Aus dem Institut für Physik der Universität Potsdam

Noise-induced Transitions and Resonant Effects in Nonlinear Systems

Habilitationschrift

zur Erlangung des akademischen Grades
Doktor rerum naturalium habilitatus
(Dr. rer. nat. habil.)
in der Wissenschaftsdisziplin Theoretische Physik

eingereicht an der
Mathematisch-Naturwissenschaftlichen Fakultät
der Universität Potsdam

von
Dr. Alexei Zaikin
geboren am 29. Januar 1973 in Moskau

Potsdam, im August 2002

Contents

Introduction

It is a fundamental question whether we need to take into consideration random fluctuations in our attempt to describe the nature. There are several reasons in favor of this stochastic approach. Our common-day experience shows that noise or fluctuations are present in every experimental measurement. This happens because real systems are sometimes embedded in the complex environment, which is very often of an irregular fluctuational structure (Fig. 1). In this case stochastic formulation of the problem is usually more elegant and apparently simple. One typical example for this situation is a movement of small pollen grains suspended in water. This phenomenon is called *Brownian Motion* [66] due to the fundamental pioneering work of Robert Brown in 1827. The simplicity of stochastic models is especially actual for climate research because to describe ocean or atmosphere dynamics one needs thousands of deterministic equations. Including noise can decrease the number of model equations and, hence, significantly speed up the solution and make forecasting more commercially profitable. On the other hand, fluctuational terms may be needed if we study a dynamics of some isolated particle in a potential, which has a local minimum. Without external forces the particle will never escape from this local minimum of the potential. To describe this escape we have to include noisy or fluctuational terms in equations (Fig. 1). An interesting example, illustrating this point, and discussing the possible causes of the Permian extinction which some 225 million years ago wiped out more than 80 percent of all species living at that time, can be found in [81]. However, it would be misleading to consider stochastic approaches as bridging between phenomenological models and microscopic description of statistical mechanics. Recent investigations show the growing interest in mesoscopic descriptions of nature, also in interdisciplinary research, and prove that fluctuations in nonlinear systems may also play the key role in nonlinear dynamics [174].

Usually noise destroys the order in the system (Fig. 2), or serves as a nuisance in the communication or any signal transmission. The street noise decreases the quality of the lecture, we suffer from noise watching the TV, or loud music does not give us the possibility to sleep. Mathematically this influence of noise consists in the fact that noise destroys the ordered structure of the trajectory. This influence of noise is illustrated in Fig. 3, where the attractors for the well-known Van-der-Pol oscillator [100] and the Lorenz model [100] are shown without noise and after adding a noisy term in the equations. It can be clearly seen that the ordered structure of the limit cycle or chaotic attractor is destroyed by adding noise. This is the usual and logical action of random fluctuations on the system.

However, intensive investigations, performed in the last three decades, have shown that
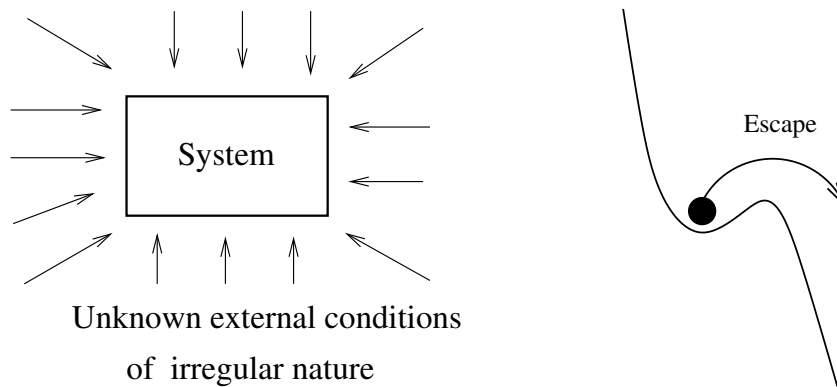
Figure 1: Real systems are often embedded in the very complex environment of external conditions (left). In this case a stochastic description is much simpler and more elegant. Another advantage of including fluctuational terms in equations is that we are able then to describe an escape of isolated from external forces particle from local minimum of the potential, which governs the behaviour of the system (right).

under certain conditions the influence of noise can be very counterintuitive, and noise can also induce ordering in nonlinear nonequlibrium systems. Now it is a well established fact, that there are many phenomena, which demonstrate noise-induced order in nonlinear systems far from equilibrium. In these phenomena the energy of noise can be used for constructive purposes in contrast to the usual role of noise as nuisance. It is very important to note, that mechanisms responsible for the appearance of noise-induced order are present in biological systems, and can be even considered as the evolutionary adaptation in living creatures. A nice example for this is a recent experiment on the stochastic resonance in sensory nervous system of a paddlefish [169]. In this experiment, the paddle fish was swimming in the aquarium, detecting the electrical signals from the planktonic prey *Daphnia* and feeding itself by capturing *Daphnia*. Some additional electric noise, supplied by putting two electrodes in the aquarium has helped the paddlefish to detect the location of the planktonic prey. As a consequence, the increase of the noise intensity resulted in the better detection. Additional investigations have shown that the detector equipment of paddlefish is tuned to use the noise from sea and planktonic conglomerations in the most optimal way.

Additionally, mechanisms of noise-induced order can be found not only in the biological systems, but also in human cognition. The effect of stochastic resonance has been found in the speed of the memory retrieval in the presence of noise[191]. The idea of the experiment was to measure the speed of memory retrieval for arithmetical multiplication rules. The average response time has been found to be minimal for some optimal noise. This result can be interpreted as a manifestation of stochastic resonance. This can be also the reason why several people prefer hearing music during the work, where they need their memory. Moreover, noise-induced phenomena have been found directly in the human brain's visual processing area: it has been found [133] that light noise, sent to one eye, improves the processing of a periodic signal, which is sent to another eye of a human subject. In what follows we are going to review state-of-the-art in the investigation of noise-induced phenomena.
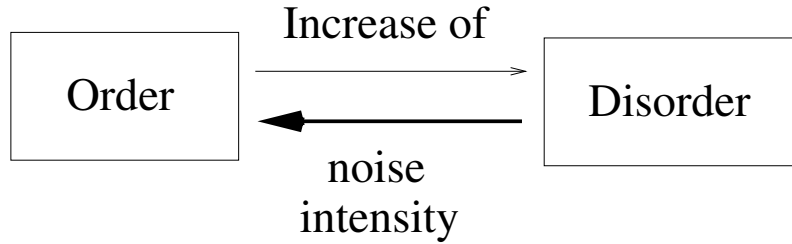
Figure 2: Usually the increase of noise intensity leads to disordering of the system. In contrast to this situation, in noise-induced effects the increase of noise may result in ordering, e.g. in synchronization with a signal or appearance of a new ordered phase.

0.1 Review of noise-induced effects

Numerous theoretical and experimental works demonstrate that there are really many nonequilibrium systems which demonstrate phenomena manifesting noise-induced ordering. Among these phenomena we can emphasize several basic ones, such as stochastic resonance (SR) [21, 53], noise-induced transitions (NIT) [81, 65][11*], coherence resonance [150], or noise-induced transport in ratchets[122, 162]. This classification does not pretend to be complete, because there are various modifications and extensions of these basic phenomena (e.g. resonance activation [39] or noise-induced pattern formation[146]). On the other hand there are phenomena which possess properties of different groups from this classification. Two interesting examples may illustrate this point: a synthesis of a ratchet mechanism and noise-induced phase transition [163] , and a synthesis of stochastic resonance and noise-induced transition [5*].

I start with **stochastic resonance** (SR), which is one of the most bright examples of noise-induced phenomena. In general case of SR, optimal amount of noise improves synchronization of the system output with input, and this improvement has resonant-like character versus the noise intensity, giving the name to SR (Fig. 4). In the classical situation SR (for review see [53], [10] and [74]) consists in the optimization of the bistable system response by noise. The term *stochastic resonance* has been introduced by Benzi, Sutera and Vulpiani [21, 47, 141], when they were exploring a model of a bistable oscillator proposed for explanation of the periodic recurrences of the Earth's ice ages. Two wells of the bistable potential represented the ice period and the optimal normal climate of the Earth. The periodic force referred to the oscillations of the eccentricity of the Earth's orbit. The problem was that according to estimations, the actual amplitude of the periodic force is far too small to force the system to switch from one state to another one. The possibility of hops has been achieved by the introduction of additional random force, i.e. noise, which induced transitions from one potential well to another by surmounting the potential barrier of the system. In 1983, SR has been studied experimentally in the Schmitt trigger system, where the Signal to Noise Ratio (SNR) was first used to describe the effect [48]. It has been shown that there is an optimal noise level at which the periodic component of the output is maximized because the SNR of the Schmitt trigger with increasing noise intensity passes through a maximum and then decreases. SR has proven to be a very general phenomenon and there are several classifications
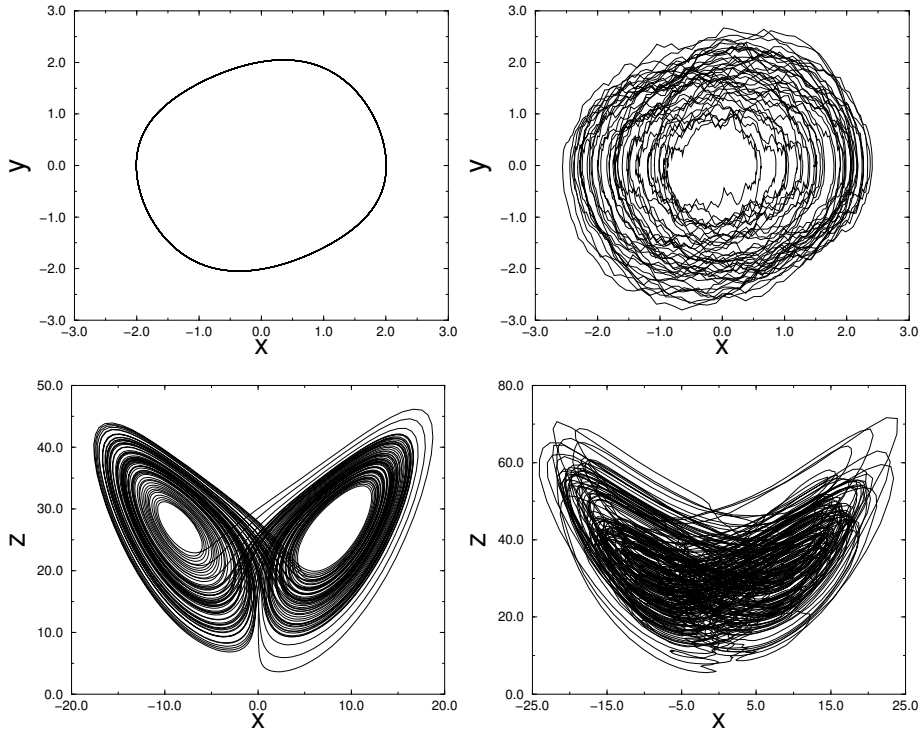
3

Figure 3: Usually adding noise in the model equations destroys the order of the trajectory structure. Top pictures: the Van-der-Pol oscillator, described by the eqs.: $\ddot{x} - 0.2\dot{x}(1 - x^2) - x = \varepsilon\xi(t)$, without noise $\varepsilon = 0$ (left) and with noise $\varepsilon = 10$ (right). Bottom pictures: the same for the Lorenz model, which demonstrate deterministic chaos, and described by eqs.: $\dot{x} = p(y - x), \dot{y} = -xz + rx - y + \varepsilon\xi(t)$, $\dot{z} = xy - bz$. Without noise $\varepsilon = 0$ (left), and with noise $\varepsilon = 40$ (right). The remaining parameters are: $p = 10$, $b = 8/3$, $r = 28$.

of SR:

1. With respect to the different situations and applications: SR has been found in in a ring laser [125], in analog systems [35, 54, 55, 56, 57] [58, 59, 70, 71, 72, 135, 211] in magnetic systems [45], in passive optical bistable systems [41], in systems with electronic paramagnetic resonance [60], in experiments with Brownian particles [180], in experiments with magnetoelastic ribbons [185], in a tunnel diode [121], in superconducting quantum interference devices (SQUIDS) [79], and in ferromagnetics and ferroelectrics [148, 137]. SR has been also observed in chemical systems[109, 42, 80], in visual perception [164, 165, 181] and even in social models [14] as well. As it was already discussed above, SR has been found in the behaviour of paddlefish[169] and in human cognition [191].

2. With respect to the class of the system: SR has been found in many different systems, e.g. in monostable [186], excitable [203], non-dynamical [69], nonpotential [9], and thresholdless [22] systems, and in systems with transient noise-induced structure [52].

3. With respect to the form of a signal: SR has been found for periodic signal [53], digital

4

or aperiodic signals [17, 18, 16], or in systems without signal [83].

4. With respect to different kinds of noise: SR has been investigated for white noise [53], colored noise [140], chaotic signal [182], or even high-frequency periodic signal, which played the role of noise [104].

Noteworthy, the effect of stochastic resonance can be extended for the case of spatially distributed systems as spatiotemporal stochastic resonance [123, 199], array enhanced stochastic resonance [112], or stochastic resonance in extended bistable systems [205, 23]. *Noise-induced propagation* is another effect, which is closely related to the effect of stochastic resonance, i.e. can be interpreted as nontrivial spatial extension of stochastic resonance. In this effect the propagation of a harmonic signal through an unforced system is increased for an optimal intensity of the additive noise. Noise-induced or noise-enhanced propagation has been reported in bistable or excitable medium [111, 209, 92, 15, 63, 147, 168].
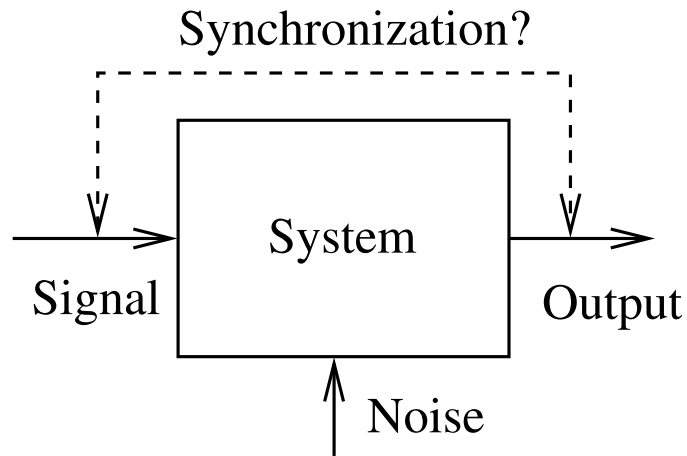

Figure 4: A scheme of stochastic resonance: optimal intensity of noise leads to the syncrhonization between input and output of the system

Noise-induced transition is an effect in which changing the noise intensity causes the transition to the new state, which is qualitatively different from the previous one. This difference can be estimated by the corresponding order parameter (Fig. 5). Noise-induced transitions in nonequilibrium systems can be considered as a generalization of phase transitions in thermodynamic equilibrium systems. Tracing the analogy between such equilibrium phase transitions and nonequilibrium noise-induced transitions, one can say, that the noise intensity plays the role of the temperature of the system, and the order parameter determines the phase of the system [75]. Noise-induced transitions (NIT) can be classified into three main groups:

1. NIT which lead to the appearance of additional extrema (maxima) in the system's probability distribution,

2. NIT which lead to the excitation of oscillations,

3. NIT in spatially extended systems, which lead to breaking of symmetry and the creation of a mean field.

NIT, which lead to the appearance of additional extrema (maxima) in the system's probability distribution (for the review see the book [81]) or disappearance of old ones [49], occur in zero-dimensional systems with multiplicative noise. Such transitions have been investigated in the Verhulst model to study the dynamics of population growth in biological systems [81], in the genetic model to describe the genotype dynamics in the fluctuational environment ([81] and experimentally in [183]), in chemical reactions under the action of the fluctuating light [32] and in bistable systems [166]. Additionally, NIT of this type have been found experimentally in an electrical parametric oscillator [90, 91] and in analog circuits [89, 183]. The mechanism, responsible for these NIT, is the fact, that multiplicative noise changes the "stochastic" potential, which effectively governs the behaviour of the system. For such transitions the order parameter will be the location of extrema in the system probability distribution.
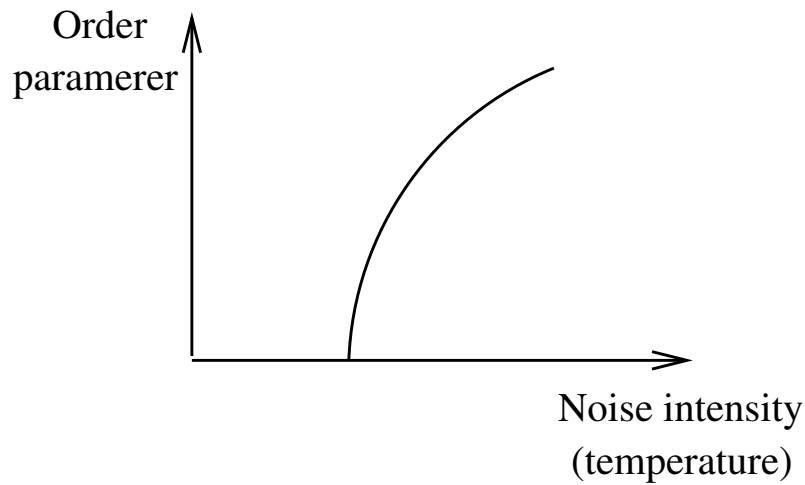

Figure 5: Noise-induced transition: changing the intensity of noise, which plays the role of temperature, results in qualitative change of the order parameter, which can be the extremum in the system probability distribution, an amplitude of oscillations, or a mean field.

NIT which lead to the excitation of oscillations (for the review see [100, 103, 102]), appear in oscillatory systems, for example, in the pendulum with randomly vibrated suspension axis [25*]. In this case, the order parameter is the average of the instantaneous amplitude of oscillations or average of its square. If the noise intensity is below its critical value, there is no oscillations in the system, but if the noise intensity is increased above the critical value, oscillations are excited. Hence, the reason of these NIT is the parametric excitation of oscillations, performed by multiplicative noise, which changes the frequency of the system in the random way. In addition to mechanical systems, this type of NIT can be found in nonlinear models, which describe the dynamics of childhood epidemics [24*][11*]. Noteworthy, that noise-induced oscillations possess the property of on-off-intermittency [20*] and can be controlled by additional periodic action [21*][156]. Finally, there exist a hypothesis, that such NIT occur in open subsonic submerged jets in the appearance and evolution of the turbulence [101][15*]. In particular, it can be especially potential for applications, that turbulence as noise-induced oscillations can be controlled by a periodic additional force (acoustic wave or sound).

NIT which lead to breaking of symmetry and the creation of a mean field (for review see [65]) occur in spatially extended systems, e.g. in systems of noisy coupled nonlinear oscillators. In this case the order parameter, which determines a phase of a system, is the mean field In 1979 Mikhailov reported a noise-induced phase transition of this type in a biological system with diffusion [129]. In [62, 195, 64, 196] generic models, in particular Ginzburg-Landau equation, which demonstrate the noise-induced transition and formation a mean fields, have been considered. If oscillators in these models are coupled via the especial form of coupling,*a la Swift-Hohenberg*, then a transition will lead to the formation of spatially ordered patterns [146]. Noteworthy, the effect of colored noise is crucial for these transitions, because additional memory of noise is disordering a system [119, 120]. A mechanisms, which are responsible for these transitions, namely, a joint action of multiplicative noise and coupling, are described in [196] and [172]. With respect to experimental application of the theory of these noise-induced transitions, the understanding of these NIT will certainly help in the investigation of liquid nematic crystals [93, 207], of noise-induced bistability in Helium-IV [73], in electronic circuits [1], as well as in systems, which demonstrate noise-induced shift of the phase transition, e.g, in: photosensitive chemical reactions [128, 32], or Rayleigh-Bénard convection [127].
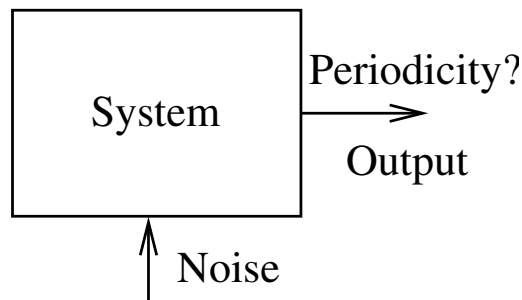

Figure 6: Coherence resonance: increase of the noise intensity improves the periodicity of the system output.

The effect of **coherence resonance** (CR) is another manifestation of the noise-induced order, in which noise shows the surprising ability to increase level of periodicity in the output of the nonlinear nonequlibrium system (Fig. 6). CR has been reported in different kinds of systems, in particular, it has been found that some noise amplitude exists at which the coherence of spiking in the output of the system can be significantly enhanced in an isolated Fitz-Hugh Nagumo (FHN) system [150], in the Hodgkin-Huxley [106] and Plant/Hindmarsh-Rose neuron models [115], and in dynamical systems close to the onset of bifurcations [138] (note also experimental verifications of CR in optical systems [68]). In addition, CR has been found in the behaviour of a dynamical system, which shows jumps between several attractors [144]. Hence, two basic mechanisms of CR have been reported, CR in excitable systems via the competition between the constant excursion time and waiting time, which in optimal regime is negligibly small, and CR in a system with two attractors via jumps of the trajectory between these attractors after one period of being on each of them.

In recent years, there has been a great interest in the CR behaviour of spatially extended

systems consisting of many interacting elements[77, 139]. It has been shown that matching the noise-related characteristic time scales of the coupled excitable elements results in noise-induced synchronization regimes very similar to those for coupled limit cycles (for the review on synchronization phenomena see [151]). Moreover, *array-enhanced CR* has been reported, in which constructing an array of coherence-resonance oscillators significantly improves the periodicity of the output [82, 210]. It is important to note that understanding of CR mechanisms is very important for the modelling of the generation of different rhythms in the description of several natural processes, such as locomotion [29] or playing piano [44].
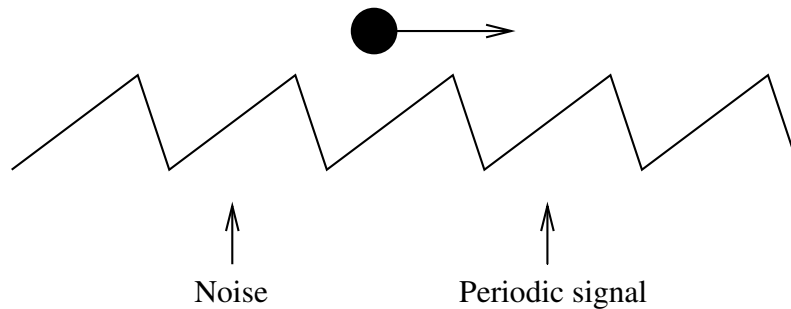

Figure 7: Stochastic transport in ratchets: noise induces directed motion of particles in the periodic assymetric potential, which is harmonically changed.

Stochastic transport in spatially extended systems with a periodic assymetric potential far from equilibrium, or **ratchets** (Fig. 7), is still very actual topic in the investigation of noise-induced effects (for the review see [162]). In 1963 Feynman has predicted that in the presence of a second heat bath a ratchet effect will manifest itself [50]. Further on, previously known results in the frame of the concept of molecular motors and pumps [85, 177, 178], have been developed in numerous works on ratchet effects [24, 192, 107, 30, 12, 13, 190, 202]. Ratchet effect in the form of voltage rectification by a dc-SQUID in the presence of a magnetic field and an unbiased ac-current has been experimentally observed and theoretically interpreted in [34, 33, 20]. Two main ratchet scheme have been mainly investigated, tilted ratchet [117] and on-off ratchet [8]. A synthesis of a noise-induced phase transition and a ratchet effect has been considered in [163]. Up to now ratchets belong to the actual topic of modern physics [173, 25, 161, 105, 145].

0.2 The aim and content of this work

Despite really intensive investigations, carried on in the last three decades, not all mechanisms, responsible for the appearance of noise-induced order have been discovered and analyzed. Especially interesting are situations, in which a system is under the action of several noise sources, e.g. an interplay between additive and multiplicative noise can be observed. In particular, it is still not clear which role can be played by additive noise in the effect of noise-induced transitions or noise-induced phase transitions, usually induced by multiplicative noise. Also it has not been investigated, that noise-induced order can occur due to the scenario, in which the role of noise is twofold: first noise creates the necessary feature in

the system, and then this feature is used by noise to induce the order. The question which naturally arises in this considerations is: is it possible to generalize noise-induced resonant phenomena for systems which do not have necessary features? Hence, the problem is whether we can observe noise-induced phenomena due to this property which is also induced by noise and, therefore, use the energy of noise even more efficiently. We call these phenomena as *doubly stochastic effects* (DSE), and investigate whether one can apply this concept to basic noise-induced phenomena, such as stochastic resonance, noise-induced propagation, or coherence resonance. Doubly stochastic effects also occur due to the interplay between multiplicative and additive noises, and hence this problem is closely related to the investigation of the role of additive noise in transitions, which are induced by multiplicative noise. To be complete, it is neccessary to note that for ratchets, some kind of DSE have been found in [163]. Finally, there are many other noise-induced effects and effects related to the action of the noise, which have not been investigated. This was the motivation of the present research, and hence, **the aim of this work** is the investigation of nonlinear systems under the action of multiplicative and additive noise for the determination of new mechanisms responsible for the appearance of noise-induced order, especially via doubly stochastic effects, and for finding the appropriate applications of these effects.

According to this aim the following problems are considered in this work:

1. we study the effect of additive noise in noise-induced transitions,

2. we study doubly stochastic effects: doubly stochastic resonance, noise-induced propagation in monostable media, and doubly stochastic coherence,

3. we study new effects: noise-induced frequency selection of the propagation frequency, vibrational resonance in a noise-induced structure, system size resonance in coupled noisy systems, and coherence resonance in inhibitory coupled excitable oscillators,

4. we study possible applications for these findings, in particular, we design the electronic circuit for doubly stochastic resonance, we study experimentally coherence resonance via noise-induced symmetry, and we study experimentally a vibrational resonance in bistable systems.

The research presented in this work is organized as follows. This work is devoted to the investigation of new mechanisms responsible for the noise-induced ordering in nonlinear systems, to the development of the concept of doubly stochastic effects, and to some new effects, which demonstrate the counterintuitive ability of noise to induce order in nonequlibrium systems. In the first chapter we start with the investigation of the role of **additive noise in noise-induced transitions**. If we deal with noise-induced transitions, usually only multiplicative noise or the joint action of multiplicative noise and coupling is responsible for the appearance of the transition. In noise-induced transitions, which lead to the appearance of new maxima in the system probability distribution, the transition happens, because due to the multiplicative noise some additional terms appear in the "stochastic" potential, which governs the behaviour of the system[81]. In noise-induced transitions, which lead to the excitations of oscillations, the transition occurs due to the parametric action of the multiplicative

noise[102]. In noise-induced transitions, which lead to the breaking of symmetry and creation of the mean field, the transition occurs again due to the multiplicative noise which induces short-time bistability, and then due to coupling, which freezes a system in this bistable state [65]. Meanwhile additive noise can also play a crucial and very nontrivial role in the effect of noise-induced transition [11*,24*,19*,18*]. First, we investigate a transition in the presence of additive noise in a pendulum with randomly vibrated suspension axis. We show that additive noise smoothes a transition and influences the effect of on-off intermittency, which is a characteristical feature of noise-induced oscillations [11*,20*]. Then, on the model, which describe the behaviour of childhood epidemics, we show that additive noise is able to stabilize noise-induced oscillations, which appear as a result of noise-induced phase transition [11*]. Finally, we show that additive noise itself can induce a phase transition in the spatially extended system of coupled noisy oscillators. This transition, induced by additive noise, can be of the second- [19*] and first- order [12*]. In the latter case, the order parameter , here a mean field, is a discontinuous function of the noise intensity. If the oscillators coupled via a coupling *a la Swift-Hohenberg*, then additive noise can induce a formation of spatially ordered patterns, as a result of noise-induced phase transition [18*].
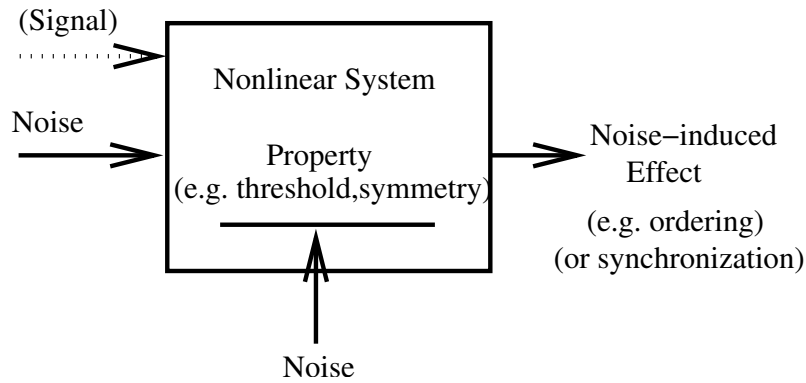

Figure 8: A concept of doubly stochastic effects: noise creates a property of the system which is used by another noise to induce the effect in the nonlinear nonequlibrium system. Usually it occurs due to the interplay between multiplicative and additive noise.

After an investigation of new mechanisms, which causes noise-induced order in systems via phase transitions, in the second chapter we develop **a concept of doubly stochastic effects** (Fig. 8). The idea of this concept is the following. Usually, if we observe noise-induced order in an nonlinear system, it occurs due to the presence of some intrinsic property of a system, which works as a mechanism of a noise-induced phenomenon. For example, in the effect of stochastic resonance this feature is a threshold, which presents in the system. Coming noise interacts with this feature, and we observe a noise-induced order. Meanwhile, this mechanism, responsible for the noise-induced effect, can be also induced by noise. In this case we deal with doubly stochastic effect, in which noise-induced order appears according to the scenario, when noise-induced order is created in a system due to the feature, which was, in its turn, also induced by noise. This is the idea of the concept of doubly stochastic effects. Certainly, in such effects, the energy of noise is used more efficiently, because it is used not only for the noise-induced ordering, but also for the mechanism, which is used in this process.

10

The first effect, which has been found and investigated by us in frames of this concept is doubly stochastic resonance [5*]. In this effect, multiplicative noise induces bistability in the spatially extended system via a phase transition, and additive noise optimizes a signal processing, i.e. synchronizes output with input, in this bistable system due to the principle of stochastic resonance. To suggest a possible experimental implementation of doubly stochastic resonance, we have designed a simple electronic circuit [4*]. The idea of doubly stochastic effects can be developed not only for effects, based on the principle of stochastic resonance, but also for coherence resonance effects. To do this, we consider the effect of doubly stochastic coherence, which demonstrate a periodicity via noise-induced symmetry [34*]. It is important to note that usually noise is able only to destroy a symmetry, as it happens in noise-induced phase transitions. In contrast to this situation, in doubly stochastic coherence, multiplicative noise induces a symmetry in the system, and then this symmetry helps to generate a periodic output due to additive noise. We study doubly stochastic coherence on the paradigmatic model, explain its behaviour by the consideration of an "effective" model, and finally confirm these idea by experimental measurements on the electronic circuit.

As discussed above, SR can be extended for the case of spatially extended systems, as the effect of noise-induced or noise-enhanced propagation. Nevertheless, these effects have been sobserved only in bistable or excitable media, and not in deterministically *monostable* media, which certainly describe a rather wide class of systems. Application of the concept of doubly stochastic effects leads to the discovery of **new effects in noise-induced propagation**. We discuss one of such effect in the third chapter, where we describe a noise-induced propagation in monostable media [3*]. The idea of this effect is the following. First, a joint action of multiplicative noise and coupling induces a bistability in the spatially extended system via a noise-induced phase transition. Then additive noise is able to enhance a propagation of a periodic signal through this system. Interesting that propagation of a signal does not destroy a bistability, which is a collective effect. Discussing noise-induced propagation, we study also another effect, which is related to the concept of doubly stochastic effects. Namely, we study a propagation of a bichromatic signal through a bistable media in the presence of noise, and find that under certain conditions noise is able to select a propagation frequency.

In the fourth chapter we study **noise-induced effects and resonant effects in the presence of noise**, some additional new effects, which have been investigated during the development of the concept of doubly stochastic effects. We start with the investigation of vibrational resonance in a noise-induced structure [7*]. In this effect, an addition of high-frequency optimizes a response of the system at the frequency of a low frequency signal, due to the bistability, which has been created by joint action of multiplicative noise and coupling. The effective model, responsible for this effect, is also studied experimentally on the electronic circuit [7*]. Further on, we study a new effect, which appear only in the presence of noise, namely, system size resonance [153]. The effect consists in the fact, that when a small periodic force on the ensemble of coupled noisy systems, the linear response of the system has a maximum at a certain system size, similar to stochastic resonance phenomenon. This effect can be observed if we change a size of a system of coupled bistable oscillators, but, in particular, this effect can be also demonstrated for systems with noise-induced bistability. After that, we study a coherence resonance in a system of coupled noisy excitable elements,

based in the new mechanism [5*]. For this we consider a system of two or three excitable oscillators with inhibitory coupling. A new mechanism of noise-induced periodic output is based on anti-phase motion of coupled oscillators, whereas for other mechanisms of coherence resonance in spatially extended systems, in-phase movement was necessary. In the last chapter we summarize the results, obtained in this work, and discuss possible direction of the future research.

Chapter 1

Additive noise in noise-induced nonequilibrium transitions

As mentioned in the introduction doubly stochastic effects occur in a nonlinear system due to the interplay between two noise sources, usually sources of multiplicative and additive noise. One noise induces a new state in the system or a new property of the system, and other noise uses this new state to work out noise-induced effect. The effect of noise-induced transition already consists in the creation of the new state or in the transition to the new state. Hence, logically the question arises, what additionally can happen, if we have two noise sources in the system. Since usually transitions are induced by multiplicative noise, we formulate the problem as follows: what is the role of additive noise in transitions, which occur in nonlinear systems due to the action of multiplicative noise. We start with a study of the transition which leads to noise-induced oscillations and happens in a pendulum with randomly vibrated axis. This model can be considered as a paradigmatic model for such a transition, besides, a pendulum is a classical and universal object of investigation in theoretical physics.

CHAPTER 1. ADDITIVE NOISE IN NOISE-INDUCED NONEQUILIBRIUM
TRANSITIONS

1.1 Transitions in the presence of additive noise. On-off intermittency

A pendulum with randomly vibrated suspension axis is a typical example of oscillatory system, in which parametric action of noise can lead to the excitation of oscillations via a second-order phase transition [25*,24*,11*]. In this case the intensity of multiplicative noise plays the role of temperature and the average amplitude is the order parameter. Here we discuss the question what happens if additionally additive noise is acting upon the system. Therefore we consider a pendulum whose suspension axis is vibrating in the direction making the angle γ with respect to the vertical (Fig. 1.1). As shown in [11*], for moderately small vibrations of a suspension axis, i.e. in the presence of additive noise, the equation of motion can be written as follows:

$$\ddot{\varphi} + 2\beta\left(1 + \alpha\dot{\varphi}^2\right)\dot{\varphi} + \omega_0^2\left(1 + \xi_1(t)\right)\sin\varphi = \omega_0^2\xi_2(t), \tag{1.1}$$

where φ is the pendulum angular deviation from the equilibrium position, ω_0 is the natural frequency of small free pendulum's oscillations, β is the damping factor, α is the coefficient of nonlinear friction, $\xi_1(t)$ and $\xi_2(t)$ are comparatively broad-band random processes with zero mean values.

We assume that the suspension axis vibration is moderately small in amplitude, i.e. the pendulum oscillations can be considered small enough for φ to be substituted in place of $\sin\varphi$ in Eq. (1.1).

We start with an approximate analytical solution of this problem, which can be obtained from the assumptions that $\beta/\omega_0 \sim \varepsilon$, $\xi_1(t) \sim \sqrt{\varepsilon}$, and $\xi_2(t) \sim \sqrt{\varepsilon}$, where ε is a certain small parameter which should be put equal to unity in the final results. Eq. (1.1) can then be solved by the Krylov–Bogolyubov method; to do this we set $\varphi = A(t)\cos\psi(t) + \varepsilon u_1 + \ldots$, where $\psi(t) = \omega_0 t + \phi(t)$,

$$\dot{A} = \varepsilon f_1 + \ldots, \quad \dot{\phi} = \varepsilon F_1 + \ldots, \tag{1.2}$$

$u_1, \ldots, f_1, \ldots, F_1, \ldots$, are unknown functions. By using the Krylov–Bogolyubov technique for stochastic equations (see [187]), we find expressions for the unknown functions f_1 and F_1. Substituting these expressions into Eqs. (1.2) we obtain

$$\dot{A} = -\beta\left(1 + \frac{3}{4}\alpha\omega_0^2 A^2\right)A + \omega_0\overline{g_1(A,\psi(t),\xi_1(t),\xi_2(t))}, \tag{1.3}$$

$$\dot{\phi} = \omega_0\overline{g_2(A,\psi(t),\xi_1(t),\xi_2(t))}, \tag{1.4}$$

where

$$g_1(A,\phi,t) = \frac{A}{2}\xi_1(t)\sin 2\psi(t) - \xi_2(t)\sin\psi(t),$$

$$g_2(A,\phi,t) = \xi_1(t)\cos^2\psi(t) - \frac{1}{A}\xi_2(t)\cos\psi(t),$$

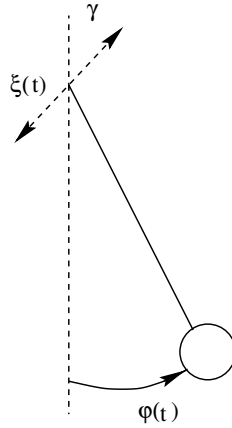the bar over the expression denotes averaging over time.

Figure 1.1: A scheme of a pendulum with randomly vibrated suspension axis. The direction
of this vibration is not vertical, and this provides additive noise in the model equation.

As follows from [187], the Fokker–Planck equation associated with Eqs. (1.3), (1.4) is

$$\frac{\partial w(A,\phi,t)}{\partial t} = -\frac{\partial}{\partial A}\left[\left(-\beta\left(1+\frac{3}{4}\alpha\omega_0^2 A^2\right)A + \omega_0^2 R_1\right)w(A,\phi,t)\right] - \omega_0^2 R_2\frac{\partial w(A,\phi,t)}{\partial\phi} +$$

$$\frac{\omega_0^2}{2}\left\{\frac{\partial^2}{\partial A^2}\left(\left(\frac{K_{11}}{4}A^2 + K_{12}\right)w(A,\phi,t)\right) + \left(K_{21} + \frac{K_{22}}{A^2}\right)\frac{\partial^2 w(A,\phi,t)}{\partial\phi^2}\right\}, \qquad (1.5)$$

where

$$R_1 = \int\limits_{-\infty}^{0}\left(\left\langle\overline{\frac{\partial g_1(A,\phi,t)}{\partial A}g_1(A,\phi,t+\tau)}\right\rangle + \left\langle\overline{\frac{\partial g_1(A,\phi,t)}{\partial\phi}g_2(A,\phi,t+\tau)}\right\rangle\right)d\tau, \qquad (1.6)$$

$$R_2 = \int\limits_{-\infty}^{0}\left(\left\langle\overline{\frac{\partial g_2(A,\phi,t)}{\partial A}g_1(A,\phi,t+\tau)}\right\rangle + \left\langle\overline{\frac{\partial g_2(A,\phi,t)}{\partial\phi}g_2(A,\phi,t+\tau)}\right\rangle\right)d\tau, \qquad (1.7)$$

the angular brackets denotes averaging over the statistical ensemble,

$$K_{11} = \frac{1}{2}\kappa_{\xi_1}(2\omega_0), \quad K_{12} = \frac{1}{2}\kappa_{\xi_2}(\omega_0), \qquad (1.8)$$

and

$$K_{21} = \frac{1}{4}\left(\kappa_{\xi_1}(0) + \frac{1}{2}\kappa_{\xi_1}(2\omega_0)\right), \quad K_{22} = \frac{1}{4}\left(\kappa_{\xi_2}(0) + \frac{1}{2}\kappa_{\xi_2}(\omega_0)\right), \qquad (1.9)$$

and

$$\kappa_\xi(\omega) = \int\limits_{-\infty}^{\infty}\langle\xi(t)\xi(t+\tau)\rangle\cos\omega\tau\,d\tau$$

is the power spectrum density of the process $\xi(t)$ at the frequency ω.

Let us now calculate the integrals (1.6) and (1.7) taking account of the expressions for g_1

and g_2. As a result we obtain:

$$R_1 = \frac{3A}{8} \int\limits_{-\infty}^{0} \langle \xi_1(t)\xi_1(t+\tau) \rangle \cos 2\omega_0\tau \, d\tau + \frac{1}{2A} \int\limits_{-\infty}^{0} \langle \xi_2(t)\xi_2(t+\tau) \rangle \cos \omega_0\tau \, d\tau$$

$$= \frac{3K_{11}}{8}A + \frac{K_{12}}{2A}, \tag{1.10}$$

$$R_2 = \frac{1}{4} \int\limits_{-\infty}^{0} \langle \xi_1(t)\xi_1(t+\tau) \rangle \sin 2\omega_0\tau \, d\tau - \frac{1}{A^2} \int\limits_{-\infty}^{0} \langle \xi_2(t)\xi_2(t+\tau) \rangle \sin \omega_0\tau \, d\tau. \tag{1.11}$$

The value of R_2 depends on the characteristics of the random processes $\xi_1(t)$ and $\xi_2(t)$: if they are white noises then $R_2 = 0$; but if, for example, $\xi_2(t)$ is white noise and $\xi_1(t)$ has a finite correlation time and its power spectrum density is

$$\kappa_{\xi_1}(\omega) = \frac{a_1^2 \kappa_{\xi_1}(2\omega_0)}{(\omega - 2\omega_0)^2 + a_1^2},$$

then

$$R_2 = -\frac{a_1 \omega_0 \kappa_{\xi_1}(2\omega_0)}{4\left(16\omega_0^2 + a_1^2\right)}.$$

It should be noted that in this case R_2 is negative, that results in a decrease of the mean oscillation frequency with an increase of noise intensity. The Langevin equations which can be related to the Fokker-Planck equation (1.5) in view of (1.10) and (1.11) are presented the following:

$$\dot{A} = \beta\left(\eta - \frac{3\omega_0^2}{4}\alpha A^2\right)A + \frac{\omega_0^2}{2A}K_{12} + \frac{\omega_0}{2}A\zeta_{11}(t) + \omega_0\zeta_{12}(t),$$

$$\dot{\phi} = \omega_0^2 M + \omega_0\left(\zeta_{21}(t) + \frac{\zeta_{22}(t)}{A}\right), \tag{1.12}$$

where $\zeta_{11}(t)$, $\zeta_{12}(t)$, $\zeta_{21}(t)$, and $\zeta_{22}(t)$ are white noises with zero mean value and uncorrelated with A. The intensities of these noises are K_{11}, K_{12}, K_{21}, and K_{22}, respectively. We note that even in the case with $\kappa_{\xi_2} = 0$ Eqs. (1.12) differ from that derived in [187]. The reason is that there the variable $u = \ln A$ in place of A was used, i.e. the correlation between the noise $\xi(t)$ and the amplitude A was implicitly ignored [100][25*,22*].

First we consider **the case when additive noise is absent**, i.e. $\kappa_{\xi_2} \equiv 0$. In this case the steady-state solution of Eq. (1.5), satisfying the condition of zero probability flux, is

$$w(A,\phi) = \frac{C}{2\pi A^2} \exp\left\{\frac{3}{1+\eta}\left(\eta \ln A - \frac{aA^2}{2}\right)\right\}, \tag{1.13}$$

where $a = 3\alpha\omega_0^2/4$ is the nonlinear parameter and $\eta = 3\omega_0^2 K_{11}/8\beta - 1$. The constant C is deter-
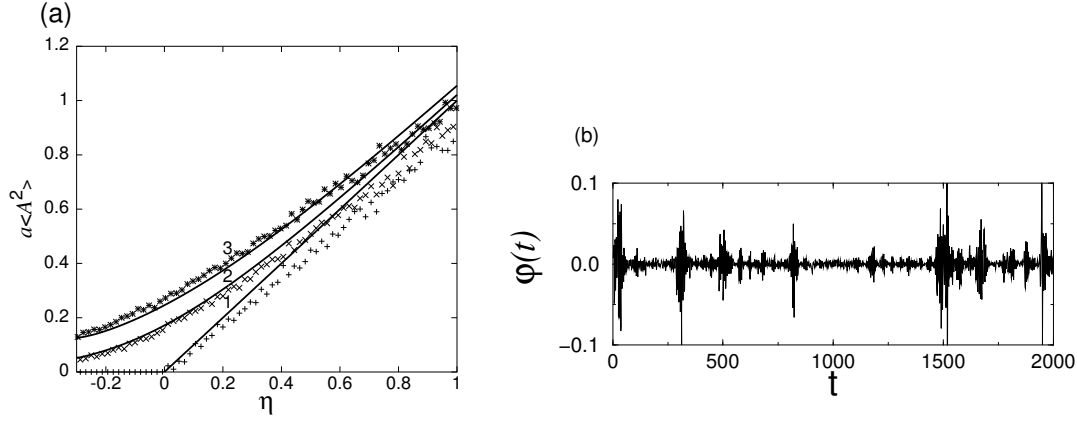
Figure 1.2: (a) A noise-induced phase transition in a pendulum with randomly vibrated suspension axis (Eq.(1.1)). The dependence of the averaged amplitude squared multiplied by the parameter $a = 3\alpha\omega_0^2/4$ on η, where η is an extent on which multiplicative noise intensity exceeds the threshold value. Without additive noise $q_0 = 0$ (curve 1), and with increasing additive noise $q_0 = 0.005$ (curve 2) and 0.02 (curve 3). The remaining parameters are $\beta = 0.1$, $\alpha = 100$, and $\omega_0 = 1$. Analytical and numerical results are shown by solid and symbol curves, respectively. (b) On-off intermittency for subcritical values of multiplicative noise intensity. In contrast to this situation, if additive noise is absent, on-off intermittency is observed near a threshold but for supercritical values of the multiplicative noise intensity.

mined from the normalization condition

$$\int\limits_0^{2\pi} \int\limits_0^\infty w(A,\phi)A\,dA\,d\phi = 1.$$

Upon integrating (1.13) over ϕ, we find the expression for the probability density w of the oscillations amplitude

$$w(A) = CA^{(2\eta-1)/(1+\eta)} \exp\left(-\frac{3aA^2}{2(1+\eta)}\right). \tag{1.14}$$

From the normalization condition we get

$$C = 2 \begin{cases} \left(\dfrac{3a}{2(1+\eta)}\right)^{3\eta/2(1+\eta)} \dfrac{1}{\Gamma\left(3\eta/2(1+\eta)\right)} & \text{for } \eta \geq 0 \\[4mm] 0 & \text{for } \eta \leq 0. \end{cases} \tag{1.15}$$

Hence,

$$w(A) = 2 \begin{cases} \left(\dfrac{3a}{2(1+\eta)}\right)^{3\eta/2(1+\eta)} \dfrac{A^{(2\eta-1)/(1+\eta)}}{\Gamma\left(3\eta/2(1+\eta)\right)} \exp\left(-\dfrac{3aA^2}{2(1+\eta)}\right) & \text{for } \eta \geq 0 \\[4mm] \delta(A) & \text{for } \eta \leq 0. \end{cases} \tag{1.16}$$

The fact that for $\eta \leq 0$ the probability density of the amplitude turns out to be a δ-function is associated with the absence of additive noise (see below).
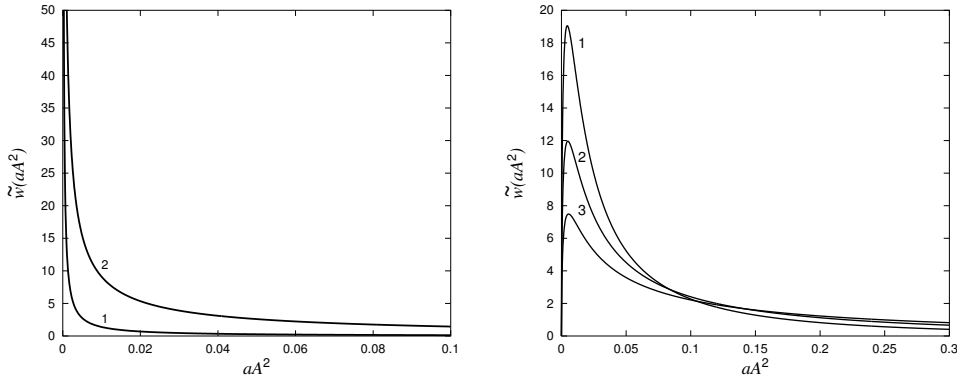
20

Figure 1.3: The system probability distribution for a pendulum. (a) The case without additive noise. The probability distribution $\tilde{w}(aA^2) = w(A)/2aA$ for $\eta = 0.01$ (curve 1), and $\eta = 0.2$ (curve 2). (b) The case with additive noise. The dependence of $\tilde{w}(aA^2) = w(A)/2aA$ for $q = 0.01/(1+\eta)$ and $\eta = -0.2$, 0 and 0.2 for curves 1–3 respectively.

Using (1.16), we can determine $\langle A \rangle$ and $\langle A^2 \rangle$:

$$\langle A \rangle = \begin{cases} \sqrt{\dfrac{3}{2a(1+\eta)}} \dfrac{\Gamma\big((4\eta+1)/2(1+\eta)\big)}{\Gamma\big(3\eta/2(1+\eta)+1\big)}\eta & \text{for } \eta \geq 0 \\[4mm] 0 & \text{for } \eta \leq 0 \end{cases} \tag{1.17}$$

$$\langle A^2 \rangle = \begin{cases} \dfrac{\eta}{a} & \text{for } \eta \geq 0 \\[3mm] 0 & \text{for } \eta \leq 0 \end{cases} \tag{1.18}$$

Therefore, it is evident that for $\eta > 0$ the parametric excitation of pendulum oscillations occurs under the influence of multiplicative noise. This manifests itself in the fact that the mean values of the amplitude and of the amplitude-squared become non-zero (Fig. 1.2, curve 1). This parametric excitation implies a transition of the system to a new state, that can be treated as a phase transition. The condition $\eta = 0$ is the threshold for the onset of this phase transition. It follows that, in the absence of additive noise, the critical value of the multiplicative noise intensity is

$$\kappa_\xi^{\text{cr}}(2\omega_0) \equiv \kappa_{\text{cr}} = \frac{16\beta}{3\omega_0^2}. \tag{1.19}$$

Hence, the parameter η characterizes the extent to which the intensity of multiplicative noise component exceeds its critical value.

It should be noted that, for $\eta > 0$, the steady state $A = 0$ loses its stability and the state $A \neq 0$ becomes stable. At the same time, eq. (1.16) implies that the probability density of A^2 is monotonically decreasing with increasing A^2 for any value of $\eta > 0$. Hence, in contrast to the transitions considered in [81], the appearance of a new stable state needs not to be accompanied by the appearance of a new maxima in the system probability distribution (see Fig. 1.3, a).

21

Now let us consider **the case when the intensity of additive noise is not equal to
zero**. The steady-state solution of Eq. (1.5), satisfying the condition of zero probability flux,
is conveniently written as

$$w(A, \phi) = \frac{Ca}{2\pi(aA^2 + q)} \exp\left\{ \int \frac{3\left(\eta - aA^2\right)aA^2 + q}{(1+\eta)(aA^2 + q)A} \, dA \right\}, \tag{1.20}$$

where $q = 4aK_{12}/K_{11}$ characterizes the ratio between the intensities of additive and multiplicative noise.

Following the calculations presented in the detail in [11*], we get an expression for

$$a\langle A^2 \rangle \approx (1+\eta)\left[\frac{4\mu}{3}\Gamma(2\mu)\Gamma\left(\frac{3}{2} - 2\mu\right)(1+2\mu)\left(2(1-2\mu) + (5-4\mu)\frac{3q}{2(1+\eta)}\right) - \right.$$

$$\left. \frac{3q}{2(1+\eta)}\left(\sqrt{\pi}\Gamma(-2\mu)(1-2\mu)\left(\frac{3q}{2(1+\eta)}\right)^{2\mu} + 2\Gamma(2\mu)\Gamma\left(\frac{3}{2} - 2\mu\right)(1+2\mu)\right)\right] \times$$

$$\left[\frac{\sqrt{\pi}}{2}\Gamma(-2\mu)(1-2\mu)\left(\frac{3q}{2(1+\eta)}\right)^{2\mu}\left(2(1+2\mu) + \frac{9q}{2(1+\eta)}\right) + \right.$$

$$\left. \Gamma(2\mu)\Gamma\left(\frac{3}{2} - 2\mu\right)(1+2\mu)\left(2(1-2\mu) + \frac{3(3-4\mu)q}{2(1+\eta)}\right)\right]^{-1}. \tag{1.21}$$

where $\mu = 3(\eta + q)/4(1+\eta)$. Note that similarly to the case without additive noise, after a
transition no additional maxima appear in the system probability distribution and the shape
of this distribution is not qualitatively changed (Fig. 1.3, b).

Next we compare these analytical results with numerical simulations. The corresponding
dependence of $a\langle A^2 \rangle$ on η for different values of the parameter q_0 is illustrated in Fig. 1.2. We
see that additive noise of the small intensity results in a smoothing of the dependence of the
mean oscillation amplitude-squared on the multiplicative noise intensity: it becomes without
fracture inherent in a phase transition induced by only multiplicative noise. If we increase
additive noise intensity, the transition becomes less detectable (Fig. 1.2, curve 3).

In numerical experiment it is more convenient to calculate the variance of the corresponding variable instead of the mean amplitude squared. It is evident that the dependencies of
these values on the noise intensity should be similar. Indeed, in the case when the amplitude
A is a slowly changing function, the variance is equal to $\langle A^2 \rangle/2$. The dependencies of $a\langle A^2 \rangle$ on
η found by numerical simulation of Eq. (1.1) for both the presence of additive noise and its
absence are shown also in Fig. 1.2. We find that near the threshold the simulations match
the analytical results very good and that the dependencies for $q = 0$ can be approximated by
a straight line intersecting the abscissa at $\eta = 0$. With an increase of η, the growth rate of
the variance in numerical simulations is smaller than in the analytical results. This can be
explained by the fact that the Krylov-Bogolyubov method is valid only near a threshold.

Now let us discuss how additive noise influences the effect of on-off intermittency. Numerical simulation of the original Eq.(1.1) shows that if the noise intensity is slightly over
a threshold, then in the absence of additive noise on-off intermittency can observed in the

form of oscillations [20*]. This means that for the same external action the system is sometimes in the state "on" (the amplitude is large), which is intermittent with the state "off" (the amplitude is rather small). The additive noise influences the effect of on-off intermittency in the following way. For supercritical values of the multiplicative noise intensity on-off intermittency is now hidden and not observable in the form of oscillations, but can be detected for subcritical values, below a threshold (see Fig.1.2 b). Hence in the presence of additive noise on-off intermittency, a sign of noise-induced transition, can be observed even before this transition occurs with respect to the increase of the control parameter.

It is necessary to note that in the same system chaotic oscillations can be observed, if the external parametric action is periodic. A comparison with this case is discussed in [25*]. Chaotic pendulum's oscillations are very similar in its form to noise-induced oscillations. However, a calculation of the probability distribution of the average amplitude squared allows to distinguish between both cases of the external action by means of the Rytov-Dimentberg criterion [25*].

As is shown by further examples, this effect of transition smoothing and influence on on-off intermittency is not a single effect of additive noise in oscillatory systems.

1.2 Stabilization of noise-induced oscillations performed by additive noise

In this section we study again a system under the action of noise, which has both additive and multiplicative components. The aim now is to show that, in contrast to a pendulum, here additive noise can have also another form of influence, namely, stabilize noise-induced oscillations. To demonstrate this effect, we use a standard epidemiological model for the dynamics of children diseases [37]. Two variants of excitation are possible, either by periodic force [143, 43] or by noise [24*]. In both cases this system exhibits chaotic or noise-induced oscillations which closely resemble oscillations observed in experimental data.

We analyze the influence of additive component of noise in the following model system [24*]:

$$
\begin{aligned}
\dot{S} &= e(1-S) - bSI, \dot{E} = bSI - (e+l)E, \\
\dot{I} &= lE - (e+g)I
\end{aligned}
\tag{1.22}
$$

where S, E, and I denote the number of susceptible, exposed but not yet infected, and invective children, respectively. An independent equation for the variable R, which denotes the number of recovered children, can be added to this system of equations: $\dot{R} = gI - mR$. Mutual relations between the components, involved in the model, are illustrated schematically by Fig.1.4.
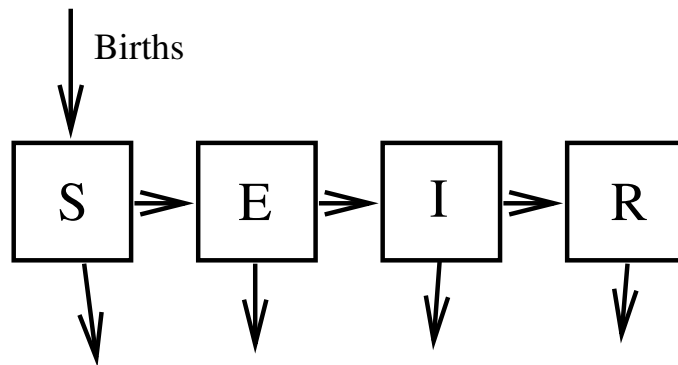
Figure 1.4: Diagram illustrating mutual relations between different components in the model of childhood epidemics

The parameters $1/e$, $1/l$, $1/g$ are the average expectancy, latency and infection periods of time. The contact rate b is the parameter of excitation and equal to $b = b_0(1 + b_1\xi(t))$ where $\xi(t)$ is a harmonic noise with the peak of spectral density at the circle frequency 2π (seasonal noisy oscillations with a period equal to one year) and the parameter b_1 is the amplitude of noise. The excited oscillations are executed in the vicinity of the stable singular point with

Figure 1.5: (a) Noise-induced oscillations (epidemics)in the epidemiological model Eqs.(1.24).
(b) The dependence of oscillation variance for the variable x on the parameter b_1, which is
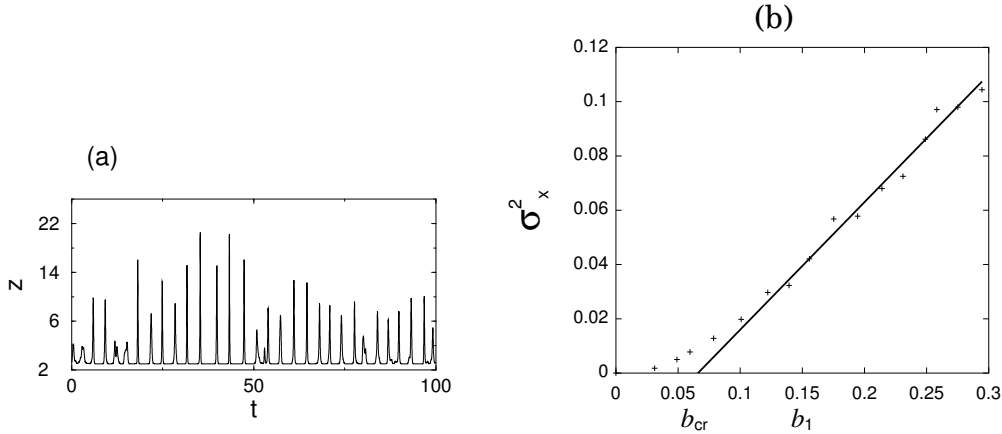responsible for the noisy variation of a contact rate (see the text).

the coordinates (S_0, E_0, I_0):

$$S_0 = \frac{(m+a)(m+g)}{ab_0}, \quad E_0 = \frac{m}{m+a} - \frac{m(m+g)}{ab_0}, \quad I_0 = \frac{am}{(m+a)(m+g)} - \frac{m}{b_0} \qquad (1.23)$$

Hence, one can easily rewrite the equations for the new variables $x = S/S_0 - 1$, $y = E/E_0 - 1$,
and $z = I/I_0 - 1$ which are deviations from the equilibrium point:

$$
\begin{aligned}
\dot{x} + ex &= -b_0 I_0 (1 + b_1 \xi(t))(x + z + xz) - b_0 b_1 I_0 \xi(t), \\
\dot{y} + (e+l)y &= (e+l)(1 + b_1 \xi(t))(x + z + xz) + (e+l)b_1 \xi(t), \\
\dot{z} + (e+g)z &= (e+g)y.
\end{aligned}
\qquad (1.24)
$$

This form of eqs. clearly shows that the action of noise is multiplicative as well as additive.

An increase of the noise intensity causes noise-induced oscillations of the variables S, I, E
(Fig. 1.6 (a)). Their oscillatory behaviour closely resembles observed epidemiological data
(compare Fig. 1.6 (a) with figures in [157]). These oscillations are excited after a noise-induced
transition (see Fig. 1.6 (b)). There the variance of oscillations together with an approximating
straight line is shown. The point where the straight line crosses the abscissa-axis can be
taken as a critical point of the transition. To prove this, we remove artificially the additive
component of noise from eqs.(1.24). In this case the variance of oscillations is equal to zero
if $b_1 < b_{1cr}$ and goes to infinity shortly after the noise intensity exceeds its critical value.
So, multiplicative noise indeed induces a transition. What is even more interesting, if the
additive and multiplicative components of noise act together, as in the model, a stabilization
of noise-induced oscillations occurs: in this case the dependence of the variance on the noise
intensity does not increase to infinity, that is not a case if multiplicative component of noise
acts separately.

Noteworthy, the same model can demonstrate deterministic chaotic oscillations, which are
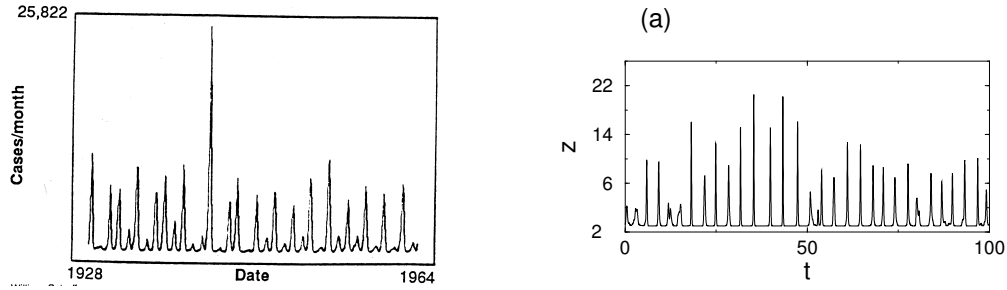
Figure 1.6: Left: experimentally measured epidemics[157], Right: chaotic solution of the model with periodically varied contact rate [24*].

very irregular, and closely resembles in its form both to experimental data [157] and to noise-induced oscillations [24*]. Hence, the problem arises whether we can distinguish the nature of oscillations if we analyze time series. These noise-induced and chaotic oscillations can be distinguished by use of the Rytov-Dimentberg criterion, initially proposed in [171, 38] to solve the problem of distinguishing between noise passed through a linear narrow-band filter and periodic but noisy self-oscillations. According to this criterion, the probability distributions for the process itself and for the instantaneous amplitude squared are monotonic in the case of noise-induced oscillations, whereas for chaotic oscillations these distributions have to have peaks [24*,25*]. The instantaneous amplitude can be calculated by means of the Hilbert transform [167].

1.3 Phase transitions induced by additive noise

1.3.1 Second-order phase transitions. Noise-induced pattern formation

Now we extend our study to spatially extended systems and show that additive noise is able to induce second- and first-order phase transitions. We start with an investigation of a nonlinear lattice of overdamped coupled stochastic oscillators [146][18*] under the action of noise. In this system a transition manifests itself in the formation of spatially ordered patterns, as a consequence of a special form of coupling *a la* Swift-Hohenberg. The system is described by a scalar field $x_{\mathbf{r}}$, defined on a spatial lattice with points $\mathbf{r}$:

$$\dot{x}_{\mathbf{r}} = f(x_{\mathbf{r}}) + g(x_{\mathbf{r}})\xi_{\mathbf{r}} + \mathcal{L}x_{\mathbf{r}} + \zeta_{\mathbf{r}} \qquad (1.25)$$

with f and g taken in the form (for the discussion, which functions can be chosen to observe a transition see [172])

$$f(x) = -x(1 + x^2)^2 \quad g(x) = a^2 + x^2 \qquad (1.26)$$

and $\xi_{\mathbf{r}}$, $\zeta_{\mathbf{r}}$ are independent zero-mean-value Gaussian white noises:

$$\langle \xi_{\mathbf{r}}(t)\xi_{\mathbf{r}'}(t') \rangle = \sigma_m^2 \delta_{\mathbf{r},\mathbf{r}'}\delta(t - t') \qquad (1.27)$$
$$\langle \zeta_{\mathbf{r}}(t)\zeta_{\mathbf{r}'}(t') \rangle = \sigma_a^2 \delta_{\mathbf{r},\mathbf{r}'}\delta(t - t').$$

Note that for these functions $f(x)$ and $g(x)$ the transitions described are *pure* noise-induced phase transitions, in the sense that they do not exist in the system without noise. The coupling operator $\mathcal{L}$ is a discretized version of the Swift-Hohenberg coupling term $-D(q_0^2 + \nabla^2)^2$ [18*].

To study the influence of the additive noise, we consider two limiting cases of correlation between additive and multiplicative noise : strong correlation ($\zeta_{\mathbf{r}} = 0$ and parameter a is varied), and no correlation ($a = 0$ and the intensity of $\zeta_{\mathbf{r}}$ is varied).

Using the generalized Weiss mean field theory (MFT) [65], the conditions of phase transition can be found. Substituting the value of the scalar variable $x_{\mathbf{r}'}$ at the sites coupled to $x_{\mathbf{r}}$ by its special average:

$$\langle x_{\mathbf{r}'} \rangle = \langle x \rangle \cos[\mathbf{k} \cdot (\mathbf{r} - \mathbf{r}')], \qquad (1.28)$$

we obtain for $x = x_{\mathbf{r}}$

$$\dot{x} = f(x) + g(x)\xi(t) + D\omega(\mathbf{k})x - D_{\text{eff}}(x - \langle x \rangle) + \zeta(t), \qquad (1.29)$$

where

$$D_{\text{eff}} = \left[\left(\frac{2d}{\Delta^2} - q_0^2\right)^2 + \frac{2d}{\Delta^2} + \omega(\mathbf{k})\right]D \qquad (1.30)$$
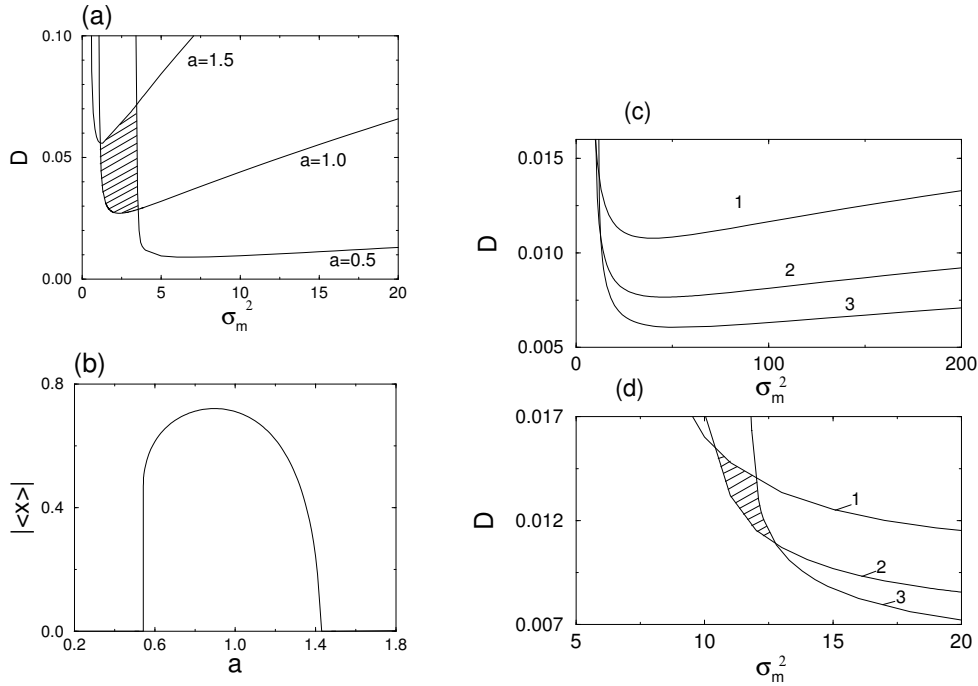
Figure 1.7: Additive noise induced phase transition in a nonlinear lattice Eqs.(1.25): predictions of the mean field theory. (a) The boundaries of the transition on the plane (σ_m^2, D) for different values of a Eqs.(1.26). It is clearly seen that by variation of a a point from the dashed region is a point of the transition induced by additive noise. (b) Dependence of order parameter $|\langle x \rangle|$ if the additive noise intensity is varied. (c) The transition lines for the case when additive and multiplicative noise are independent: $\sigma_a^2 = 1$ (label 1), 0.5 (label 2), and 0.3 (label 3). (d) Large scaled region from the plot in (c).

and a dispersion relation $\omega(\mathbf{k}) = 0$ for the most unstable mode, which is only of interest here [146].

Now the value $\langle x \rangle$ plays the role of the amplitude of the spatial patterns with an effective diffusion coefficient D_{eff}. The steady state solution of the Fokker-Planck equation corresponding to Eq.(1.28) is written then as follows

$$w_{st}(x) = \frac{C(\langle x \rangle)}{\sqrt{\sigma_m^2 g^2(x) + \sigma_a^2}} \exp\left(2 \int_0^x \frac{f(y) - D_{\text{eff}}(y - \langle x \rangle)}{\sigma_m^2 g^2(y) + \sigma_a^2} \, dy \right), \tag{1.31}$$

and $C(\langle x \rangle)$ is the normalization constant.

For the mean field value $\langle x \rangle$ we obtain [208]

$$\langle x \rangle = \int x w_{st}(x, \langle x \rangle) dx. \tag{1.32}$$

Solving eq.(1.32) with parameters D, σ_m^2, and σ_a^2, we obtain a boundary between two phases: a disordered ($|\langle x \rangle| = 0$) and an ordered one ($|\langle x \rangle| \neq 0$). The ordered phase corresponds to the appearance of spatially ordered patterns, because its average amplitude be-

30
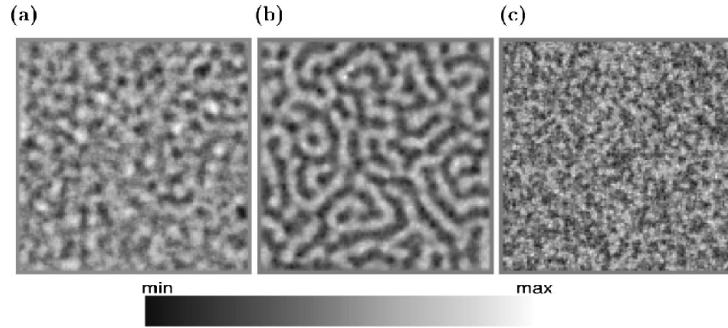
Figure 1.8: Snapshots of the field for $D = 1.0$, $\sigma_m^2 = 1.8$, and $\sigma_a^2 = 0$. The parameter a is equal to (a) 0.1, (b) 1.0, and (c) 10.0. The increase of additive noise induces spatial patterns.
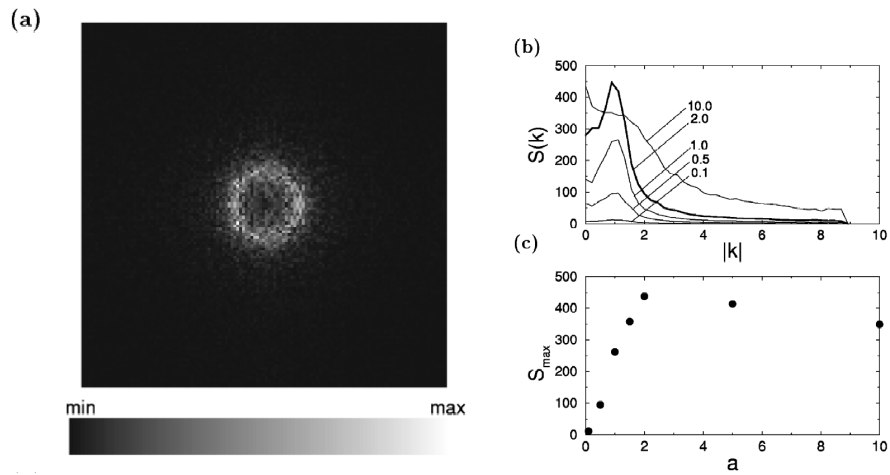
Figure 1.9: (a)2D Fourier transform of the pattern shown in the previous Fig. Rotationally symmetry is observed. (max,min) values are (1337,0.1). (b) Fourier transform averaged over angles for D=1.0 and $\sigma_m^2 = 1.8$. values of parameter a are shown in the figure. (c) Dependence of $S_{\max}$ on a

31
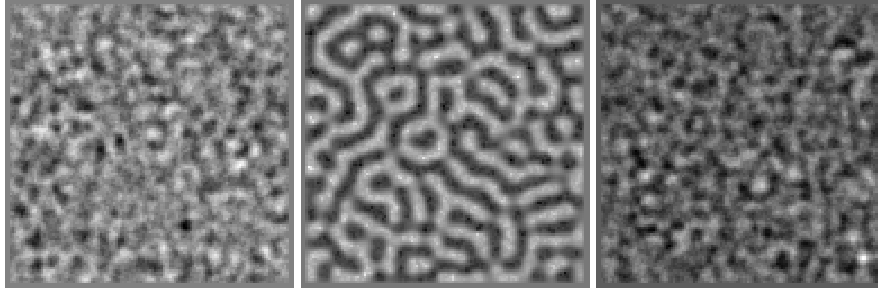
Figure 1.10: A formation of spatial patterns induced by additive noise. From left to right
the intensity of additive noise is increased ($a = 0$): $\sigma_a^2 = 0.001$, 0.7 and 10 (from left to right).
The field in the nonlinear lattice of 128x128 elements is coded from white (minimum) to black
(maximum) colours.

comes nonzero. This happens due to the special form of coupling which includes wave length
of these patterns q_0. It is known that in the considered system multiplicative noise induces a
phase transition [146]. We focus our attention to the influence of additive noise. The bound-
ary of the phase transition on the plane (σ_m^2, D) is shown in Fig. 1.7 (a), which demonstrates
that variation of the intensity of correlated additive noise (the parameter a in Eq.(1.26))
causes a shift of the transition boundary. The most interesting situation occurs in the dashed
region. Here, the increase of the additive noise intensity causes the reentrant (disorder-
order-disorder) phase transition. The corresponding dependence of the order parameter on
the parameter a is shown in Fig. 1.7 (b). Hence changing additive noise can lead to the for-
mation of spatially ordered patterns (Fig. 1.8). The pattern, which corresponds to the ordered
case, has rotational symmetry, which can be clearly observed in the two-dimensional Fourier
transform of the field, represented in Fig.1.9. To make a transition more evident we have
plotted the Fourier transform of the field averaged over the angles of the wave vector. It is
shown in the Fig. 1.8 for different values of a. With increase of a a maximum in this structure
function is found.

For the case of uncorrelated additive noise ($a = 0$), the observed behaviour is qualitatively
the same (Fig. 1.7 (c,d)). Here the transition lines are plotted on the plane (σ_m^2, D) and the
intensity σ_a^2 of uncorrelated additive noise is varied. It is evident that again dashed region
corresponds to the phase transition. If we take parameters from this dashed region (in both
cases of correlation), and change the intensity of additive noise (varying the parameter a or
σ_a^2) we observe a formation of patterns and further their destroying (see results of numerical
simulations in Fig. 1.10).

To understand the mechanism behind this transition, it is necessary to note that there
is no bistability either in the "usual" potential or in the so-called "stochastic" potential [81].
Nevertheless, using some approximations it can be shown [196][18*] that the short-time evo-
lution of the mean field can be described by the "effective" potential, which becomes to be
bistable after a transition. If D, and σ_a^2 vanish, the time evolution of the first moment of a
single element is simply given by the drift part in the corresponding Fokker-Planck equation
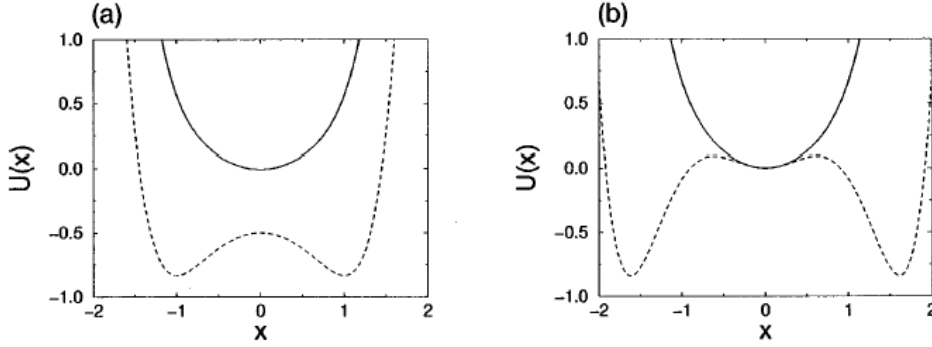
Figure 1.11: An "effective" potential for the short time evolution of the mean field. (a) $\sigma_m^2 = 2$: solid line, $a^2 = 0.1$; dashed line, $a^2 = 1.0$. (b) a=0: solid line, $\sigma_m^2 = 2$; dashed line, $\sigma_m^2 = 5$. In case (a) the short time behaviour can be described by the bistable potential if the constant a is sufficiently large. In case (b) the situation is more complicated: the zero state remains stable, but large enough additive noise can force a system to leave the zero state and form a mean field.

(Stratonovich case)

$$\langle \dot{x} \rangle = \langle f(x) \rangle + \frac{\sigma_m^2}{2} \langle g(x) g'(x) \rangle. \tag{1.33}$$

As it was argued in [196], the mechanism of the noise-induced transition in coupled systems can be explained by means of a short time evolution approximation [2]. It means that we start with an initial Dirac δ function, follow it only for a short time, such that fluctuations are small and the probability density is well approximated by a Gaussian. A suppression of fluctuations, performed by coupling, makes this approximation appropriate in our case[193]. The equation for the maximum of the probability, which is also the average value in this approximation $\bar{x} = \langle x \rangle$, takes the following form

$$\dot{\bar{x}} = f(\bar{x}) + \frac{\sigma_m^2}{2} g(\bar{x}) g'(\bar{x}), \tag{1.34}$$

which is valid if $f(\langle x \rangle) >> \langle \delta x^2 \rangle f''(\langle x \rangle)$. For this dynamics an "effective" potential $U_{\text{eff}}(x)$ can be derived, which has the form

$$U_{\text{eff}}(x) = U_0(x) + U_{\text{noise}} = - \int f(x) dx - \frac{\sigma_m^2 g^2(x)}{4}, \tag{1.35}$$

where $U_0(x)$ is a monostable potential and U_{noise} represents the influence of the multiplicative noise. In the ordered region, this "effective" potential has additional to $x = 0$ minima, that explain the non-zero solutions for the amplitude of spatial patterns [18*] (see Fig. 1.11).

Here I have considered a second-order phase transition induced by additive noise in a spatially extended system. Due to the special form of coupling, the phase transition manifested itself in the formation of ordered spatial patterns. In what follows, I will demonstrate that additive noise can also induce *first-order* phase transition in such systems.

1.3.2 First-order phase transitions.

In [136] a first-order phase transition has been reported, which is induced by multiplicative noise. Now we show that *first-order* nonequilibrium transitions in spatially extended systems can be also induced by additive noise. It is important, that in contrast to second-order transitions, in a first-order transition very tiny fluctuation of the control parameter can lead to a drastical change of the order parameter. The study is performed on a nonlinear lattice of coupled stochastic overdamped oscillators introduced in [195] and further studied in [196, 119][18*,19*]. The time evolution of the system is described by the following set of Langevin equations:

$$\dot{x}_i = f(x_i) + g(x_i)\xi_i(t) + \frac{D}{2d}\sum_j (x_j - x_i) + \zeta_i(t), \tag{1.36}$$

where $x_i(t)$ represents the state of the i-th oscillator, and the sum runs over all nearest neighbors of cell i. The strength of the coupling is measured by D, and d is the dimension of the lattice, which has $N = L^d$ elements. The noise terms $\xi_i(t)$ and $\zeta_i(t)$ are the same as defined in Eqs. (1.27): mutually uncorrelated, gaussianly distributed, with zero mean and white in both space and time. The functions $f(x)$ and $g(x)$ are defined in Eqs.(1.26).

We study the behaviour of this system by means of a standard MFT procedure. Solving the corresponding Eq.(1.32) with respect to the variable $m = \langle x \rangle$, and w_{st} defined by Eq.(1.31) with $D_{eff} = D$, one can set the transition boundaries. In this way obtained order-disorder transition lines are shown in Fig. 1.12 (a). Here we consider only the case when $\sigma_a^2 = 0$ and the parameter a is varied. Curve 1 separates regions of disorder (below the curve) and order (above the curve) for small multiplicative noise intensity. In this case, the ordered region is characterized by three self-consistent solutions of Eq. (1.32), one of them unstable ($m = 0$) and the other two stable and symmetrical. These new solutions appear continuously from $m = 0$ in the course of the transition. Hence, if we fix the coupling strength e.g. $D = 20$, and increase the intensity of additive noise (the parameter a) a *second-order* phase transition from disorder to order occurs, followed by a reentrant transition back to disorder, also of second order.

The *first-order* transition can be observed when the multiplicative noise intensity increases. In that case (curve 2 in Fig. 1.12 (a)), a region appears where Eq. (1.32) has five roots, three of which ($m = 0$ and two symmetrical points) are stable. This region is marked dashed in the figure. Thus, for large enough values of D, a region of coexistence appears in the transition between order and disorder. This region is limited by discontinuous transition lines between $m = 0$ and a nonzero, finite value of m. Hence, additive noise is seen to induce a *first-order* phase transition in this system for large enough values of the coupling strength and multiplicative noise intensity. The reentrant transition is again of second order. When the first-order phase transition appears, hysteresis can be expected to occur in the coexistence region (if a certain algorithm is applied [3]). The dependence of the order parameter m on the control parameter a as predicted by MFT is shown in Fig. 1.12 (b) with a solid line. The region of possible hysteresis is bounded by dotted lines.

In order to contrast the analytical results, we have performed simulations of the complete model (1.36) using the numerical methods described in [65, 196]. The order parameter m_n is computed as $m_n = \left\langle \left| \frac{1}{L^2} \sum_{i=1}^{N} x_i \right| \right\rangle$, where $\langle \rangle$ denotes time average. Results for a two-dimensional
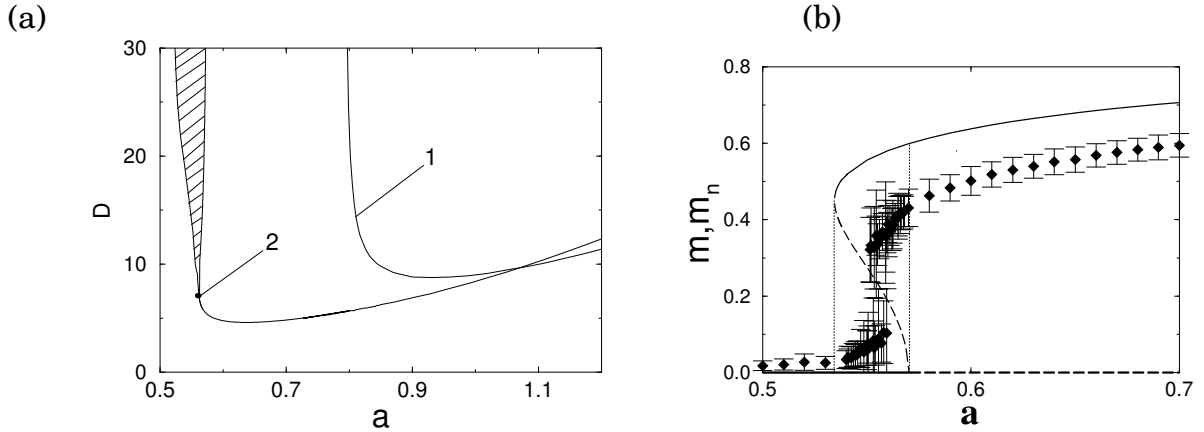
(a)

(b)

Figure 1.12: Characteristics on the phase transition in the nonlinear lattice Eqs.(1.36): (a) Transition lines on the plane (a, D) for $\sigma_a = 0$ and two different intensities of the multiplicative noise (curve 1: $\sigma_m^2 = 1.6$; curve 2: $\sigma_m^2 = 3.0$). The dashed region (starting with the dot) corresponds to the coexistence of disordered and ordered phase. (b) The corresponding dependence of the order parameters m, m_n on a for $D = 20$, $\sigma_m^2 = 3.0$ and $\sigma_a^2 = 0.0$ are plotted by solid line (MFT predictions) and by diamonds (numerical simulations). The dotted line delimits the coexistence region exhibited by MFT (a region of the hysteresis effect). The unstable state is plotted by the dashed line.
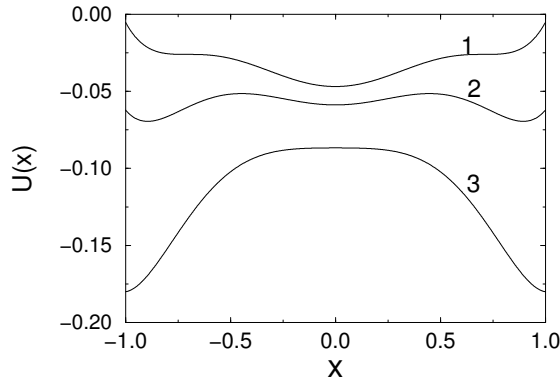
Figure 1.13: An "effective" potential for the short-time evolution of m in the lattice Eqs(1.36),for $a^2 =$: 0.25 (curve 1), 0.28 (curve 2), and 0.34 (curve 3). Other parameters are $\sigma_m^2 = 3.0$ and $\sigma_a^2 = 0.0$. A coexistence of ordered and disordered phases is observed for the curve 2.

lattice with lateral size $L = 32$ are shown with diamonds in Fig. 1.12 (b). Analyzing this figure one can observe that MFT overestimates the size of the coexistence region. This effect, analogous to what was observed for multiplicative-noise induced transitions [195], can be explained in terms of an "effective potential" derived for the system at short times (see discussion below). For instance, as a increases the system leaves the disordered phase not when this state becomes unstable but earlier, when the potential minima corresponding to the ordered states

36

become much lower than the minimum corresponding to the state $m = 0$. It should also be mentioned that the numerical simulations did not show hysteresis, because in the coexistence region the system occupied any of the three possible states, independently of the initial conditions. It can be explained by the small size of the simulated system, which permits jumps between steady states when the system is sufficiently perturbed (*e.g.* by slightly changing the parameter a).

We have thus seen so far that numerical simulations qualitatively confirm the existence of a first-order phase transition induced by additive noise in this system, as predicted by MFT. We note that the transition occurs in the two limiting cases of correlation between multiplicative and additive noise. We also emphasize that variation of both the multiplicative noise intensity and the coupling strength can change the order of this transition.

Let us now discuss a possible mechanism behind this effect. As pointed above, the collective behaviour of this system can be described by the "effective" potential (see Eq.(1.35)). We can trace the behavior of this potential in the presence of multiplicative noise, for the case $\sigma_a^2 = 0$ and $a \neq 0$. Its evolution for increasing a is shown in Fig. 1.13. This approach can be clearly seen to successfully explain the mechanism of the first-order transition: first, only the zero state is stable (curve 1), then there is a region where three stable states coexist (curve 2), and finally, the disordered state becomes unstable (curve 3). This approach also explains why a variation of the multiplicative noise intensity influences the order of the transition: for another (lower) σ_m^2 there is no region where ordered and disordered phases simultaneously exist. We emphasize that the "effective" potential is derived only for short-time evolution, and should not be confused with the "stochastic" potential [81], which for this system remains always monostable. For the other case of correlation between multiplicative and additive noise, in the region of additive noise induced transition, the "effective" potential always has three minima (two symmetric minima are lower than the central one). Sufficiently large (above a threshold of the transition) additive noise causes an escape from zero state and leads to the transition. The value of a critical additive noise intensity for this transition can be estimated by the "effective" potential approach, only by MFT. Here we have considered only a case of strong correlation between multiplicative and additive noise. As described in [12*], if additive noise is independent, it can also induce a first-order phase transition. The level of correlation between additive and multiplicative noise can be considered as an additional parameter in this system, what we leave as an open question here.

Chapter 2

Doubly stochastic effects

In what follows, I consider a concept of doubly stochastic effects and application of this concept to several basic noise-induced phenomena. In this chapter two doubly stochastic effects are demonstrated: doubly stochastic resonance and doubly stochastic coherence. This is the result of application of the concept of doubly stochastic effects to the effect of stochastic resonance and of coherence resonance. In both these effects we are interested in the behavior of the system output as a whole. In contrast to it, in propagation effects, it is not the response of the system as a whole, but the propagation of a signal that is studied. Concerning the propagation, doubly stochastic effect can also be found: this effect, called noise-induced propagation in monostable media will be considered in Chapter 3, together with other new effects of propagation.

2.1 Doubly stochastic resonance

Doubly stochastic resonance is at the borderline of two basic noise-induced phenomena. The first class of phenomena is noise-induced phase transitions. The second basic phenomenon is stochastic resonance. SR has been found and investigated in a large variety of different class of systems (see Introduction). However, SR has not been considered in systems with a noise-induced structure [4]. Here a new type of SR is presented in a system with a noise-induced nonequilibrium phase transition resulting in a bistable behaviour of the mean field. This effect is called *doubly stochastic resonance* (DSR) to emphasize that additive noise causes a resonance-like behaviour in the structure, which in its own turn is induced by multiplicative noise.

This DSR is demonstrated on a nonlinear lattice of coupled overdamped oscillators firstly introduced in [195] and further studied in [196, 119][18*,19*]. The following set of Langevin equations describes the considered system:

$$\dot{x}_i = f(x_i) + g(x_i)\xi_i(t) + \frac{D}{2d}\sum_j(x_j - x_i) + \zeta_i(t) + A\cos(\omega t + \varphi), \tag{2.1}$$

where $x_i(t)$ represents the state of the ith oscillator, $i = 1,...,L^d$, in the cubic lattice of the size L in d dimensions and with $N = L^d$ elements. The sum runs over $2d$ nearest neighbors of the ith cell, and the strength of the coupling is measured by D. The noisy terms $\xi_i(t)$ and $\zeta_i(t)$ represent mutually uncorrelated Gaussian noise, with zero mean and uncorrelated both in space and time

$$\langle\xi_i(t)\xi_j(t')\rangle = \sigma_m^2\delta_{i,j}\delta(t - t'), \tag{2.2}$$

$$\langle\zeta_i(t)\zeta_j(t')\rangle = \sigma_a^2\delta_{i,j}\delta(t - t'). \tag{2.3}$$

The last item in (2.1) stands for an external periodic force with amplitude A, frequency ω and initial phase φ.

For the sake of simplicity, the functions $f(x)$ and $g(x)$ are taken to be of the form [195]:

$$f(x) = -x(1 + x^2)^2, \quad g(x) = 1 + x^2. \tag{2.4}$$

In the absence of external force ($A = 0$) this model can be solved analytically by means of a standard mean-field theory (MFT) procedure [65]. The mean-field approximation consists in replacing the nearest-neighbor interaction by a global term in the Fokker-Planck equation corresponding to (2.1). In this way, one obtains the following steady-state probability distribution w_{st}:

$$w_{\text{st}}(x,m) = \frac{C(m)}{\sqrt{\sigma_m^2 g^2(x) + \sigma_a^2}} \exp\left(2\int_0^x \frac{f(y) - D(y - m)}{\sigma_m^2 g^2(y) + \sigma_a^2}\,dy\right), \tag{2.5}$$

where $C(m)$ is a normalization constant and m is a mean field, defined by the equation:
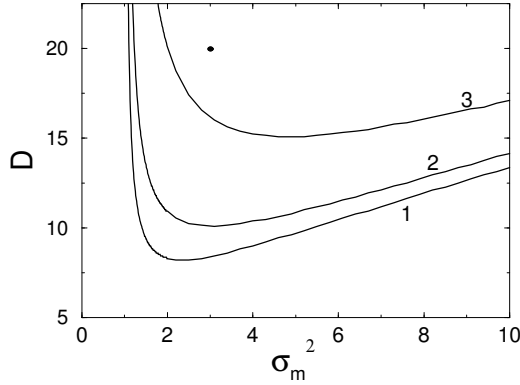
Figure 2.1: Transition lines between ordered and disordered phase on the plane $(\sigma_m^2; D)$ for different intensities of the additive noise $\sigma_a^2 = 0$ (1); 1 (2), and 5 (3). The black point corresponds to $D = 20$, $\sigma_m^2 = 3$.

$$m = \int_{-\infty}^{\infty} x w_{\mathrm{st}}(x, m) dx. \tag{2.6}$$

Solving Eq. (3.4) self-consistently with respect to the variable m one determines transitions between ordered ($m \neq 0$) and disordered ($m = 0$) phases. Transition boundaries between different phases are shown in Fig. 2.1 and the corresponding dependence of the order parameter on σ_m^2 is presented in Fig. 2.3. In addition to [195], we show influence of additive noise resulted in the shift of transition lines. For $\sigma_a^2 = 0$ an increase of the multiplicative noise causes a disorder-order phase transition, which is followed by the reentrant transition to disorder [195]. In the ordered phase the system occupy one of two symmetric possible states with the mean fields $m_1 = -m_2 \neq 0$, depending on initial conditions (for a visualization of this transition see Fig. 2.2).

Now let us turn to the problem, how the system (1) responses to periodic forcing ($A_i = A$). We have taken a set of parameters $(\sigma_m^2; D)$ within the region of two coexisting ordered states with nonzero mean field. In particular, we choose values given by the dot in Fig. 2.1. As for the network, we take a two-dimensional lattice of $L^2 = 18 \times 18$ oscillators, which is simulated numerically [97] with a time step $\Delta t = 2.5 \times 10^{-4}$ under the action of the harmonic external force. The amplitude of the force A has to be set sufficiently small to avoid hops in the absence of additive noise during the simulation time of a single run which is much larger than the period of the harmonic force [5]. Jumps between $m_1 \leftrightarrow m_2$ occur only if additive noise is additionally switched on. Runs are averaged over different initial phases.

Time series of the mean field and the corresponding periodic input signal are plotted in Fig. 2.4 for three different values of σ_a^2. The current mean field is calculated as $m(t) = \frac{1}{L^2} \sum_{i=1}^{N} x_i(t)$. For a small intensity of the additive noise, hops between the two symmetric states m_1 and m_2 are rather seldom and not synchronized to the external force. If we increase the intensity σ_a^2, we achieve a situation when hops occur with the same periodicity as the external force and, hence, the mean field follows with high probability the input force. An increase of additive
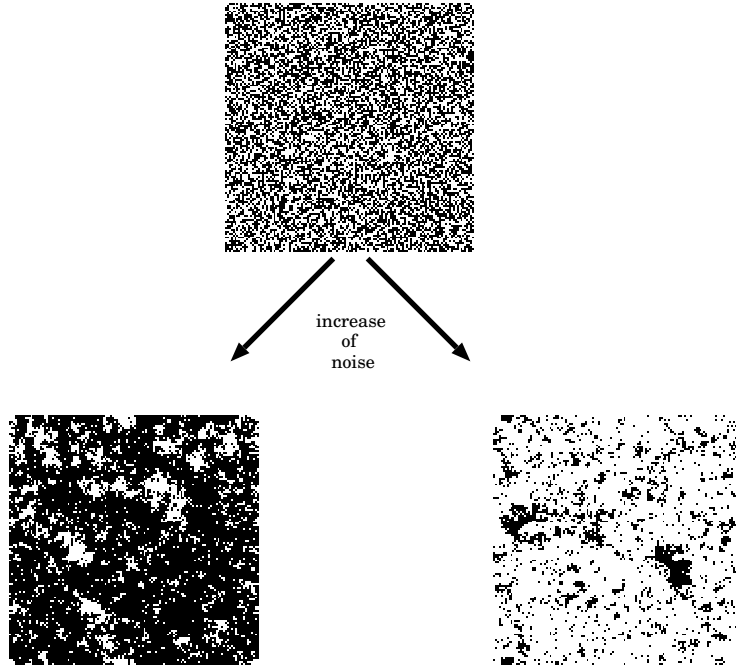
Figure 2.2: A symbolic visualization of a phase transition in the model Eqs.(2.1), which leads to the formation of a mean field. In the disordered phase the mean field is zero due to the random deviation of different elements around zero (up). In the ordered phase, induced by noise, the symmetry is broken and the mean field is either positive (right) or negative (left). The elements in the lattice 128×128 are coded in accordance to its sign: if positive or zero - white, if negative - black.

noise provides an optimization of the output of the system which is stochastic resonance. If σ_a^2 is increased further, the order is again destroyed, and hops occur much more frequently than the period of the external force. Note also that for large σ_a^2 the value of the mean field which corresponds to the stable state is becoming smaller. It is caused by the fact that additive noise influences also transition lines [18*,19*][119]. An increase of σ_a^2 results in the reduction of the ordered region (Fig. 2.1, curves 2 and 3) and decreasing the value $m_1 = -m_2$ (Fig. 2.3, curves 2 and 3).

Fig. 2.4 illustrates that additive noise is able to optimize the signal processing in the system (1). In order to characterize this SR-effect we have calculated signal-to-noise ratio (SNR) by the extracting the relevant phase-averaged power spectral density $S(\omega)$ and taking the ratio between its signal part with respect to the noise background [53]. The dependence of SNR on the intensity of the additive noise is shown in the Fig. 2.5 for the mean field (filled points) and the mean field in a 2-state approximation (opaque point). In this 2-states approximation we have replaced $m(t)$ by its sign and put approximately $m(t) = +1$ or $m(t) = -1$, respectively. Both curves exhibit the well known bell shaped dependence on σ_a^2 typically for SR. Since the bimodality of the mean field is a noise-induced effect we call that whole effect *Doubly Stochastic Resonance*. For the given parameters and $A = 0.1$, $\omega = 0.1$ the maximum of the SNRs is approximately located near $\sigma_a^2 \sim 1.8$.

Next we intend to give analytic estimates of the SNR. If A, D, and σ_a^2 vanish, the time
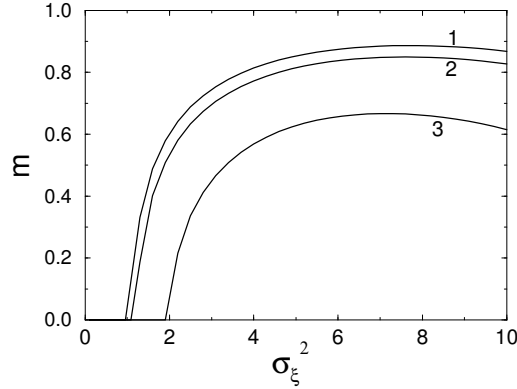
Figure 2.3: The order parameter $|m|$ vs the intensity of multiplicative noise for $D = 20$ and $\sigma_a^2 = 0$ (label 1), 1 (label 2), and 5 (label 3). Inside the ordered region for fixed value of σ_m^2 an increase of the additive noise intensity leads to the decrease of the order parameter.

evolution of the first moment of a single element is given simply by the drift part in the corresponding Fokker-Planck equation (Stratonovich case)

$$\langle \dot{x} \rangle = \langle f(x) \rangle + \frac{\sigma_m^2}{2} \langle g(x)g'(x) \rangle. \tag{2.7}$$

As it was argued in [196], the mechanism of the noise-induced transition in coupled systems can be explained by means of a short time evolution approximation [2]. It means that we start with an initial Dirac δ function, follow it only for a short time, such that fluctuations are small and the probability density is well approximated by a Gaussian. A suppression of fluctuations, performed by coupling, makes this approximation appropriate in our case[193]. The equation for the maximum of the probability, which is also the average value in this approximation $\bar{x} = \langle x \rangle$, takes the following form

$$\dot{\bar{x}} = f(\bar{x}) + \frac{\sigma_m^2}{2} g(\bar{x})g'(\bar{x}), \tag{2.8}$$

which is valid if $f(\langle x \rangle) >> \langle \delta x^2 \rangle f''(\langle x \rangle)$. For this dynamics an "effective" potential $U_{\text{eff}}(x)$ can be derived, which has the form where $U_0(x)$ is a monostable potential and U_{noise} represents the influence of the multiplicative noise. In the ordered region, inside the transition lines (Fig. 2.1), the potential $U_{\text{eff}}(x)$ is of the double-well form, e.g. $U(x)_{\text{eff}} = -x^2 - 0.25x^4 + x^6/6$, for given $f(x)$, $g(x)$ and $\sigma_m^2 = 3$.

Now we consider a conventional SR problem in this potential with an external periodic force of the amplitude A and the frequency ω. If we neglect intrawell dynamics and follow linear response theory the SNR is well known [53, 124, 141, 6]

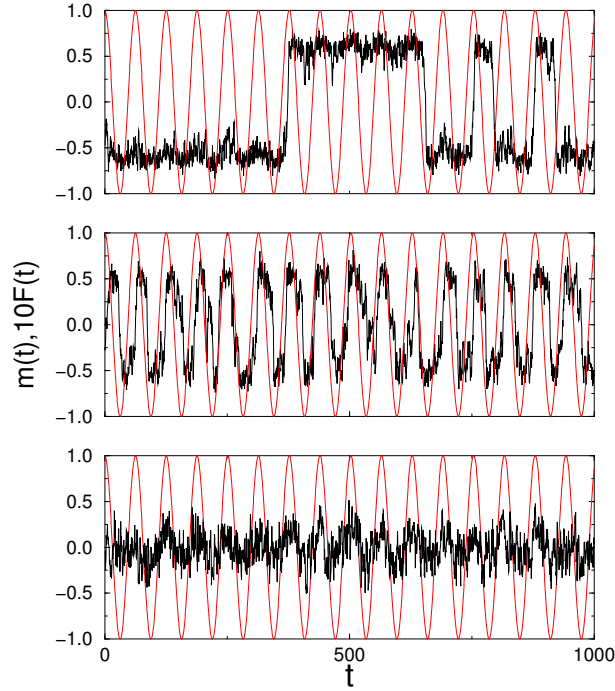$$SNR_1 = \frac{4\pi A^2}{\sigma_a^4} r_k \tag{2.9}$$

46

Figure 2.4: Example of input/output synchronization. The time evolution of the current mean field (output) and the periodic external force $F(t)$ (input) for different intensities of additive noise (from top to bottom) $\sigma_a^2 = 0.01$, 1.05, and 5.0. If the intensity of the additive noise is close to their optimal value (middle row), hops occur with the period of the external force. The remaining parameters are: $A = 0.1$, $\omega = 0.1$, $D = 20$, and $\sigma_m^2 = 3$.

where r_k is the corresponding Kramers rate [99]

$$r_k = \frac{\sqrt{(U''_{\text{eff}}(x)|_{x=x_{\min}} |U''_{\text{eff}}(x)|_{x=x_{\max}})}}{2\pi} \exp\left(-\frac{2\Delta U_{\text{eff}}}{\sigma_a^2}\right) \qquad (2.10)$$

for surmounting the potential barrier ΔU_{eff}. Using Eqs.(4.6),(2.19), and (2.20) we get an analytical estimates for a single element inside the lattice. Further on, rescaling this value by the number N of oscillators in the lattice [175] and taking into account the processing gain G and the bandwidth Δ in the power spectral density [124, 141, 6], the SNR_N of the mean field of the network of N elements can be obtained

$$SNR_N = SNR_1 \frac{NG}{\Delta} + 1. \qquad (2.11)$$

This dependence is shown in the Fig. 2.4 by the solid line and demonstrates despite the rough approximation a good agreement with the results of the numerical simulations. Nearly exact agreement is found in the location of the maximum as well as for the quantitative values of the SNR ("scalloping loss" [124, 141, 6] has been avoided in simulations by setting the frequency ω to be centered on one of the bins in the spectrum).
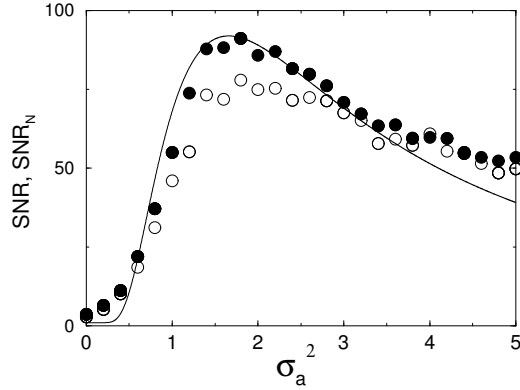
Figure 2.5: The dependence of SNR on the additive noise intensity for the output (filled points) and its 2-states approximation (opaque points). The solid line corresponds to the analytical estimation SNR_{N} (2.21), performed on the base of derivation of the "effective" potential and linear response theory. The parameters are the same as for Fig. 2.4 and the processing gain $G = 0.7$.

$$U_{\mathrm{eff}}(x) = U_0(x) + U_{\mathrm{noise}} = -\int f(x)dx - \frac{\sigma_m^2 g^2(x)}{4}, \qquad (2.12)$$

Some remarks should be added. Firstly, we have considered a system which undergoes a *pure* noise-induced transition, in the sense that a transition is impossible in the absence of noise. This is an important distinction of the DSR effect from SR in any variation of the mean-field model [134]. Secondly, despite the coexistence of the two states in the considered system, the so-called "stochastic" potential [81] for a single oscillator in the lattice (which differs from (4.6)) always remains monostable. Thirdly, there are clear distinctions between SR and DSR behaviour, because, in contrast to SR, in DSR additive noise does not only help an input/output synchronization, but also changes the properties of the system in the absence of the external force (see Fig. 2.1 and 2.3). As a consequence, completely different to standard SR, in DSR amplitude of hops is decreased (bistability dissappears) for large noise intensities σ_a^2 (compare Fig. 2.4 and Fig. 4 from [53]). Finally, not arbitrary system with noise-induced bistability will demonstrate DSR, e.g. we did not find DSR in zero-dimensional systems, which are described in [81].

Noteworthy, noise-induced bistability, described here can be used not only for a synchronization between output and input of the system, but also for other effects, observed in bistable systems. For example, in 4.2 a system size resonance, which occur in spatially distributed system of coupled bistable oscillators, has been also demonstrated for the case of noise-induced bistability.

2.2 A simple electronic circuit model for doubly stochastic resonance

We expect that these theoretical findings resulted from study of DSR will stimulate experimental works to verify DSR in real physical systems (for the first experimental observation of noise-induced bistability see [73]). Appropriate situations can be found in electronic circuits [1], as well as in systems, which demonstrate noise-induced shift of the phase transition, e.g, in: liquid crystals [93, 207], photosensitive chemical reactions [128, 32], or Rayleigh-Bénard convection [127]. It can be crucial for such experiments, that, in contrast to conventional SR, in DSR the energy of noise is used in a more profitable way: not only for the optimization of the signal processing, but also for the support of the potential barrier to provide this optimization.

Here we design an electronic circuit for the observation of DSR. The most direct way is the realization through analog circuits but there are complicated due to the complex construction of every unit, hence it is worth to look for a simpler electronic circuit model which exhibits the DSR property. With this aim we consider an electrical circuit which consists of N coupled elements (i, j). A circuit of one element is shown in Fig. 2.6. Three ingredients in this circuit are important: input current, time-varying resistor (TVR) and a nonlinear resistor. Every element is coupled with its neighbours by the resistor R_c (i.e. by diffusive coupling). The capacitor is shown by C. The nonlinear resistor R_N can be realized with a set of ordinary diodes [86, 28], whose characteristic function is a piecewise-linear function

$$i_N = f_1(V) = \begin{cases} G_b V + (G_a - G_b) B_p & \text{if } V \leq -B_p, \\ G_a V & \text{if } |V| < B_p, \\ G_b V - (G_a - G_b) B_p & \text{if } V \geq B_p, \end{cases} \qquad (2.13)$$

where i_N is the current through the nonlinear resistor(R_N), V is the voltage across the capacitor(C), and parameters G_a, G_b and B_p determine the slopes and the breakpoint of the piecewise-linear characteristic curve. Another way to realize the nonlinear resistor is via a third-order polynomial function:

$$i_N = f_2(V) = g_1 V + g_2 V^3.$$

The next important ingredient is a time-varying resistor(TVR)[142, 28]. The conductance $G(t)$ of TVRs varies with time. Presently, we consider the case that the function which represents the variation of the TVR is a Gaussian $\delta-$correlated in space and time noise, i.e. $G(t) = \xi(t)$, where

$$\langle \xi_i(t) \xi_j(t') \rangle = \sigma_m^2 \delta_{i,j} \delta(t - t').$$

An external action on the circuit is performed by the current input $I(t)$, which is a periodic signal (with amplitude A, frequency ω, and initial phase φ), additively influenced by

49
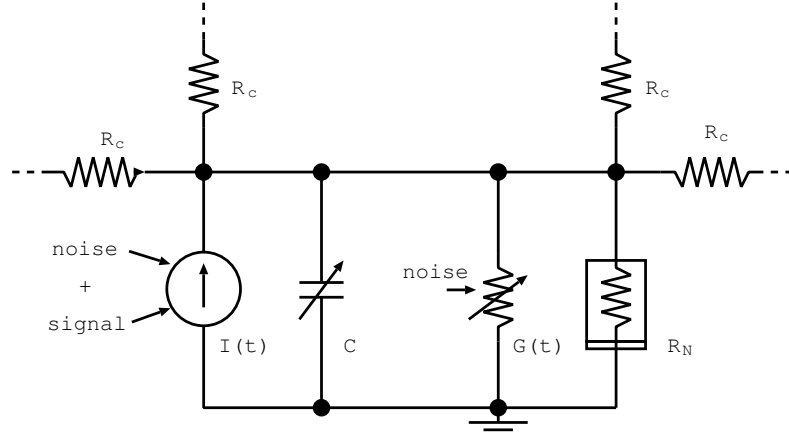
Figure 2.6: The electronic circuit of the element (i, j).

independent Gaussian noise $\zeta(t)$

$$I(t) = \zeta(t) + A\cos(\omega t + \varphi),$$

where

$$\langle \zeta_i(t)\zeta_j(t')\rangle = \sigma_a^2\delta_{i,j}\delta(t - t').$$

The electronic circuit with respect to the element (i, j) can be described by a set of Kirchoff's equations:

$$
\begin{aligned}
C\frac{dV_{i,j}}{dt} &= I(t) - G(t)V_{i,j} - f_{1,2}(V_{i,j}) \\
&+ \frac{1}{R_c}(V_{i+1,j} + V_{i-1,j} + V_{i,j+1} + V_{i,j-1} - 4V_{i,j})
\end{aligned}
\tag{2.14}
$$

Hence, the following set of Langevin equations describes the considered system:

$$
\begin{aligned}
\frac{dV_{i,j}}{dt} &= -f_{1,2}(V_{i,j}) + V_{i,j}\xi_{i,j}(t) \\
&+ \frac{D}{4}(V_{i+1,j} + V_{i-1,j} + V_{i,j+1} + V_{i,j-1} - 4V_{i,j}) \\
&+ \zeta_{i,j}(t) + A\cos(\omega t + \varphi),
\end{aligned}
\tag{2.15}
$$

where C is set to unity by normalization of time and D denotes a strength of coupling equal to $\frac{4}{CR_c}$. In the case when f_2 represents the TVR, the model is the time-dependent Ginzburg-Landau equation, which is a standard model to describe phase transitions and critical phenomena in both equilibrium and nonequilibrium situations [65]. It is important that we consider only the situation when the potential of one element is monostable ($G_a = 0.5$, $G_b = 10$, $B_p = 1$ for f_1, and $g_1 > 0, g_2 = 1$ for f_2), avoiding the possibility to observe SR without multiplicative noise

We are interested in the behaviour of the mean field $m(t) = \frac{1}{N}\sum_{i=1}^{N}\sum_{j=1}^{N}V_{i,j}(t)$ and consider it
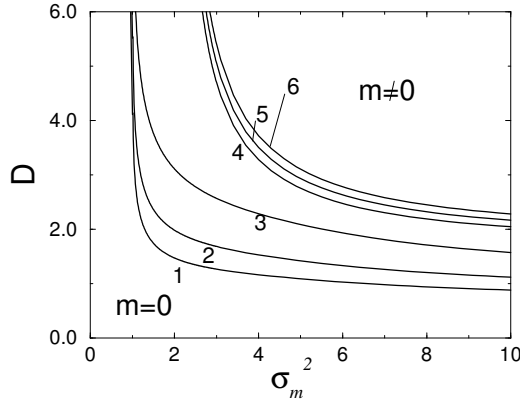
Figure 2.7: Transition lines for the equation with function f_1: $\sigma_a^2 = 0.3$ (label 1), 0.5 (label 2) and 1 (label 3). Also the case with f_2 (the potential of every element is monostable: $g_1 > 0, g_2 = 1$); $g_1 = 1$, $\sigma_a^2 = 0.8$ (label 4), 0.9 (label 5) and 1 (label 6).

as an output and the periodic signal as an input of the whole system. SR behaviour can be expected if the system is bistable for the chosen set of parameters. Regions of bistability can be determined by means of a standard mean-field theory (MFT) procedure [65]. The mean-field approximation consists in replacing the nearest-neighbor interaction by a global term in the Fokker-Planck equation corresponding to (2.15). In this way, we obtain the following steady-state probability distribution w_{st}:

$$
w_{\mathrm{st}}(x,m) =
\frac{C(m)}{\sqrt{\sigma_m^2 g^2(x) + \sigma_a^2}} \exp\left(2 \int\limits_0^x \frac{f_{1,2}(y) - D(y-m)}{\sigma_m^2 g^2(y) + \sigma_a^2} \, dy \right),
\tag{2.16}
$$

where $C(m)$ is a normalization constant and m is a mean field, defined by the equation:

$$
m = \int_{-\infty}^{\infty} x w_{\mathrm{st}}(x,m) dx.
\tag{2.17}
$$

Self-consistent solution of Eq. (3.4) determines the mean field and the transition lines between ordered bistable ($m \neq 0$) and disordered monostable ($m = 0$) phases. Transition boundaries for functions f_1 and f_2 are shown in Fig. 2.7. Note that bistability is impossible without multiplicative noise and without coupling between elements. Since SR effect, described below, appears due to the variation of additive noise, it is also important that a change of the additive noise intensity shifts transition boundaries.

Next we estimate signal-to-ratio (SNR) analytically. Following short-time evolution approximation, first introduced in [196] and further developed in [18*,5*], the dynamics of the mean field is governed by an "effective" potential $U_{\mathrm{eff}}(x)$ which has the form

$$
U_{\mathrm{eff}}(V) = U_0(V) + U_{\mathrm{noise}} = \int f(V)dx - \frac{\sigma_m^2 V^2}{4},
\tag{2.18}
$$

where $U_0(V)$ is a monostable potential and U_{noise} represents the influence of the multiplicative

noise. Note that this approach is valid only if a suppression of fluctuations, performed by the coupling, is sufficient. It means that the coupling strength should tend to infinity, or actually be large enough. DSR is expected for the regions where this effective potential has a bistable form. To obtain an analytical estimation of SNR for one element we use a standard linear response theory [53, 124], yielding

$$SNR_1 = \frac{4\pi A^2}{\sigma_a^4} r_k, \tag{2.19}$$

where r_k is the corresponding Kramers rate [99]

$$r_k = \frac{\sqrt{(|U_{\text{eff}}''(V)|_{V=v_{\min}} |U_{\text{eff}}''(V)|_{V=v_{\max}})}}{2\pi} \exp(-\frac{2\Delta U_{\text{eff}}}{\sigma_a^2}). \tag{2.20}$$

Further we rescale this value by the number N of elements in the circuit [175] and take into account the processing gain G and the bandwidth Δ in the power spectral density [124]. The SNR_{N} of the mean field of the whole system of N elements is then

$$SNR_{\text{N}} = SNR_1 \frac{NG}{\Delta} + 1. \tag{2.21}$$

For the parameters, used below for numerical simulations ($\sigma_m^2 = 3$, $A = 0.1$, $N = 324$, $G = 0.7$, $\Delta = 0.012$), we obtain the analytic estimation of SNR, shown in Fig. 2.8a by the solid line. Except for the application for electronic circuits this calculation shows also that DSR can be observed not only in the specific model described in [5*].

In order to verify the results obtained by our rough analytical approximation, we have performed simulations of the model (2.15) using numerical methods described in [97]. We have taken a set of parameters within the region of two coexisting ordered states with nonzero mean field. As a total system, we take a two dimensional lattice of 18×18 elements, which was simulated numerically with a time step $\Delta t = 2.5 \times 10^{-4}$. The amplitude of the external signal was set to 0.1, i.e. sufficiently small to avoid hops between two states in the absence of additive noise. To describe the SR effect quantitatively, we have calculated SNR by extracting the relevant phase-averaged power spectral density $S(\omega)$ and taking the ratio between its signal part with respect to the noise background [53]. The dependence of SNR on the intensity of the additive noise is shown in Fig. 2.8a for the mean-field (filled points) and the mean field in a two-state approximation (opaque points). In this two-state approximation, we have replaced the value of the mean field in time-series by its sign before calculating the power spectral density, using method of symbolic dynamics [206], standardly used to investigate SR [53]. Both curves demonstrate well-known bell-shaped dependence which is typical for SR. In contrast to two-states approximation, for the mean field, SNR tends to infinity for small values of multiplicative noise intensity (see black points for $\sigma_a^2 < 0.1$). It can be explained by intrawell dynamics in the same way as in the conventional SR [53]. Numerical simulations agree very good with our theoretical estimation despite the very rough approximation via "effective" potential.

Note that this SR effect is created by multiplicative noise, since a bimodality is induced by the combined actions of the multiplicative noise and the coupling. If we decrease only the intensity of multiplicative noise, other parameters fixed, the SR effect is not observed, as it is
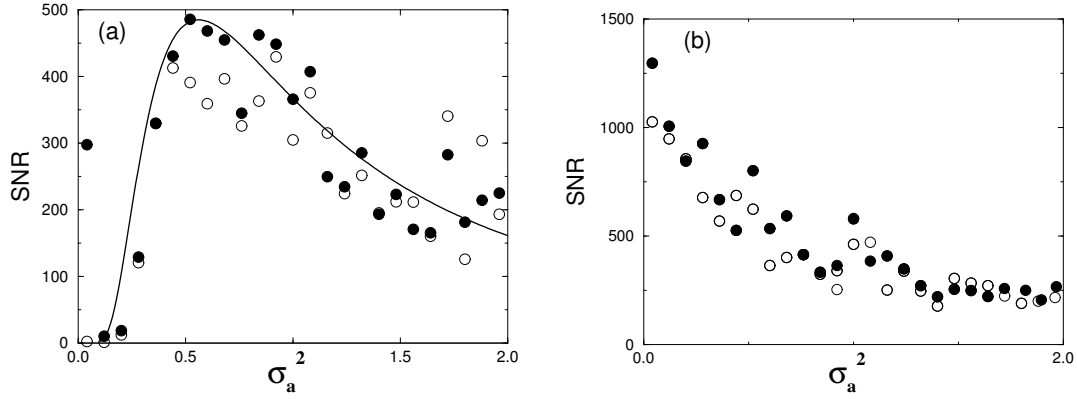
Figure 2.8: (a) Numerical SNR (points) vs analytical estimation (solid line) for the equation with f_1 and $D = 3$, $\sigma_m^2 = 3$. Numerical results are shown by black points for the mean field and opaque points for its two-state approximation. The stochastic resonance effect is supported by noise. If we decrease the intensity of multiplicative noise, we do not observe it; e.g. for (b) $D = 3$, $\sigma_m^2 = 0.5$.

shown in Fig. 2.8b. The reason is that in this case our system is not bistable (see Fig. 2.7) For f_2 the behaviour is similar: DSR is observed for $g_1 = 1$, $g_2 = 1$, $D = 5$, $\sigma_m^2 = 5$, but not for $\sigma_m^2 = 3$, $D = 5$. For experimental setup a minimal number of elements, which are neccessary for DSR observation, can be important. Reduction of the elements number in this system leads to the fact, that a system can spontaneously (even in the absence of forcing) perform a hop between two states. These jumps hide DSR effect, since they destroy a coherence between input and output. For the system size 18×18, considered here, such jumps are rather seldom [136] and do not hinder DSR. Our calculations have shown that a size 10×10 is still satisfactory, whereas further decrease of the elements number will destroy the effect.

2.3 Doubly stochastic coherence: periodicity via noise-induced symmetry in bistable neural models

Above we have suggested the concept of doubly stochastic effects. The idea is that ordering occurs due to interplay of two noise sources and hence an optimization of both noise intensities is needed. Here we investigate doubly stochastic coherence (DSC), which appears via to the noise-induced symmetry in the excitable system. Rhythm generation is a long-standing problem in science, in particular, in biological and cognitive science contexts [204, 44]. A paradigm of this kind of self-sustained oscillating behavior in nonlinear systems is offered by limit cycles. But even in the absence of limit cycles, internal rhythms can be generated in nonlinear systems by the effect of noise. An early realization of this phenomenon was reported in a two-dimensional autonomous system when operating close to a limit cycle, and was interpreted as a manifestation of stochastic resonance in the absence of external forcing [83]. An optimal amount of noise was also seen to lead to a maximally coherent output in an excitable system [150]. This effect, called *coherence resonance*, was studied in the well-known FitzHugh-Nagumo model, which has been extensively used to describe the dynamics of neural systems [94].

A complete understanding of these different mechanisms of coherence resonance is very important for the study of rhythm generation in biological systems [44, 29], and in particular in neural tissue. On the other hand, increasing experimental evidence has established in recent years that certain types of neurons frequently operate in a bistable regime [84]. Thus, the question arises whether noise can excite an autonomous coherent output in *bistable* neural systems. In this direction, both standard stochastic and coherence resonance have been observed in a symmetrically bistable FitzHugh-Nagumo model [110]. Here we show that coherence can also be generated in the general asymmetric case, where the stability of the two stable steady states is not necessarily the same. We demonstrate that the mechanism of coherence enhancement in this situation is utterly different from the standard one, being based on the restoration of symmetry induced by a multiplicative source of noise. This effect vividly contrasts with standard noise-induced phase transitions, where noise usually leads to the breaking of symmetry [65].

Doubly stochastic coherence (DSC) can be observed in an asymmetric system under the action of multiplicative and additive noises. Once multiplicative noise induces a symmetric bistable state in the system, an optimal amount of additive noise can maximize coherence in the output [110]. Hence, the resulting coherence is *doubly stochastic*, since simultaneous optimization of two noise intensities is required in order to get the phenomenon. Here the occurrence of DSC is reported on a modified version of the well-known FitzHugh-Nagumo (FHN) model.

We consider the following version of the FHN model:

$$\varepsilon \frac{du}{dt} = (u(1-u)(u-a)-v)$$
$$\frac{dv}{dt} = bu - v - uv\xi(t) + \zeta(t). \tag{2.22}$$

In a neural context, $u(t)$ represents the membrane potential of the neuron and $v(t)$ is related to the time-dependent conductance of the potassium channels in the membrane [94]. The dynamics of u is much faster than that of v, as indicated by the small time-scale-ratio parameter ε. There are two mutually uncorrelated noise sources, represented by the $\delta-$correlated Gaussian noises $\xi(t)$ and $\zeta(t)$, with zero mean and correlations $\langle \xi(t)\xi(t')\rangle = \sigma_m^2 \delta(t-t')$ and $\langle \zeta(t)\zeta(t')\rangle = \sigma_a^2 \delta(t-t')$. The multiplicative noise $\zeta(t)$ is interpreted in the Stratonovich sense [65].

In what follows we use the parameters $a = 0.15$, $b = 0.12$, and $\varepsilon = 0.01$, for which the deterministic system has two stable fixed points with different stability (i.e. with different thresholds of escape through the extrema of the u-nullcline), as shown in Fig. 2.9 (curve 1 and its crossing points with the u-nullcline). Additive noise induces here jumps between these two states, but the escape times are very different in the two states. This behavior is shown in Fig. 2.11(a), as obtained from numerical simulations of model (2.22) for the above-mentioned parameters.
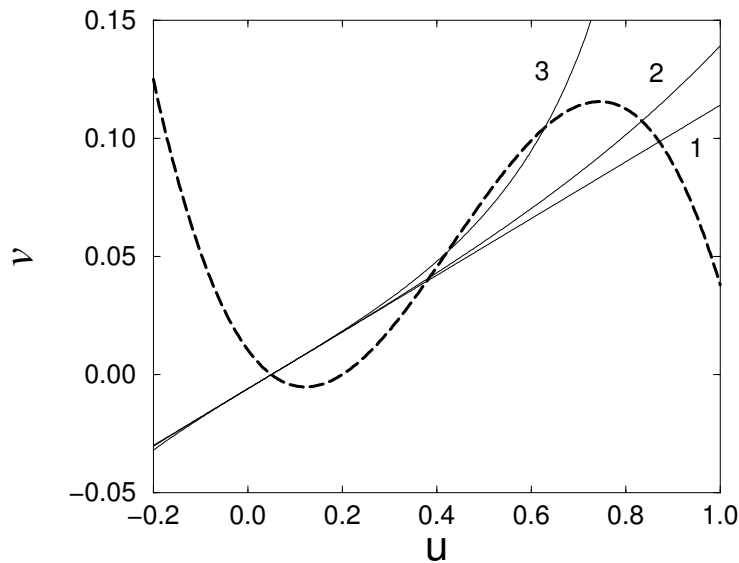
Figure 2.9: Nullcline plot of the FHN model (2.22). Dashed line: u-nullcline ($\dot{u} = 0$); solid lines: v-nullclines ($\dot{v} = 0$) for three different values of the multiplicative noise intensity: $\sigma_m^2 = 0.0$ (curve 1), 0.2 (curve 2), and 2 (curve 3). Multiplicative noise changes the relative stability of the stable points and induces the symmetric situation.

The effect of multiplicative noise in this system can be determined by analyzing the systematic effect it produces in the system dynamics due to the fact that the corresponding fluctuating term in the v equation has a nonzero average value. Computation of this average value by means of standard techniques [172] leads to the following effective deterministic model, which can be considered as a first order approximation in a small-noise expansion of

Figure 2.10: Coherence parameter R vs. intensity of the multiplicative (left) and additive (right) noises. $\sigma_a^2 = 2 \times 10^{-4}$ and $\sigma_m^2 = 0.5$ rsp. The curves have clearly defined minimum, which corresponds to the most periodic behaviour.

$\xi(t)$ [65]:

$$\varepsilon \frac{\partial u}{\partial t} = (u(1-u)(u-a)-v) \tag{2.23}$$

$$\frac{\partial v}{\partial t} = bu - v + \frac{\sigma_m^2}{2} u^2 v, \tag{2.24}$$
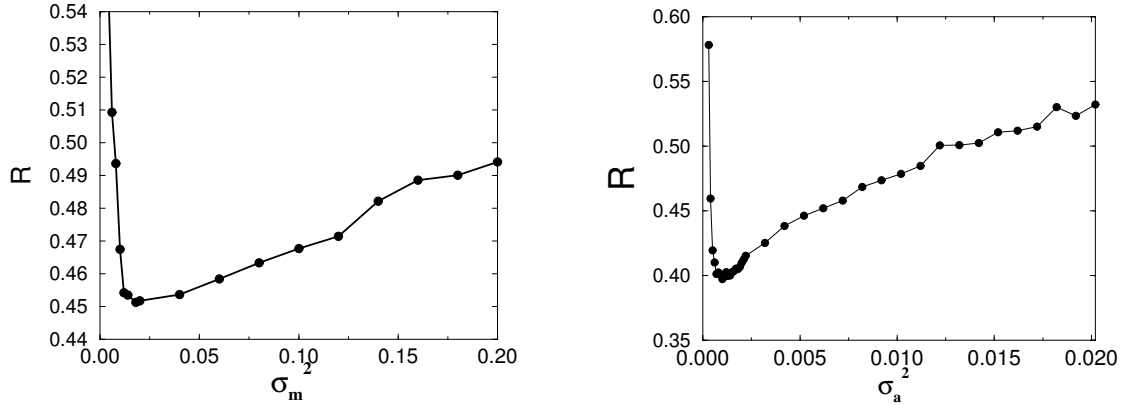
The nullclines of this model for two nonzero values of σ_m^2 are shown in Fig. 2.9, as curves 2 and 3. It can be seen that for an intermediate value of σ_m^2, corresponding to curve 2, the two states are equally stable and the escape times are basically identical. As a result, jumps in the output of the system in the presence of an optimal amount of additive noise are more equidistant (2.11(b)). Hence, an increase of multiplicative noise enhances coherence via noise-induced symmetry. For larger multiplicative noise intensity the asymmetry arises again, this time reversed (curve 3 in the Fig. 2.9) and the coherence is strongly reduced [Fig. 2.11(c)]. In fact, in this extreme case the upper steady state has turned unstable, and the system becomes excitable.

To quantify this coherence enhancement, we have measured the normalized variance of subsequent periods T_i. The illustration of the definition of T_i is depicted in Fig. 2.11(a). The normalized variance, which is called coherence parameter [150], is determined as $R = \sqrt{\sigma_T^2} / \langle T_i \rangle$, where σ_T^2 is the variance of the sequence T_i, and $\langle T_i \rangle$ is its average value. The dependence of R on the multiplicative noise intensity for the time series depicted in Fig. 2.11(a-c) is shown in the Fig.2.10 left. It is clearly seen that R first decreases to some minimum value and then increases again. The minimal R corresponds to the highest degree of periodicity in the system output, and is a manifestation of stochastically induced coherence. A similar behavior occurs for varying the strength of the additive noise as well, as shown in the inset of Fig. 2.10 right. Hence, both noise intensities need to be tuned in order to optimize periodicity in the output (see Fig. 2.11 (d)), and hence we call this effect doubly stochastic coherence (DSC). Different values of the excitation threshold correspond to different optimal intensities of the noise. Hence, to optimize the periodicity one can vary either the threshold (provided by
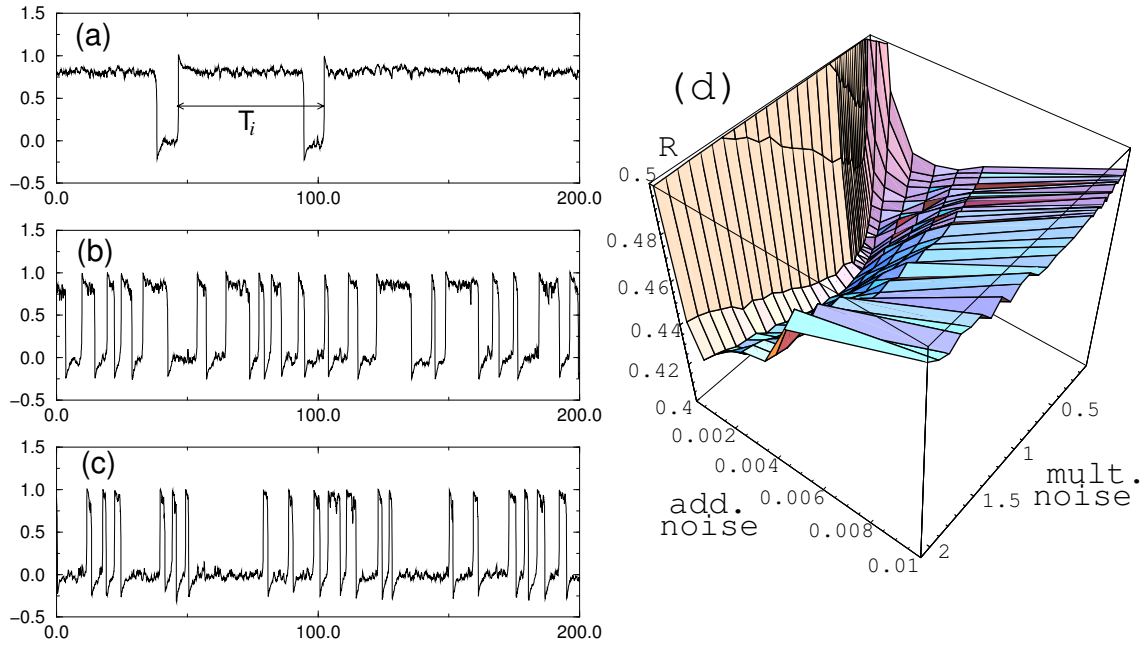
Figure 2.11: (a-c): Time evolution of the activator variable u for three multiplicative noise intensities: (a) σ_m^2=0.0, (b) 0.2, (c) 2. The intensity of additive noise is fixed to $\sigma_a^2 = 2 \times 10^{-4}$, other parameters are given in the text. (d): 3D plot of the coherence parameter R vs. intensity of the multiplicative and additive noises.

multiplicative noise), or the intensity of additive noise.

With the aim of confirming experimentally the phenomenon of DSC via noise-induced symmetry, we have designed a circuit (Fig. 2.12), which has two asymmetrically stable steady states. In this circuit, the difference between the positive and negative voltages feedings the operational amplifier provides the asymmetry in the stability of the two fixed points. Multiplicative noise acts on the positive voltage V_+, which is a parameter that changes the stability of the higher voltage fixed point of the circuit [19]. A second source of noise, which acts as a signal, induces jumps between the two stable states, and acts as an additive noise. The noise is produced electronically by amplifying shot noise from a junction diode [114].

Following the numerical approach, we fix the intensity of additive noise and increase that of multiplicative noise. First, the upper steady state is more stable than the lower one, and the system spends more time in the former [Fig. 2.13(a)]. As the strength of multiplicative noise increases the situation is reversed [Fig. 2.13(c)], passing through a symmetric regime for intermediate noise [Fig. 2.13(b)]. Calculating the coherence parameter R for the experimental time traces, we find clearly the effect of doubly stochastic coherence [Fig. 2.13(d)].

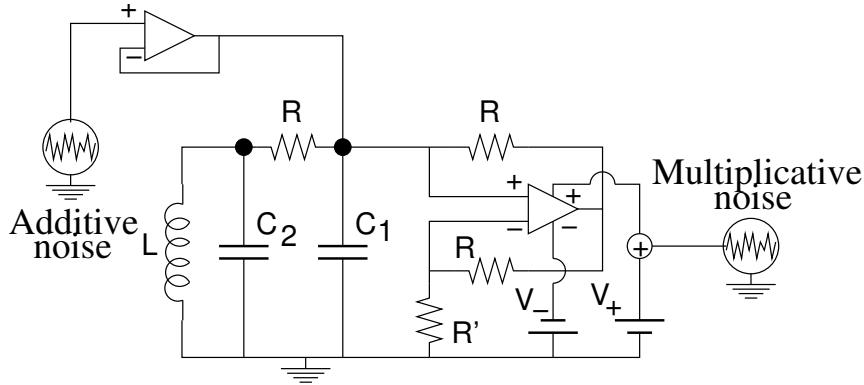We have also examined the effect of spatial coupling on a set of distributed bistable FHN

Figure 2.12: Nonlinear electronic circuit with two asymmetrically stable steady states. The values of the elements are: $R = 270\,\Omega$, $L = 10\,mH$, $C_1 = 1\,nF$, $C_2 = 10\,nF$, $R' = 220\,\Omega$, $V_- = 5\,V$, and $V_+ = 2\,V$. The operational amplifier is taken from a TL082 integrated circuit.

oscillators subject to two noise sources. The model is now given by:

$$
\begin{aligned}
\varepsilon\frac{\partial u_i}{\partial t} &= (u_i(1-u_i)(u_i-a)-v_i) \\
&\qquad +\frac{D}{2}(u_{i+1}+u_{i-1}-2u_i) \\
\frac{\partial v_i}{\partial t} &= bu_i - v_i - u_i v_i \xi_i(t) + \zeta_i(t),
\end{aligned}
\tag{2.25}
$$

where D denotes the strength of coupling and the noise terms are now δ-correlated also in space, with $\langle \xi_i(t)\xi_j(t')\rangle = \sigma_m^2\delta(t-t')\delta_{ij}$ and $\langle \zeta_i(t)\zeta_j(t')\rangle = \sigma_a^2\delta(t-t')\delta_{ij}$.

We now study the joint effect of additive and multiplicative noise on the spatiotemporal evolution of this extended system, using a binary coding for the activator variable $u_i(t)$, associating black or white to each one of the two fixed points of the local bistable dynamics. The numerical simulation results are shown in Fig. 2.14 for three values of σ_m^2 and a fixed σ_a^2. As expected, the local dynamics becomes more regular for an optimal amount of multiplicative noise, as happens with an isolated FHN element. However, remarkably enough, the most temporally coherent case corresponds also to the most spatially uniform behavior of the system as a whole. To characterize such a synchronized coherence we calculate the coherence parameter R for the mean field $m(t) = \sum_i u_i$. The dependence of this parameter vs the intensity of multiplicative noise is shown in Fig. 2.15 (a) for a system of 50 coupled elements. The dependence is non-monotonic, reflecting the DSC characteristic of isolated elements, although in this case the parameter measures also the degree of synchronization in the system. Furthermore, Fig.2.15 (b) shows that increasing the number of elements in the ensemble first increases the coherence of the output (R initially decreases), due to the synchronization of the elements, but further increase of the system size leads to a loss of synchronization, and thus R increases again. The result is a system-size coherence resonance (cf with system-size stochastic resonance, which happens in externally forced systems [153]). In a neural context, this property could explain why neurons are coupled in networks of optimal size for the organization of a pacemaker.
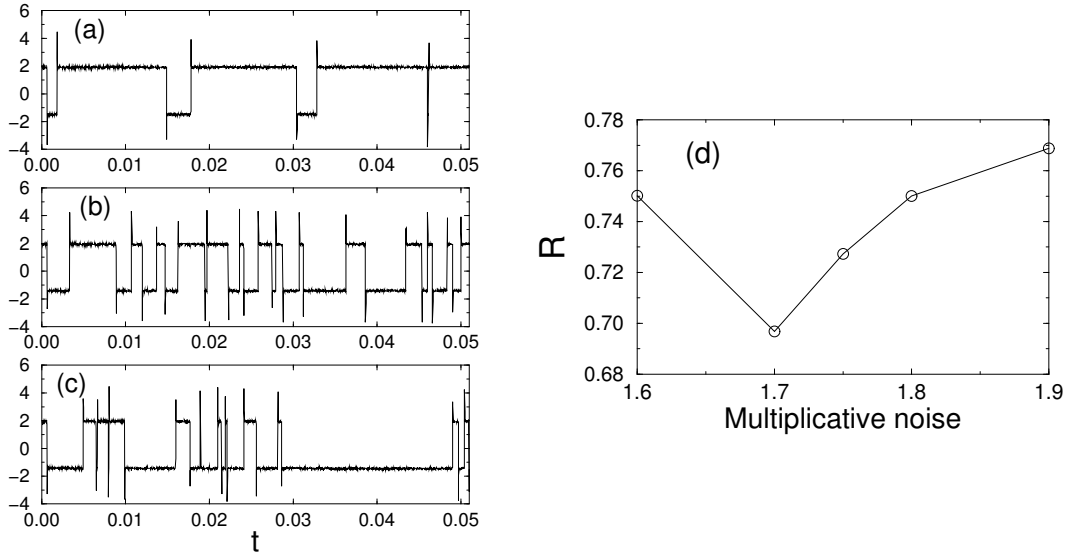
Figure 2.13: Time evolution of the voltage drop through condenser C_1 for the circuit represented in Fig. 2.12, for three different intensities of the multiplicative noise (measured as peak-to-peak amplitude of the random voltage): (a) 1.6 V, (b) 1.7 V, and (c) 1.9 V. Additive noise intensity is fixed to 0.88 V. (d): coherence parameter vs multiplicative noise intensity for the previous case.

In conclusion of this chapter, it has been shown that bistable neural systems exhibit doubly stochastic coherence via noise-induced symmetry. This mechanism of rhythm generation arises whenever the two stable steady states of the system have different escape thresholds. An optimal amount of multiplicative noise renders the two fixed points equally stable, and tuning the additive noise in this noise-induced symmetric situation maximizes the coherent behavior in the system. The influence of multiplicative noise can be explained in terms of an effective model that contains the systematic effect of the noise term. These results have been confirmed by experimental measurements on a bistable nonlinear electronic circuit. From a second standpoint, it has been shown that this effect leads to synchronized behavior in spatially distributed systems. In this case, this coherence enhancement also exhibits a resonance with respect to the size of the system, i.e. there is some optimal size of the system for which the output is the most periodic one. Our study has been performed in the general framework of the paradigmatic FHN model, in a bistable asymmetric regime which is realistic for biological systems, and hence we expect that our findings could be of importance for understanding the mechanisms of periodicity generation in neural and other excitable media.

Figure 2.14: Spatiotemporal evolution of a chain of FHN oscillators in the bistable regime for three intensities of the multiplicative noise. From left to right, $\sigma_m^2 = 0.01, 0.2 ; 4$. Additive noise is fixed to $\sigma_a^2 = 4 \times 10^{-4}$. Coding is binary, with black corresponding to the upper fixed point, and white to the lower one. Other parameters are $D = 30$, $a = 0.15$, $b = 0.12$, and $\varepsilon = 0.01$.

Figure 2.15: (a): Coherence parameter R of the mean field $m(t)$ vs intensity of the multiplicative noise for a system with 50 coupled elements. (b): the dependence of R on the size of the system ($\sigma_m^2 = 0.005$).

Chapter 3

New effects in noise-induced propagation

3.1 Noise induced propagation in monostable media

In previous sections we have shown that in DSR the energy of fluctuations can be used even more efficiently in spatially extended systems, by using noise twofold: to synchronize output hops across a potential barrier with an external signal, and also to optimally construct the barrier itself. Another important and nontrivial phenomenon connected with SR in spatially distributed systems is the phenomenon of *noise enhanced propagation*, in which the propagation of a harmonic forcing through an unforced bistable or excitable medium is increased for an optimal intensity of the additive noise [111, 209, 15].

The idea of doubly stochastic effects in the application to propagation leads to a new propagation phenomenon in monostable media. We show that noise can enhance propagation in deterministically *monostable* media, without any deterministic threshold, provided bistability is induced by a second (multiplicative) noise and coupling through a noise-induced phase transition. Although numerous works about noise-induced propagation exist (cf. [63, 147, 168], for instance), to our knowledge propagation in *monostable* media,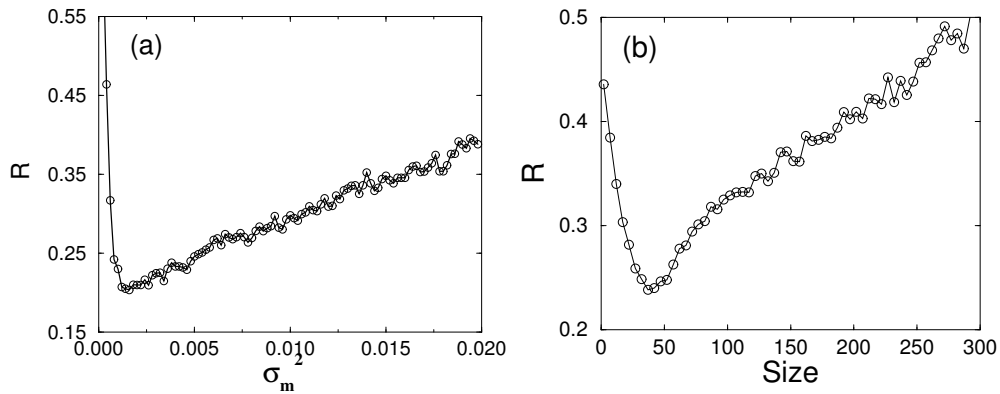 which is a very important class of dynamical systems, has not been considered before. Some exception is the work [160], where noise-induced propagation in systems with one stable state has been considered, however the system was nonpotential and hence not with a monostable potential. In what follows, we present noise-induced propagation in a general model of overdamped coupled monostable nonlinear oscillators. Subsequently, and for the sake of concreteness, the phenomenon is analyzed in particular in a simple model of coupled electronic circuits.

We begin by studying a general class of spatially distributed systems, which are locally coupled and periodically forced:

$$\dot{x}_i = f(x_i) + g(x_i)\xi_i(t) + \frac{D}{4}\sum_{j\in nn(i)}(x_j - x_i) + \zeta_i(t) + A_i\cos(\omega t + \varphi),\qquad(3.1)$$

where x_i is defined in a two-dimensional discrete space of $N \times N$ cells, with i denoting the cell position ($i = i_x + N(i_y - 1)$, where i_x and i_y run from 1 to N). The sum in the right-hand side runs over all nearest neighbors of site i [$nn(i)$]. The additive and multiplicative noise terms are mutually uncorrelated Gaussian distributed with zero mean, and white both in space and time, i.e. $\langle \zeta_i(t)\zeta_j(t')\rangle = \sigma_a^2\delta_{ij}\delta(t-t')$ and $\langle \xi_i(t)\xi_j(t')\rangle = \sigma_m^2\delta_{ij}\delta(t-t')$. The results are averaged over the initial phase φ of a harmonic forcing, which has amplitude A_i and frequency ω.

In the absence of periodic forcing ($A_i = 0$), different types of noise-induced phase transitions can be obtained for different deterministic and stochastic forces $f(x_i)$ and $g(x_i)$ [172]. In particular, a system with a monostable deterministic potential can undergo a phase transition to a noise-induced bistable state for a suitable stochastic forcing $g(x_i)$ [195]. There, in the presence of a global harmonic forcing, DSR is observed [5*]. We consider here the case that the periodic forcing is applied coherently along only one side, as shown in Fig. 3.1 [$A_i = A(\delta_{i_x,1} + \delta_{i_x,2} + \delta_{i_x,3})$], and study the propagation of this forcing action into the non-excited portion of the system.

Even though the results shown below are very general, for a quantitative study we choose particular functions $f(x)$ and $g(x)$. These functions model the local dynamics of the electronic
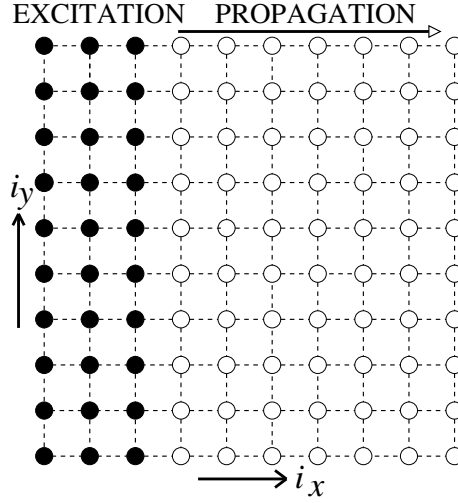
Figure 3.1: Scheme of the spatially distributed system. The periodic excitation is performed only from one side, elements under the direct periodic action are denoted by black. All oscillators are under the influence of noise. To study the behavior of both driven and non-driven elements, first three columns ($i_x = 1, 2, 3$) are periodically driven, however to achieve propagation it is sufficient to excite only one column.

circuit designed theoretically (i.e. it is so far a thought experiment) and displayed in Fig. 2.6. This circuit consists of a capacitor with capacitance C, a time-varying resistor (TVR) with conductance $G(t)$, a current generator $I(t)$, four coupling resistors R_c (responsible for the diffusive coupling with the neighbors), and a nonlinear resistor R_N, which is realized with a set of ordinary diodes or operational amplifiers [4*], and has the characteristic function

$$i_N = h(V) = \begin{cases} G_b V + (G_a - G_b)B_p & \text{if } V \leq -B_p, \\ G_a V & \text{if } |V| < B_p, \\ G_b V - (G_a - G_b)B_p & \text{if } V \geq B_p, \end{cases} \tag{3.2}$$

where i_N is the current through the nonlinear resistor (R_N), V is the voltage drop across it, and the parameters G_a, G_b and B_p determine the slopes and the breakpoint of its piecewise-linear characteristic curve.

We now consider that the conductance of the TVR fluctuates randomly in time, in the form of a Gaussian noise δ−correlated in space and time [$G_i(t) = \xi_i(t)$], and that the input current $I(t)$ has the form of a periodic signal to which an uncorrelated Gaussian noise $\zeta(t)$ is added [$I_i(t) = \zeta_i(t) + A_i \cos(\omega t + \varphi)$]. Under these conditions, the dynamics of the spatially coupled system is described by Eq. (3.1), where x_i now represents the voltage drop across the nonlinear resistor of circuit i, and the forces are $f(x) = -h(x)$ and $g(x) = x$ [4*]. Additionally, $C = 1$ by an appropriate time normalization, and the coupling strength $D = \frac{4}{CR_c}$.

SR behavior can be expected if the system is bistable for the chosen set of parameters. Regions of bistability can be determined approximately by means of a standard mean-field procedure [65]. The mean-field approximation consists of replacing the nearest-neighbor interaction by a global term in the Fokker-Planck equation corresponding to (3.1) in the absence

of external forcing. In this way, we get the steady-state probability distribution P_{st}:

$$P_{\text{st}}(x,m) = \frac{C(m)}{\sqrt{\sigma_m^2 g^2(x) + \sigma_a^2}} \exp\left(2\int_0^x \frac{f(y) - D(y-m)}{\sigma_m^2 g^2(y) + \sigma_a^2}\,dy\right), \tag{3.3}$$

where $C(m)$ is a normalization constant and m is the mean field, defined implicitly by:

$$m = \int_{-\infty}^{\infty} x P_{\text{st}}(x,m)\,dx. \tag{3.4}$$

The value of m is obtained by the self-consistent solution of Eq. (3.4), which enables to determine the transition lines between the ordered bistable ($m \neq 0$) and the disordered monostable ($m = 0$) phases. These transition boundaries are shown in Fig. 3.2 in the $D - \sigma_m^2$ plane for three different values of the additive noise intensity. Note that bistability requires *both* multiplicative noise and coupling between elements. We also find that an increase in additive noise reduces the bistable region. This gives DSR a special character with respect to standard SR [5*].

Now we place ourselves within the bistable regime supported by multiplicative noise and coupling (e.g. $D = 3$, $\sigma_m^2 = 3$), and investigate the propagation of a wave through the system. To that end, we harmonically excite the lattice from one side, as shown in Fig. 3.1, with boundary conditions periodic in the vertical direction and no-flux in the horizontal direction. The propagation will be quantified by the system's response at the excitation frequency, computed as $Q^{(j)} = \sqrt{Q_{\sin}^{(j)^2} + Q_{\cos}^{(j)^2}}$, with

$$Q_{\sin}^{(j)} = \frac{\omega}{n\pi} \int_0^{2\pi n/\omega} 2m_j(t)\sin(\omega t)dt\,, \tag{3.5}$$

$$Q_{\cos}^{(j)} = \frac{\omega}{n\pi} \int_0^{2\pi n/\omega} 2m_j(t)\cos(\omega t)dt\,, \tag{3.6}$$

where $m_i(t)$ is the field (voltage) averaged along the vertical column (Fig. 3.1), i.e. $m_j(t) = \frac{1}{N}\sum_{k=1}^N x_{i+(k-1)N}(t)$.

The value of $Q^{(j)}$ for different oscillators along the chain is shown in Fig. 3.3(a), for increasing intensities of additive noise within the noise-induced bistable regime. The forcing amplitude is taken to be large enough to produce hops between the two wells in the bistable oscillators, without the need of additive noise. Therefore, for the first oscillators an increase of additive noise leads only to a decreasing response at the forcing frequency, whereas for distant oscillators the situation changes qualitatively. There, a response is induced that depends non-monotonically on the additive noise intensity. Clearly, a certain amount of additive noise exists for which propagation of the harmonic signal is optimal. For smaller multiplicative-noise intensity [Fig. 3.3(b)] the system leaves the bistable region; hence the response is small and always monotonically decreasing. Hence, the resonant-like effect requires suitable intensities of *both* the additive and multiplicative noises.

A propagation of the harmonic signal can also be obtained for values of the forcing amplitude small enough so that hops are not produced in the directly excited sites in the absence of additive noise. This is the regime in which DSR really occurs in the excited part of the system,
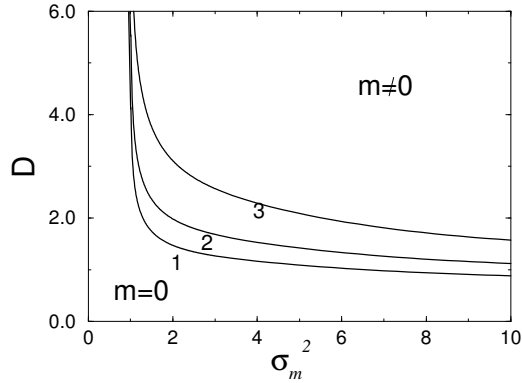
Figure 3.2: Mean-field transition lines between disordered monostable ($m = 0$) and ordered bistable ($m \neq 0$) phases for model (3.1): $\sigma_a^2 = 0.3$ (label 1), $\sigma_a^2 = 0.5$ (label 2) and $\sigma_a^2 = 1.0$ (label 3). Other parameters are $G_a = 0.5$, $G_b = 10$ and $B_p = 1$.

and the excitation propagates through the rest of the lattice enhanced by noise. Now all the oscillators have a non-monotonic dependence on the additive noise intensity for a multiplicative noise within the bistable region [Fig. 3.3(c)], and a monotonic one for a multiplicative noise within the monostable region [Fig. 3.3(d)]. The former case corresponds to a spatiotemporal propagation in the DSR medium, and we call this phenomenon *spatiotemporal doubly stochastic resonance* (SDSR).

The mechanism of this phenomenon can be explained theoretically on the basis of a mean-field approximation. We give a first qualitative glimpse of this analysis in what follows; quantitative details will be published elsewhere. Due to coupling and multiplicative noise, the system becomes bistable with the behavior approximately governed by a mean-field effective potential [5*]

$$U_{\text{eff}}(x) = U_0(x) + U_{\text{noise}} = -\int f(x)dx - \frac{\sigma_m^2 x^2}{4}. \tag{3.7}$$

Now the effect can be understood in the frame of a standard SR mechanism [53], where the external signal is provided by the periodic force for the directly excited oscillators, and by the influence of the left neighbors for the non-excited oscillators. For large forcing, only the latter need an additive noise to hop synchronously between wells, whereas for small forcing, both the excited and the non-excited oscillators display SR. These two behaviors correspond to the situations depicted in Figs. 3.3(a) and 3.3(c), respectively.

At this point it is worth making several remarks to the phenomenon described above. First, SDSR and noise-induced propagation in monostable media are strongly different to spatiotemporal SR [123, 199] or noise enhanced propagation [111, 209] in bistable media. The effect presented here can be controlled by multiplicative noise, which modifies the depth and separation of the two potential wells. Therefore, an optimal amount of multiplicative noise is required to support the bistable structure. Nothing similar occurs in array-enhanced SR [112] or in SR in extended bistable systems [23, 205]. On the other hand, an increase of additive noise also leads to a loss of bistability (see Fig. 3.2), and hence a decrease of Q for large additive noise is explained not only by the fact that disordered hops are produced by
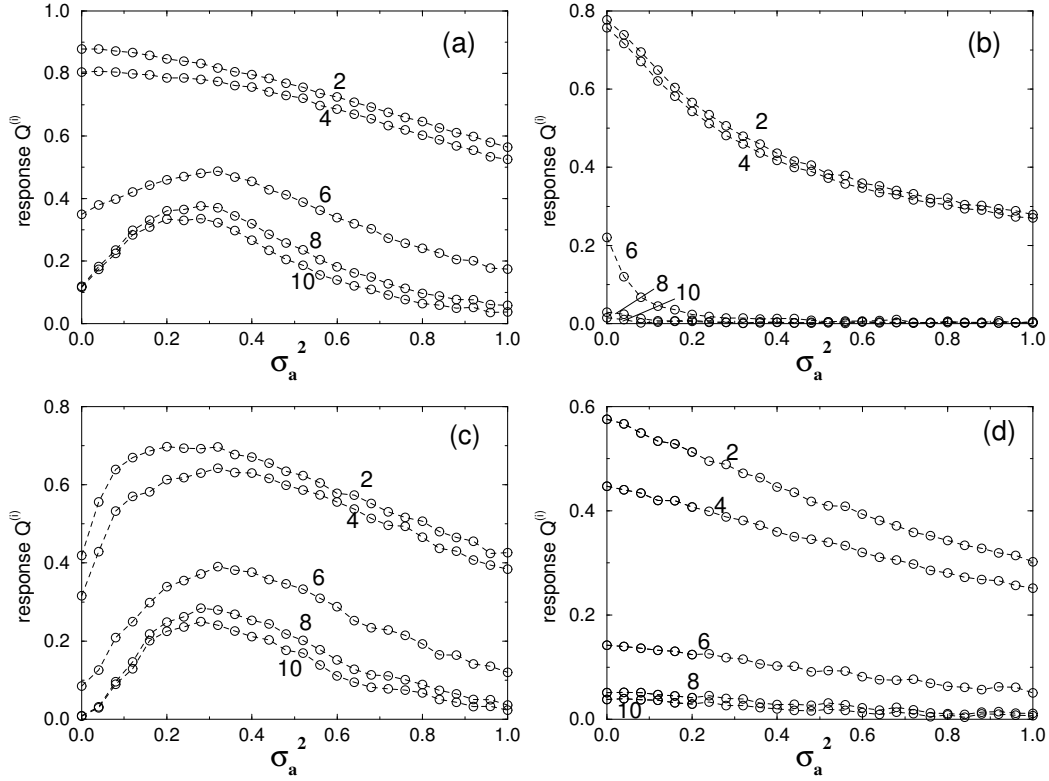
Figure 3.3: Response $Q^{(j)}$ to a periodic excitation in different oscillators (the order j is shown in the curve labels) vs. additive-noise intensity (a,c) inside the bistability region ($\sigma_m^2 = 3$), and (b,d) outside that region ($\sigma_m^2 = 0.5$). As shown in Fig. 3.1, the oscillators with index $j = i_x = 1, 2, 3$ are directly excited by the periodic force, and oscillators with $j = i_x > 3$ are excited through the excitation propagation. Parameters are those of Fig. 3.2, and $D = 3$. The amplitude is: (a,b) $A = 0.3$ (noise-induced propagation) and (c,d) $A = 0.2$ (spatiotemporal doubly stochastic resonance).

intense noise, as in standard SR, but also by the loss of bistability.

Second, noise-induced propagation in monostable media is very intriguing from the viewpoint of the theory of extended systems with noise and cannot be directly predicted from DSR. The noise-induced bistability, on which DSR is based, is a collective phenomenon, which can be observed only for a positive value of coupling. The coupling causes the situation when all elements are close to the same position. In contrast to it, here we have shown that a propagation, which implies that different cells are simultaneously in different states, can occur in such a system without destroying the mechanism of bistability. Moreover this propagation can be enhanced by additive noise and controlled by multiplicative noise. An interesting question is, how high can the frequency of the external signal be and still display propagation in this medium.

In conclusion, we have reported the existence of a propagation phenomenon, in which noise induces wave propagation in monostable media. The joint action of multiplicative noise and spatial coupling induces bistability, and additive noise enhances the propagation of harmonic forcing in the stochastically induced bistable medium. Due to its nontrivial propagation mechanism, this effect is interesting from a theoretical viewpoint, and can be considered as a contribution to the theory of extended systems with noise. We also expect that these theoretical findings will stimulate experimental work. Especially, such kind of a propagation can be of great importance in communications, due to the fact that the energy of noise is used in a very efficient way, both to construct the potential barrier and to provide propagation enhancement in the noise-supported bistable system. We have demonstrated noise-induced propagation in monostable media in a simple realistic model, but in a general framework. Due to the generality of the model we expect that this effect can be also found in several more complicated real extended systems with noise-induced bistability. Probable experimental implementations include the same as for DSR experimental situations: arrays of simple electronic circuits as a communication system [4*], analog circuits [1], electronic cellular neural networks [149, 11, 158], and are expected to be achieved in several real spatially distributed systems, such as liquid crystals [93], photosensitive chemical reactions [128], Rayleigh-Bénard convection [127] or liquid helium [73].

3.2 Noise-induced propagation and frequency selection of bichromatic signals in bistable media

Information needs to be transmitted in many different contexts, including for instance cell signalling in biological systems [94] and optical communications in technological networks [7]. Biological systems, and in particular neural tissue (where signal transmission is of utmost importance), are subjected to a large amount of noise of different origins. This fact underlies the current interest in examining the effects of random fluctuations in signal transmission processes. Actually, contrary to intuition, recent investigations have revealed the constructive role of noise in the effect of noise-induced propagation. Numerical investigations have shown that random fluctuations enhance propagation of harmonic (monochromatic) signals through bistable [209, 111] and even monostable [1*] media (see the previous chapter). In those cases, the periodic response to a harmonic forcing being applied to one end of the system propagates the farthest when the amount of noise acting on all elements is optimal. The phenomenon has all ingredients characteristic of stochastic resonance [125]; one can say in fact that the system exhibits locally the noise-induced amplification of a weak periodic signal coming from the neighboring sites. Here we are interested in the propagation of a signal which contains more than one frequency.

Noise-enhanced propagation has also been observed for aperiodic signals [63]. But between the two limiting cases of purely harmonic (single frequency) and completely aperiodic signals, the intermediate case of signals consisting of a finite number of harmonic modulations is worth being studied. This kind of signals is commonly used, for instance, in multichannel optical communication systems based on wavelength-division multiplexing (WDM) [7]. In a different type of application, probing methods based on the propagation of two-frequency signals are used, for example, to determine the size and abundance of plankton [132], to analyze evoked potentials in the human visual cortex [198], and to diagnose the physical conditions of the Antarctic ice sheet [51]. Here we analyze the effect of noise on the propagation of such kind of bichromatic signals. Two main conclusions can be drawn from this study. First, noise enhances propagation of the two harmonic components of the driving, similarly to what happens with standard monochromatic driving [209, 111]. Second, and more importantly, noise can be used to select the frequency which is propagated with higher efficiency. We observe that for small noise levels the harmonic with lower frequency is propagated better than the one with higher frequency, where for large noise levels the reverse property is found. These two different effects will be analyzed in the following paragraphs.

We consider a one-dimensional chain of N coupled overdamped oscillators under the action of spatiotemporal noise. The dynamics of this system can be described by the following set of equations:

$$\dot{x}_n = f(x_n) + \varepsilon(x_{n-1} - x_n) + \varepsilon(x_{n+1} - x_n) + \xi_n(t) \tag{3.8}$$

where $n = 1 \ldots N$ denotes the different oscillators, ε represents the strength of coupling between them, and $\xi_n(t)$ is a Gaussian noise, δ-correlated in space and time with intensity σ_a^2. The form of the deterministic force $f(x)$, which is assumed equal for all oscillators, is chosen

to correspond to a bistable dynamics:

$$f(x) = k_1 x - k_2 x^3, \tag{3.9}$$

with k_1, $k_2 > 0$. In what follows, we will use the values $k_1 = 4.74$ and $k_2 = 7.48$. The boundary conditions of the model are such that the ends of the chain are free ($x_0 = x_1$, $x_{N+1} = x_N$). Moreover, an input signal is introduced at one end of the chain by forcing its first element with two harmonic drivings:

$$\dot{x}_1 = f(x_1) + \varepsilon(x_2 - x_1) + \xi_1(t) + A_1 \cos(\omega_1 t) + A_2 \cos(\omega_2 t) \tag{3.10}$$

We aim to analyze the propagation of this combined signal through the chain. We choose non-commensurate frequencies and different amplitudes of the two harmonic components, to avoid interference effects due to their superposition. An example of this signal is shown in Fig. 3.4.
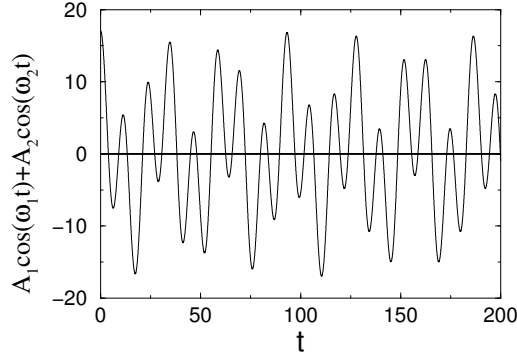
Figure 3.4: Two-frequency signal injected in one end of the chain. Its parameters are $A_1 = 7$, $A_2 = 10$, $\omega_1 = 0.2$, and $\omega_2 = \omega_1 e \approx 0.54$, where e is the base of a natural logarithm.

To estimate the quality of signal transmission at a certain oscillator k along the chain and at a particular frequency ω_i, we have calculated the response $Q^{(k)}(\omega_i)$ as the Fourier component of the spectrum of the corresponding time series $x_k(t)$ at this frequency:

$$Q^{(k)}(\omega_i) = \sqrt{Q_{\sin}^2 + Q_{\cos}^2}, \tag{3.11}$$

where

$$Q_{\sin} = \frac{\omega_i}{n\pi} \int_0^{2\pi n/\omega_i} x_k(t) \sin(\omega_i t) dt, \tag{3.12}$$

and

$$Q_{\cos} = \frac{\omega_i}{n\pi} \int_0^{2\pi n/\omega_i} x_k(t) \cos(\omega_i t) dt. \tag{3.13}$$

We have performed numerical simulations of model (3.8) in the presence of the signal shown in Fig. 3.4, and have analyzed the response of the different oscillators at the two driving frequencies, as a function of the intensity of the spatiotemporal noise. The results

for the first oscillators of the chain are shown in Fig. 3.5. We first note that for the second
and third oscillators (left and middle plot of the figure), the response at both frequencies
decreases with noise intensity. The reason for this behavior is that the amplitudes of the two
harmonic signals acting on the first oscillator are large enough to produce in it jumps between
the two wells of the bistable potential even without noise. This noiseless periodic output
pervades the neighboring oscillators (in this case the second and third ones). Therefore, any
amount of noise decreases the quality of the response. On the other hand, far enough from
the input end of the chain (depending on the value of the coupling strength; in this case,
where $\varepsilon = 4$, it occurs at the fourth oscillator; for smaller coupling it occurs earlier, but the
response is weaker) the system does not jump spontaneously, and noise is needed to induce
the switchings between wells. For that reason, the response function of the fourth oscillator
(right plot in Fig. 3.5) initially increases with noise intensity. Naturally, for large noise levels
disorder comes into play and the response function decreases again. The result is that there
exist intermediate amounts of noise for which the response at each one of the two driving
frequencies is optimal, a characteristic signature of stochastic resonance. Hence, one can say
that noise enhances propagation of the two-frequency signal in this system, with the optimal
noise intensity being slightly different for each one of the two frequencies.

Figure 3.5: Response of the system in the 2nd (left), 3rd (middle), and 4th (right) oscillators
at frequencies ω_1 (thick line) and ω_2 (thin line). The number of oscillators in the chain is 32.

Another feature that can be observed in Fig. 3.5 is that the response in the first oscilla-
tors is larger at the high frequency than at the low one, for all values of the noise intensity.
As the signal travels farther away from the input end of the chain, the response decreases
monotonously. However, the decrease is fastest for the high frequency than for the low fre-
quency signal, an effect which is more pronounced for low noise levels. As a result, for oscilla-
tors far down the chain and for small enough noise, the response is larger at the low frequency
than at the high one. This can be seen in Fig. 3.6, which represents the response at the two
frequencies for the fifth, sixth and eigth oscillators. For the fifth and sixth oscillators, the
crossover between the two response regimes at an intermediate noise intensity can be clearly
seen. For the eight oscillators and at large noise, the response is approximately equally low
at the two frequencies. The result is that, for a certain set of oscillators along the chain, noise
selects the frequency which is being transmitter with better efficiency: the high-frequency
harmonic for large noise intensity and the low-frequency one for small enough noise. It is
worth to note that due to the intrinsic properties of the bistable chain, the high frequency

is always better suppressed, hence this noise-induced selection is possible only under the condition of different initial amplitudes.
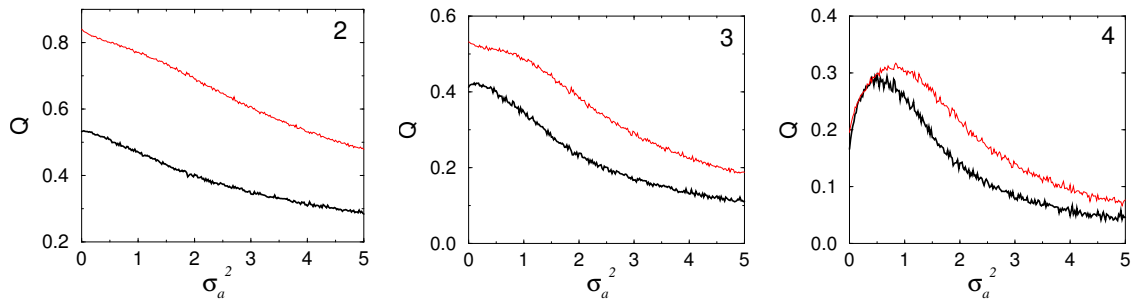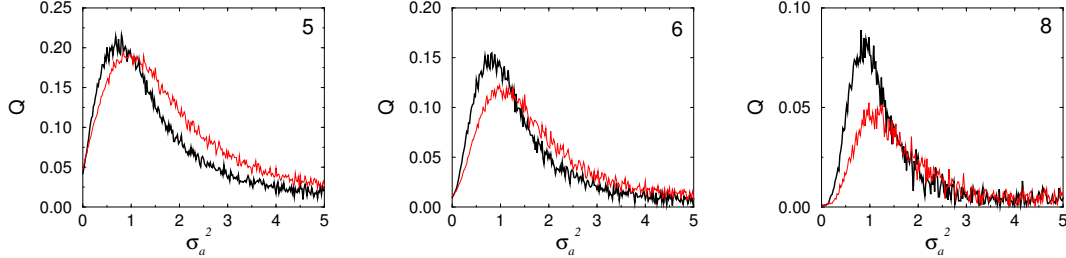

Figure 3.6: Response of the system in the 5th (left), 6th (middle), and 8th (right) oscillators at frequencies ω_1 (thick line) and ω_2 (thin line).

In order to visualize the noise-induced frequency selection effect described above, we have performed a symbol coding of two time series for different amounts of noise. These results are shown in Fig. 3.7. It can be clearly seen that for $\sigma_a^2 = 0.65$ (second plot from above) the low-frequency harmonic (top plot) is better transmitted, whereas for $\sigma_a^2 = 2.0$ (third plot from above) propagation is better for the high-frequency signal (bottom plot). The behavior of the 5th oscillator in Fig. 3.7 can be compared with the corresponding response curves in Fig. 3.6.
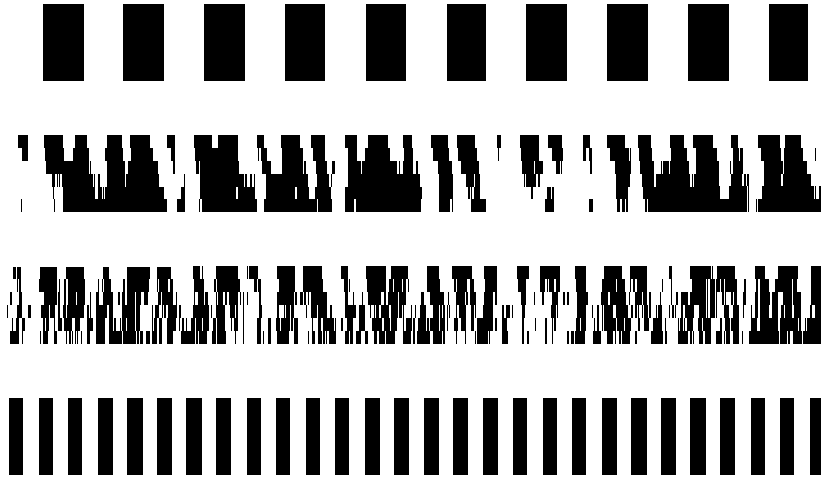
Figure 3.7: Symbol coding of the spatio-temporal evolution of the system. Time evolves along the horizontal axis, space along the vertical one. From top to bottom: low-frequency component of the signal ($cos(\omega_1 t)$); first six oscillators for $\sigma_a^2 = 0.65$; first six oscillators for $\sigma_a^2 = 2.0$; high-frequency component of the signal ($cos(\omega_2 t)$).

In conclusion, here we have analyzed the constructive effect of additive noise in the propagation of two-frequency (bichromatic) harmonic signals through discrete bistable media. The results show that noise enhances propagation of such signals, similarly to what happens with simpler monochromatic driving. Furthermore, we have shown that by changing the

noise intensity one is able to select the propagation frequency. We expect this effects to be also present with more general multifrequency signals. Hence, this results could be relevant in biological and technological contexts where harmonic signals with many frequencies are present or used.

Chapter 4

Noise-induced resonant effects and resonant effects in the presence of noise

4.1 Vibrational resonance in a noise-induced structure

It has been pointed out that stochastic resonance like phenomena can be also observed in systems where a chaotic signal is used instead of noise [182]. Moreover, in [104] it has been shown that a high-frequency periodic force can work as a noise and amplify the response to the low frequency periodic signal in bistable systems. This effect has been called Vibrational Resonance (VR) [104], analogously to SR. In VR the dependence of the system response versus the amplitude of the high-frequency action has a well-known bell-shaped resonant form. Since two-frequency signals are very often used in communication technologies [131], it means that an optimal high-frequency modulation may improve processing of a low-frequency signal. It is important to mention that two-frequency signals are also object of intensive interest in laser physics [188], acoustics[118], neuroscience[198], or physics of the ionosphere[67]. Here we investigate whether VR can be achieved in noise-induced structures, which do not have any threshold or a potential barrier in the absence of noise. For this purpose we consider a spatially extended system consisting of a network of coupled monostable noisy oscillators under the action of low- and high-frequency periodic signals. In this system a collective action of coupling and multiplicative noise results in the organization of bistability of the mean field. If the amplitude of a low-frequency signal is not enough for a synchronous response of the system, then the high-frequency force is applied. We find that an increase of the high-frequency amplitude leads to a non-monotonous change of the system response with a clearly defined maximum. Therefore, we present a new phenomenon, *vibrational resonance in a noise-induced structure*, which is a variation of SR.

We study this effect on a nonlinear lattice of coupled overdamped oscillators introduced in [195] and further studied in [196][5*]. The following set of Langevin equations describes the considered system:

$$\dot{x}_i = f(x_i) + g(x_i)\xi_i(t) + \frac{D}{2d}\sum_{j \in nn(i)}(x_j - x_i) + A\cos(\omega t) + B\cos(\Omega t), \qquad (4.1)$$

where $x_i(t)$ represents the state of the ith oscillator, $i = 1, ..., L^d$, in the cubic lattice of size L in d dimensions with $N = L^d$ elements. The sum runs over the $2d$ nearest neighbors of the ith cell [$nn(i)$], and the strength of the coupling is measured by D. The noisy term $\xi_i(t)$ represents Gaussian noise, with zero mean and uncorrelated both in space and time

$$\langle \xi_i(t)\xi_j(t') \rangle \quad = \quad \sigma_m^2 \delta_{i,j}\delta(t - t'). \qquad (4.2)$$

The last terms in (4.1) stand for external periodic forces, representing a low frequency signal with amplitude A, frequency ω, and a high-frequency signal with amplitude B and frequency Ω, where $\Omega >> \omega$ and these frequencies can be incommensurable.

For the sake of simplicity, the functions $f(x)$ and $g(x)$ are taken to be of the form [4*]:

$$f(x) = \begin{cases} -G_b x - (G_a - G_b)B_p & \text{if } x \leq -B_p, \\ -G_a x & \text{if } |x| < B_p, \\ -G_b x + (G_a - G_b)B_p & \text{if } x \geq B_p, \end{cases} \qquad (4.3)$$

79
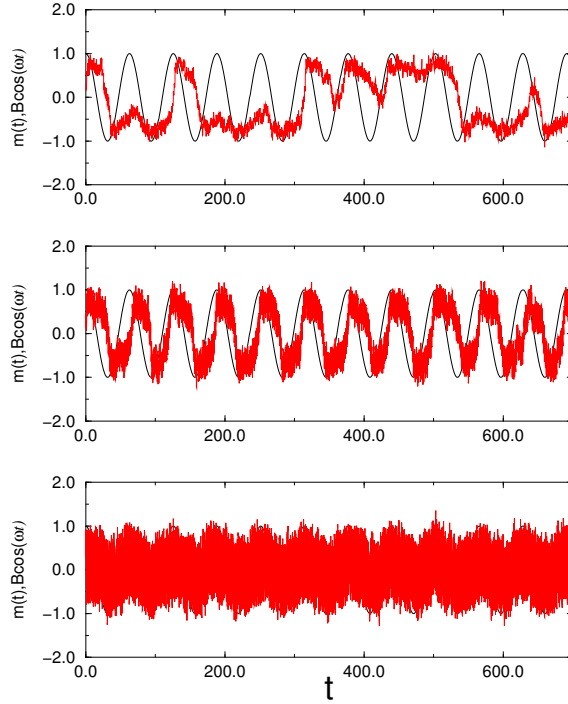
Figure 4.1: Time series of the mean field of the system (eq. 4.1) compared with the low-frequency signal $A\cos(\omega t)$ (not in scale) for different intensities of high-frequency vibration. From top to bottom, B=0.5, 1.5, and 4.0. $\Omega = 5.0, \omega = 0.1, A = 0.15, \sigma_m^2 = 3.0$. This intensity of multiplicative noise corresponds to the bistable region.

$$g(x) = x, \tag{4.4}$$

where the parameters $G_a = 0.5$, $G_b = 10$ and $B_p = 1$ determine the slopes and the breakpoint of the piecewise-linear characteristic curve (an approximation of the function $f(x) = -x - x^3$). Such forms of functions describe a realistic electronic circuit designed in [5*]. In the absence of the external force ($A = 0, B = 0$) this model can be solved analytically by means of a standard mean-field theory (MFT) procedure [65]. The mean-field approximation consists in replacing the nearest-neighbor interaction by a global term in the Fokker-Planck equation corresponding to (4.1). Using this mean-field approximation, one determines transitions between ordered ($m \neq 0$) and disordered ($m = 0$) phases[5*], where m is the mean field, defined as $m(t) = \frac{1}{L^d} \sum_{i=1}^{N} x_i(t)$. This analysis shows that the joint action of multiplicative noise and coupling between the elements leads to the bistability of the mean-field (ordered phase). If we fix the coupling strength above its critical value, then an increase of the multiplicative noise induces a disorder-order phase transition, which is followed by a reentrant transition to disorder [195]. In the ordered phase the system occupies one of two possible symmetric states with the mean fields $m_1 = -m_2 \neq 0$, depending on the initial conditions. This bistability disappears if we switch off the multiplicative noise.

Now let us turn to the problem, how the system (1) responds to a periodic signal which

Figure 4.2: Vibrational resonance in the noise-induced structure. Numerical simulations (a) vs experimental results for the effective model (b). Response Q of the system vs. the amplitude of the high-frequency force. In (a): $\sigma_m^2 = 3$ (label 1), 0.5 (label 2), and 0 (label 3); other parameters are the same as in Fig. 4.1
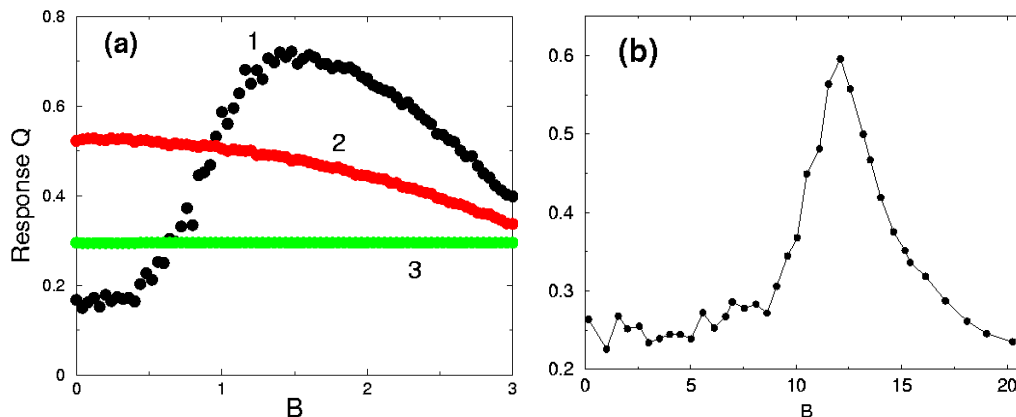
contains two very different frequencies (e.g. $\omega = 0.1$ and $\Omega = 5$). First, we analyze the behavior of the system in the parameter region (the parameters being the coupling strentgh and the multiplicative noise intensity) where the noise-induced bistability is provided. We set the amplitude of the low frequency signal A fixed and sufficiently small (e.g. $A = 0.15$), which is not enough to cause jumps between two potential wells. The time series of the mean field $m(t)$ and the corresponding periodic input signal are plotted in Fig. 4.1 for three different values of B (increasing from top to bottom). For a small amplitude B we observe rare jumps between the two symmetric states m_1 and m_2 in the output, which are not synchronized with the low-frequency signal (here $d = 2$ and $N = 10$). If we increase B to its optimal value (in the middle), it is clearly seen that hops occur with the same periodicity as the input signal. Hence, the high-frequency modulation optimizes signal processing in this noise-induced bistable structure. Further increase of B leads to oscillations-hops at the high frequency, which completely hide the signal at the low frequency. The situation differs qualitatively when we choose another intensity of multiplicative noise corresponding to the monostable region. In this case, an increase of B leads only to the destruction of synchronization between input and output. Hence, the high-frequency modulation is unable to improve the quality of signal processing at low frequency in this case. Therefore, the system considered exhibits *vibrational resonance in a noise-induced structure* only when a collective bistability has been created by multiplicative noise and coupling. To characterize this VR-effect quantitatively, we calculate the dependence of the system response Q at the signal frequency on the amplitude of the high-frequency force (Fig. 4.2 a). For the bistable regime the response curve (label 1) exhibits a clearly defined maximum for the optimal value of B, which gives evidence for the presence of VR. Note that this effect disappears if we decrease (label 2) or switch off (label 3) the multiplicative noise: in this case an increase of the amplitude of a high-frequency force may lead only to the decrease
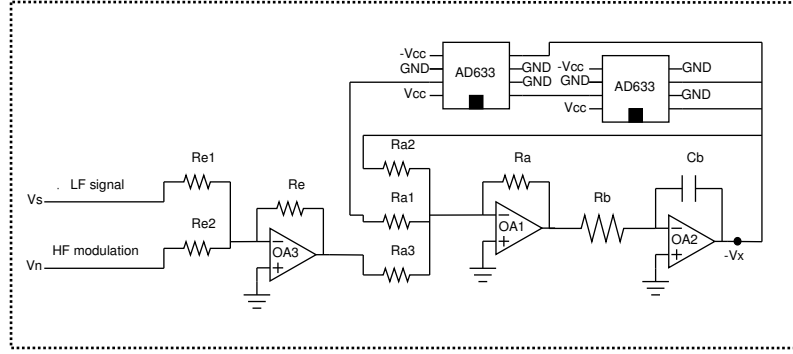
Figure 4.3: Electronic circuit for the effective model (eq. 4.7).

of the system response.

The mechanism of this effect can be understood as follows. As it has been shown above, the equation for the maximum of the probability, which is also the average value $\bar{x} = \langle x \rangle$ in this approximation, takes the following form

$$\dot{x} = f(\bar{x}) + \frac{\sigma_m^2}{2} g(\bar{x}) g'(\bar{x}), \tag{4.5}$$

which is valid if $f(\langle x \rangle) >> \langle \delta x^2 \rangle f''(\langle x \rangle)$. For this dynamics an "effective" potential $U_{\text{eff}}(x)$ can be derived, which has the form

$$U_{\text{eff}}(x) = U_0(x) + U_{\text{noise}} = - \int f(x)dx - \frac{\sigma_m^2 g^2(x)}{4}, \tag{4.6}$$

where $U_0(x)$ is a monostable potential and U_{noise} represents the influence of the multiplicative noise. In the region, where VR in the noise-induced structure is observed, this potential has a bistable form due to the input provided by multiplicative noise. This effect may be understood assuming a model of an overdamped system with a bistable potential under the action of a high- and a low-frequency periodic force:

$$\dot{m} = F(m) + A\cos(\omega t) + B\cos(\Omega t) + \xi(t), \tag{4.7}$$

where $m(t)$ is the mean-field of the initial system, and the function $F(x)$ describes a bistable potential. The noisy term $\xi(t)$ denotes tiny fluctuations, which are present in every real system.

To verify the behavior of this effective model, we have constructed an electronic circuit (Fig. 4.3), which is composed of two main parts. The first part is an adder, whose function is to add a low and a high frequency signal (operational amplifier OA3 and resistors R_e, R_{e1}, and R_{e2}). The second part is the integrator in the double-well potential, which consists of another adder ($R_a, R_{a1}, R_{a2}, R_{a3}$ and OA1), two multiplyers (AD633 with coefficient α), and an integrator (R_b, C_b and OA2). Taking into account that the output of OA2 is $-V_x$, the equation describing
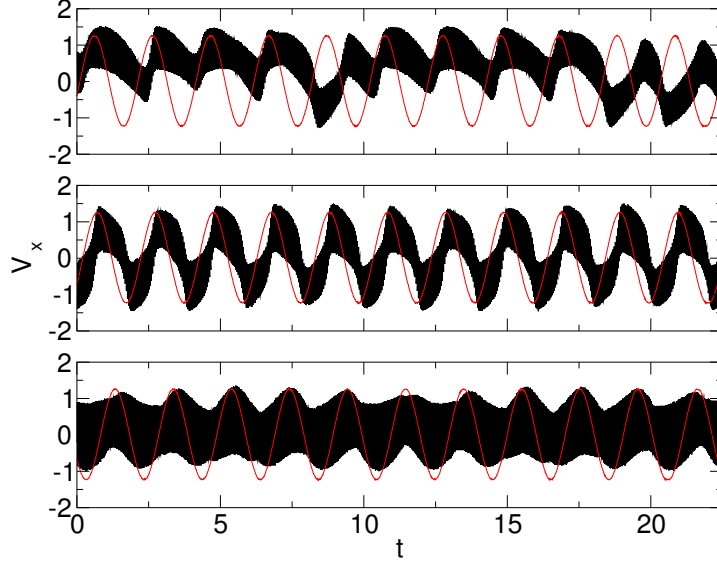
Figure 4.4: Vibrational resonance in the experiment (Fig. 3): in the middle plot the processing is optimal. From top to bottom: increase of the amplitude of the high frequency $B = 9.57, 10.88, 15.41$.

the behavior of the circuit is given by

$$R_b C_b \dot{V} x = -V_{HL} \frac{R_a}{R_{a3}} + V_x \frac{R_a}{R_{a2}} - \alpha^2 \frac{R_a}{R_{a1}} V_x^3, \qquad (4.8)$$

where α is a parameter introduced by the multiplier circuits and V_{HL} is the weighted sum of the low and high-frequency signals.

The experimental results from a digital oscilloscope are shown in Fig. 4.4. In the upper panel the jumps between wells are very rare ; in (Fig. 4.4 down) the amplitude is so high that the "particle" always overcome the potential barrier. However, for intermediate values of the high-frequency signal the jumps of the particle are synchronized with the low frequency signal showing the VR phenomenon described here, (Fig. 4.4 middle). Hence, by this experiment we have shown qualitatively that the "effective" model undergoes the effect of VR, which in the initial system occurs in the noise-induced structure.

It is worth to note that not every system with noise-induced bistability exhibits vibrational resonance. For example, zero-dimensional systems, described in [81], demonstrate noise-induced bistability due to the bistability of a so called "stochastic" potential but do not show a pronounced VR. Although it is possible to observe a small maximum in the response of the system, a further increase of the multiplicative noise, which provides bistability, decreases

83

the response of the system.

In conclusion, we have described the novel phenomenon of the existence of vibrational resonance in a noise-induced structure. This effect is a synthesis of a noise-induced phase transition and vibrational resonance. High-frequency carrier force is able to optimize signal processing, and this process can be controlled by multiplicative noise. Numerical simulations for a spatially extended system has been confirmed by a experimental results for a zero-dimensional "effective" model. We expect that due to its generality, this effect can be of a great importance in communication technologies.

These theoretical findings can stimulate experimental work in order to verify VR in noise-induced structures in real physical systems (for the first experimental observation of noise-induced bistability see [73]). Appropriate situations can be found in electronic circuits [5*], electronic cellular [149, 11, 158], as well as in systems which show a noise-induced shift of the phase transition, e.g, in: liquid crystals [93], photosensitive chemical reactions [128], or Rayleigh-Bénard convection [127]. The results presented here might be crucial for such experiments because in the noise-induced structure presented here, the bistability of the mean-field is controlled by noise.

4.2 System size resonance in coupled noisy systems

In 2.1 we have shown that noise-induced bistability can lead to stochastic resonance phenomena in the presence of additional signal. Here we investigate another effect, system size resonance, and show that it is also possible in systems with noise-induced bistability. In stochastic resonance there exists a "resonant" noise intensity at which the response to a periodic force is maximally ordered. Being first discussed in the context of a simple bistable model, stochastic resonance has been also studied in complex systems consisting of many elementary bistable cells [87, 134, 26, 61, 88]. Again, as in the conventional SR one observes a resonance-like dependence on the noise intensity, moreover, the resonance may be enhanced due to coupling [112, 113]. Here we discuss another type of resonance in such systems, namely the *system size resonance*, when the dynamics is maximally ordered at a certain number of interacting subsystems. Contrary to previous reports of array-enhanced stochastic resonance phenomena (cf. [112, 113]), here we fix the noise strength, coupling, and other parameters; only the the size of the ensemble changes.

The basic model to be considered below is the ensemble of noise-driven bistable overdamped oscillators, governed by the Langevin equations

$$\dot{x}_i = x_i - x_i^3 + \frac{\varepsilon}{N} \sum_{j=1}^{N} (x_j - x_i) + \sqrt{2D}\xi_i(t) + f(t) . \tag{4.9}$$

Here $\xi_i(t)$ is a Gaussian white noise with zero mean: $\langle \xi_i(t)\xi_j(t') \rangle = \delta_{ij}\delta(t-t')$; ε is the coupling constant; N is the number of elements in the ensemble, and $f(t)$ is a periodic force to be specified later. In the absence of periodic force the model (4.9) has been extensively studied in the thermodynamic limit $N \to \infty$. It demonstrates an Ising-type phase transition from the disordered state with vanishing mean field

$$X = N^{-1} \sum_i x_i \tag{4.10}$$

to the "ferromagnetic" state with a nonzero mean field $X = \pm X_0$. A theory of this transition, based on the nonlinear Fokker-Planck equation, was developed in [36], where also the expressions for the critical coupling ε_c are given.

While in the thermodynamic limit the full description of the dynamics is possible, for finite system sizes we have mainly a qualitative picture. Formally, for finite ensembles the average of the mean field $\langle X \rangle$ vanishes for all couplings. However, in the ordered phase (i.e. for $\varepsilon > \varepsilon_c$) the mean field X switches between the values $\pm X_0$. The rate of switchings depends on the system size and tends to zero as $N \to \infty$. The asymptotic dynamics in this limit has been discussed in [31].

For us, of the main importance is the fact that qualitatively the behavior of the mean field can be represented as the dynamics of a nonlinear noise-driven variable, with the effective noise vanishing in the thermodynamic limit. A nonlinear potential of this effective dynamics has one minimum in the disordered phase (at $X = 0$) and has two symmetric minima (at $X = \pm X_0$) in the ordered phase. Now we can apply the ideas of the stochastic resonance to

this effective noise-driven oscillator. In the bistable case, (i.e. in the ordered phase for small enough noise or for large enough coupling), one can expect a resonant-like behavior of the response to a periodic external force when the intensity of the effective noise is changed. Because this intensity is inverse proportional to N, we obtain the resonance-like curve of the response in dependence of the system size.

The main idea behind the system size resonance is that in finite ensembles of noise-driven systems the dynamics of the mean field can be represented as driven by the effective noise whose variance is inverse proportional to the system size. For the rigorous proof of the validity of this approach see [31]. This idea has been applied to description of a transition to collective behavior in [152]. In [154] it was demonstrated that the finite-size fluctuations can cause a transition that disappears in the thermodynamic limit. The description of finite-size effects in deterministic chaotic systems using the effective noise concept has been suggested in [155, 76]. We emphasize that noise plays an essential role in this picture: with $D = 0$ (4.9) is a deterministic oscillator (double or single well, depending on ε), whose response to a periodic force does not depend on N.

Before proceeding to a quantitative analytic description of the phenomenon, we illustrate it with direct numerical simulations of the model (4.9), with a sinusoidal forcing term $f(t) = A\cos(\Omega t)$. Figure 4.5 shows the linear response function, i.e. the ratio of the spectral component in the mean field at frequency Ω and the amplitude of forcing A, in the limit $A \to 0$. For a given frequency Ω the dependence on the system size is a bell-shaped curve, with a pronounced maximum. The dynamics of the mean field $X(t)$ is illustrated in Fig. 4.6, for three different system sizes and for a particular frequency. The resonant dynamics (Fig. 4.6b) demonstrates a typical for stochastic resonance synchrony between the driving periodic force and the switchings of the field between the two stable positions. For non-resonant conditions (Fig. 4.6a,c) the switchings are either too frequent or too rare, as a result the response is small.

To describe the system size resonance analytically, we use, following [36], the Gaussian approximation. In this approximation one writes $x_i = X + \delta_i$ and assumes that δ_i are independent Gaussian random variables with zero mean and the variance M. Assuming furthermore that

$$\frac{1}{N}\sum_i \delta_i^2 = M\,,$$

and neglecting the odd moments $N^{-1}\sum_i \delta_i$, $N^{-1}\sum_i \delta_i^3$, as well as neglecting the correlations between δ_i and δ_j, we obtain from (4.9) the equations for X and M:

$$\dot{X} \;=\; X - X^3 - 3MX + \sqrt{\frac{2D}{N}}\eta(t) + f(t)\,, \tag{4.11}$$

$$\frac{1}{2}\dot{M} \;=\; M - 3X^2M - 3M^2 - \varepsilon M + D\,, \tag{4.12}$$

where η is the Gaussian white noise having the same properties as $\xi_i(t)$. In the thermodynamic limit $N \to \infty$ the noisy term η vanishes. If the forcing term is absent ($f = 0$), the equations coincide with those derived in [36]. This system of coupled nonlinear equations (4.11,4.12) exhibits a pitchfork bifurcation of the equilibrium $X = 0$, $M > 0$ at $\varepsilon_c = 3D$. This
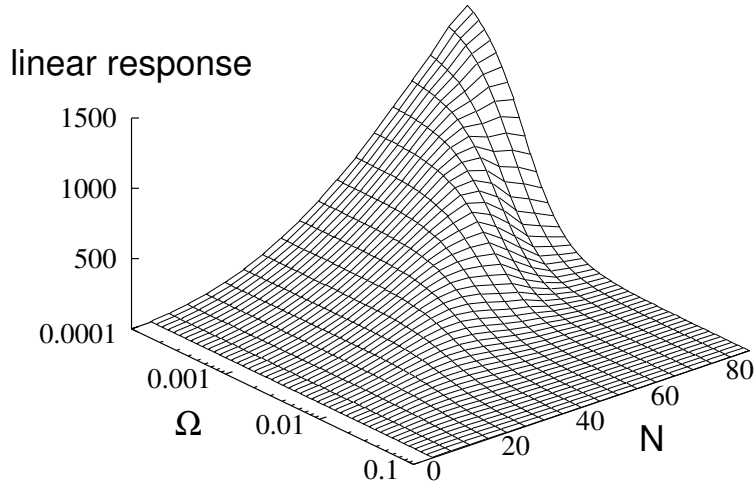
Figure 4.5: Dependence of the linear response of the ensemble (4.9) of noise-driven bistable systems ($D = 0.5$, $\varepsilon = 2$) on the frequency of forcing and the system size N. The response to forces with smaller frequencies is shifted to larger system sizes, where the effective noise, and, consequently, the switching rate, is smaller. The linear response is obtained by virtue of the fluctuation-dissipation theorem.
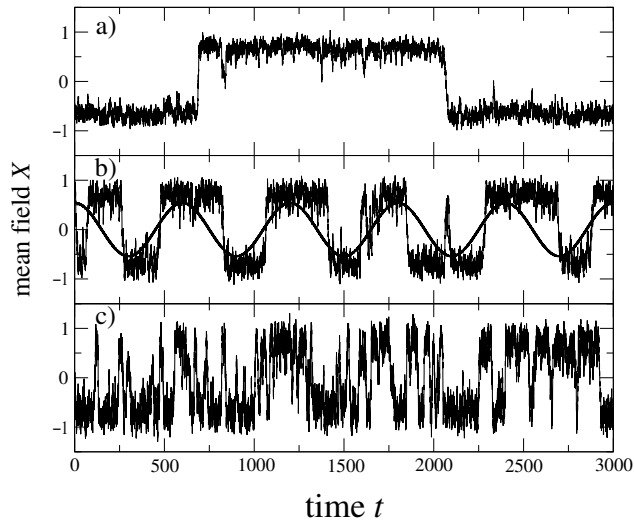
Figure 4.6: The time dependence of the mean field in the ensemble (4.9) for $D = 0.5$, $\varepsilon = 2$, $A = 0.02$, $\Omega = \pi/300$, and different sizes of the ensemble: (a) $N = 80$, (b) $N = 35$, and (c) $N = 15$. In (b) we also depict the periodic force (its amplitude is not in scale) to demonstrate the synchrony of the switchings with the forcing.

bifurcation is supercritical for $D > 2/3$ in accordance with the exact solution given in [36], below we consider only this case. For $\varepsilon > \varepsilon_c$ the system is bistable with two symmetric stable

fixed points

$$X_0 = \pm(2 - \varepsilon + \sqrt{(2+\varepsilon)^2 - 24D})^{1/2}/2, \qquad (4.13)$$

$$M_0 = (2 + \varepsilon - \sqrt{(2+\varepsilon)^2 - 24D})/12,$$

and the unstable point $X = 0$, $M = (1 - \varepsilon + \sqrt{(1-\varepsilon)^2 + 12D})/6$. Now, with the external noise η and with the periodic force $f(t)$ the problem reduces to a standard problem in the theory of stochastic resonance, i.e. to the problem of the response of a noise-driven nonlinear bistable system to an external periodic force (because the noise affects only the variable X, it does not lead to unphysical negative values of variance M, since $\dot{M}$ is strictly positive at $M = 0$). This response has a maximum at a certain noise intensity, which according to (4.11) is directly related to the system size.

To obtain an analytical formula, we perform further simplification of the system (4.11),(4.12). Near the bifurcation point the dynamics of X is slower than that of M, and we can exclude the latter one assuming $\dot{M} \approx 0$. Then from (4.12) we can express M as a function of X and substitute to (4.11). Near the bifurcation point we obtain a standard noise-driven bistable system

$$\dot{X} = aX - bX^3 + \sqrt{\frac{2D}{N}}\eta(t) + f(t), \qquad (4.14)$$

where $a = 1 + 0.5(\varepsilon - 1) - 0.5\sqrt{(\varepsilon-1)^2 + 12D}$, $b = -0.5 + 1.5(\varepsilon - 1)((\varepsilon-1)^2 + 12D)^{-1/2}$. A better approximation valid also beyond a vicinity of the critical point can be constructed if we use $\bar{b} = aX_0^{-2}$ instead of b, where the fixed point X_0 is given by (4.13). Having written the ensemble dynamics as a standard noise-driven double-well system (4.14) (cf. [53]), we can use the analytic formula for the linear response. It reads

$$\eta = \frac{NX_0^2}{2Da}\left(\frac{\mathcal{D}_{-3/2}(-\sqrt{s})}{\mathcal{D}_{-1/2}(-\sqrt{s})}\right)^2 \left[1 + \frac{\pi^2 \Omega^2}{2a^2}\exp(s)\right]^{-1} \qquad (4.15)$$

where $s = aNX_0^2/(2D)$, and $\mathcal{D}$ are the parabolic cylinder functions. We compare the theoretical linear response function with the numerically obtained one in Fig. 4.7. The qualitative correspondence is good, moreover, the maxima of the curves are rather good reproduced with the formula (4.15). This shows that the resonant system size is quite good quantitatively described by the Gaussian approximation, see Fig. 4.8.

Above we concentrated on the properties of the linear response. Numerical simulations with the finite forcing amplitude yielded the results similar to that presented in Figs. 4.5,4.7. However, for large amplitudes of forcing (e.g., $A > 0.1$ for $\Omega = 0.01$, $D = 0.5$, $\varepsilon = 2$) a saturation was observed: here the response grows monotonically with N. This is in full agreement with the corresponding property of the stochastic resonance in double-well systems of type (4.14), where the saturation occurs for small noise intensities (cf. Fig. 7 in [53]). Qualitatively, the saturation is due to the disappearance of multistability for large forcing amplitudes, so that the oscillator (4.14) switches at every period of the forcing, contrary to the case of small amplitudes, where the switchings are rare (Fig. 4.6a).

Above we have considered the system of globally coupled nonlinear oscillators (4.9). The
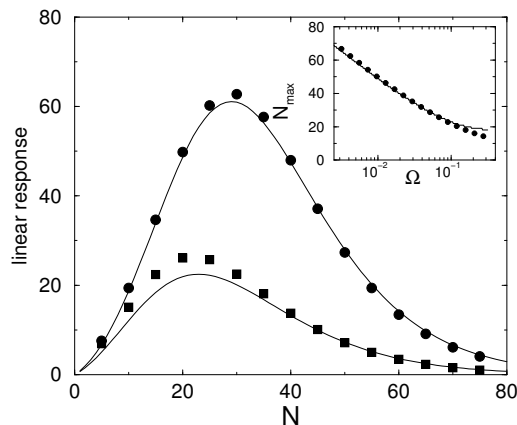
Figure 4.7: Comparison of the system-size dependencies of the linear response function for frequencies $\Omega = 0.05$ (circles) and $\Omega = 0.1$ (squares) with theory (4.15). The parameters are $D = 1$ and $\varepsilon - \varepsilon_c = 2.5$ (where the the exact ε_c and the approximate $\varepsilon_c = 3D$ are used for the ensemble and the Gaussian approximation, respectively).
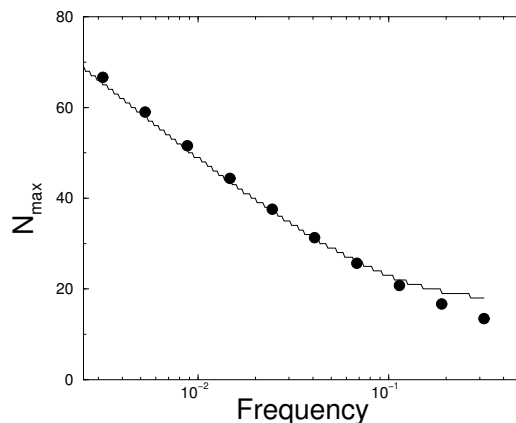
Figure 4.8: Dependence of the system size yielding maximal linear response on the driving frequency Ω. Circles: simulations of the ensemble (4.9), line is obtained by maximizing the expression (4.15).

same effect of system size resonance can be observed in a lattice with nearest neighbors coupling as well. Then, instead of (4.9), we have

$$\dot{x}_i = x_i - x_i^3 + \frac{\varepsilon}{K} \sum_{\langle ij \rangle} (x_j - x_i) + \sqrt{2D}\xi_i(t) + f(t) \,, \qquad (4.16)$$

where the number of nearest neighbors K depends on the geometry of the lattice and on the dimension of the space. In the thermodynamic limit, the Ising-type phase transition occurs in the lattice (if its dimension is larger than one). Similar to the globally coupled ensemble, in finite lattices in the ordered phase the switchings between the two stable states of the mean field are observed. With the same argumentation as above we can conclude that the response of the mean field to a periodic forcing $f(t)$ can have a maximum at a certain lattice size,

while all other parameters (noise intensity, coupling strength, etc.) are kept constant. We illustrate this in Fig. 4.9. Here the two-dimensional lattice with periodic boundary conditions is studied. In order to keep the lattice of nearly quadratic form, we have chosen the lattices with sizes either l^2 or $l(l+1)$, with $l = 2, 3, 4, \dots$. The response to the periodic force has a pronounced maximum at a certain size of the system.
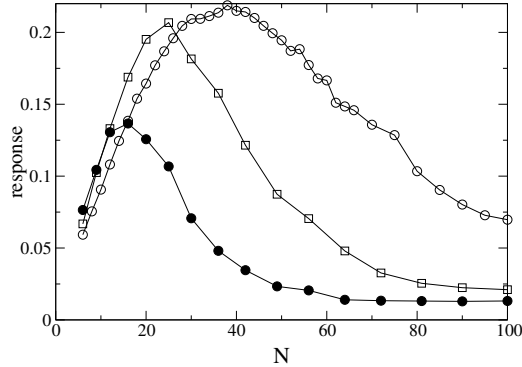
Figure 4.9: Filled circles: Response of a rectangular two-dimensional lattice of N nonlinear bistable noise-driven elements (4.16) to a periodic force with amplitude $A = 0.02$ and period $T = 500$. The noise intensity is $D = 0.5$, the parameter of nearest-neighbors coupling $\varepsilon = 4$. Squares: Response of system (4.17) (a two-dimensional lattice with $D = 1.25$, $\varepsilon = 30$, $A = 0.1$ and $T = 140$). Circles: the same as squares, but for a globally coupled lattice with $D = 1$, $\varepsilon = 20$, $A = 0.1$ and $T = 100$.

As the last example of the system size resonance we consider a lattice where each individual element does not exhibit bistable noisy dynamics, but such a behavior appears due to interaction and multiplicative noise. This model is described by the set of Langevin equations (see for details the section 2.1)

$$
\begin{aligned}
\dot{x}_i &= -x_i(1 + x_i^2)^2 + \frac{\varepsilon}{K}\sum_j (x_j - x_i) \\
&\quad + \sqrt{2D}\xi_i(t)(1 + x_i^2) + A\cos(2\pi t/T) \ .
\end{aligned}
\tag{4.17}
$$

The difference to the model (4.9) is that the noise is multiplicative and the on-site potential has only one minimum. K is the number of elements to which the oscillator i is coupled, for global coupling $K = N$ and for a lattice of dimension d with nearest-neighbors coupling $K = 2d$. As has been demonstrated in [194, 195], in some region of couplings ε system (4.17) exhibits the Ising-type transition, characterized in the thermodynamic limit $N \to \infty$ by the onset of nonzero mean field X. Due to the symmetry of (4.17), there are states with positive and negative mean field. If an additional additive noise is added to (4.17), then one observes transitions between these states and the so-called double stochastic resonance in the presence of the periodic forcing [4*,5*]. As is evident from the considerations above, such transitions occur even in the absence of the additive noise if the system is finite. Thus, the system size resonance should be observed in the lattice (4.17) as well. We confirm this in Fig. 4.9.

Another possible field of application of the system size resonance is the neuronal dynamics (see, e.g., [189]). Individual neurons have been demonstrated to exhibit stochastic reso-

nance [116, 40]. While in experiments one can easily adjust noise to achieve the maximal sensitivity to an external signal, it may be not obvious how this adjustment takes place in nature. The above consideration shows, that changing the number of elements in a small ensemble of coupled bistable elements to the optimum can significantly improve the sensitivity (cf. [87]). Moreover, changing its connectivity and/or coupling strength, a neuronal system can tune itself to signals with different frequencies.

Concluding, we have shown that in populations of coupled noise-driven elements, exhibiting in the thermodynamic limit the Ising-type transition, in the ordered phase (i.e. for relatively small noise and large coupling) the response to a periodic force achieves maximum at a certain size of the system. We demonstrated this effect for lattices and globally coupled ensembles noisy oscillators. We expect the system size resonance to occur also in purely deterministic systems demonstrating the Ising-type transition, e.g. in the Miller-Huse coupled map lattice [130]. The system size resonance is described theoretically by reducing the dynamics of the mean field to a low-dimensional bistable model with an effective noise that is inverse proportional to the system size. The stochastic resonance in the mean field dynamics then manifests itself as the system size resonance.

4.3 Coherence resonance and polymodality in inhibitory coupled excitable oscillators

Coherence resonance(CR) has been reported in different kinds of systems, in particular, it has been found that some noise amplitude exists at which the coherence of spiking in the output of the system can be significantly enhanced in an isolated Fitz-Hugh Nagumo (FHN) system [150], in the Hodgkin-Huxley [106] and Plant/Hindmarsh-Rose neuron models [115], in dynamical systems close to the onset of bifurcations [138], or in experimentally studied laser [68]. On the base of another mechanism, in contrast to excitable systems, CR has been also found in the behaviour of a dynamical system, which shows jumps between several attractors [144].

The CR behaviour have been also studied in spatially extended systems consisting of many interacting elements[77, 139]. It has been shown that matching the noise-related characteristic time scales of the coupled excitable elements results in noise-induced synchronization regimes very similar to those for coupled limit cycles. Moreover, *array-enhanced CR* has been reported, in which constructing an array of coherence-resonance oscillators significantly improves the periodicity of the output [82, 210]. To our knowledge, all these studies of the CR behaviour have been performed in systems with coupling via fast variable exchange or pulsed coupling which activates the neighbors. These modes of coupling lead to many collective phenomena, including noise-induced spiral waves [88] and "clustering" of FHN stochastic oscillators [184]. As a consequence of this form of activatory coupling in spatially extended system, CR may happen only if coupled oscillators move synchronously and *in-phase*. However, other interactions between stochastic oscillators, for example inhibitory coupling, are also very interesting and reported to be important in numerous physical[95], electronical [170] and chemical systems[197, 27]. To be particular, the inhibitory form of coupling is used to explain morphogenesis in Hydra regeneration and animal coat pattern formation [126, 98], or to provide the understanding of pattern formation in an electron-hole plasma and low temperature plasma [95]. In chemistry, the effective increase of inhibitor diffusion by reducing of activator diffusivity via the complexation of iodide (activator) with the macromolecules of starch results in a Turing structure formation [108]. It is interesting to note that systems with inhibitory coupling in its rhythmogenic activity resemble very much systems with time delay [96, 159].

Following this motivation, here we study a system of noise-driven FHN elements, which are coupled, in contrast to previous studies of CR, by the slow variable, i.e. by a diffusive inhibitory coupling. This delays the firing of an element, if its neighbors are firing. We show that a system of two coupled excitable elements demonstrates CR, which is intrinsically based on *the anti-phase behaviour* of the elements. This is a new mechanism of CR, which works via noise-induced synchronization in antiphase [151] of excitable elements. We demonstrate that this effect is connected to the fact, that such systems have very rich dynamics in the generation of rhythms, and, as a result, generate a polymodal interspike distribution. It is important to note that the generation of polyrythms is an important problem in the description of several natural processes, such as locomotion [29] or playing piano [44]. Recently,

many model investigations have been motivated by experimental studies of the firing activity of neurons that revealed polymodality in the interspike interval histograms (ISIH) [46], [179] or studies of locomotor behaviour of halobacterium [176]. The most interesting feature of such systems is the appearance of polymodality even without additional forcing. In this study, we show that the application of an inhibitory coupling in a system of excitable oscillators is another possible mechanism for the generation of polymodality without any external periodic stimuli. We study this behaviour in systems of two and three coupled elements and show how the degree of coherence can be controlled by the noise amplitude and the coupling strength. Such a nontrivial behaviour can be expected from the possibility of noise-induced generation of coupling-dependent transient out-of-phase stochastic attractors in the phase space. For two-dimensional FHN limit cycles, inhibitory coupling results in the appearance of out-of-phase limit cycles which are stable in large areas of the parameter space if the stiffness is large. The overlapping of the in-phase and the anti-phase limit cycles is typical for two or three coupled oscillators and depends on the stiffness[200, 201].

We begin with the study of two FHN systems, coupled via diffusive exchange of the recovery (slow) variable, which is a kind of mutual inhibition of motion of the phase points along the slow part of the FHN N-shaped nullcline. The equations of motion for identical bidirectionally coupled elements are

$$\frac{dx_{1,2}}{dt} = A - y_{1,2} + C(x_{2,1} - x_{1,2}) + \xi_{1,2} \tag{4.18}$$

$$\varepsilon \frac{dy_{1,2}}{dt} = x_{1,2} - y_{1,2}^3/3 + y_{1,2} \tag{4.19}$$

Here, $\varepsilon << 1$ is a small parameter, which determines that y_i are the fast variables and A is responsible for the excitatory properties of the isolated elements. It is well known that for $|A| > 1$ the only attractor is a stable fixed point. For $|A| < 1$, the limit cycle generates a periodic sequence of spikes. The choice of ranges for ε and A is crucial in this study. We fix A close to the bifurcation in the interval $(1.01 \div 1.03)$ in order not to use high-level noise (parameter D) to excite oscillation and thereby to avoid masking of the fine structure of the ISIHs. Here ε is in the range $(.001 \div .0001)$, which is significantly smaller compared to those that are commonly used [150], [139]. To emphasize this specifically small value of ε, the term "relaxator" will be used instead of "very relaxation oscillator". The stochastic forcing is represented by Gaussian white noise ξ_i with zero mean and intensity $2D$: $\langle \xi_i(t)\xi_j(t+\tau)\rangle = 2D\delta(\tau)\delta_{i,j}$.

For numerics we take the standard constant-step Runge-Kutta fourth-order routine with the white noise added according to the algorithm [78]. In cases of any doubt, control runs have been done with smaller steps. The ISIH usually contains about 10,000 interspike intervals, ensuring a reasonable statistical accuracy. The numerical results are presented in Fig. 4.10. For weak noise (Fig. 4.10*left*(a)) the distribution is polymodal with equidistant positions of the peaks and progressively decreasing peak amplitudes. Hence, the inhibitory coupling really provides a mechanism for polyrhythm generation in a system of FHN oscillators. A 2.5-fold increase of the noise amplitude shifts the peak positions and their relationships. The second peak becomes now the main one (Fig. 4.10*left*(b)); however, the polymodal structure of the ISIH is still preserved. A further increase in the noise amplitude results in the disappearance
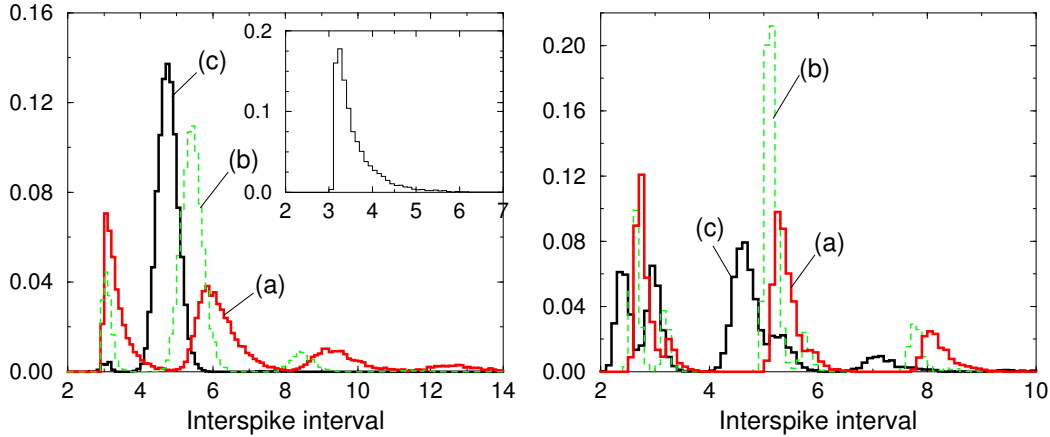
Figure 4.10: (left) Interspike interval histograms for two coupled very stiff ($\varepsilon = .0001$) relaxators Eqs.(1,2) for A=1.01, C=0.1: (a) $D = 10^{-6}$, (b) $D = 2.5 \times 10^{-6}$, (c) $D = 10^{-5}$; (right) The same for a larger coupling C=0.6: (a) $D = 10^{-6}$, (b) $D = 10^{-5}$, (c) $D = 10^{-3}$. The built-in plot corresponds to the typical histogram for a system with activatory coupling ($C = 1.5$).

of polymodality because of the global dominance of the second peak (Fig.4.10 *left* (c)). The spiking behavior becomes highly regular. This simple ISIH shape is observed in a broad range of noise amplitudes (at least up to $D = 10^{-3}$). For comparison, in the similar system but with an activatory coupling, the ISIH has always the same structure with one peak, as it is shown in the built-in plot in the Fig. 4.10*left*.

These qualitative changes in the ISIH shape may be explained by analyzing the stochastic time series. As in [150], the characteristic time of isolated stochastic oscillations is the sum of the activation and excursion times. The former is the waiting time of the appropriate excitation and fluctuates in a broad range; the latter is almost constant ($T_{ex} \approx 3$ for our parameters). At low noise amplitudes and low coupling strengths, the shape and position of the first peak in Fig.4.10 *left*(a) are very similar to those of the entire ISIH for each isolated element and for activatory coupled elements (built-in plot in Fig. 4.10*left*). The origin of the ISIH polymodality is seen from the time dependences of the slow variables as presented in Fig.4.11(a). At this particular noise amplitude, the average activation time is such that the order of spike generation by the two relaxators excited near the steady state does not depend on the coupling. However, as soon as one element fires, the phase point of the other element moves away from the excitation threshold due to a slow variable exchange (see Fig.4.11(b)). In other words, when the noise amplitude is low, the second element is unlikely to fire, while its neighbor makes an excursion. This simple consideration explains why the average interpeak interval equals nT_{ex}. Obviously, the probability of three consecutive firings of the same element is lower than that of two consecutive firings; therefore, the greater the number of the peak, the lower the peak amplitude. If the noise amplitude increases at a fixed coupling strength, the activation time becomes shorter, and the antiphase noise-induced regime as well as the previously described random excitations begin to compete. Their competition enlarges the second peak in the ISIH and shifts it to the left (Fig. 4.10 *left*(b)), because the augmented noise may induce one element to fire slightly before the other finishes its excursion. A further in-
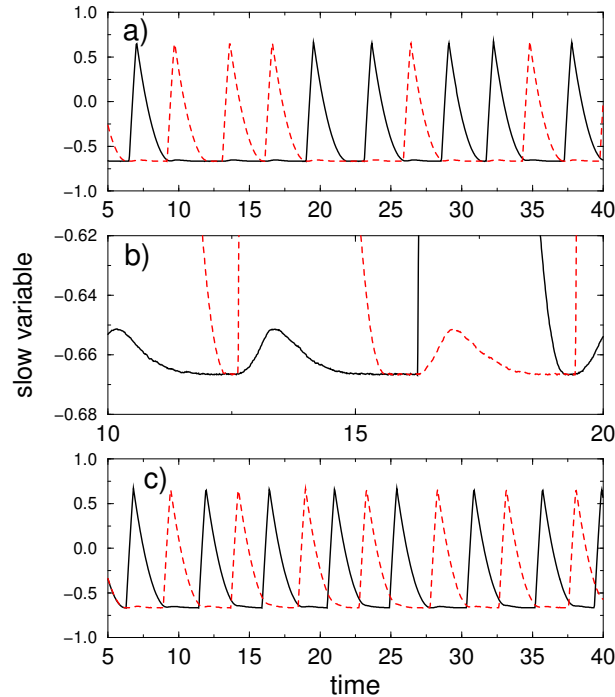
Figure 4.11: Typical waveforms of the slow variables for the cases (a) and (c) in Fig.4.10 left. (b) - the zoom of (a) in the area near the firing point.

crease in the noise amplitude leads to the full dominance of antiphase stochastic oscillations (Fig. 4.11*left*(c)), as can be seen from the waveforms presented in Fig.4.11(c).

Additional calculations (as in [200, 201]) show that the dominance of the antiphase regime is not surprising because the basin of attraction of the antiphase deterministic limit cycle (e.g., for A=.98) is significantly larger for coupling strengths $.1 < C < .3$ than the in-phase regime basin. This is not the case for larger values of coupling, for which even strong noise is unable to induce coherency via antiphase motion. Fig. 4.10 *right* shows the ISIH for C=0.6 and for different noise levels. In the case of low-level noise, the ISIH shape is as in the Fig. 4.10 *left*(a), because changes in the coupling strength are not significant for the mechanism of equidistant polymodality. The other two histograms, Fig. 4.10 *right*(b) and (c), are different from those in Fig. 4.10 *left* in that (i) anti-phase stochastic oscillations are not dominant in them, and (ii) their peaks are split (especially the first peak of histograms). The effect of peak splitting is a bright manifestation of the dual role of the coupling we consider: on the one hand, it causes the phase points to move more slowly when they are on different branches of the nullcline; on the other hand, it reduces the phase shift between them when they are on the same branch.

Hence, at A=1.01, we find two main scenarios (Figs. 4.10 *left* and *right*), how noise controls the evolution of ISIH polymodality. Both regimes, which differs in the value of coupling, demonstrate polymodality, but only for small values of coupling noise is able to suppress this behaviour and induces a coherent motion via anti-phase oscillations. These observations hold not only if the system is very close to the bifurcation point. For example, for A=1.03, the main

Figure 4.12: (*left*) Coherence resonance in inhibitory coupled noise-driven excitable oscillators. Correlation time τ_c vs the noise intensity for different coupling stren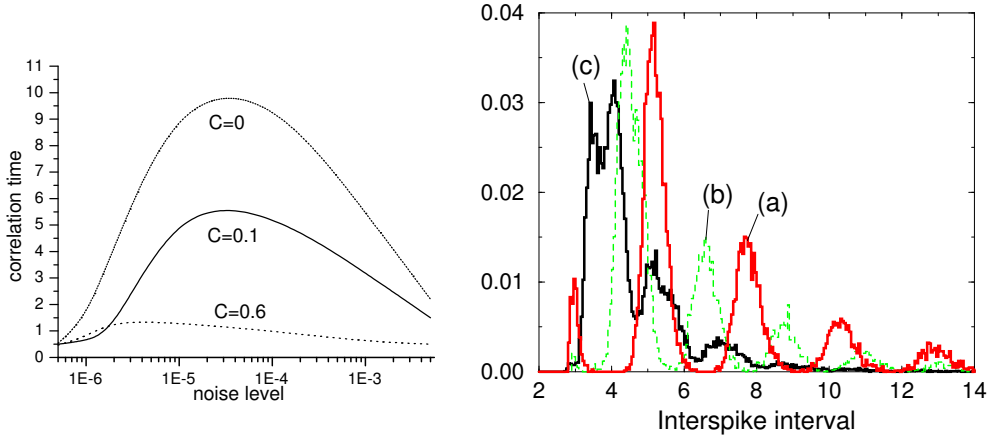gths C. $A = 1.01$; (*right*)Interspike interval histograms for a ring of three very stiff relaxators ($\varepsilon = .0001$ for C=0.1, A=1.01). (a) $D = 2 \times 10^{-6}$, (b) $D = 10^{-5}$, (c) $D = 10^{-4}$.

steps of the ISIH evolution do not change, but a significantly stronger noise is required for overcoming the threshold.

The changes in the ISIH structure with the noise amplitude increasing in the range from 10^{-6} to 10^{-3} clearly indicate a growing coherence of ISIs, which is especially strong for small values of coupling. In order to characterize this effect quantitatively, we compute the normalized autocorrelation function of the slow variable: $C(\tau)= <x(t)x(t+\tau)>/<x(t)^2>$, $x(t)$=x(t)-$<$x$>$. An important characteristic of the autocorrelation function is the correlation time: $\tau_c = \int C(t)^2 dt$. Fig. 4.12 *left* shows τ_c as a function of the noise level for weak and strong coupling strengths. The coherence resonance is clearly seen from this figure; its significant dependence on the coupling strength is evident. The increase in τ_c with the noise level can be easily understood from the above considerations of the ISIH evolution. The reason for smaller τ_c at higher noise amplitudes is as in [150]: in this region, the ISIH dispersion grows up more rapidly with the noise level than does the average ISI value. Note, however, that two stochastic relaxators are running mainly in antiphase, hence the underlying mechanism of this new form of CR is significantly different from CR effects reported till now in ensembles of excitable systems [77, 139, 82, 210].

The next important question is how the degree of ISIH polymodality depends on the number of interacting relaxators. We consider only the simplest extension, a system of three elements with cyclic boundary conditions. For this ring of three oscillators, large regions of the phase diagram are co-occupied mainly by the following attractors [200, 201]: (i) in-phase oscillations and the anti-phase regime in which two oscillators move in phase with each other and in anti-phase with the third one; (ii) the in-phase limit cycle and different types of the rotating waves (all phase differences are equal to one third of the period); and (iii) the anti-phase regime and rotating waves [200, 201]. It has been shown recently [170] that several additional attractors arise when three inhibitorily coupled relaxators are slightly detuned. It is natural to expect that the underlying attractors determine the richness of noise-induced

97

behavior, although any particular attractor manifests itself only temporarily in the case of stochastic relaxators. The noise-dependent evolution of the ISIH in the ring with a low excitation threshold (A=1.01) and a low coupling strength (C=0.1) is presented in Fig. 4.12 *right*. The qualitative properties of the distributions are not sensitive to C if $C \in (0.05 \div 0.3)$ and to A if $A \in (1.01 \div 1.03)$. The main difference between the histograms in Fig. 4.12 *right* and Fig. 4.10 *left* is in the number of detectable peaks, which grows with the number of elements. However, even in this case, due to the mechanism of out-of-phase motion, provided by inhibitory coupling, the increase of noise leads to an increase of coherency. It manifests itself in the dominance of only one peak in the corresponding ISIH (see the evolution in Fig. 4.12 *right* a,b,c) and based on the transient out-of-phase motion of any two oscillators. If the coupling is strong, it can split all peaks of the ISIH, but the detailed analysis of this phenomenon is beyond the volume of the Letter.

In summary, we have demonstrated two related phenomena, induced by inhibitory coupling in a system of excitable oscillators: i) The first effect is the generation of nontrivial polymodal distributions of interspike intervals without any periodic stimuli. Instead of external characteristic times, the time delays of the motion caused by the inhibitor exchange modulate the probability of the firing. The values of these delays define the peak's positions in the ISIHs. ii) The second effect is the coherence resonance which appears for this polymodal regime if we increase the noise amplitude. This CR has in the background the noise-dependent dominance of some out-of-phase attractor (anti-phase one for two coupled relaxators). This type of CR is slightly weaker than the classical CR; it is based on a completely different mechanism and seems to be quite perspective for the selective interactions of coupled relaxators with signals of different periods and forms. We have demonstrated these two effects on a simple model but in a general framework, and, therefore, we expect that these theoretical findings can be detected and used in different experimental systems with inhibitory coupling in physics [95], biology[126], electronics [170], or chemistry [197, 27].

Chapter 5

Main results and conclusions

In this thesis I have investigated analytically, numerically, and experimentally several new mechanisms of noise-induced transitions, new phenomena in the frame of the concept of doubly stochastic effects, and I have reported several new effects in nonlinear systems, which lead to noise-induced order. In particular, the following results have been presented in this work:

1. I have studied an interplay of additive and multiplicative noises in nonequilibrium transitions, and have shown that the role of additive noise in noise-induced transitions can be very nontrivial. Consideration of a pendulum under the action of multiplicative and additive noise has shown that if a transition occurs in the presence of additive noise, it is blurred by this noise - this behaviour has been described analytically. Moreover, additive noise hides on-off intermittency, but causes this intermittency before a transition, i.e. for subcritical values of the noise intensity. Consideration of an epidemiological model has shown that an action of additive noise can stabilize oscillations.

2. I have shown that in spatially extended systems additive noise can induce second-order phase transitions, which lead to breaking of the symmetry and the creation of a nonzero mean field. Moreover, if a coupling term is *a la Swift and Hohenberg*, then additive noise is able to induce spatially ordered patterns as a result of reentrant phase transition. Under certain parameters of the system, additive noise is able to induce also a first-order phase transition, in which the order parameter is changed not continuously versus the additive noise intensity.

3. I have suggested and developed a concept of doubly stochastic effects. According to this concept, a noise-induced order may appear in a nonlinear system in the following scenario: one noise source creates some property of the system, and then another noise induces the order in the system due to this property. Hence, the mechanism of a noise-induced order is also induced by noise. It means that energy of noise is used more efficiently for constructive purposes. The first effect, which is reported in the frame of this concept is doubly stochastic resonance. Doubly stochastic resonance is a combined effect which consists of a noise-induced phase transition and conventional stochastic resonance. Multiplicative noise induces a bistability, and then this bistability is used by additive noise to synchronize the output of the system with the incoming periodic

signal. Doubly stochastic resonance has been investigated numerically, and confirmed by analytical estimation

4. A simple electronic circuit for experimental implementation of doubly stochastic resonance has been designed and numerically investigated. The main advantage is that the energy of noise can be used more efficiently, not only for a synchronization as in conventional stochastic resonance, but also for the creation of a potential barrier, needed for this synchronization, and hence, this effect can be more commercially profitable. This effect has been explained by a consideration of the "effective" model.

5. A new effect in neural models, doubly stochastic coherence via noise-induced symmetry, has been reported. In this effect multiplicative noise creates symmetry in the system, which is deterministically asymmetric, and additive noise generates periodic output of the system. An optimization of both noise intensities is needed, and, hence, this effect is also a doubly stochastic effect. The behaviour is explained in terms of the "effective" model and confirmed by experimental measurements. For this an excitable electronic circuit has been designed and measured. Additionally, it has been shown that this effect can be enhanced in spatially extended system by coupling of elements. This enhancement has a resonance with respect to the size of the system, i.e. there is an optimal size of the system. Probably it explains the time generation in ensembles of neurons due to noise and due to optimal size of the neuron network.

6. Another new phenomenon in the frame of the concept of doubly stochastic effects is a noise-induced propagation in monostable media. The noise-induced propagation has been reported only for excitable or bistable media (or systems without local potential). In this work it has been shown that this effect can be also observed in deterministically monostable media. Combined action of multiplicative noise and coupling induces a bistability, and additive noise enhances the propagation of a periodic signal in this noise-supported bistable structure. Possible experimental implementations of this effect include arrays of simple electronic circuits as a communication system, analog circuits, electronic cellular neural networks, liquid crystals, photosensitive chemical reactions, or liquid helium.

7. Studying the noise-induced propagation, the constructive effect of additive noise in the propagation of a bichromatic signals through bistable media has been analyzed. Our results have shown that noise enhances propagation of such signals, similarly to what happens with simpler monochromatic driving. Moreover, it has been shown that by changing the noise intensity one is able to select the propagation frequency. These findings are potentially important for communication technologies.

8. Vibrational resonance in the noise-induced structure has been reported. This effect is a synthesis of a noise-induced phase transition and a conventional vibrational resonance. In this effect an additional high frequency force is able to optimize a signal processing in the system whose bistability is created by noise. The effect has been explained by the "effective" model, and this model has been tested in the experiment with a simple electronic circuit.

9. The effect of system size resonance in systems of coupled noisy elements has been reported. It has been shown that in populations of coupled noise-driven elements, in the ordered phase the response to a periodic force achieves maximum at a certain size of a system. This effect has been also demonstrated in deterministically monostable elements under the condition that bistability is created by multiplicative noise and coupling.

10. Excitable systems with inhibitory coupling have been studied and two related phenomena have been demonstrated: a generation of nontrivial polymodal distributions of interspike intervals without any periodic stimuli and a new mechanism of coherence resonance, that is based on the noise-dependent dominance of out-of-phase attractor (antiphase one for two coupled relaxators).

Especial attention in this work has been paid to possible application of these theoretical findings. Let me summarize this discussion and results. The results, concerning the influence of additive noise in noise-induced transitions can be applied for mechanical systems [25*], models of epidemics [24*], and systems with a pattern formation [18*]. For the effect of doubly stochastic resonance a simple electronic circuit has been designed [4*]. Also, it is discussed that understanding of such doubly stochastic resonance effects, as doubly stochastic resonance and noise-induced propagation in monostable media, can be potentially helpful in the investigation of liquid nematic crystals [93, 207], noise-induced bistability in Helium-IV [73], electronic circuits [1], as well as systems, which demonstrate noise-induced shift of the phase transition, e.g, in: photosensitive chemical reactions [128, 32], or Rayleigh-Bénard convection [127]. For communication technologies it can been important that in these doubly stochastic effects the energy of noise is used more efficiently for constructive purposes. For an experimental implementation of doubly stochastic coherence, an especial electronic circuit has been constructed and investigated [34*]. New results, which show the possibility of noise-induced selection of propagation frequency of bichromatic signal in bistable media, can be used in communication technologies. A possible field of application of the system size resonance is neural dynamics [189]. Finally, a new mechanism of coherence resonance, discussed here, can be found in numerous systems with inhibitory coupling, e.g. in physical[95], electronical [170], chemical systems[197, 27], in particular, in morphogenesis of Hydra regeneration and in the animal coat pattern formation [126], in the pattern formation in an electron-hole plasma and low temperature plasma [95], or in chemical systems, where the effective increase of inhibitor diffusion is achieved by reducing of activator diffusivity via the complexation of iodide (activator) with the macromolecules of starch results in Turing structure formation [108].

In the conclusion I would like to outline some perspective of the further research. It is important to note that the topic of nonequilibrium phenomena which lead to noise-induced order is rather new. I see three main directions in the study of these effects:

1. Theory of noise-induced phenomena which lead to ordering in nonlinear systems. The phenomena described here are demonstrated by a large variety of models, and the question naturally arises what is the complete classification of such effects. At the moment one can distinguish in this classification between several basic phenomena such

as stochastic resonance, noise-induced transitions, ratchets and so on. Nevertheless, recent researches, including this work, have shown that a synthesis of these basic phenomena is possible. This makes the complete classification as an open question up to now. Another and closely connected direction of theoretical research is finding of new phenomena and new mechanisms, which demonstrate or create noise-induced order. In particular, in the nearest future it will be very interesting to investigate the role of colored noise in doubly stochastic effects, the effect of system size resonance in the generation of periodic output in neuronal networks, i.e. ensembles of excitable system, vibrational propagation in the chains of noisy elements, or hidden transitions induced by additive noise in oscillatory systems due to the autoparametric effect. We expect that doubly stochastic resonance or its modifications can be found not only in the system, described here, but probably in oscillatory systems, or systems with a bistable "stochastic" potential.

2. Experimental implementation and confirmation of theoretical findings developed in the study of noise-induced effects, and, in particular, in this work. During the research, presented here, we have paid an especial attention to possible experimental situations, which can be considered as an application of this theory. Nevertheless, despite to the discussed results, an experimental research and commercial use of noise-induced effects is not sufficiently developed, and we leave it as a perspective direction of the future research in physics, chemistry, and living sciences.

3. Modelling transitions and irregular oscillations observed in experimental data by stochastic models. As has been shown in this work, already known phenomena which have been explained in the framework of a deterministic theory, could be also successfully described by stochastic models. Deterministic and noise-induced processes are very difficult to distinguish in many situations. Moreover, sometimes a noisy excitation looks more justified. For example, in the recently outlined hypothesis it is mentioned that turbulence in non-closed flows is a result of noise-induced phase transition. Also we expect that noise-induced processes may be very important for understanding of complex natural systems studied in neuroscience or such as microseismic oscillations, or phase transitions observed in physiological systems, especially in bimanual movements. Another open question, closely associated with modelling is the identification of the excitation mechanism by the analysis of irregular time-series. This problem is of high importance because to model a system one should know the physical mechanism of an excitation. At the same time, time-series are often the single source of the information about a nonlinear system - "black box". At this point, it is essential to note that classical methods of analysis, such as a spectral analysis or a calculation of correlation dimension are sometimes unable to distinguish between noise-induced irregular oscillations and chaotic oscillations of deterministic nature.

Acknowledgements

Collection of papers

1*. A. Zaikin, J. Garcia-Ojalvo, L. Schimansky-Geier, and J. Kurths, "Noise-induced propagation in monostable media", Phys. Rev. Lett. 88, 010601 (2002).

2*. A. Pikovksy, A.Zaikin, and M.A. de la Casa, "System size resonance in coupled noisy systems", Phys. Rev. Lett. 88, 050601 (2002).

3*. A. Zaikin, D. Topaj, and J. Garcia-Ojalvo, "Noise-induced propagation of bichromatic signals", Fluctuations and Noise Letters 2, L45-49 (2002).

4*. A.A. Zaikin, K. Murali, and J. Kurths, "A Simple Electronic Circuit Model for Doubly Stochastic Resonance", Phys. Rev. E, Rapid Communication 63, 020103 (R) (2001).

5*. A. Zaikin , J. Kurths , and L. Schimansky-Geier, "Doubly Stochastic Resonance", Phys. Rev. Lett. 85, 227 (2000).

6*. J.P. Baltanas, A.Zaikin, F.Feudel, J.Kurths, and M.A.F. Sanjuan, "Noise-induced effects in tracer dynamics", Physics Letters A 297 396-401 (2002)

7*. A.A. Zaikin, and J. Kurths, "Additive noise in Noise-induced Nonequilibrium Transitions", CHAOS 11(3), 570 (2001).

8*. Landa P.S., Zaikin A. and Schimansky-Geier L., "Effect of the potential shape and of a Brownian particle mass on noise-induced transport", Chaos, Solitons & Fractals, 12 (8) (2001) pp. 1459-1471.

9*. Landa P.S. and Zaikin A., Fluctuational transport of a Brownian particle in ratchet-like gravitational potential field , Chaos, Solitons & Fractals, 13 (1) (2002) pp. 109-113.

10*. Landa,P.S., Zaikin,A.A., and Kurths,J., "On Noise-induced Transitions in Nonlinear Oscillators", in "Stochastic Processes in Physics, Chemistry, and Biology, Editors: J.A. Freund, T. Poeschel, Springer 2000.

11*. Landa,P.S., Zaikin,A.A., Ushakov,V.G. and Kurths,J., "Influence of additive noise on transitions in nonlinear systems", Phys. Rev. E, Vol. 61, 5, 4809 (2000).

12*. A.A. Zaikin, J. Garcia-Ojalvo, and L. Schimansky-Geier, "Nonequilbrium first-order phase transition induced by additive noise", Phys. Rev. E, Rapid Communication, Vol.60, p. R6275, (1999).

13*. A.A. Zaikin, J. Kurths, "Additive Noise and Noise-induced Nonequilibrium Phase Transitions", in "Unsolved Problems of Noise and fluctuations", edited by D. Abbott and L.B. Kish, AIP Conf. Proc. No. 511 (AIP, Melville, New York, 1999), pp. 303-313.

14*. A.A. Zaikin, J. Kurths, " Modeling Cognitive Control in Simple Movements", in "Computing Anticipatory systems", AIP 517, (1999).

15*. P.S. Landa, A.A. Zaikin, A.S. Ginevsky, and Ye.V. Vlasov, "Turbulence and coherent structures in subsonic submerged jets. Control of the turbulence.", Int. J. of Bif. and Chaos, Vol.9, No.2, pp. 397-414 (1999).

16*. A.A. Zaikin, L. Schimansky-Geier, "Ordering Role of Additive Noise in Extended Media", International Journal of Computing Anticipatory Systems, CHAOS, ed. by Daniel M. Dubois, Vol. 3, pp. 251-273 (1998).

17*. P.S. Landa, A.A. Zaikin, "Noise-induced Phase Transitions in Nonlinear Oscillators", in "Computing Anticipatory Systems", AIP Conference Proceedings 465, pp.419-435, CASYS'98, Liege, Belgium (1998).

18*. A.A. Zaikin and L. Schimanksy-Geier, "Spatial Patterns Induced by Additive Noise", Phys.Rev.E 58(4),pp. 4355-4360, (1998).

19*. P.S. Landa, A.A. Zaikin, and L. Schimansky-Geier, "Influence of additive noise on noise-induced phase transitions in nonlinear chains", Chaos, Solitons & Fractals, Vol.9, No. 8, pp.1367-1372,(1998).

20*. P.S. Landa, A.A. Zaikin, M.G. Rosenblum, and J.Kurths, "On-off Intermittency Phenomena in a Pendulum with a Randomly Vibrating Suspension Axis", Chaos, Solitons & Fractals, Vol. 9, No.1/2, pp. 157-169, (1998).

21*. P.S. Landa, A.A. Zaikin, M.G. Rosenblum, and J. Kurths, "Control of Noise-induced Oscillations of a Pendulum with a Randomly Vibrating Suspension Axis", Phys.Rev.E. 56(2), pp. 1465-1470, (1997).

22*. P.S. Landa and A.A. Zaikin, "Nonequilibrium Noise-induced Phase Transitions in Simple Systems", JETP 84 (1),pp.197-208, (1997), translation of Zh. Eksp. Teor. Fiz. , 1997, t. 111, vup.1, str. 359-378.

23*. C. Scheffczyk, A. Zaikin, M.Rosenblum, R.Engbert, R.Krampe, and J.Kurths, "Modeling Qualitative Changes in Bimanual Movements", Int. J. of Bif. and Chaos, Vol.7, No.6 , pp. 1441-1450 (1997).

24*. P.S. Landa and A.A. Zaikin, "Random and chaotic oscillations in the model of childhood infections caused by the seasonal variations of the contact rate", in "Applied Nonlinear Dynamics and Stochastic Systems near Millenium", AIP conference proceedings 411, San Diego, CA July 1997, pp.321-329 (1997).

25*. P.S. Landa, A.A. Zaikin, "Noise-induced Phase Transitions in a Pendulum with a Randomly Vibrating Suspension Axis", Phys.Rev.E, 54(4), pp. 3535-3544,(1996).

26*.C. Scheffczyk, R. Engbert, R. Krampe, J. Kurths, M. Rosenblum, and A.Zaikin, "Nonlinear Modelling of Polyrhythmic Hand Movements", Medical & Biological Engineering & Computing, Vol. 34, Supplement 1, Part 1, 1996, The 10th Nordic-Baltic Conference on Biomedical Engineering, June 9-13, 1996, Tampere, Finland.

27*. A.A. Zaikin and O.V. Rudenko, "A Nonlinear Model of the Helmholtz Resonator with a Movable Wall", Acoustical Physics, Vol.42, No.3,pp. 329-333 (1996).

28*. A.A. Zaikin and O.V. Rudenko, "Shock Wave Effect on Resonance Sound Absorbers", Moscow University, Physics Bulletin, Vol. 50, No.6, pp.35-40, (1995), 1996 by Allerton Press.

29*. A.S. Ginevsky, P.S. Landa, and A.A. Zaikin, "Self-excitation of Impinging Jets with Regard to Acoustic Feedback", Proceedings of Third International Congress on Air- and Structure-Borne Sound and Vibrations, June 13-15, Montreal, Canada, (1994), pp. 1191-1196.

30*. A.A. Zaikin and O.V. Rudenko, "Acoustic Nonlinearity of Nonuniform Flow of an Oscillating Liquid", Moscow University, Physics Bulletin, Vol. 48, No. 6, pp. 56-58, (1993),1993 by Allerton Press.

31*. A. M. Correig, M. Urguizu, V.B. Ryabov, and A.A. Zaikin, "On the dynamics of microseism time series", Chaos, Solitons, and Fractals, (in press).

32*. E.I. Volkov, M.N. Stolyarov, A. A. Zaikin, and J. Kurths, "Coherence resonance and polymodality in inhibitory coupled excitable oscillators", (submitted).

33*. A. A. Zaikin, L. Lopez, J.P. Baltanas, J. Kurths, and M.A.F. Sanjuan, "Vibrational resonance in noise-induced structures", Phys. Rev. E 66, 011106 (2002).

34*. A. Zaikin, J. García-Ojalvo, R.Bascones, E.Ullner, and J. Kurths, "Doubly stochastic coherence via noise-induced symmetry in bistable neural models" (submitted).

35*. E. Ullner, A.Zaikin, R.Bascones, J. Garcia-Ojalvo, and J. Kurths, "Vibrational resonance and propagation in excitable systems" (submitted).

36*. A. Zaikin, "Doubly stochastic effects", Fluctuations and Noise Letters, (submitted).

37* A. Zaikin, P. Saparin, S. Prohaska, J. Kurths, W. Gowin, "Bone modeling and structural measures of complexity", Proceedings of the "Symposium Life in Space for Life on Earth", Stockgolm 2002 (submitted).

List of appendixes

1. A. Zaikin, "Doubly stochastic effects", Fluctuations and Noise Letters, (submitted).

2. A. Zaikin, J. García-Ojalvo, R.Bascones, E.Ullner, and J. Kurths, "Doubly stochastic coherence via noise-induced symmetry in bistable neural models" (submitted).

3. A. Zaikin, J. Garcia-Ojalvo, L. Schimansky-Geier, and J. Kurths, "Noise-induced propagation in monostable media", Phys. Rev. Lett. 88, 010601 (2002).

4. A. Pikovksy, A.Zaikin, and M.A. de la Casa, "System size resonance in coupled noisy systems", Phys. Rev. Lett. 88, 050601 (2002).

5. A.A. Zaikin, K. Murali, and J. Kurths, "A Simple Electronic Circuit Model for Doubly Stochastic Resonance", Phys. Rev. E, Rapid Communication 63, 020103 (R) (2001).

6. A. Zaikin , J. Kurths , and L. Schimansky-Geier, "Doubly Stochastic Resonance", Phys. Rev. Lett. 85, 227 (2000).

7. A.A. Zaikin, and J. Kurths, "Additive noise in Noise-induced Nonequilibrium Transitions", CHAOS 11(3), 570 (2001).

8. Landa,P.S., Zaikin,A.A., Ushakov,V.G. and Kurths,J., "Influence of additive noise on transitions in nonlinear systems", Phys. Rev. E, Vol. 61, 5, 4809 (2000).

9. A.A. Zaikin, J. Garcia-Ojalvo, and L. Schimansky-Geier, "Nonequilbrium first-order phase transition induced by additive noise", Phys. Rev. E, Rapid Communication, Vol.60, p. R6275, (1999).

10. A.A. Zaikin and L. Schimanksy-Geier, "Spatial Patterns Induced by Additive Noise", Phys.Rev.E 58(4),pp. 4355-4360, (1998).

Bibliography

[1] Private communication with F. Moss.

[2] Note that not always the effective potential description appropriately explains the phase transition in this system [A.A. Zaikin, J. García-Ojalvo and L. Schimansky-Geier, Phys. Rev. E **60**, R6275 (1999)].

[3] The hysteresis may appear if we slowly change c^* during integration, i.e., the solution x_i for the previous value $c^* = c - \Delta c$ is the initial condition for the next point $c^* = c$ by a monotonical variation of c^*, where c^* is a control parameter (a or σ_a^2) and variated upwards and downwards.

[4] Note that SR in connection with a noise-induced transition has been considered in [A.Fuliński, Phys. Rev E (**52**), 4523, 1995], but in a zero-dimensional system with noise-induced *transient* states and with specific non-Markovian dichotomic noise.

[5] For small L hops can be observed even without external force [R. Müller, K. Lippert, A. Kühnel, and U. Behn, Phys. Rev. E **56**, 2658 (1997)]. With $L = 18$ such hops are very rare.

[6] H.S. Wio, Phys. Rev. E **54**, R3075 (1996); S. Bouzat and H.S. Wio, Phys. Rev. E **59**, 5142 (1999).

[7] G.P. Agrawal. *Fiber-Optic Communication Systems*. John Wiley & Sons, New York, 1992.

[8] A. Ajdari and J. Prost. *C. R. Acad. Sci. Paris*, t. 315, Serie II:1635, 1992.

[9] T. Alarcón, A. Pérez-Madrid, and J.M.Rubí. Stochastic resonance in nonpotential systems. *Phys. Rev. E*, 57(5):4979–4985, 1998.

[10] V. S. Anishchenko, A. B. Neiman, F. Moss, and L. Schimansky-Geier. Stochastic resonance: noise-enhanced order. *Sov. Phys. Usp.*, 42:7, 1999.

[11] P. Arena, R. Caponetto, L. Fortuna, and A. Rizzo. *IEEE Trans.*, 48:360, 2001.

[12] R.D. Astumian and M. Bier. Fluctuation driven ratchets: molecular motors. *Phys. Rev. Lett.*, 72:1766, 1994.

BIBLIOGRAPHY

[13] R.D. Astumian and M. Bier. Mechanochemical coupling of the motion of molecular motors to atp hydrolysis. *Biophys. J.*, 70:637, 1996.

[14] P. Babinec. *Phys. Lett. A*, 225:179, 1997.

[15] G. Balázsi, L.B. Kiss, and F.E. Moss. Unsolved problems of noise and fluctuations. *AIP Conference Proceeding 511*, 1999.

[16] S. Barbay, G. Giacomelli, and F. Marin. Stochastic resonance in vertical cavity surface emitting lasers. *Phys. Rev. E*, 61:157, 2000.

[17] S. Barbay, G. Giacomelli, and F. Martin. Experimental evidence of binary aperiodic stochastic resonance. *Phys. Rev. Lett.*, 85:4652, 2000.

[18] S. Barbay, G. Giacomelli, and F. Martin. Noise-assisted transmission of binary information: Theory and experiment. *Phys. Rev. E*, 63:051110, 2001.

[19] R. Báscones, J. García-Ojalvo, and J.M. Sancho. Pulse propagation sustained by noise in arrays of bistable electronic circuits. *Phys. Rev. E*, 65:061108, 2002.

[20] V.I. Belinicher and B.I. Sturman. The photogalvanic effect in media lacking a center of symmetry. *Sov. Phys. Usp.*, 23:199, 1980. (Usp. Fiz. Nauk. 130 (1980) 415).

[21] R. Benzi, A. Sutera, and A. Vulpiani. The mechanism of stochastic resonance. *J. Phys. A*, 14:L453, 1981.

[22] S.M. Bezrukov and I. Vodyanoy. In search for a possible statistical basis of stochastic resonance. In D. Abbott and L.Kiss, editors, *Unsolved Problems of Noise and fluctuations*, , 1999. AIP Conference Proceedings. (in press).

[23] S. Bouzat and H.S. Wio. *Phys. Rev. E*, 59:5142, 1999.

[24] S.M. Braxton. Synthesis and use of a novel class of atp carbamates and a ratchet diffusion model for directed motion in muscle. *PhD thesis, Washington State University, Pullman, WA*, 1998.

[25] G. Carapella and G. Costabile. Ratchet effect: Demonstration of a relativistic fluxon diode. *Phys. Rev. Lett.*, 87:077002, 2001.

[26] J.M. Casado and M. Morillo. *Phys. Rev. E*, 52:2088, 1995.

[27] V. Castets, E. Dulos, J. Boissonade, and P. De Kepper. *Phys. Rev. Lett.*, 64:2953, 1990.

[28] L.O. Chua, C.A. Desoer, and E.S. Kuh. *Linear and Nonlinear Circuits*. McGraw-Hill Book Co., New-York, 1987.

[29] J.J. Collins and I.N. Stewart. *J. Nonlinear Science*, 3:349, 1993.

[30] N.J. Cordova, B. Ermentrout, and G.F. Oster. Dynamics of signle-motor molecules: The termal ratchet model. *Proc. Natl. Acad. Sci. USA*, 89:339, 1992.

[31] D. Dawson and J. Gärtner. *Stochastics*, 20:247, 1987.

[32] P. de Kepper and W. Horsthemke. Experimental evidence of noise-induced transition in an open chemical system. In *Synergetics: Far From Equilibrium*. Springer, New York, 1979.

[33] A. de Waele and R. de Bruin Outober. Quantum-interference phenomena in point contacts between two supercondactors. *Physica (Utrecht)*, 41:225, 1969.

[34] A. de Waele, W.H. Kraan, R. de Bruin Outober, and K.W. Taconis. *Physica (Utrecht)*, 37:114, 1967.

[35] G. Debnath, T. Zhou, and F. Moss. *Phys. Rev. A*, 39:4323, 1989.

[36] R.C. Desai and R. Zwanzig. *J. Stat. Phys.*, 19:1, 1978.

[37] K. Dietz. The incidence of infectious diseases under the influence of seasonal fluctuations. *Lect. Notes Biomath.*, 11:1–15, 1976.

[38] M.F. Dimentberg. *Nonlinear Stochastic Problems of Mechanical Oscillations*. Nauka, Moscow, 1980. (in Russian).

[39] C.R. Doering and J.C. Gadoua. Resonant activation over a fluctuating barrier. *Phys. Rev. Lett.*, 69:2318, 1992.

[40] J.K. Douglas, L. Wilkens, and L. Pantazelou. *Nature*, 365:337–340, 1993.

[41] M.I. Dykman. *Pis'ma Zh. Eksp. Teor. Fiz.*, 53:182, 1991.

[42] M.I. Dykman, T. Horita, and J. Ross. *J. Chem. Phys.*, 103:966, 1995.

[43] R. Engbert and F.R. Drepper. Chance and chaos in population biology — models of recurrent epidemics and food chain dynamics. *Chaos, Solitons and Fractals*, 4(7):1147–1169, 1994.

[44] R. Engbert, C. Scheffczyk, R. T. Krampe, M. Rosenblum, J. Kurths, and R. Kliegl. Tempo-induced transitions in polyrhythmic hand movements. *Phys. Rev. E*, 56:5823, 1997.

[45] A.N. Grigorenko et al. *J. Appl. Phys.*, 76:6335, 1994.

[46] J. Rose et al. *J. Neurophysiol.*, 30:769, 1967.

[47] R. Benzi et al. *Tellus*, 34:10, 1982.

[48] S. Fauve and F. Heslot. *Phys. Lett. A*, 97:5, 1983.

[49] I.I. Fedchenia. Boundary stochastic problems, multistability in the presence of fluctuations and noise-induced phase transitions. *Physica A*, 125A:577–590, 1984.

[50] R.P. Feynman, R.B. Leighton, and M. Sands. *The Feynman lectures on physics*, volume Vol.1, chapter 46. Addison Wesley, Reading MA, 1963.

[51] S. Fujita, H. Maeno, S. Uratsuka, T. Furukawa, S. Mae, Y. Fujii, and O. Watanabe. Nature of radio echo layering in the antarctic ice sheet detected by a two-frequency experiment. *Journal of Geophys. research - solid earth*, 104:13013, 1999.

[52] A. Fuliński. Relaxation, noise-induced transitions, and stochastic resonance driven by non-markovian dichotomic noise. *Phys. Rev. E*, 52(4):4523–4526, 1995.

[53] L. Gammaitoni, P. Hänggi, P. Jung, and F. Marchesoni. Stochastic resonance. *Rev. Mod. Phys.*, 70:223, 1998.

[54] L. Gammaitoni, F. Marchesoni, M. Martinelli, L. Pardi, and S. Santucci. *Phys. Lett. A*, 158:449, 1989.

[55] L. Gammaitoni, F. Marchesoni, M. Martinelli, L. Pardi, and S. Santucci. *Phys. Rev. Lett.*, 62:349, 1989.

[56] L. Gammaitoni, F. Marchesoni, M. Martinelli, L. Pardi, and S. Santucci. *Phys. Rev. Lett.*, 65:2607, 1990.

[57] L. Gammaitoni, F. Marchesoni, M. Martinelli, L. Pardi, and S. Santucci. *Phys. Rev. Lett.*, 71:3625, 1993.

[58] L. Gammaitoni, F. Marchesoni, M. Martinelli, L. Pardi, and S. Santucci. *Phys. Rev. E*, 49:4878, 1994.

[59] L. Gammaitoni, F. Marchesoni, M. Martinelli, L. Pardi, and S. Santucci. *Phys. Rev. E*, 51:R3799, 1995.

[60] L. Gammaitoni, M. Martinelli, L. Pardi, and S. Santucci. Observation of stochastic resonance in bistable electron-paramagnetic-resonance systems. *Phys. Rev. Lett.*, 67:1799, 1991.

[61] H. Gang, H. Haken, and X. Fagen. *Phys. Rev. Lett.*, 77:1925, 1996.

[62] J. García-Ojalvo, A. Hernández-Machado, and J.M. Sancho. Effects of external noise on the swift-hohenberg equation. *Phys. Rev. Lett.*, 71:1542, 1993.

[63] J. García-Ojalvo, A.M. Lacasta, F. Sagués, and J.M. Sancho. *Europhys. Lett.*, 50:427, 2000.

[64] J. García-Ojalvo, J. M. R. Parrondo, J. M. Sancho, and C. Van den Broeck. Reentrant transition induced by multiplicative noise in the time-dependent ginzburg–landau model. *Phys. Rev. E*, 54:6918, 1996.

[65] J. García-Ojalvo and J. M. Sancho. *Noise in Spatially Extended Systems*. Springer, New York, 1999.

[66] C.W. Gardiner. *Handbook of Stochastic Methods*. Springer, Berlin, 1985.

[67] V.E. Gherm, N.N. Zernov, B. Lundborg, and A. Vastberg. The two-frequency coherence function for the fluctuating ionosphere: Narrowband puls propagation. *Journ. of Atmospheric and Solar-terrestrial physics*, 59:1831, 1997.

[68] G. Giacomelli, M. Giudici, S. Balle, and J. R. Tredicce. Experimental evidence of coherence resonance in an optical system. *Phys. Rev. Lett.*, 84:3298, 2000.

[69] Z. Gingl, L. Kiss, and F. Moss. *Europhys. Lett.*, 29:191, 1995.

[70] D. Gong, G. hu, X. Wen, C. Yang, G.R. Qin, R. li, and D. Ding. *Phys. Rev. A*, 36:4243, 1992.

[71] D. Gong, G. hu, X. Wen, C. Yang, G.R. Qin, R. li, and D. Ding. *Phys. Rev. E*, 48:4862, 1992.

[72] D. Gong, G.R. Qin, G. Hu, and X.D. Weng. *Phys. Lett. A*, 159:147, 1991.

[73] D. Grisowld and J.T. Tough. *Phys. Rev. A*, 36:1360, 1987.

[74] P. Haenggi. Stochastic resonance in biology. *ChemPhysChem*, 3:285–290, 2002.

[75] H. Haken. *Synergetics*. Springer-Verlag, Berlin, 1978.

[76] A. Hamm. *Physica D*, 142:41, 2000.

[77] S. K. Han, T.G. Yim, D.E. Postnov, and O.V. Sosnovtseva. *Phys. Rev. Lett.*, 83:1771, 1999.

[78] E. Helfand. *Bell Sys. Tech. J.*, 58:2289, 1979.

[79] A.D. Hibbs. *Nuovo Cimento*, 17D:811, 1995.

[80] W. Hohmann, J. Muller, and F.W. Schneider. *J. Phys. Chem*, 100:5388, 1996.

[81] W. Horsthemke and R. Lefever. *Noise-Induced Transitions*. Springer, Berlin, 1984.

[82] B. Hu and C. Zhou. *Phys. Rev. E*, 61:R1001, 2000.

[83] Hu Gang, T. Ditzinger, C.Z. Ning, and H. Haken. Stochastic resonance without external periodic force. *Phys. Rev. Lett.*, 71(6):807, 1993.

[84] S.W. Hughes, D.W. Cope, T.I. Tóth, S.R. WIlliams, and V. Crunelli. *J. Physiol.*, 517:805, 1999.

[85] A.F. Huxley. Muscle structure and theories of contraction. *Prog. Biophys.*, 7:255, 1957.

[86] N. Inaba, T. Saito, and S. Mori. Chaotic phenomena in a circuit with a negative resistance and an ideal switch of diodes. *The Trans. of the IEICE*, E70(8):744–754, August 1987.

[87] P. Jung, U. Behn, E. Pantazelou, and F. Moss. *Phys. Rev. A*, 46:R1709, 1992.

[88] P. Jung and G. Mayer-Kress. *Phys. Rev. Lett.*, 74:2130, 1995.

BIBLIOGRAPHY

[89] S. Kabashima. Observation of phase transition due to external fluctuations. (not published).

[90] S. Kabashima and T. Kawakubo. Observation of a noise-induced phase transition in a parametric oscillator. *Phys. Lett.*, A70:375, 1970.

[91] S. Kabashima, S. Kogure, T. Kawakubo, and T. Okada. Oscillatory-to-nonoscillatory transition due to external noise in a parametric oscillator. *J. Appl. Phys*, 50(10):6296–6302, 1979.

[92] S. Kádár, J. Wang, and K. Showalter. Noise-supported traveling waves in sub-excitable media. *Nature*, 391:770, 1998.

[93] S. Kai, T. Kai, and M. Takata. *J. Phys. Soc. Jpn.*, 47:1379, 1979.

[94] J. Keener and J. Snyder. *Mathematical Physiology*. Springer, New York, 1998.

[95] B.S. Kerner and V.V. Osipov. *Soviet Phys. Uspekhi*, 33:679, 1990.

[96] S. Kim, S.H. Park, and C.S. Ryu. Noise-enhanced multistability in coupled oscillator systems. *Phys. Rev. Lett.*, 78(9):1616–1619, 1997.

[97] P.E. Kloeden and E. Platen. *Numerical Solution of Stochastic Differential Equations*. Springer-Verlag, Berlin Heidelberg, 1992.

[98] A.J. Koch and H. Meinhardt. *Rev. Mod. Phys.*, 66:1482, 1994.

[99] H.A. Kramers. Brownian motion in a field of force and the diffusion model of chemical reactions. *Physica*, 7(4):284–304, 1940.

[100] P.S. Landa. *Nonlinear Oscillations and Waves in Dynamical Systems*. Kluwer Academic Publ., Dordrecht–Boston–London, 1996.

[101] P.S. Landa. Turbulence in nonclosed fluid flows as a noise-induced phase transition. *Europhys. Lett.*, 36:401–406, 1996.

[102] P.S. Landa. *Nonlinear Oscillations and Waves*. Nauka, Moscow, 1997. (in Russian).

[103] P.S. Landa and P.V.E. McClintock. Changes in dynamical behavior of nonlinear systems induced by noise. *Physics Reports*, 323:1, 2000.

[104] P.S. Landa and P.V.E. McClintock. Vibrational resonance. *J. Phys.A: Math.Gen*, 33:L433, 2000.

[105] G. Lattanzi and A. Maritan. Force dependence of the michaelis constant in a two-state ratchet model for molecular motors. *Phys. rev. Lett.*, 86:1134, 2001.

[106] S.G. Lee, A. Neiman, and S. Kim. *Phys. Rev. E*, 57:3292, 1998.

[107] S. Leibler and D.A. Huse. A physical model for motor proteins. *C.R. Acad. Sci Paris*, t. 313, Serie III:27, 1991.

[108] I. Lengyel and I.R. Epstein. *Science*, 251:650, 1990.

[109] D.S. Leonard and L.E. Reichl. *Phys. Rev. E*, 1994.

[110] B. Lindner and L. Schimansky-Geier. Coherence and stochastic resonance in a two-state system. *Phys. Rev. E*, 61:6103, 2000.

[111] J.F. Lindner, S. Chandramouli, A.R. Bulsara, M. Löcher, and W. Ditto. Noise enhanced propagation. *Phys. Rev. Lett.*, 81:5048, 1998.

[112] J.F. Lindner, B.K. Meadows, W.L. Ditto, M.E. Inchiosa, and A.R. Bulsara. *Phys. Rev. Lett.*, 75:3, 1995.

[113] J.F. Lindner, B.K. Meadows, W.L. Ditto, M.E. Inchiosa, and A.R. Bulsara. Scaling laws for soatiotemporal synchronization and array enhanced stochastic resonance. *Phys. Rev. E*, 53:2081, 1996.

[114] M. Löcher, D. Cigna, and E.R. Hunt. Noise sustained propagation of a signal in coupled bistable electronic elements. *Phys. Rev. Lett.*, 80(23):5212, 1998.

[115] A. Longtin. *Phys. Rev. E*, 55:868, 1997.

[116] A. Longtin, A. Bulsara, and F. Moss. *Phys. Rev. Lett*, page 656, 1991.

[117] M.O. Magnasco. Forced thermal ratchets. *Phys. Rev. Lett.*, 71:1477, 1993.

[118] A.O. Maksimov. On the subharmonic emission of gas bubbles under two-frequency excitation. *Ultrasonics*, 35:79, 1997.

[119] S. Mangioni, R. Deza, H. S. Wio, and R. Toral. Disordering effects of color in nonequilibrium phase transitions induced by multiplicative noise. *Phys. Rev. Lett.*, 79:2389, 1997.

[120] S.E. Mangioni, R.R. Deza, R.Toral, and H.S. Wio. Nonequlibrium phase transitions induced by multiplicative noise: Effects of self-correlation. *Phys. Rev. E*, 61:223, 2000.

[121] R.N. Mantegna and B. Spagnolo. *Phys. Rev. E*, 49:R1792, 1994.

[122] F. Marchesoni. *Physics Letters A*, 237:126, 1998.

[123] F. Marchesoni, L. Gammaitoni, and A.R. Bulsara. *Phys. Rev. Lett.*, 78:2886, 1997.

[124] B. McNamara and K. Wiesenfeld. Theory of stochastic resonance. *Phys. Rev. A*, 39(9):4854–4869, 1989.

[125] B. McNamara, K. Wiesenfeld, and R. Roy. *Phys. Rev. Lett.*, 60:2626, 1988.

[126] H. Meinhardt. *Models of Biological Pattern Formation*. Academic Press, New York, 1982.

[127] C.W. Meyer, G. Ahlers, and D.S. Cannell. *Phys. Rev. A*, 44:2514, 1991.

[128] J.C. Micheau, W. Horsthemke, and R. Lefever. *J. Chem. Phys.*, 81:2450, 1984.

[129] A.S. Mikhailov. Noise-induced phase transition in a biological system with diffusion. *Phys. Lett. A*, 73:143, 1979.

[130] J. Miller and D.A. Huse. *Phys. Rev. E*, 48:2528, 1993.

[131] V.A. Mironov and V.M. Sokolov. Detection of broadband phase-code-modulated two-frequency signals through calculation of their cross-correlation function. *Radiotekhnika i electronika*, 41:1501, 1996. (inRussian).

[132] R.B. Mitson, Y. Simard, and C. Goss. *ICES J. Marine Science*, 53:209–215, 1996.

[133] T. Mori and S. Kai. Noise-induced entrainment and stochastic resonance in human brain waves. *Physical Review Letters*, 88:218101, 2002.

[134] M. Morillo, J. Gómez-Ordonez, and J.M. Casado. Stochastic resonance in a mean-field model of cooperative behaviour. *Phys. Rev. E*, 52(1):316–320, 1995.

[135] F. Moss. *Ber. Bunsenges. Phys. Chem.*, 95:303, 1991.

[136] R. Müller, K. Lippert, A. Kühnel, and U. Behn. First-order nonequilibrium phase transition in a spatially extended system. *Phys. Rev. E*, 56:2658–2662, 1997.

[137] Z. Neda. *Phys. Lett. A*, 210:125, 1996.

[138] A. Neiman, P. I. Saparin, and L. Stone. *Phys. Rev. E*, 56:270, 1997.

[139] A. Neiman, L. Schimansky-Geier, A. Cornell-Bell, and F. Moss. Noise-enhanced phase synchronization in excitable media. *Phys. Rev. Lett.*, 83:4896–4899, 1999.

[140] A. Neiman and W. Sung. Memory effects on stochastic resonance. *Phys. Lett. A*, 223:341, 1996.

[141] C. Nicolis. *Tellus*, 34:1, 1982.

[142] Y. Nishio and S. Mori. Chaotic phenomena in nonlinear circuits with time-varying resistors. *IEICE Trans. Fundamentals*, E76-A(3):467–475, March 1993.

[143] L.F. Olsen and W.M. Schaffer. Chaos versus noisy periodicity: Alternative hypothesis for childhood epidemics. *Science*, 249:499–504, 1990.

[144] C. Palenzuela, R. Toral, C.R. Mirasso, O. Calvo, and J.D. Gunton. *Europhysics Lett.*, 56:347, 2001.

[145] J. M. R. Parrondo, G. P. Harmer, and D. Abbott. New paradoxical games based on brownian ratchets. *Phys. Rev. Lett.*, 85:5226, 2000.

[146] J. M. R. Parrondo, C Van den Broeck, J. Buceta, and F. J. de la Rubia. *Physica A*, 224:153, 1996.

[147] R. Perazzo, L. Romanelli, and R. Deza. *Phys. Rev. E*, 61:R3287, 2000.

[148] A. Perez-Madrid and J.M. Rubi. *Phys. Rev. E*, 51:4159, 1995.

[149] V. Pérez-Muñuzuri, V. Pérez-Villar, and L.O. Chua. *IEEE Trans.*, 40:174, 1993.

[150] A. Pikovksy and J. Kurths. Coherence resonance in a noise-driven excitable system. *Phys. Rev. Lett.*, 78:775, 1997.

[151] A. Pikovsky, M. Rosenblum, and J. Kurths. *Synchronization. A Universal Concept in Nonlinear Sciences*. Cambridge University Press, Cambridge, 2001.

[152] A. Pikovsky and S. Ruffo. *Phys. Rev. E*, 59:1633, 1999.

[153] A. Pikovsky, A. Zaikin, and M.A. de la Casa. System size resonance in coupled noisy systems and in the ising model. *Phys. Rev. Lett.*, 88:050601, 2002.

[154] A. S. Pikovsky, K. Rateitschak, , and J. Kurths. *Z. Physik B*, 95:541, 1994.

[155] A.S. Pikovsky and J. Kurths. Do globally coupled maps really violate the law of large numbers. *Phys. Rev. Lett.*, 72:1644, 1994.

[156] J. Plata. Effect of a parametric driving force on noise-induced transitions: Analytical results. *Phys. Rev. E*, 59:2439–2442, 1999.

[157] R. Pool. *Science*, 243:25, 1989.

[158] M. Rabinovich, A. Volkovskii, P. Lecanda, R. Huerta., H.D.I. Abarbanel, and G. Laurent. *Phys. Rev. Lett.*, 87:068102, 2001.

[159] D.V. Ramana Reddy, A. Sen, and G.L. Johnston. *Phys. Rev. Lett.*, 85:3381, 2000.

[160] R. Reigada, A. Sarmiento, and K. Lindenberg. Thermal resonance in signal transmission. *Phys. Rev. E*, 63:066113, 2001.

[161] P. Reimann. Supersymmetric ratchets. *Phys. Rev. Lett.*, 86:4992, 2001.

[162] P. Reimann. Brownian motors: noisy transport far from equilibrium. *Physics Reports*, 361:57–265, 2002.

[163] P. Reimann, R. Kawai, C. Van den Broeck, and P. Hänggi. Coupled brownian motors: anomalous hysteresis and zero-bias negative conductance. *Europhys. Lett.*, 45:545, 1999.

[164] M. Riani and E. Simonotto. *Phys. Rev. Lett.*, 72:3120, 1994.

[165] M. Riani and E. Simonotto. *Nuovo Cimento D*, 17:903, 1995.

[166] S.D. Robinson, F.E. Moss, and P.V.E. McClintock. Experimental observation of stochastic posponements of critical onsets in a bistable system. *J. Phys. A*, 18:L89–94, 1985.

[167] M. Rosenblum, A. Pikovsky, and J. Kurths. *Phys. Rev. Lett.*, 76:1804, 1996.

[168] A.C.H. Rowe and P. Etchegoin. *Phys. Rev. E*, 64:031106, 2001.

[169] D.F. Russel, L.A. Wilkens, and F. Moss. Use of behavioural stochastic resonance by paddle fish for feeding. *Nature*, 402:291–294, 1999.

[170] D. Ruwisch, M.Bode, D.V. Volkov, and E.I.Volkov. *Int. J. Bifurcation and Chaos*, 9:1969, 1999.

[171] S.M. Rytov. *Introduction to Statistical Radiophysics*. Nauka, Moscow, 1966. (In Russian).

[172] J.M. Sancho and J. García-Ojalvo. Noise-induced order in extended systems: A tutorial. In J.A. Freund and T. Pöschel, editors, *Stochastic Processes in Physics, Chemistry, and Biology*, pages 235–246. Springer, New York, 2000.

[173] H. Schanz, R. Ketzmerick M. Otto, and T. Dittrich. Classical and quantum hamiltonian ratchets. *Phys. Rev. Lett.*, 87:070601, 2001.

[174] L. Schimansky-Geier and T. Pöschel, editors. *Stochastic dynamics*. Springer, Berlin, 1997.

[175] L. Schimansky-Geier and U. Siewert. A glauber-dynamics approach to coupled stochastic resonators. In L. Schimansky-Geier and T. Pöschel, editors, *Stochastic Dynamics*, page 245. Springer, Heidelberg, 1997.

[176] A. Schimz and E. Hildebrand. *PNAS*, 89:457, 1992.

[177] E.H. Serpersu and T.Y. Tsong. Stimulation a oubain-sensitive rb+ uptake in human erthrocytes with an external electric field. *J. Membr. Biol.*, 74:191, 1983.

[178] E.H. Serpersu and T.Y. Tsong. Activation of electrogenic rb+ transport of (na,k)-atpase by an electric field. *J. Biol. Chem.*, 259:7155, 1984.

[179] R.M. Siegel. *Physica D*, 42:385, 1990.

[180] A. Simon and A. Libchaber. *Phys. Rev. Lett.*, 68:3375, 1992.

[181] E. Simonotto, M. Riani, C. Seife, M.Roberts, J. Twitty, and F. Moss. Visual perception of stochastic resonance. *Phys. Rev. Lett.*, 78:1186, 1997.

[182] S. Sinha. Noise-free stochastic resonance in simple chaotic systems. *Physica A*, 270:204, 1999.

[183] J. Smythe, F. Moss, and P.V.E. McClintock. Observation of a noise-induced phase transition with a analog simulator. *Phys. Rev. Lett.*, 51:1062–1065, 1983.

[184] O.V. Sosnovtseva, A.I. Fomin, D.E. Postnov, and V.S. Anishenko. *Phys. Rev. E*, 64:026204, 2001.

[185] M.L. Spano, M. Wun-Folge, and W.L. Ditto. *Phys. rev. A*, 46:5253, 1992.

[186] N.G. Stocks, N.D. Stei, and P.V.E. McClintock. Stochastic resonance in monostable systems. *J. Phys. A*, 26:385, 1993.

[187] R.L. Stratonovich. *Topics in the Theory of Random Noise*, volume 1. Gordon and Breach, New York, 1963.

[188] D.C. Su, M.H. Chiu, and C.D. Chen. Simple two-frequency laser. *Precision Engineering-journal*, 18:161, 1996.

[189] P.A. Tass. *Phase Resetting in Medicine and Biology. Stochastic Modelling and Data Analysis*. Springer-Verlag, Berlin, 1999.

[190] T.Y. Tsong and R.D. Astumian. Absorbtion and conversion of electric field energy by membrene bound atpase. *Biolectochem. Bioenerg.*, 15:457, 1986.

[191] M. Usher and M. Feingold. Stochastic resonance in the speed of memory retrieval. *Biological Cybernetics*, 83:L11–L16, 2000.

[192] R.D. Vale and F. Oosawa. Protein motors and maxwell's demons: Does mechanochemical transduction involve a thermal ratchet? *Adv. Biophys.*, 26:97, 1990.

[193] C. Van den Broeck. From stratonovich calculus to noise-induced phase transitions. In L. Schimansky-Geier and T. Pöschel, editors, *Stochastic Dynamics*, page 7. Springer, Heidelberg, 1997.

[194] C. Van den Broeck, J. M. R. Parrondo, J. Armero, and A. Hernández-Machado. Mean field model for spatially extended systems in the presence of multiplicative noise. *Phys. Rev. E*, 49(4), 1994.

[195] C. Van den Broeck, J. M. R. Parrondo, and R. Toral. Noise-induced nonequilibrium phase transition. *Phys. Rev. Lett.*, 73:3395, 1994.

[196] C. Van den Broeck, J. M. R. Parrondo, R. Toral, and R. Kawai. Nonequilibrium phase transitions induced by multiplicative noise. *Phys. Rev. E*, 55:4084–4094, 1997.

[197] V.K. Vanag, L.F. Yang, M. Dolnik, A.M. Zhabotinky, and I.R. Epstein. *Nature*, 406:389, 2000.

[198] J.D. Victor and M.M. Conte. Two-frequency analysis of interactions elicited by vernier stimuli. *Visual Neuroscience*, 17:959, 2000.

[199] J.M.G. Vilar and J.M. Rubí. Spatiotemporal stochastic resonance in the swift-hohenberg equation. *Phys. Rev. Lett.*, 1997.

[200] E.I. Volkov and M.N. Stolyarov. *Phys. Lett. A*, 159:61, 1991.

[201] E.I. Volkov and M.N. Stolyarov. *Biol. Cybern.*, 71:451, 1994.

[202] H.V. Westerhoff, T.Y. Tsong, P.B. Chock, and R.D. Astumian. How enzymes can capture and transmit free energy from oscillatins electric field. *Proc. Natl. Acad. Sci. USA*, 83:4734, 1986.

[203] K. Wiesenfeld, D. Pierson, E. Pantazelou, C. Dames, and F. Moss. Stochastic resonance on a circle. *Phys. Rev. Lett.*, 72(14):2125–2129, 1994.

[204] A.T. Winfree. *The Geometry of Biological Time*. Springer, Berlin, 1980.

[205] H.S. Wio. *Phys. Rev. E*, 54:R3075, 1996.

[206] A. Witt, A. Neiman, and J. Kurths. *Phys. Rev. E*, 55:5050, 1997.

[207] M. Wu and C.D. Andereck. *Phys. Rev. Lett.*, 65:591, 1990.

[208] A.A. Zaikin and L. Schimansky-Geier. Spatial patterns induced by additive noise. *Phys. Rev. E*, 58(4):4355–4360, 1998.

[209] Y. Zhang, G. Hu, and L. Gammaitoni. *Phys. Rev. E*, 58:2952, 1998.

[210] C. Zhou, J. Kurths, and B. Hu. *Phys. Rev. Lett.*, 87:098101, 2001.

[211] T. Zhou and F. Moss. *Phys. Rev. A*, 41:4255, 1990.

DOUBLY STOCHASTIC EFFECTS

A. ZAIKIN

Institut für Physik, Universität Potsdam,
Am Neuen Palais 10, 14469 Potsdam, Germany
zaikin@agnld.uni-potsdam.de

Doubly stochastic effects are effects in which an optimization of both multiplicative and additive noise intensities is necessary to induce ordering in a nonlinear system. I review recent achievements in the investigation of these effects and discuss two phenomena: doubly stochastic resonance and noise-induced propagation in monostable medium. Finally I discuss possible experimental implementations of these phenomena.

Keywords: Stochastic resonance; multiplicative; additive; noise; doubly stochastic.

1. Introduction

It is not surprising nowadays that noise or random fluctuations can induce counter-intuitive effects, in which noise exhibits a constructive, leading to ordering, role in the behaviour of dynamical systems. Many phenomena have confirmed this ability of noise, among these noise-induced phenomena, one can distinguish between several basic ones, such as noise-induced transitions [1–6], stochastic resonance [7,8], coherence resonance [9], or stochastic transport in ratchets [10]. The most popular example of noise-induced ordering, which can be also found in the behaviour of biological objects [11] as well as in human recognition [12] or in human brain waves [13], is the effect of stochastic resonance (SR). In the most standard situation SR consists in an optimization by noise of the response of a bistable system to a weak periodic signal. In addition to this conventional situation, due to its generality and universality SR has been found in a large variety of systems, as monostable [14], excitable [15], non-dynamical [16], and thresholdless [17] systems, in systems without an external force (called coherence resonance) [9,18], and in systems with transient noise-induced structure [19].

Noteworthy, the principle of SR can be also extended for the case of spatially distributed systems. In such systems an optimal intensity of noise may lead to noise-enhanced propagation, in which the propagation of a harmonic forcing through an unforced bistable or excitable medium is increased for an optimal intensity of addi-

tive noise [20,21]. This phenomenon has all ingredients characteristic of SR, because the system exhibits locally the noise-induced amplification of a weak periodic signal coming from the neighboring sites. It is important to note that, although numerous works about noise-induced propagation exist (e.g. [22–24]), to our knowledge propagation in monostable media, which is a very important class of dynamical systems, has not been considered before. An interesting exception to this point is the thermal resonance in a signal transmission [25], where noise-induced propagation has been found in monostable systems, but without a local potential and with nonlinear coupling.

In this review we discuss several phenomena in the frame of a concept of doubly stochastic effects, which also demonstrate an improvement of signal processing or signal propagation in nonlinear dynamical systems. This concept has been recently introduced as new mechanism leading to noise-induced ordering in nonequlibrium systems. The idea of this concept is the following. If we observe noise-induced order in a nonlinear system, it occurs due to the presence of some intrinsic property of a system, which together with noise results in noise-induced ordering. For example, in the conventional scenario of SR this feature is a threshold, which is present in the system. Coming noise interacts with this feature, and improves a response of the system to the external periodic signal. Meanwhile, a crucial property of a system, a potential threshold in this case, can be also induced by noise. Usually it happens if we have an interplay of multiplicative and additive noise in the system. In this case multiplicative noise induces a property of a system and additive noise maximizes an ordering in a system with this property. Hence, such effects can be called *doubly stochastic effects* (DSE), because for maximal ordering an optimization of both noise intensities is necessary. Certainly, in such effects an energy of noise is used more efficiently, because it is used not only for noise-induced ordering, but also for system property, which is necessary for this ordering.

In this paper we review two DSE, doubly stochastic resonance (DSR) [26] and noise-induced propagation (NIP) in monostable media [27]. After an introduction of a model and reviewing of noise -induced phase transitions, demonstrated by this model, we describe the effect of DSR. In DSR multiplicative noise (in combination with spatial coupling) induces bistability in a deterministically monostable system, and additive noise induces synchronization with the external signal in this noise-induced bistable regime. Following this, we show that this system can exhibit doubly stochastic effects which lead to signal propagation, if the system is periodically excited from one side. Finally we discuss a possible experimental implementation of suggested theoretical findings in designed simple electronic circuit [28]. In the conclusion we discuss the obtained results and possible directions of the future research.

2. A Model and Noise-induced Phase Transition

We study a general class of spatially distributed systems of elements, which are locally coupled and periodically forced:

$$\dot{x}_i = f(x_i) + g(x_i)\,\xi_i(t) + \frac{D}{4}\sum_{j\in nn(i)} (x_j - x_i) + \zeta_i(t) + A_i\,\cos(\omega t + \varphi)\,, \quad (1)$$

where x_i is defined in a two-dimensional discrete space of $N \times N$ cells, with i denoting the cell position ($i = i_x + N(i_y - 1)$, where i_x and i_y run from 1 to N). The sum in the right-hand side runs over all nearest neighbors of site i [$nn(i)$]. The additive and multiplicative noise terms are mutually uncorrelated Gaussian distributed with zero mean, and white both in space and time, i.e. $\langle \zeta_i(t)\zeta_j(t') \rangle = \sigma_a^2 \delta_{ij}\delta(t - t')$ and $\langle \xi_i(t)\xi_j(t') \rangle = \sigma_m^2 \delta_{ij}\delta(t - t')$.

In the absence of periodic forcing ($A_i = 0$), different types of noise-induced phase transitions can be obtained for different forces $f(x_i)$ and $g(x_i)$. In particular, a system with a monostable local deterministic potential can exhibit a phase transition to a noise-induced bistable state [3, 29]. This transition breaks a symmetry and ergodicity of a system and leads to the formation of a non-zero mean field (see Fig. 1). The reason of this phase transition is the common effect of short time bistability induced by multiplicative noise and coupling. To understand which forces $f(x_i)$ and $g(x_i)$ are necessary for the demonstration of noise-induced transition, let us consider the following argumentation [30]. The time evolution of the first moment of a single element can be found by the drift part in the corresponding Fokker-Planck equation (Stratonovich case)

$$\langle \dot{x} \rangle = \langle f(x) \rangle + \frac{\sigma_m^2}{2} \langle g(x)g'(x) \rangle. \tag{2}$$

Next if we start with an initial Dirac δ function, follow it only for a short time, such that fluctuations are small and the probability density is well approximated by a Gaussian. A suppression of fluctuations, performed by coupling, which is absolutely necessary for the transition under consideration, makes this approximation appropriate in our case [31]. The equation for the maximum of the probability, which is also the average value in this approximation $\bar{x} = \langle x \rangle$, has the following form

$$\dot{\bar{x}} = f(\bar{x}) + \frac{\sigma_m^2}{2} g(\bar{x})g'(\bar{x}), \tag{3}$$

which is valid if $f(\langle x \rangle) >> \langle \delta x^2 \rangle f''(\langle x \rangle)$. For this dynamics an "effective" potential $U_{\text{eff}}(x)$ can be derived, which has the form

$$U_{\text{eff}}(x) = U_0(x) + U_{\text{noise}} = -\int f(x)dx - \frac{\sigma_m^2 g^2(x)}{4}, \tag{4}$$

where $U_0(x)$ is a monostable potential and U_{noise} represents the influence of the multiplicative noise. If this effective potential is bistable for some intensity of multiplicative noise, then with some approximation the system can undergo noise-induced phase transition, which leads to bistability of the mean field.

More precisely, a borderline of the phase transition can be found analytically by means of the standard mean-field theory procedure [3]. This mean-field approximation is based on replacing the nearest-neighbor interaction by a global term in the Fokker-Planck equation corresponding to (1) for $A_i = 0$. A steady-state solution of Fokker-Planck eq. then gives:

$$w_{\text{st}}(x, m) = \frac{C(m)}{\sqrt{\sigma_m^2 g^2(x) + \sigma_a^2}} \exp\left(2\int_0^x \frac{f(y) - D(y - m)}{\sigma_m^2 g^2(y) + \sigma_a^2} dy\right), \tag{5}$$

Fig. 1. A visualization demonstration of the phase transition in the model (1). In the disordered phase the mean field is zero due to the random deviation of different elements around zero (middle). In the ordered phase, induced by noise, the symmetry is broken and the mean field is either positive (right) or negative (left). The elements in the lattice 128×128 are coded in accordance to its sign: if positive or zero - white, if negative - black.

where $C(m)$ is a normalization constant and m is the mean field, defined by the equation:

$$m = \int_{-\infty}^{\infty} x w_{\text{st}}(x, m) dx. \tag{6}$$

The self-consistent solution of eq.(6) determines transitions between ordered ($m \neq 0$) and disordered ($m = 0$) phases. Below we consider two examples of functions $f(x)$ and $g(x)$, which provide a possibility of a noise-induced phase transition.

3. Doubly Stochastic Resonance

DSR is a synthesis of noise-induced phase transition and conventional SR. To demonstrate DSR the functions $f(x)$ and $g(x)$ in eq.(1) are taken to be of the form [29]:

$$f(x) = -x(1 + x^2)^2, \qquad g(x) = 1 + x^2. \tag{7}$$

With these forces, a system (1) undergoes a phase transition, whose transition boundaries between different phases are shown in Fig. 2 (left) and the corresponding dependence of the order parameter on σ_m^2 is presented in Fig. 2 (right).

Next we consider how the system (1) responses to the global periodic forcing ($A_i = A$). We have taken a set of parameters ($\sigma_m^2; D$) within the region of two coexisting ordered states with a nonzero mean field. In particular, we choose values given by the dot in Fig. 2 (left). As for the network, we take a two-dimensional lattice of $L^2 = 18 \times 18$ oscillators, which is simulated numerically [32] with a time step $\Delta t = 2.5 \times 10^{-4}$ under the action of the harmonic external force. The amplitude of the force A has to be set sufficiently small to avoid hops in the absence of additive noise. Jumps between $m_1 \leftrightarrow m_2$ occur only if additive noise is additionally switched on. Runs are averaged over different initial phases. Time series of the mean field and the corresponding periodic input signal are plotted in Fig. 3 left for three different values of the intensity of additive noise σ_a^2. The current mean field is calculated as $m(t) = \frac{1}{L^2} \sum_{i=1}^{N} x_i(t)$. For small σ_a^2, hops between the two symmetric states m_1 and m_2 are rather seldom and not synchronized to the external force. If we increase the intensity σ_a^2, we achieve a situation when hops occur with the same periodicity as the external force and, hence, the mean field follows with high probability the input force. An increase of additive noise provides a synchronization of the output of the
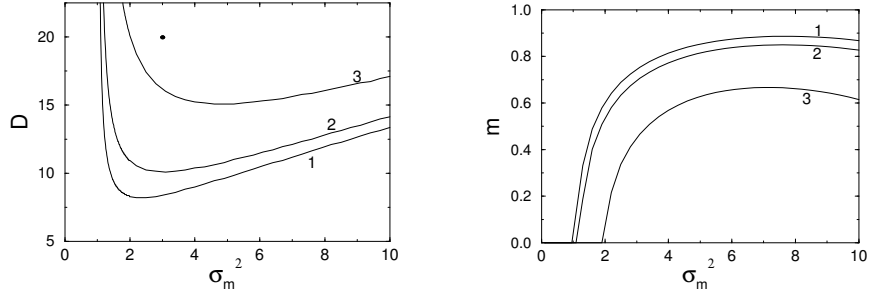
Fig. 2. Left: Boundaries of the bistable regime on the plane $(\sigma_m^2; D)$ for different intensities of the additive noise $\sigma_a^2 = 0$ (1); 1 (2), and 5 (3). The black point corresponds to $D = 20$, $\sigma_m^2 = 3$. Right: The order parameter $|m|$ vs the intensity of the multiplicative noise for $D = 20$ and $\sigma_a^2 = 0$ (label 1), 1 (label 2), and 5 (label 3). Inside the ordered region for fixed value of σ_m^2 an increase of the additive noise intensity leads to the decrease of the order parameter.

system with input forcing. If σ_a^2 is increased further, the order is again destroyed, and hops occur much more frequently than the period of the external force. Note also that for large σ_a^2 the value of the mean field which corresponds to the stable state is becoming smaller. It is caused by the fact that additive noise influences also transition lines. An increase of σ_a^2 results in a reduction of the ordered region (Fig. 2 (left), curves 2 and 3) and decreasing the value $m_1 = -m_2$ (Fig. 2 (right), curves 2 and 3).

To quantify this DSR-effect, we have calculated the signal-to-noise ratio (SNR) by extracting the relevant phase-averaged power spectral density $S(\omega)$ and taking the ratio between its signal part with respect to the noise background [8]. The dependence of SNR on the intensity of the additive noise is shown in the Fig. 3 (right) for the mean field (filled points) and the mean field in a 2-state approximation (opaque point). In this 2-states approximation we have replaced $m(t)$ by its sign and put $m(t) = +1$ or $m(t) = -1$, respectively. Both curves exhibit the well known bell shaped dependence on σ_a^2 typically for SR. Since the bimodality of the mean field is a noise-induced effect we call that whole effect *Doubly Stochastic Resonance*. For the given parameters and $A = 0.1$, $\omega = 0.1$ the maximum of the SNRs is approximately located near $\sigma_a^2 \sim 1.8$.

To obtain analytic estimates of the SNR, an approximation of "effective" potential (4) can be used. For this we consider a conventional SR problem in this potential with an external periodic force of the amplitude A and the frequency ω. If we neglect intrawell dynamics and follow linear response theory the SNR is well known [8, 33]

$$SNR_1 = \frac{4\pi A^2}{\sigma_a^4} r_k \tag{8}$$

where r_k is the corresponding Kramers rate [34]

$$r_k = \frac{\sqrt{(U_{\text{eff}}''(x)|_{x=x_{\min}} |U_{\text{eff}}''(x)|_{x=x_{\max}})}}{2\pi} \exp(-\frac{2\Delta U_{\text{eff}}}{\sigma_a^2}) \tag{9}$$
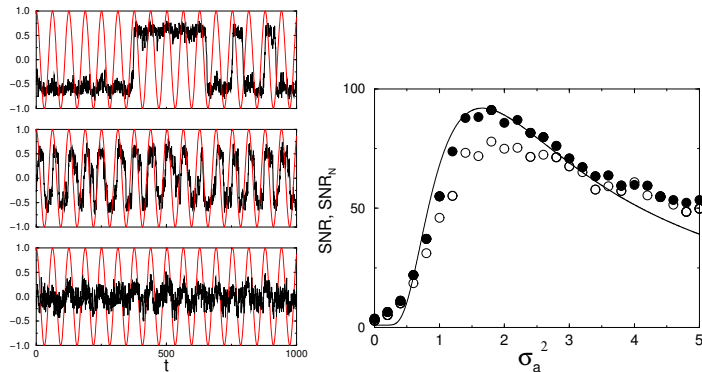
Fig. 3. Left: The time evolution of the current mean field (output) and the periodic external force $F(t)$ (input) for different intensities of additive noise (from top to bottom) $\sigma_a^2 = 0.01$, 1.05, and 5.0. If the intensity of the additive noise is close to their optimal value (middle row), an input/output synchronization occurs. The remaining parameters are: $A = 0.1$, $\omega = 0.1$, $D = 20$, and $\sigma_m^2 = 3$. Right: The dependence of SNR on the additive noise intensity for the output (filled points) and its 2-states approximation (opaque points). The solid line corresponds to the analytical estimation SNR_N (10). The processing gain is $G = 0.7$.

for surmounting the potential barrier ΔU_{eff}. Using Eqs.(4),(8), and (9) we get an analytical estimates for a single element inside the lattice. Further on, rescaling this value by the number N of oscillators in the lattice [35] and taking into account the processing gain G and the bandwidth Δ in the power spectral density [33, 36, 37], the SNR_N of the mean field of the network of N elements can be obtained

$$SNR_N = SNR_1 \frac{NG}{\Delta} + 1. \tag{10}$$

This dependence is shown in the Fig. 3 right by the solid line and demonstrates despite the rough approximation a good agreement with the results of the numerical simulations. Nearly exact agreement is found in the location of the maximum as well as for the quantitative values of the SNR ("scalloping loss" [33] has been avoided in simulations by setting the frequency ω to be centered on one of the bins in the spectrum).

4. Noise-induced Propagation in Monostable Media

Next we study a propagation in the system (1). In this case the periodic forcing is applied to the system (1) coherently along only one side, as shown in Fig. 4 (left) $[A_i = A(\delta_{i_x,1} + \delta_{i_x,2} + \delta_{i_x,3})]$. Even though the results shown below are very general, for a quantitative study we choose particular functions $f(x) = -f_1(x)$(see eq.(12)) and $g(x) = x$ [28]. Regions of bistability can be as above determined approximately by means of a standard mean-field procedure [3] and are shown in Fig. 4(right) in the $D - \sigma_m^2$ plane for three different values of the additive noise intensity.

Now we place ourselves within the bistable regime supported by multiplicative noise and coupling (e.g. $D = 3$, $\sigma_m^2 = 3$), and investigate the propagation of a wave through the system. The boundary conditions are periodic in the vertical direction

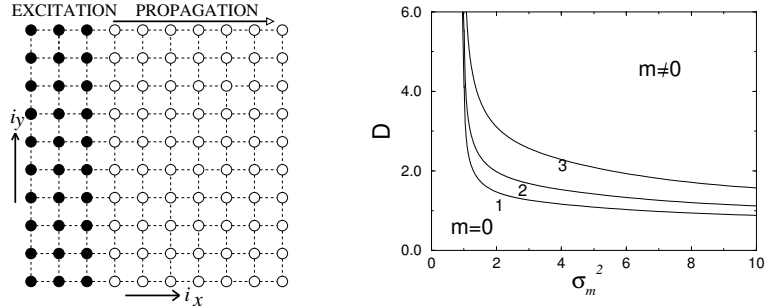Fig. 4. Left: A lattice which is excited only from one side: elements under the direct periodic action are denoted by black; the first three columns ($i_x = 1, 2, 3$) are periodically driven; all oscillators are under the influence of noise. Right: Mean-field transition lines between disordered monostable ($m = 0$) and ordered bistable ($m \neq 0$) phases for model (see Sec. 3): $\sigma_a^2 = 0.3$ (label 1), $\sigma_a^2 = 0.5$ (label 2) and $\sigma_a^2 = 1.0$ (label 3). Other parameters are $G_a = 0.5$, $G_b = 10$ and $B_p = 1$.

and no-flux in the horizontal direction. The propagation will be quantified by the system's response at the excitation frequency, computed as $Q^{(j)} = \sqrt{Q_{\sin}^{(j)}{}^2 + Q_{\cos}^{(j)}{}^2}$, with

$$Q_{\sin}^{(j)} = \frac{\omega}{n\pi} \int_0^{2\pi n/\omega} m_j(t) \sin(\omega t) dt \,, Q_{\cos}^{(j)} = \frac{\omega}{n\pi} \int_0^{2\pi n/\omega} m_j(t) \cos(\omega t) dt \,, \quad (11)$$

where $m_i(t)$ is the field (voltage) averaged along the vertical column (Fig. 4), i.e. $m_j(t) = \frac{1}{N} \sum_{k=1}^N x_{i+(k-1)N}(t)$.

The value of $Q^{(j)}$ for different oscillators along the chain is shown in Fig. 5(a) for increasing intensities of additive noise within the noise-induced bistable regime. The forcing amplitude is taken to be large enough to produce hops between the two wells in the bistable oscillators, without a need of additive noise. Therefore, for the first oscillators an increase of additive noise leads only to a decreasing response at the forcing frequency, whereas for distant oscillators the situation changes qualitatively. There, a response is induced that depends non-monotonically on the additive noise intensity. Clearly, a certain amount of additive noise exists for which the propagation of the harmonic signal is optimal. For smaller multiplicative-noise intensity [Fig. 5(b)] the system leaves the bistable region; hence the response is small and always monotonically decreasing. Hence, the resonant-like effect requires suitable intensities of *both* the additive and multiplicative noises.

A propagation of the harmonic signal can also be obtained for values of the forcing amplitude small enough so that hops are not produced in the directly excited sites in the absence of additive noise. This is the regime in which DSR really occurs in the excited part of the system, and the excitation propagates through the rest of the lattice enhanced by noise. Now all the oscillators have a non-monotonic dependence on the additive noise intensity for a multiplicative noise within the bistable region [Fig. 5(c)], and a monotonic one for a multiplicative noise within the monostable region [Fig. 5(d)]. The former case corresponds to a spatiotemporal propagation in the DSR medium, and we call this phenomenon *spatiotemporal doubly stochastic resonance* (SDSR).
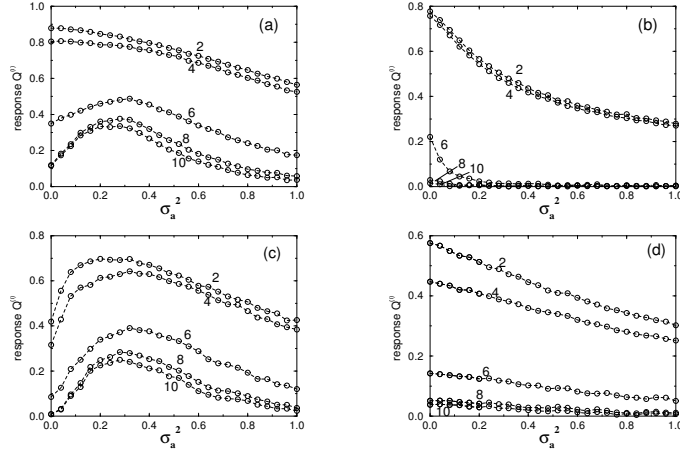
Fig. 5. Response $Q^{(j)}$ to a periodic excitation in different oscillators (the order j is shown in the curve labels) vs. additive-noise intensity (a,c) inside the bistability region ($\sigma_m^2 = 3$), and (b,d) outside that region ($\sigma_m^2 = 0.5$). As shown in Fig. 1, the oscillators with index $j = i_x = 1, 2, 3$ are directly excited by the periodic force, and oscillators with $j = i_x > 3$ are excited through the excitation propagation. Parameters are those of Fig. **??**, and $D = 3$. The amplitude is: (a,b) $A = 0.3$ (noise-induced propagation) and (c,d) $A = 0.2$ (spatiotemporal doubly stochastic resonance).

Using an approximation of "effective" potential this effect can be understood in the frame of a standard SR mechanism [8], where the external signal is provided by the periodic force for the directly excited oscillators, and by the influence of the left neighbors for the non-excited oscillators. For large forcing, only the latter need an additive noise to hop synchronously between the wells, whereas for small forcing, both the excited and the non-excited oscillators display SR. These two behaviors correspond to the situations depicted in Figs. 5(a) and 5(c), respectively.

5. Experimental Implementation

We expect that these theoretical findings will stimulate experimental works to verify DSR in real physical systems (for the first experimental observation of noise-induced bistability see [38]). Appropriate situations can be found in electronic circuits [**?**], as well as in systems, which demonstrate a noise-induced shift of the phase transition, e.g, in: liquid crystals [39, 40], electronic cellular neural networks [41–43], photosensitive chemical reactions [44, 45], or Rayleigh-Bénard convection [46]. It can be crucial for such experiments, that in doubly stochastic effects the energy of noise is used in a more profitable way: not only for the optimization of the signal processing or propagation, but also for the support of the potential barrier to provide this optimization.

Here we discuss a design of a simple electronic circuit which can be used for the demonstration of these phenomena [28]. This electrical circuit consists of N coupled elements (i, j). A circuit of one element is shown in Fig. 6 (a). Three ingredients in this circuit are important: input current, time-varying resistor (TVR) and a

nonlinear resistor. Every element is coupled with its neighbours by the resistor R_c (i.e. by diffusive coupling). The capacitor is shown by C. The nonlinear resistor R_N can be realized with a set of ordinary diodes [47, 48], whose characteristic function is a piecewise-linear function

$$i_N = f(V) = \begin{cases} G_bV + (G_a - G_b)B_p & \text{if } V \leq -B_p, \\ G_aV & \text{if } |V| < B_p, \\ G_bV - (G_a - G_b)B_p & \text{if } V \geq B_p, \end{cases} \tag{12}$$

where i_N is the current through the nonlinear resistor(R_N), V is the voltage across the capacitor(C), and parameters G_a, G_b and B_p determine the slopes and the breakpoint of the piecewise-linear characteristic curve. The next important ingredient is a time-varying resistor(TVR) [48, 49]. The conductance $G(t)$ of TVRs varies with time. Presently, we consider the case that the function which represents the variation of the TVR is a Gaussian $\delta-$correlated in space and time noise, i.e. $G(t) = \xi(t)$, where

$$\langle \xi_i(t)\xi_j(t') \rangle = \sigma_m^2 \delta_{i,j}\delta(t - t').$$

An external action on the elements under direct excitation in the circuit is performed by the current input $I(t)$, which is a periodic signal (with amplitude A, frequency ω, and initial phase φ), additively influenced by independent Gaussian noise $\zeta(t)$ with intensity σ_a^2

$$I(t) = \zeta(t) + A_i\cos(\omega t + \varphi), \quad \langle \zeta_i(t)\zeta_j(t') \rangle = \sigma_a^2 \delta_{i,j}\delta(t - t').$$
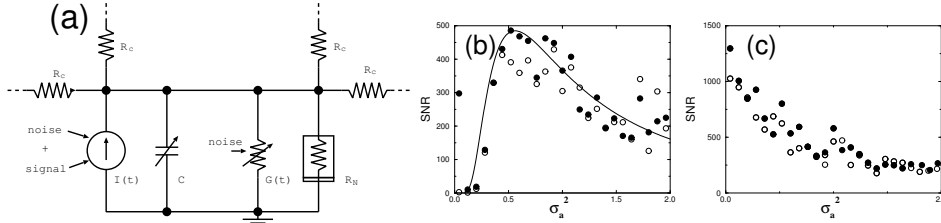
Fig. 6. (a) The electronic circuit of the element (i, j). (b) Numerical SNR (points) vs analytical estimation (solid line) for the equation with f_1 and $D = 3$, $\sigma_m^2 = 3$. Numerical results are shown by black points for the mean field and opaque points for its two-state approximation. The stochastic resonance effect is supported by noise. If we decrease the intensity of multiplicative noise, we do not observe it; e.g. for (c) $D = 3$, $\sigma_m^2 = 0.5$.

The electronic circuit with respect to the element (i, j) can be described by a set of Kirchoff's equations:

$$C\frac{dV_{i,j}}{dt} = I(t) - G(t)V_{i,j} - f(V_{i,j}) + \frac{1}{R_c}(V_{i+1,j} + V_{i-1,j} + V_{i,j+1} + V_{i,j-1} - 4V_{i,j})$$

Hence, the following set of Langevin equations describes the considered system:

$$\begin{aligned} \frac{dV_{i,j}}{dt} &= -f(V_{i,j}) + V_{i,j} + \zeta_{i,j}(t) + A_i\cos(\omega t + \varphi)\xi_{i,j}(t) \\ &+ \frac{D}{4}(V_{i+1,j} + V_{i-1,j} + V_{i,j+1} + V_{i,j-1} - 4V_{i,j}), \end{aligned} \tag{13}$$

where C is set to unity by normalization of time and D denotes a strength of coupling equal to $\frac{4}{CR_c}$. In the case when f_2 represents the TVR, the model is the time-dependent Ginzburg-Landau equation, which is a standard model to describe phase transitions and critical phenomena in both equilibrium and nonequilibrium situations [3]. It is important that we consider only the situation when the potential of one element is monostable ($G_a = 0.5$, $G_b = 10$, $B_p = 1$), hence avoiding the possibility to observe SR without multiplicative noise.

Due to the noise-induced bistability (transitions boundaries are shown in the Fig. 4 right), this circuit will demonstrate both DSE effects considered above. We focus on the case of DSR, i.e. an external excitation is applied to each element and $A_i = A$. An analytical estimation of DSR effect, calculated as in Sec. 2, is shown in the Fig. 6 (b). The DSR effect is clearly observed in the behaviour of SNR of the output mean voltage vs. the intensity of additive noise. To verify the analytical results numerically, we have also performed simulations of the model (13. We have taken a set of parameters within the region of two coexisting ordered states with nonzero mean field. As a total system, we take a two dimensional lattice of 18×18 elements, which was simulated numerically with a time step $\Delta t = 2.5 \times 10^{-4}$. The amplitude of the external signal was set to 0.1, i.e. sufficiently small to avoid hops between two states in the absence of additive noise. The numerically obtained dependence of SNR on the intensity of the additive noise is shown in Fig. 6(b) for the mean-field (filled points) and the mean field in a two-state approximation (opaque points). In this two-state approximation, we have replaced the value of the mean field in time-series by its sign before calculating the power spectral density. Both curves demonstrate well-known bell-shaped dependence which is typical for SR. Let us note, that for these version of the model SNR for the mean field tends to infinity for small values of additive noise intensity (see black points for $\sigma_a^2 < 0.1$). Numerical simulations agree very good with our theoretical estimation despite the very rough approximation via "effective" potential (we will study the question, what is the parameters regions of its validity, in a following paper).

The fact that this SR effect is created by multiplicative noise, can be illustrated as the following. If we decrease only the intensity of multiplicative noise, other parameters fixed, the SR effect is not observed, as it is shown in Fig. 6(c). The reason is that in this case our system is not bistable (see Fig. 4 right) For experimental setup a minimal number of elements, which are necessary for DSR observation, can be important. Reduction of the elements number in this system leads to the fact, that a system can spontaneously (even in the absence of forcing) perform a hop between two states. These jumps hide DSR effect, since they destroy a coherence between input and output. For the system size 18×18, considered here, such jumps are rather seldom and do not hinder DSR. Our calculations have shown that a size 10×10 is still satisfactory, whereas further decrease of the elements number will destroy the effect.

6. Summary and Outlook

I have reviewed recent findings on doubly stochastic effects. I have considered two doubly stochastic phenomena, DSR and noise-induced propagation in monostable media. In these phenomena the role of noise is twofold: first multiplicative noise (to-

gether with coupling) induces a bistability in the spatially distributed system, and then additive noise optimizes a processing or propagation of the input signal. An optimization of both noise intensities is necessary for the demonstration of these doubly stochastic phenomena. Noteworthy, DSR and NIP in monostable media, considered here, differ substantially from the conventional SR and different variations of spatiotemporal SR or NIP in bistable or excitable systems (see discussion in [26, 27]).

One can distinguish between two possible directions of future research on doubly stochastic effects. First, one can search for doubly stochastic effects in other classes of systems, or doubly stochastic effects, which lead to noise-induced ordering of other type. For example, we are going to study doubly stochastic coherence in excitable systems [50], where ordering means a generation of a coherent output in neuron systems. Second, we hope that our theoretical findings will encourage observers to perform experiments to study doubly stochastic effects. Here we have suggested a simple electronic circuit as a possible experimental implementation of doubly stochastic effects, in [26, 27] we have discussed other appropriate experimental situations. We hope that due to its generality the concept of doubly stochastic effects will be confirmed by experiments and used in applications, especially in signal processing systems, such as communication systems or neuron populations.

Acknowledgments

References

[1] J. Smythe, F. Moss, and P. McClintock, *Phys. Rev. Lett.* **51** (1983) 1062.

[2] W. Horsthemke and R. Lefever, *Noise-Induced Transitions* (Springer, Berlin, 1984).

[3] J. García-Ojalvo and J. M. Sancho, *Noise in Spatially Extended Systems* (Springer, New York, 1999).

[4] P. Landa, A. Zaikin, V. Ushakov, and J. Kurths, *Phys. Rev. E* **61** (2000) 4809.

[5] P. Landa and P. McClintock, *Phys. Reports.* **323** (2000) 4.

[6] A. Zaikin and J. Kurths, *Chaos* **11** (2001) 570.

[7] R. Benzi, A. Sutera, and A. Vulpiani, *J. Phys. A* **14** (1981) L453.

[8] L. Gammaitoni, P. Hänggi, P. Jung, and F. Marchesoni, *Rev. Mod. Phys.* **70** (1998) 223.

[9] A. Pikovksy and J. Kurths, *Phys. Rev. Lett.* **78** (1997) 775.

[10] P. Reimann, *Physics Reports* **361** (2002) 57.

[11] D. Russel, L. Wilkens, and F. Moss, *Nature* **402** (1999) 291.

[12] V. S. Anishchenko, A. B. Neiman, F. Moss, and L. Schimansky-Geier, *Sov. Phys. Usp.* **42** (1999) 7.

[13] T. Mori and S. Kai, *Physical Review Letters* **88** (2002) 218101.

[14] N. Stocks, N. Stei, and P. McClintock, *J. Phys. A* **26** (1993) 385.

[15] K. Wiesenfeld *et al.*, *Phys. Rev. Lett.* **72** (1994) 2125.

[16] Z. Gingl, L. Kiss, and F. Moss, *Europhys. Lett.* **29** (1995) 191.

[17] S. Bezrukov and I. Vodyanoy, *Nature* **378** (1995) 362.

[18] H. Gang, T. Ditzinger, C. Ning, and H. Haken, *Phys. Rev. Lett.* **71** (1993) 807.

[19] A. Fuliński, *Phys. Rev. E* **52** (1995) 4523.

[20] J. Lindner *et al.*, *Phys. Rev. Lett.* **81** (1998) 5048.

[21] G. Balázsi, L.B. Kiss, and F.E. Moss, in *Unsolved Problems of Noise and fluctuations*, edited by D. Abbott and L. Kiss (AIP Conf. Proc. 511, 1999).

[22] J. García-Ojalvo, A. Lacasta, F. Sagués, and J. Sancho, *Europhys. Lett.* **50** (2000) 427.

[23] R. Perazzo, L. Romanelli, and R. Deza, *Phys. Rev. E* **61** (2000) R3287.

[24] A. Rowe and P. Etchegoin, *Phys. Rev. E* **64** (2001) 033106.

[25] R. Reigada, A. Sarmiento, and K. Lindenberg, *Phys. Rev. E* **63** (2001) 066113.

[26] A. Zaikin, J. Kurths, and L. Schimansky-Geier, *Phys. Rev. Lett.* **85** (2000) 227.

[27] A. Zaikin, J. García-Ojalvo, L. Schimansky-Geier, and J. Kurths, *Phys. Rev. Lett.* **88** (2002) 010601.

[28] A. Zaikin, K. Murali, and J. Kurths, *Phys. Rev. E* **63** (2001) 020103(R).

[29] C. Van den Broeck, J. M. R. Parrondo, and R. Toral, *Phys. Rev. Lett.* **73** (1994) 3395.

[30] C. Van den Broeck, J. M. R. Parrondo, R. Toral, and R. Kawai, *Phys. Rev. E* **55** (1997) 4084.

[31] C. Van den Broeck, in *Stochastic Dynamics*, edited by L. Schimansky-Geier and T. Pöschel (Springer, Heidelberg, 1997), p. 7.

[32] P. Kloeden and E. Platen, *Numerical Solution of Stochastic Differential Equations* (Springer-Verlag, Berlin Heidelberg, 1992).

[33] B. McNamara and K. Wiesenfeld, *Phys. Rev. A* **39** (1989) 4854.

[34] H. Kramers, *Physica* **7** (1940) 284.

[35] L. Schimansky-Geier and U. Siewert, in *Stochastic Dynamics*, edited by L. Schimansky-Geier and T. Pöschel (Springer, Heidelberg, 1997), p. 245.

[36] C. Nicolis, *Tellus* **34** (1982) 1.

[37] H.S. Wio, *Phys. Rev. E* **54** (1996) R3075; S. Bouzat and H.S. Wio, *Phys. Rev. E* **59** (1999) 5142.

[38] D. Grisowld and J. Tough, *Phys. Rev. A* **36** (1987) 1360.

[39] S. Kai, T. Kai, and M. Takata, *J. Phys. Soc. Jpn.* **47** (1979) 1379.

[40] M. Wu and C. Andereck, *Phys. Rev. Lett.* **65** (1990) 591.

[41] V. Pérez-Muñuzuri, V. Pérez-Villar, and L. Chua, *IEEE Trans.* **40** (1993) 174.

[42] P. Arena, R. Caponetto, L. Fortuna, and A. Rizzo, *IEEE Trans.* **48** (2001) 360.

[43] M. Rabinovich *et al.*, *Phys. Rev. Lett.* **87** (2001) 068102.

[44] J. Micheau, W. Horsthemke, and R. Lefever, *J. Chem. Phys.* **81** (1984) 2450.

[45] P. de Kepper and W. Horsthemke, *Synergetics: Far From Equilibrium* (Springer, New York, 1979).

[46] C. Meyer, G. Ahlers, and D. Cannell, *Phys. Rev. A* **44** (1991) 2514.

[47] N. Inaba, T. Saito, and S. Mori, *The Trans. of the IEICE* **E70** (August 1987) 744.

[48] L. Chua, C. Desoer, and E. Kuh, *Linear and Nonlinear Circuits* (McGraw-Hill Book Co., New-York, 1987).

[49] Y. Nishio and S. Mori, *IEICE Trans. Fundamentals* **E76-A** (March 1993) 467.

[50] A. Zaikin, J. García-Ojalvo, R. Báscones,E. Ullner, and J. Kurths, (2002), (submitted).

Doubly Stochastic Coherence via Noise-Induced Symmetry in Bistable Neural Models

A. Zaikin,[1] J. García-Ojalvo,[2] R. Báscones,[2] E. Ullner,[1] and J. Kurths[1]

[1]*Institut für Physik, Potsdam Universität, Am Neuen Palais 10, D-14469 Potsdam, Germany*
[2]*Departament de Física i Enginyeria Nuclear, Universitat Politècnica de Catalunya, Colom 11, E-08222 Terrassa, Spain*
(Received 13 July 2002; published 23 January 2003)

The generation of coherent dynamics due to noise in an activator-inhibitor system describing bistable neural dynamics is investigated. We show that coherence can be induced in deterministically asymmetric regimes via symmetry restoration by multiplicative noise, together with the action of additive noise which induces jumps between the two stable steady states. The phenomenon is thus *doubly stochastic,* because both noise sources are necessary. This effect can be understood analytically in the frame of a small-noise expansion and is confirmed experimentally in a nonlinear electronic circuit. Finally, we show that spatial coupling enhances this coherent behavior in a form of system-size coherence resonance.

Rhythm generation is a long-standing problem in science, particularly in biological and cognitive science contexts [1,2]. A paradigm of this kind of self-sustained oscillating behavior in nonlinear systems is offered by limit cycles. But even in the absence of limit cycles, internal rhythms can be generated in nonlinear systems by the effect of noise. An early realization of this phenomenon was reported in a two-dimensional autonomous system when operating close to a limit cycle and was interpreted as a manifestation of stochastic resonance in the absence of external forcing [3]. An optimal amount of noise was also seen to lead to a maximally coherent output in an excitable system [4]. This effect, called *coherence resonance,* was studied in the well-known FitzHugh-Nagumo model, which has been extensively used to describe the dynamics of neural systems [5]. Coherence resonance has been confirmed in several experimental situations, such as in laser systems [6]. Furthermore, it has also been predicted in a system with two chaotic attractors [7] and in excitable media coupled via an inhibitor concentration, provided the coupled elements behave in antiphase [8].

A complete understanding of these different mechanisms of coherence resonance is very important for the study of rhythm generation in biological systems [2,9] and, in particular, in neural tissue. On the other hand, increasing experimental evidence has established in recent years that certain types of neurons frequently operate in a bistable regime [10]. Thus, the question arises whether noise can excite an autonomous coherent output in *bistable* neural systems. In this direction, both standard stochastic and coherence resonance have been observed in a symmetrically bistable FitzHugh-Nagumo model [11]. In the present Letter, we show that coherence can also be generated in the general asymmetric case, where the stability of the two stable steady states is not necessarily the same. We demonstrate that the mechanism of coherence enhancement in this situation is utterly different from the standard one, being based on the restoration of

symmetry induced by a multiplicative source of noise. This effect vividly contrasts with standard noise-induced phase transitions, where noise usually leads to the breaking of symmetry [12].

Doubly stochastic coherence (DSC) can be observed in an asymmetric system under the joint action of multiplicative and additive noises. Once multiplicative noise induces a symmetric bistable state in the system, due to the presence of optimal additive noise, coherence can be maximized in the output. Hence, the resulting coherence is *doubly stochastic,* since simultaneous optimization of two noise intensities is required in order to observe the phenomenon. The concept of doubly stochastic effects has been introduced recently as a new mechanism of noise-induced phenomena in the context of harmonically driven systems [13]. These effects are usually possible due to the interplay between additive and multiplicative noise. In [13], multiplicative noise (in combination with spatial coupling) induces bistability in a simple monostable extended system, and additive noise induces synchronization with the external signal in that noise-induced bistable regime. Such doubly stochastic resonance has been reported in simple electronic circuit models [14]. Following those lines, we have shown recently that doubly stochastic effects lead also to signal propagation in simple monostable media [15]. The synthesis of noise-induced transitions and noise-induced transport reported in [16] is also related to this kind of effects. In this Letter, we report the occurrence of DSC in a modified version of the well-known FitzHugh-Nagumo (FHN) model. The mechanism is explained theoretically in the framework of a small-noise expansion of the model, which extracts the systematic contribution of the multiplicative noise that accounts for the symmetry restoration. The results of this analysis and numerical results are confirmed by experiments on an electronic circuit. Finally, we show that this effect can be generalized for the case of spatially extended systems, where it leads to synchronization induced by multiplicative noise.

We consider the following version of the FHN model:

$$\varepsilon \frac{du}{dt} = u(1 - u)(u - a) - v,$$
$$\frac{dv}{dt} = bu - v - uv\xi(t) + \zeta(t). \tag{1}$$

In a neural context, $u(t)$ represents the membrane potential of the neuron and $v(t)$ is related to the time-dependent conductance of the potassium channels in the membrane [5]. The dynamics of u is much faster than that of v, as indicated by the small time-scale-ratio parameter ε. There are two mutually uncorrelated noise sources, represented by the δ-correlated Gaussian noises $\xi(t)$ and $\zeta(t)$, with zero mean and correlations $\langle \xi(t)\xi(t')\rangle = \sigma_m^2 \delta(t - t')$ and $\langle \zeta(t)\zeta(t')\rangle = \sigma_a^2 \delta(t - t')$. The additive noise is inserted in the slow-variable equation, as in most studies of coherence resonance [4]. The multiplicative noise $\zeta(t)$ is interpreted in the Stratonovich sense [12].

In what follows we use the parameters $a = 0.15$, $b = 0.12$, and $\varepsilon = 0.01$, for which the deterministic system has two stable fixed points with different stability (i.e., with different thresholds of escape through the extrema of the u nullcline), as shown in Fig. 1(a) (curve 1 and its crossing points with the u nullcline). Additive noise induces here jumps between these two states, but the escape times are very different in the two states. This behavior is shown in Fig. 1(b), as obtained from numerical simulations of model (1) for the above-mentioned parameters.

The effect of multiplicative noise in this system can be determined by analyzing the systematic effect it produces in the system dynamics due to the fact that the corresponding fluctuating term in the v equation has a nonzero average value. Computation of this average value by means of standard techniques [17] leads to the following effective deterministic model, which can be considered as a first order approximation in a small-noise expansion of $\xi(t)$ [12]:
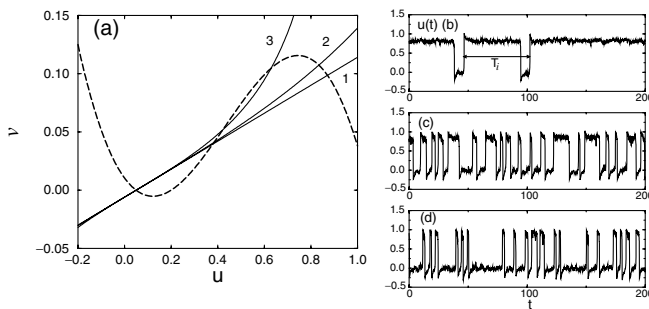
$$\varepsilon \frac{\partial u}{\partial t} = u(1 - u)(u - a) - v, \tag{2}$$

$$\frac{\partial v}{\partial t} = bu - v + \frac{\sigma_m^2}{2} u^2 v + \zeta(t). \tag{3}$$

The nullclines of this model for two nonzero values of σ_m^2 are shown in Fig. 1(a), as curves 2 and 3. It can be seen that for an intermediate value of σ_m^2, corresponding to curve 2, the two states are equally stable and the escape times are basically identical. As a result, jumps in the output of the system are more equidistant [Fig. 1(c)]. For larger multiplicative noise intensity the asymmetry increases again, this time reversed, as shown in curve 3 of Fig. 1(a), and the system spends more time in the lower state, as shown in Fig. 1(d) (in fact, in this extreme case the upper steady state has turned unstable, and the system becomes excitable).

Hence, an optimal amount of multiplicative noise optimizes the symmetric response of the system. In that situation, we can expect additive noise to be more effective in producing coherence, since the potential barrier heights (and thus the corresponding escape times) are the same in the two jump directions. To quantify this expected coherence enhancement, we have measured the normalized variance of subsequent periods T_i. The illustration of the definition of T_i is depicted in Fig. 1(b). The normalized variance, which is called the coherence parameter [4], is determined as $R = \sqrt{\sigma_T^2 / \langle T_i \rangle}$, where σ_T^2 is the variance of the sequence T_i, and $\langle T_i \rangle$ is its average value. The dependence of R on the multiplicative noise intensity for the time series depicted in Figs. 1(b)–1(d) is shown in Fig. 2 (left). It is clearly seen that R first decreases to some minimum value and then increases again. The minimal R corresponds to the highest degree of periodicity in the system output and is a manifestation of stochastically induced coherence. A similar behavior occurs for varying the strength of the additive noise as well, as shown in the inset of Fig. 2 (left). Different values of the excitation threshold correspond to different optimal intensities of the noise. To optimize the periodicity, one should vary both the threshold (provided by

FIG. 1. (a) Nullcline plot of the FHN model (1). Dashed line: u nullcline ($\dot{u} = 0$); solid lines: v nullclines ($\dot{v} = 0$) for three different values of the multiplicative noise intensity: $\sigma_m^2 = 0.0$ (curve 1), 0.2 (curve 2), and 2.0 (curve 3). (b)–(d) Time evolution of the activator variable u for the previous three multiplicative noise intensities: (b) $\sigma_m^2 = 0.0$, (c) 0.2, (d) 2.0. The intensity of additive noise is fixed to $\sigma_a^2 = 2 \times 10^{-4}$; other parameters are given in the text.
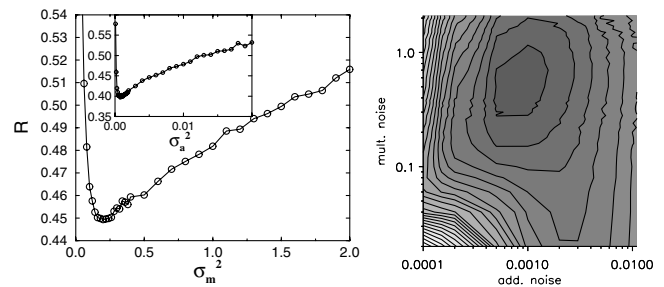

FIG. 2. Left: coherence parameter R vs intensity of the multiplicative and additive (inset plot) noises. $\sigma_a^2 = 2 \times 10^{-4}$ and $\sigma_m^2 = 0.5$, respectively. Right: contour plot of the coherence parameter R vs intensity of the multiplicative and additive noises (darker gray corresponds to smaller values of R).
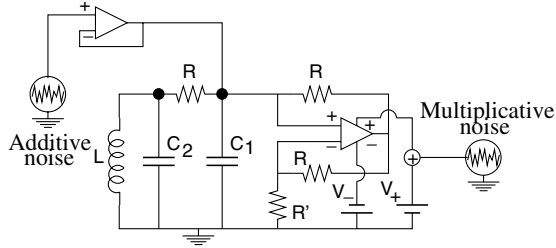
FIG. 3.   Nonlinear electronic circuit with two asymmetrically stable steady states. The values of the elements are $R = 270\ \Omega$, $L = 10$ mH, $C_1 = 1$ nF, $C_2 = 10$ nF, $R' = 220\ \Omega$, $V_- = 5$ V, and $V_+ = 2$ V. The operational amplifier is taken from a TL082 integrated circuit.

FIG. 4.   Time evolution of the voltage drop V_1 through capacitor C_1 for the circuit represented in Fig. 3, for three different intensities of the multiplicative noise (measured as peak-to-peak amplitude of the random voltage): (a) 1.6 V, (b) 1.7 V, and (c) 1.9 V. Additive noise intensity is fixed to 0.88 V. (d) Coherence parameter vs multiplicative noise intensity.

multiplicative noise) and the intensity of additive noise. Both noise intensities need to be tuned in order to optimize periodicity in the output [see Fig. 2 (right)], and hence we call this effect doubly stochastic coherence.

With the aim of confirming experimentally the phenomenon of DSC via noise-induced symmetry, we have designed a circuit (Fig. 3), which has two asymmetrically stable steady states. In this circuit, the difference between the positive and negative voltages feeding the operational amplifier provides the asymmetry in the stability of the two fixed points. Multiplicative noise acts on the positive voltage V_+, which is a parameter that changes the stability of the higher voltage fixed point of the circuit [18]. A second source of noise, which acts as a signal, induces jumps between the two stable states and acts as an additive noise. The noise is produced electronically by amplifying shot noise from a junction diode [19].

Following the numerical approach, we fix the intensity of additive noise and increase that of multiplicative noise. First, the upper steady state is more stable than the lower one, and the system spends more time in the former [Fig. 4(a)]. As the strength of multiplicative noise increases, the situation is reversed [Fig. 4(c)], passing through a symmetric regime for intermediate noise [Fig. 4(b)]. Calculating the coherence parameter R for the experimental time traces, we find clearly that multiplicative noise enhances coherence via the appearance of symmetry [Fig. 4(d)].

We have also examined the effect of spatial coupling on a set of distributed bistable FHN oscillators subject to two noise sources. The model is now given by

$$\varepsilon \frac{\partial u_i}{\partial t} = u_i(1 - u_i)(u_i - a) - v_i$$
$$+ \frac{D}{2}(u_{i+1} + u_{i-1} - 2u_i), \qquad (4)$$
$$\frac{\partial v_i}{\partial t} = bu_i - v_i - u_i v_i \xi_i(t) + \zeta_i(t),$$

where D denotes the strength of coupling and the noise terms are now δ correlated also in space, with $\langle \xi_i(t)\xi_j(t') \rangle = \sigma_m^2 \delta(t - t')\delta_{ij}$ and $\langle \zeta_i(t)\zeta_j(t') \rangle = \sigma_a^2 \delta(t - t')\delta_{ij}$.

We now study the joint effect of additive and multiplicative noise on the spatiotemporal evolution of this extended system, using a binary coding for the activator variable $u_i(t)$, associating black or white to each one of the two fixed points of the local bistable dynamics. The numerical simulation results are shown in Fig. 5 for three values of σ_m^2 and a fixed σ_a^2. As expected, the local dynamics becomes more regular for an optimal amount of multiplicative noise, as happens with an isolated FHN element. However, remarkably enough, the most temporally coherent case corresponds also to the most spatially uniform behavior of the system as a whole. To characterize such a synchronized coherence, we calculate the coherence parameter R for the mean field $m(t) = \sum_i u_i$. The dependence of this parameter on the intensity of multiplicative noise is shown in Fig. 6(a) for a system of 50 coupled elements. The dependence is nonmonotonic, reflecting the DSC characteristic of isolated elements,
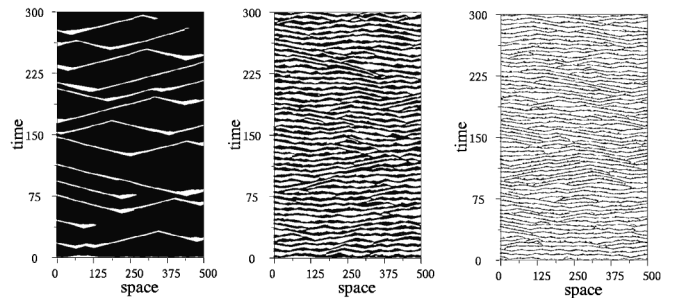
FIG. 5.   Spatiotemporal evolution of a chain of FHN oscillators in the bistable regime for three intensities of the multiplicative noise. From left to right, $\sigma_m^2 = 0.01, 0.2, 4$. Additive noise is fixed to $\sigma_a^2 = 4 \times 10^{-4}$. Coding is binary, with black corresponding to the upper fixed point and white to the lower one. Other parameters are $D = 30$, $a = 0.15$, $b = 0.12$, and $\varepsilon = 0.01$.

FIG. 6. (a) Coherence parameter R of the mean field $m(t)$ vs intensity of the multiplicative noise for a system with 50 coupled elements. (b) The dependence of R on the size of the system ($\sigma_m^2 = 0.005$).

although in this case the parameter measures also the degree of synchronization in the system. Furthermore, Fig. 6(b) shows that increasing the number of elemen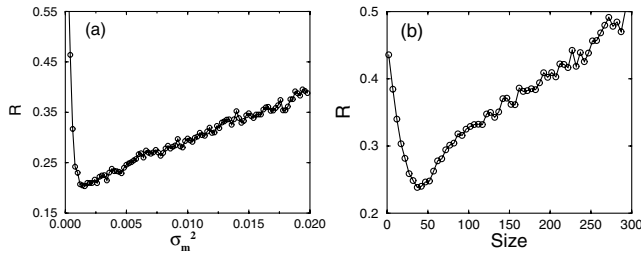ts in the ensemble first increases the coherence of the output (R initially decreases), due to the synchronization of the elements, but further increase of the system size leads to a loss of synchronization, and thus R increases again. The result is a *system-size coherence resonance* (cf. with system-size stochastic resonance, which happens in externally forced systems [20]). In a neural context, this property could imply that neurons benefit from coupling in networks of optimal size for the organization of a pacemaker.

In conclusion, we have shown that bistable models of neural dynamics exhibit doubly stochastic coherence via noise-induced symmetry. This mechanism of rhythm generation arises whenever the two stable steady states of the system have different escape thresholds. An optimal amount of multiplicative noise renders the two fixed points equally stable, and tuning the additive noise in this noise-induced symmetric situation maximizes the coherent behavior in the system. The influence of multiplicative noise can be explained in terms of an effective model that contains the systematic effect of the noise term. These results have been confirmed by experimental measurements on a bistable nonlinear electronic circuit. From a second standpoint, we have shown that this effect leads to synchronized behavior in spatially distributed systems. In this case, this coherence enhancement also exhibits a resonance with respect to the size of the system; i.e., there is some optimal size of the system for which the output is the most periodic one. Our study has been performed in the general framework of the paradigmatic FHN model, in a bistable asymmetric regime which is realistic for biological systems [10], and hence we expect that our findings could be of importance for understanding the mechanisms of periodicity generation in neural and other excitable media.

[1] A. T. Winfree, *The Geometry of Biological Time* (Springer, Berlin, 1980).
[2] R. Engbert, C. Scheffczyk, R. T. Krampe, M. Rosenblum, J. Kurths, and R. Kliegl, Phys. Rev. E **56**, 5823 (1997).
[3] G. Hu, T. Ditzinger, C. Z. Ning, and H. Haken, Phys. Rev. Lett. **71**, 807 (1993).
[4] A. Pikovksy and J. Kurths, Phys. Rev. Lett. **78**, 775 (1997).
[5] J. Keener and J. Snyder, *Mathematical Physiology* (Springer, New York, 1998).
[6] G. Giacomelli, M. Giudici, S. Balle, and J. R. Tredicce, Phys. Rev. Lett. **84**, 3298 (2000); J. M. Buldú, J. García-Ojalvo, C. R. Mirasso, M. C. Torrent, and J. M. Sancho, Phys. Rev. E **64**, 051109 (2001).
[7] C. Palenzuela, R. Toral, C. Mirasso, O. Calvo, and J. Gunton, Europhys. Lett. **56**, 347 (2001).
[8] E. Volkov, M. Stolyarov, A. Zaikin, and J. Kurths (to be published).
[9] J. Collins and I. Stewart, J. Nonlinear Sci. **3**, 349 (1993).
[10] S. W. Hughes, D. W. Cope, T. I. Tóth, S. R. Williams, and V. Crunelli, J. Physiol. (London) **517**, 805 (1999).
[11] B. Lindner and L. Schimansky-Geier, Phys. Rev. E **61**, 6103 (2000); F. Moss, J. K. Douglass, L. Wilkens, D. Pierson, and E. Pantazelou, Ann. N.Y. Acad. Sci. **706**, 26 (1993).
[12] J. García-Ojalvo and J. M. Sancho, *Noise in Spatially Extended Systems* (Springer, New York, 1999).
[13] A. Zaikin, J. Kurths, and L. Schimansky-Geier, Phys. Rev. Lett. **85**, 227 (2000).
[14] A. Zaikin, K. Murali, and J. Kurths, Phys. Rev. E **63**, 020103(R) (2001).
[15] A. Zaikin, J. García-Ojalvo, L. Schimansky-Geier, and J. Kurths, Phys. Rev. Lett. **88**, 010601 (2002).
[16] P. Reimann, R. Kawai, C. Van den Broeck, and P. Hänggi, Europhys. Lett. **45**, 545 (1999).
[17] J. M. Sancho and J. García-Ojalvo, in *Stochastic Processes in Physics, Chemistry, and Biology*, edited by J. Freund and T. Pöschel (Springer, New York, 2000), pp. 235–246.
[18] R. Báscones, J. García-Ojalvo, and J. M. Sancho, Phys. Rev. E **65**, 061108 (2002).
[19] M. Löcher, D. Cigna, and E. R. Hunt, Phys. Rev. Lett. **80**, 5212 (1998).
[20] A. Pikovksy, A. Zaikin, and M. A. de la Casa, Phys. Rev. Lett. **88**, 050601 (2002).

Noise Induced Propagation in Monostable Media

A. A. Zaikin,[1] J. García-Ojalvo,[2] L. Schimansky-Geier,[3] and J. Kurths[1]

[1]*Institut für Physik, Potsdam Universität, Am Neuen Palais 10, D-14469 Potsdam, Germany*
[2]*Departament de Física i Enginyeria Nuclear, Universitat Politècnica de Catalunya, Colom 11 E-08222 Terrassa, Spain*
[3]*Institut für Physik, Humboldt Universität zu Berlin, Invalidenstrasse 110, D-10115 Berlin, Germany*

We show that external fluctuations are able to induce propagation of harmonic signals through monostable media. This property is based on the phenomenon of doubly stochastic resonance, where the joint action of multiplicative noise and spatial coupling induces bistability in an otherwise monostable extended medium, and additive noise resonantly enhances the response of the system to a harmonic forcing. Under these conditions, propagation of the harmonic signal through the unforced medium is observed for optimal intensities of the two noises. This noise-induced propagation is studied and quantified in a simple model of coupled nonlinear electronic circuits.

       PACS numbers: 05.40.Ca, 05.70.Fh

It is a well-established fact nowadays that dynamical noise, which usually has a disordering impact, can be used to induce order in nonlinear nonequilibrium systems under certain conditions. Examples of this counterintuitive influence of random fluctuations are noise-induced transitions [1–4], stochastic transport in ratchets [5] (also in a synthesis with a transition [6]), or noise-induced pattern formation [7]. However, one of the most far-reaching examples is stochastic resonance (SR) [8], which has been experimentally observed in several physical and biological systems [9]. In the classical situation, SR consists of an optimization by noise of the response of a bistable system to a weak periodic signal. Besides this standard scenario, SR has also been found in monostable [10], excitable [11], nondynamical [12], and thresholdless [13] systems, in systems without an external force (what is called coherence resonance) [14,15], and in systems with transient noise-induced structure [16].

Additionally, it has been recently shown that the energy of fluctuations can be used even more efficiently in spatially extended systems, by using noise twofold: to synchronize output hops across a potential barrier with an external signal, and also to optimally construct the barrier itself. This phenomenon is known as *doubly stochastic resonance* (DSR) [17]. DSR occurs in systems of coupled overdamped oscillators; and it is a synthesis of two basic phenomena: SR and noise-induced phase transitions [18]. Another important and nontrivial phenomenon connected with SR in spatially distributed systems is the phenomenon of *noise enhanced propagation,* in which the propagation of a harmonic forcing through an unforced bistable or excitable medium is increased for an optimal intensity of the additive noise [19,20].

In this Letter, we present a new propagation phenomenon in monostable media. We show that noise can enhance propagation in deterministically *monostable* media, without any deterministic threshold, provided bistability is induced by a second (multiplicative) noise and coupling through a phase transition. Although numerous works

about noise-induced propagation exist (e.g., [21]), to our knowledge propagation in *monostable* media, which is a very important class of dynamical systems, has not been considered before. In what follows, we present this propagation or in a general model of overdamped coupled nonlinear oscillators. Subsequently, and for the sake of concreteness, the phenomenon is analyzed in particular in a simple model of coupled electronic circuits.

We study a general class of spatially distributed systems, which are locally coupled and periodically forced:

$$\dot{x}_i = f(x_i) + g(x_i)\xi_i(t) + \frac{D}{4}\sum_{j\in nn(i)}(x_j - x_i)$$
$$+ \zeta_i(t) + A_i\cos(\omega t + \varphi), \qquad (1)$$

where x_i is defined in a two-dimensional discrete space of $N \times N$ cells, with i denoting the cell position $[i = i_x + N(i_y - 1)$, where i_x and i_y run from 1 to $N]$. The sum in Eq. (1) runs over all nearest neighbors of site i $[nn(i)]$. The additive and multiplicative noise terms are mutually uncorrelated Gaussian distributed with zero mean, and white both in space and time, i.e., $\langle \zeta_i(t)\zeta_j(t')\rangle = \sigma_a^2\delta_{ij}\delta(t - t')$ and $\langle \xi_i(t)\xi_j(t')\rangle = \sigma_m^2\delta_{ij}\delta(t - t')$. The results are averaged over the initial phase φ of a harmonic forcing, which has amplitude A_i and frequency ω.

In the absence of periodic forcing ($A_i = 0$), different types of noise-induced phase transitions can be obtained for different forces $f(x_i)$ and $g(x_i)$ [3]. In particular, a system with a monostable deterministic potential can undergo a phase transition to a noise-induced bistable state for a suitable stochastic forcing $g(x_i)$ [18]. There, in the presence of a global harmonic forcing, DSR is observed [17]. We consider in this Letter the case that the periodic forcing is applied coherently along only one side, as shown in Fig. 1 $[A_i = A(\delta_{i_x,1} + \delta_{i_x,2} + \delta_{i_x,3})]$, and study the propagation of this forcing action into the nonexcited portion of the system.

Even though the results shown below are very general, for a quantitative study we choose particular functions
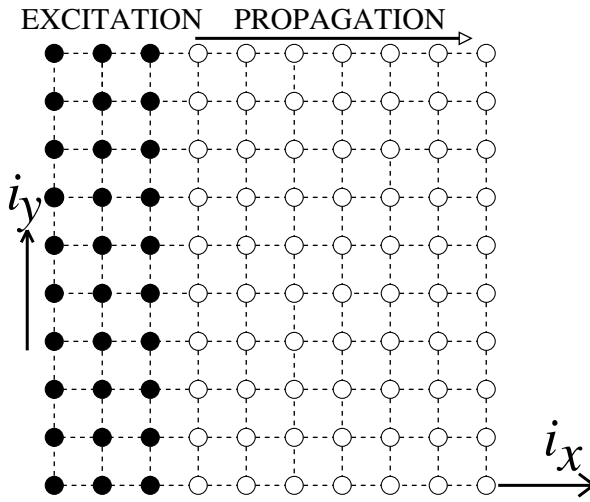
EXCITATION   PROPAGATION

FIG. 1.   Scheme of the spatially distributed system. The periodic excitation is performed only from one side, elements under the direct periodic action are denoted by black. All oscillators are under the influence of noise. To study the behavior of both driven and nondriven elements, first three columns ($i_x = 1, 2, 3$) are periodically driven; however, to achieve propagation it is sufficient to excite only one column.

$f(x)$ and $g(x)$. These functions model the local dynamics of the electronic circuit designed theoretically (i.e., it is so far a thought experiment) and displayed in Fig. 2. This circuit consists of a capacitor with capacitance C, a time-varying resistor (TVR) with conductance $G(t)$, a current generator $I(t)$, four coupling resistors R_c (responsible for the diffusive coupling with the neighbors), and a nonlinear resistor R_N, which is realized with a set of ordinary diodes or operational amplifiers [22], and has the characteristic function

$$i_N = h(V) = \begin{cases} G_b V + (G_a - G_b)B_p, & \text{if } V \le -B_p, \\ G_a V, & \text{if } |V| < B_p, \\ G_b V - (G_a - G_b)B_p, & \text{if } V \ge B_p, \end{cases} \quad (2)$$

where i_N is the current through the nonlinear resistor (R_N), V is the voltage drop across it, and the parameters G_a, G_b, and B_p determine the slopes and the break point of its piecewise-linear characteristic curve.

We now consider that the conductance of the TVR fluctuates randomly in time [$G_i(t) = \xi_i(t)$], and that the input
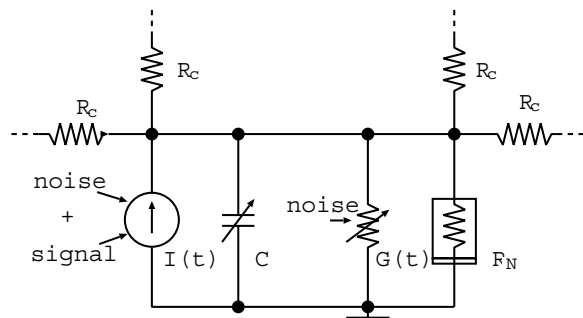
FIG. 2.   Nonlinear electronic circuit at element i.

current $I(t)$ has the form of a periodic signal to which an uncorrelated Gaussian noise $\zeta(t)$ is added [$I_i(t) = \zeta_i(t) + A_i \cos(\omega t + \varphi)$]. Under these conditions, the dynamics of the spatially coupled system is described by Eq. (1), where x_i now represents the voltage drop across the nonlinear resistor of circuit i, and the forces are $f(x) = -h(x)$ and $g(x) = x$ [22]. Additionally, $C = 1$ by an appropriate time normalization, and the coupling strength $D = \frac{4}{CR_c}$.

SR behavior can be expected if the system is bistable for the chosen set of parameters. Regions of bistability can be determined approximately by means of a standard mean-field procedure [3]. The mean-field approximation consists of replacing the nearest-neighbor interaction by a global term in the Fokker-Planck equation corresponding to (1) in the absence of external forcing. In this way, we get the steady-state probability distribution P_{st}:

$$P_{\text{st}}(x, m) = \frac{C(m)}{\sqrt{\sigma_m^2 g^2(x) + \sigma_a^2}} \\ \times \exp\left(2 \int_0^x \frac{f(y) - D(y - m)}{\sigma_m^2 g^2(y) + \sigma_a^2} dy\right), \quad (3)$$

where $C(m)$ is a normalization constant and m is the mean field, defined implicitly by:

$$m = \int_{-\infty}^{\infty} x P_{\text{st}}(x, m) \, dx. \quad (4)$$

The value of m is obtained by the self-consistent solution of Eq. (4), which enables us to determine the transition lines between the ordered bistable ($m \ne 0$) and the disordered monostable ($m = 0$) phases. These transition boundaries are shown in Fig. 3 in the (D, σ_m^2) plane for three different values of the additive noise intensity. Note that bistability requires both multiplicative noise and coupling between elements. We also find that an increase in additive noise reduces the bistable region. This gives DSR a special character with respect to standard SR [17].

Now, we place ourselves within the bistable regime supported by multiplicative noise and coupling (e.g.,

FIG. 3.   Mean-field transition lines between disordered monostable ($m = 0$) and ordered bistable ($m \ne 0$) phases for model (1): $\sigma_a^2 = 0.3$ (label 1), $\sigma_a^2 = 0.5$ (label 2), and $\sigma_a^2 = 1.0$ (label 3). Here $G_a = 0.5$, $G_b = 10$, and $B_p = 1$.

$D = 3$, $\sigma_m^2 = 3$), and investigate the propagation of a wave through the system. To that end, we harmonically excite the lattice from one side, as sho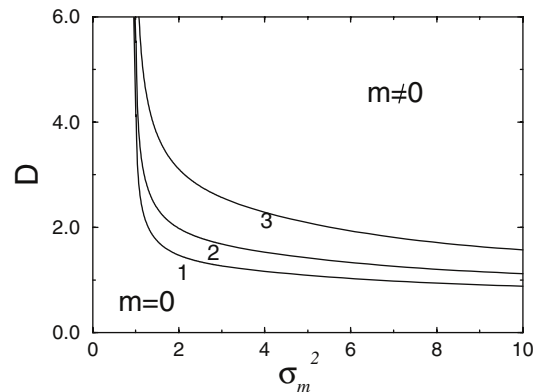wn in Fig. 1, with boundary conditions periodic in the vertical direction and no-flux in the horizontal direction. The propagation will be quantified by the system's response at the excitation frequency, computed as $Q^{(j)} = \sqrt{[Q_{\sin}^{(j)}]^2 + [Q_{\cos}^{(j)}]^2}$, with

$$Q_{\sin}^{(j)} = \frac{\omega}{n\pi} \int_0^{2\pi n/\omega} 2m_j(t) \sin(\omega t)\, dt \,, \qquad (5)$$

$$Q_{\cos}^{(j)} = \frac{\omega}{n\pi} \int_0^{2\pi n/\omega} 2m_j(t) \cos(\omega t)\, dt \,, \qquad (6)$$

where $m_j(t)$ is the field (voltage) averaged along the vertical column (Fig. 1), i.e., $m_j(t) = \frac{1}{N} \sum_{k=1}^{N} x_{j+(k-1)N}(t)$.

The value of $Q^{(j)}$ for different oscillators along the chain is shown in Fig. 4(a), for increasing intensities of additive noise within the noise-induced bistable regime. The forcing amplitude is taken to be large enough to produce hops between the two wells in the bistable oscillators, without the need of additive noise. Therefore, for the first oscillators an increase of additive noise leads only to a decreasing response at the forcing frequency, whereas for distant oscillators the situation changes qualitatively. There, a response is induced that depends nonmonotonically on the additive noise intensity. Clearly, a certain amount of additive noise exists for which propagation of the harmonic signal is optimal. For smaller σ_m^2 [Fig. 4(b)] the system leaves the bistable region; hence the response is small and always monotonically decreasing. Hence, the resonantlike

FIG. 4. Response $Q^{(j)}$ to a periodic excitation in different columns (the order j is shown in the curve labels) vs additive-noise intensity (a),(c) inside the bistability region ($\sigma_m^2 = 3$), and (b),(d) outside that region ($\sigma_m^2 = 0.5$). As shown in Fig. 1, the oscillators with index $j = i_x = 1, 2, 3$ are directly excited by the periodic force, and oscillators with $j = i_x > 3$ are excited through the excitation propagation. Parameters are those of Fig. 3, and $D = 3$. The amplitude is: (a),(b) $A = 0.3$ (noise-induced propagation) and (c),(d) $A = 0.2$ (spatiotemporal doubly stochastic resonance).

effect requires suitable intensities of *both* the additive and multiplicative noises.

A propagation of the harmonic signal can also be obtained for values of the forcing amplitude small enough so that hops are not produced in the directly excited sites in the absence of additive noise. This is the regime in which DSR really occurs in the excited part of the system, and the excitation propagates through the rest of the lattice enhanced by noise. Now all the oscillators have a nonmonotonic dependence on the additive noise intensity for a multiplicative noise within the bistable region [Fig. 4(c)], and a monotonic one for a multiplicative noise within the monostable region [Fig. 4(d)]. The former case corresponds to a spatiotemporal propagation in the DSR medium, and we call this phenomenon *spatiotemporal doubly stochastic resonance* (SDSR).

The mechanism of this phenomenon can be explained theoretically on the basis of a mean-field approximation. We give a first qualitative glimpse of this analysis in what follows; quantitative details will be published elsewhere. Because of coupling and multiplicative noise, the system becomes bistable with the behavior approximately governed by a mean-field effective potential [17]

$$U_{\text{eff}}(x) = U_0(x) + U_{\text{noise}} = -\int f(x)\, dx - \frac{\sigma_m^2 x^2}{4}. \qquad (7)$$

Now the effect can be understood in the frame of a standard SR mechanism [8], where the external signal is provided by the periodic force for the directly excited oscillators, and by the influence of the left neighbors for the nonexcited oscillators. For large forcing, only the latter need an additive noise to hop synchronously between wells, whereas for small forcing, both the excited and the nonexcited oscillators display SR. These two behaviors correspond to Figs. 4(a) and 4(c), respectively.

At this point it is worth making several remarks to the phenomenon described above. First, SDSR and noise-induced propagation in monostable media are strongly different to spatiotemporal SR [23] or noise enhanced propagation [19] in bistable media. The effect presented here can be controlled by multiplicative noise, which modifies the depth and separation of the two potential wells. Therefore, an optimal amount of multiplicative noise is required to support the bistable structure. Nothing similar occurs in array-enhanced SR [24] or in SR in extended bistable systems [25]. On the other hand, an increase of additive noise also leads to a loss of bistability (see Fig. 3), and hence a decrease of Q for large additive noise is explained not only by the fact that disordered hops are produced by intense noise, as in standard SR, but also by the loss of bistability. Second, noise-induced propagation in monostable media is very intriguing from the viewpoint of the theory of extended systems with noise and cannot be directly predicted from DSR. The noise-induced bistability, on which DSR is based, is a collective phenomenon,
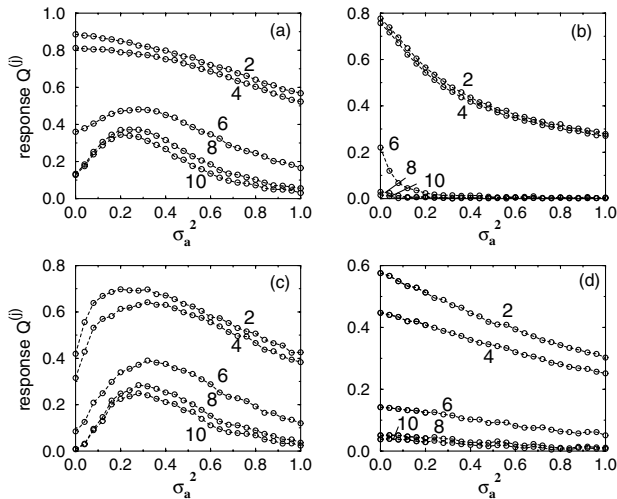
which can be observed only for a positive value of coupling enabling all elements to be close to the same position. In contrast to it, here we have shown that a propagation, which implies that different cells are simultaneously in different states, can occur in such a system without destroying the mechanism of bistability.

In conclusion, we have reported the existence of a propagation phenomenon, in which noise induces wave propagation in monostable media. The joint action of multiplicative noise and spatial coupling induces bistability, and additive noise enhances the propagation of harmonic forcing in the stochastically induced bistable medium. Because of its nontrivial propagation mechanism, this effect can be considered as a contribution to the theory of extended systems with noise. We also expect that these theoretical findings will stimulate experimental work. Especially, such kind of a propagation can be of great importance in communications, due to the fact that the energy of noise is used in a very efficient way, both to construct the potential barrier and to provide propagation enhancement in the noise-supported bistable system. We have demonstrated noise-induced propagation in monostable media in a simple realistic model, but in a general framework. Because of the generality of the model we expect that this effect can be also found in several more complicated real extended systems with noise-induced bistability. Probable experimental implementations include arrays of simple electronic circuits as a communication system [22], analog circuits [26], electronic cellular neural networks [27], and are expected to be achieved in several real spatially distributed systems, such as liquid crystals [28], photosensitive chemical reactions [29], Rayleigh-Bénard convection [30], or liquid helium [31].

---

[1] J. Smythe, F. Moss, and P. McClintock, Phys. Rev. Lett. **51**, 1062 (1983).

[2] W. Horsthemke and R. Lefever, *Noise-Induced Transitions* (Springer, Berlin, 1984).

[3] J. García-Ojalvo and J.M. Sancho, *Noise in Spatially Extended Systems* (Springer, New York, 1999).

[4] P. Landa, A. Zaikin, V. Ushakov, and J. Kurths, Phys. Rev. E **61**, 4809 (2000).

[5] P. Hänggi and R. Bartussek, in *Nonlinear Physics of Complex Systems,* edited by J. Parisi, S.C. Müller, and W. Zimmermann (Springer, Berlin, 1996).

[6] P. Reimann, R. Kawai, and C. Van den Broeck, P. Hänngi, Europhys. Lett. **45**, 545 (1999).

[7] J. García-Ojalvo, A. Hernández-Machado, and J.M. Sancho, Phys. Rev. Lett. **71**, 1542 (1993).

[8] R. Benzi, A. Sutera, and A. Vulpiani, J. Phys. A **14**, L453 (1981). L. Gammaitoni, P. Hänggi, P. Jung, and F. Marchesoni, Rev. Mod. Phys. **70**, 223 (1998).

[9] B. McNamara, K. Wiesenfeld, and R. Roy, Phys. Rev. Lett. **60**, 2626 (1988); J. Douglass, L. Wilkens, and L. Pantazelou, Nature (London) **365**, 337 (1993).

[10] N.G. Stocks, N.D. Stei, and P.V.E. McClintock, J. Phys. A **26**, L385 (1993).

[11] K. Wiesenfeld, D. Pierson, E. Pantazelou, C. Dames, and F. Moss, Phys. Rev. Lett. **72**, 2125 (1994).

[12] Z. Gingl, L. Kiss, and F. Moss, Europhys. Lett. **29**, 191 (1995).

[13] S. Bezrukov and I. Vodyanoy, in *Unsolved Problems of Noise and Fluctuations,* edited by D. Abbott and L. Kiss, AIP Conf. Proc. No. 511 (AIP, New York, 2000).

[14] H. Gang, T. Ditzinger, C. Ning, and H. Haken, Phys. Rev. Lett. **71**, 807 (1993).

[15] A. Pikovksy and J. Kurths, Phys. Rev. Lett. **78**, 775 (1997).

[16] A. Fuliński, Phys. Rev. E **52**, 4523 (1995).

[17] A. Zaikin, J. Kurths, and L. Schimansky-Geier, Phys. Rev. Lett. **85**, 227 (2000).

[18] C. Van den Broeck, J.M.R. Parrondo, and R. Toral, Phys. Rev. Lett. **73**, 3395 (1994).

[19] J. Lindner, S. Chandramouli, A.R. Bulsara, M. Löcher, and W.L. Ditto, Phys. Rev. Lett. **81**, 5048 (1998); Y. Zhang, G. Hu, and L. Gammaitoni, Phys. Rev. E **58**, 2952 (1998).

[20] S. Kadar, J. Wang, and K. Showalter, Nature (London) **391**, 770 (1998); G. Balázsi, L.B. Kiss, and F.E. Moss, in *Unsolved Problems of Noise and Fluctuations* (Ref. [13]).

[21] J. García-Ojalvo, A.M. Lacasta, and F. Sagués, J.M. Sancho, Europhys. Lett. **50**, 427 (2000); R. Perazzo, L. Romanelli, and R. Deza, Phys. Rev. E **61**, R3287 (2000); A.C.H. Rowe and P. Etchegoin, Phys. Rev. E **64**, 031106 (2001).

[22] A.A. Zaikin, K. Murali, and J. Kurths, Phys. Rev. E **63**, 020103(R) (2001).

[23] F. Marchesoni, L. Gammaitoni, and A.R. Bulsara, Phys. Rev. Lett. **76**, 2609 (1996); J.M.G. Vilar and J.M. Rubí, Phys. Rev. Lett. **78**, 2886 (1997).

[24] J.F. Lindner, B.K. Meadows, W.L. Ditto, M.E. Inchiosa, and A.R. Bulsara, Phys. Rev. Lett. **75**, 3 (1995).

[25] H.S. Wio, Phys. Rev. E **54**, R3075 (1996); S. Bouzat and H.S. Wio, Phys. Rev. E **59**, 5142 (1999).

[26] F. Moss (private communication).

[27] V. Pérez-Muñuzuri, V. Pérez-Villar, and Leon O. Chua, IEEE Trans. **40**, 174 (1993); P. Arena, R. Caponetto, L. Fortuna, and A. Rizzo, IEEE Trans. **48**, 360 (2001).

[28] S. Kai, T. Kai, and M. Takata, J. Phys. Soc. Jpn. **47**, 1379 (1979).

[29] J. Micheau, W. Horsthemke, and R. Lefever, J. Chem. Phys. **81**, 2450 (1984).

[30] C. Meyer, G. Ahlers, and D. Cannell, Phys. Rev. A **44**, 2514 (1991).

[31] D. Griswold and J.T. Tough, Phys. Rev. A **36**, 1360 (1987).

System Size Resonance in Coupled Noisy Systems and in the Ising Model

A. Pikovsky and A. Zaikin

Department of Physics, University of Potsdam, Postfach 601553, D-14415 Potsdam, Germany

M. A. de la Casa

Departamento Física Fundamental, Universidad Nacional de Educación a Distancia, 28040 Madrid, Spain
(Received 8 March 2001; published 16 January 2002)

We consider an ensemble of coupled nonlinear noisy oscillators demonstrating in the thermodynamic limit an Ising-type transition. In the ordered phase and for finite ensembles stochastic flips of the mean field are observed with the rate depending on the ensemble size. When a small periodic force acts on the ensemble, the linear response of the system has a maximum at a certain system size, similar to the stochastic resonance phenomenon. We demonstrate this effect of system size resonance for different types of noisy oscillators and for different ensembles—lattices with nearest neighbors coupling and globally coupled populations. The Ising model is also shown to demonstrate the system size resonance.

PACS numbers: 05.40.Ca, 05.45.–a, 05.50.+q

Stochastic resonance has attracted much interest recently [1]. As was demonstrated in [2], a response of a noisy nonlinear system to a periodic forcing can exhibit a resonancelike dependence on the noise intensity. In other words, there exists a "resonant" noise intensity at which the response to a periodic force is maximally ordered. Stochastic resonance has been observed in numerous experiments [3]. Noteworthy, the order in a noise-driven system can have a maximum at a certain noise level even in the absence of periodic forcing, this phenomenon being called coherence resonance [4].

Being first discussed in the context of a simple bistable model, stochastic resonance has been also studied in complex systems consisting of many elementary bistable cells [5]; moreover, the resonance may be enhanced due to coupling [6]. In this paper we discuss another type of resonance in such systems, namely, the *system size resonance,* when the dynamics is maximally ordered at a certain number of interacting subsystems. Contrary to previous reports of array-enhanced stochastic resonance (cf. also [7]), here we fix the noise strength, coupling, and other parameters; only the size of the ensemble changes.

The basic model to be considered below is the ensemble of noise-driven bistable overdamped oscillators, governed by the Langevin equations,

$$\dot{x}_i = x_i - x_i^3 + \frac{\varepsilon}{N} \sum_{j=1}^{N} (x_j - x_i) + \sqrt{2D}\,\xi_i(t) + f(t).$$

(1)

Here $\xi_i(t)$ is a Gaussian white noise with zero mean: $\langle \xi_i(t)\xi_j(t') \rangle = \delta_{ij}\delta(t - t')$; ε is the coupling constant; N is the number of elements in the ensemble, and $f(t)$ is a periodic force to be specified later. In the absence of periodic force, the model (1) has been extensively studied in the thermodynamic limit $N \to \infty$. It demonstrates an Ising-type phase transition at $\varepsilon = \varepsilon_c$ from the disordered state with vanishing mean field $X = N^{-1} \sum_i x_i$ to the "ferromagnetic" state with a nonzero mean field $X = \pm X_0$ [8].

While in the thermodynamic limit the full description of the dynamics is possible, for finite system sizes we have mainly a qualitative picture: In the ordered phase the mean field X switches between the values $\pm X_0$ and its average vanishes for all couplings. The rate of switchings depends on the system size and tends to zero as $N \to \infty$.

For us, the main importance is the fact that qualitatively the behavior of the mean field can be represented as the noise-induced dynamics in a potential with one minimum in the disordered phase (at $X = 0$) and two symmetric minima (at $X = \pm X_0$) in the ordered phase. Now, applying the ideas of the stochastic resonance, one can expect in the bistable case (i.e., in the ordered phase for small enough noise or for large enough coupling) a resonantlike behavior of the response to a periodic external force when the intensity of the effective noise is changed. Because this intensity is inverse proportional to N, we obtain the resonancelike curve of the response in dependence of the system size. The main idea behind the system size resonance is that in finite ensembles of noise-driven or chaotic systems the dynamics of the mean field can be represented as driven by the effective noise whose variance is inverse proportional to the system size [9]. This idea has been applied to the description of a transition to collective behavior in [10]. In [11] it was demonstrated that the finite-size fluctuations can cause a transition that disappears in the thermodynamic limit.

Before proceeding to a quantitative analytic description of the phenomenon, we illustrate it with direct numerical simulations of the model (1), with a forcing term $f(t) = A\cos(\Omega t)$. Figure 1 shows the linear response function, i.e., the ratio of the spectral component in the mean field at frequency Ω and the amplitude of forcing A, in the limit $A \to 0$. For a given frequency Ω the dependence on the system size is a bell-shaped curve, with a pronounced maximum. The dynamics of the mean field $X(t)$ is illustrated in Fig. 2, for three different system sizes. The resonant dynamics (Fig. 2b) demonstrates a typical for
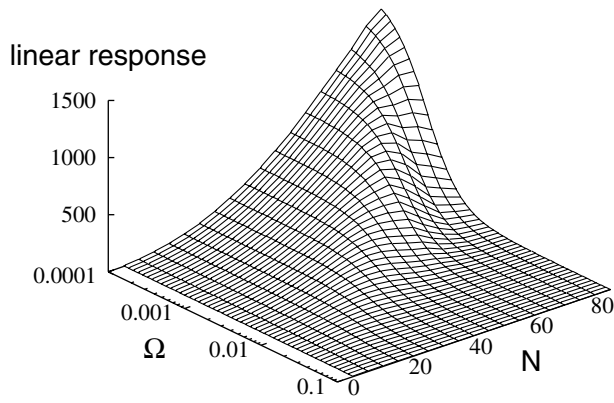
FIG. 1. Linear response of the ensemble (1) ($D = 0.5$, $\varepsilon = 2$) in dependence on the frequency and the system size N.

stochastic resonance synchrony between the driving periodic force and the switchings of the field between the two stable positions.

To describe the system size resonance analytically, we use, following [8], the Gaussian approximation. In this approximation, one writes $x_i = X + \delta_i$ and assumes that δ_i are independent Gaussian random variables with zero mean and the variance M. Assuming furthermore that $N^{-1}\sum_i \delta_i^2 = M$ and neglecting the odd moments $N^{-1}\sum_i \delta_i$, $N^{-1}\sum_i \delta_i^3$, as well as the correlations between δ_i and δ_j, we obtain from (1) the equations for X and M:

$$\dot{X} = X - X^3 - 3MX + \sqrt{\frac{2D}{N}}\,\eta(t) + f(t), \quad (2)$$

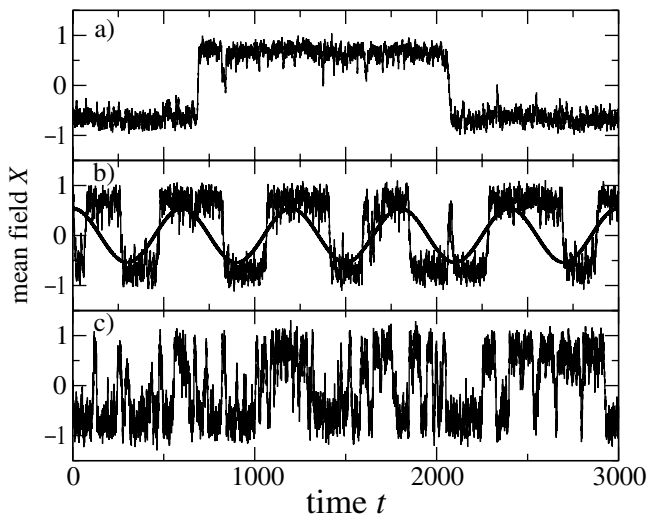$$\tfrac{1}{2}\dot{M} = M - 3X^2 M - 3M^2 - \varepsilon M + D, \quad (3)$$

FIG. 2. The time dependence of the mean field in the ensemble (1) for $D = 0.5$, $\varepsilon = 2$, $A = 0.02$, $\Omega = \pi/300$, and different sizes of the ensemble: (a) $N = 80$, (b) $N = 35$, and (c) $N = 15$. We also depict the periodic force (its amplitude is not in scale) to demonstrate the synchrony of the switchings with the forcing in (b).

where η is the Gaussian white noise having the same properties as $\xi_i(t)$. In the thermodynamic limit $N \to \infty$ the noisy term η vanishes. If the forcing term is absent ($f = 0$), the equations coincide with those derived in [8]. This system of coupled nonlinear equations exhibits a pitchfork bifurcation of the equilibrium $X = 0$, $M > 0$ at $\varepsilon_c = 3D$. This bifurcation is supercritical for $D > 2/3$ in accordance with the exact solution of (1) given in [8]; below we consider only this case. For $\varepsilon > \varepsilon_c$ the system is bistable with two symmetric stable fixed points,

$$X_0^2 = (2 - \varepsilon + S)/4, \quad M_0 = (2 + \varepsilon - S)/12 \quad (4)$$

[here $S = \sqrt{(2 + \varepsilon)^2 - 24D}$], and the unstable point $X = 0$, $M = [1 - \varepsilon + \sqrt{(1 - \varepsilon)^2 + 12D}]/6$. Now, with the external noise η and with the periodic force $f(t)$, the problem reduces to a standard problem in the theory of stochastic resonance, i.e., to the problem of the response of a noise-driven nonlinear bistable system to an external periodic force (because the noise affects only the variable X, it does not lead to unphysical negative values of variance M, since $\dot{M}$ is strictly positive at $M = 0$).

To obtain an analytical formula, we perform further simplification of the system (2) and (3). Near the bifurcation point, we can use the slaving principle to obtain a standard noise-driven bistable system:

$$\dot{X} = aX - bX^3 + \sqrt{\frac{2D}{N}}\,\eta(t) + f(t), \quad (5)$$

where $a = 1 + 0.5(\varepsilon - 1) - 0.5\sqrt{(\varepsilon - 1)^2 + 12D}$, $b = -0.5 + 1.5(\varepsilon - 1)[(\varepsilon - 1)^2 + 12D]^{-1/2}$. A better approximation valid also beyond a vicinity of the critical point can be constructed if we use $\bar{b} = aX_0^{-2}$ instead of b, where the fixed point X_0 is given by (4). Having written the ensemble dynamics as a standard noise-driven double-well system (5) (cf. [1,12]), we can use the analytic formula for the linear response R derived in [12]. It reads

$$R = \frac{NX_0^2}{2Da}\left(\frac{\mathcal{D}_{-3/2}(-\sqrt{s})}{\mathcal{D}_{-1/2}(-\sqrt{s})}\right)^2\left[1 + \frac{\pi^2\Omega^2}{2a^2}\exp(s)\right]^{-1}, \quad (6)$$

where $s = aNX_0^2/(2D)$, and $\mathcal{D}$ are the parabolic cylinder functions. We compare the theoretical linear response function with the numerically obtained one in Fig. 3. The qualitative correspondence is good; moreover, the maxima of the curves are rather good reproduced with the formula (6).

Above, we concentrated on the properties of the linear response. Numerical simulations with the finite forcing amplitude yielded the results similar to that presented in Figs. 1 and 3. However, for large amplitudes of forcing (e.g., $A > 0.1$ for $\Omega = 0.01$, $D = 0.5$, $\varepsilon = 2$) a saturation was observed: Here the response grows monotonically with N. This is in full agreement with the corresponding property of the stochastic resonance in double-well systems of type (5), where the saturation
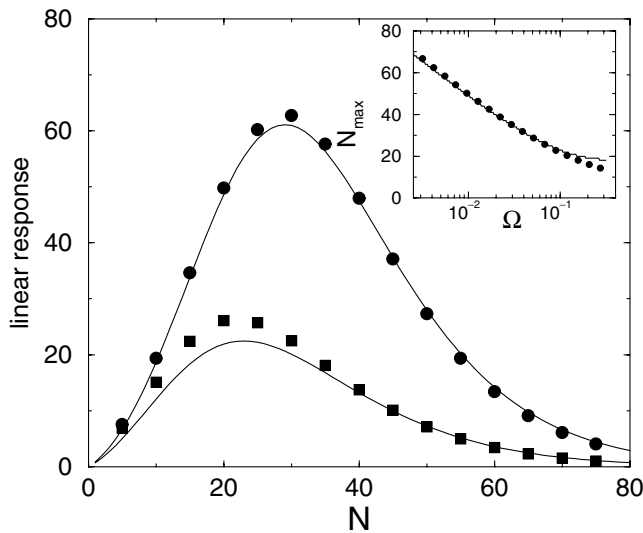
FIG. 3. Comparison of the system size dependencies of the linear response function for frequencies $\Omega = 0.05$ (circles) and $\Omega = 0.1$ (squares) with theory (6). The parameters are $D = 1$ and $\varepsilon - \varepsilon_c = 2.5$ (where the exact ε_c and the approximate $\varepsilon_c = 3D$ are used for the ensemble and the Gaussian approximation, respectively). Inset: Dependence of the system size yielding maximal linear response on the driving frequency Ω [circles: simulations of the ensemble (1), line is obtained by maximizing the expression (6)].

occurs for small noise intensities (cf. Fig. 7 in [1]), due to the disappearance of multistability for large forcing amplitudes.

It is instructive to compare the response of the noise-driven system (1) with the noise-free case $D = 0$. Without external force, the ensemble relaxes eventually to a steady state solution with some mean field X; in this state each oscillator can be in one of the stable steady positions of the potential; correspondingly, the oscillators form one or two clusters. From the clustering it follows that the linear response does not depend on the number of elements in the ensemble. Our numerical experiments demonstrated also that the response is system size independent for large forcing amplitudes as well, where, e.g., the force-induced cluster mergings occur. Thus, the effect of system size resonance essentially relies on the presence of noise, which breaks the clustering.

Above, we have considered the system of globally coupled nonlinear oscillators (1). The same effect of system size resonance can be observed in a lattice with nearest neighbors coupling as well. In the thermodynamic limit, the Ising-type phase transition occurs in the lattice (if its dimension is larger than one). Similar to the globally coupled ensemble, in finite lattices in the ordered phase the switchings between the two stable states of the mean field are observed. With the same argumentation as above, we can conclude that the response of the mean field to a periodic forcing can have a maximum at a certain lattice size, while all other parameters (noise intensity, cou-

pling strength, etc.) are kept constant. We illustrate this in Fig. 4.

As the next example we consider the two-dimensional nearest neighbor Ising model in the presence of a time-dependent external field. The Hamiltonian of the system reads

$$H = -J \sum_{\langle ij \rangle} s_i s_j - A \cos(\Omega t) \sum_i s_i, \qquad (7)$$

where $J > 0$ and $s_i = \pm 1$. We are interested in the dependence of the response of the mean magnetization $m(t) = \frac{1}{N} \sum_i s_i(t)$ on the system size N (for the usual stochastic resonance in the Ising model, i.e., for the dependence of the response on the temperature, see [13]). To calculate the linear response, we used the fluctuation-dissipation theorem and obtained this quantity by virtue of the power spectrum of fluctuations of $m(t)$. The latter was found using the Metropolis Monte Carlo method on a lattice with helical boundary conditions [14]. The results presented in Fig. 5 demonstrate the system size resonance of the linear response in the two-dimensional Ising model.

As the last example of the system size resonance, we consider a lattice where each individual element does not exhibit bistable noisy dynamics, but such a behavior appears due to interaction and multiplicative noise. This model is described by the set of Langevin equations [15,16]:

$$\dot{x}_i = -x_i(1 + x_i^2)^2 + \frac{\varepsilon}{K} \sum_j (x_j - x_i)$$
$$+ \sqrt{2D}\, \xi_i(t)(1 + x_i^2) + f(t). \qquad (8)$$

As has been demonstrated in [15], in some region of couplings the ε system (8) exhibits the Ising-type transition.

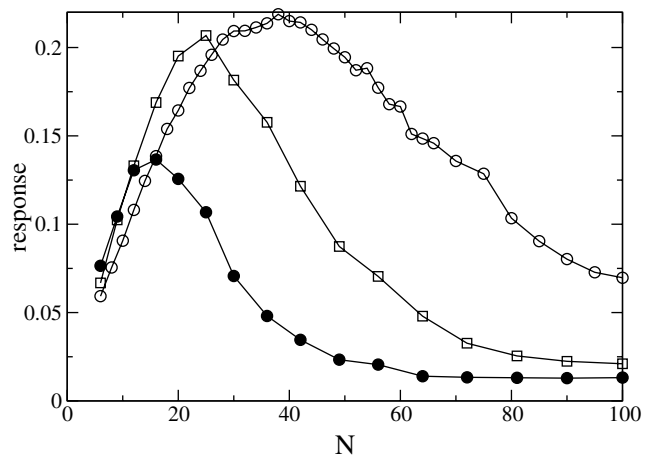FIG. 4. Filled circles: Response of a two-dimensional lattice of N with nearest neighbors coupling for $A = 0.02$, $T = 500$, $D = 0.5$, and $\varepsilon = 4$. Squares: Response of system (8) (a two-dimensional lattice with $D = 1.25$, $\varepsilon = 30$, $A = 0.1$, and $T = 140$). Circles: The same as squares, but for a globally coupled lattice with $D = 1$, $\varepsilon = 20$, $A = 0.1$, and $T = 100$.
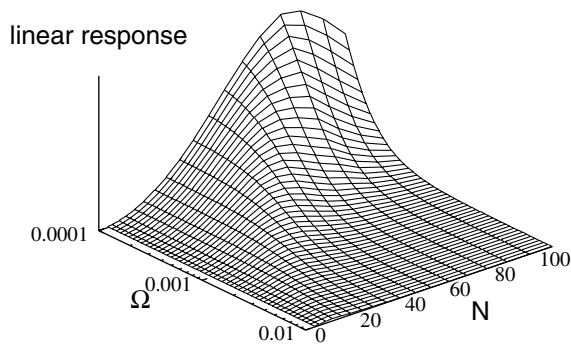
linear response

FIG. 5.   Linear response (in arbitrary units) of the Ising model (7) for the temperature $T = 2J$ slightly below the critical temperature $T_c = 2.269J$.

If an additional additive noise is added to (8), then one observes transitions between these states and the so-called double stochastic resonance in the presence of the periodic forcing [17]. As is evident from the considerations above, such transitions occur even in the absence of the additive noise if the system is finite. Thus, the system size resonance should be observed in the lattice (8) as well. We confirm this in Fig. 4.

Another possible field of application of the system size resonance is the neuronal dynamics (see, e.g., [18]). Individual neurons have been demonstrated to exhibit stochastic resonance [3,19]. While in experiments one can easily adjust noise to achieve the maximal sensitivity to an external signal, it may not be obvious how this adjustment takes place in nature. The above consideration shows that changing the number of elements in a small ensemble of coupled bistable elements to the optimum can significantly improve the sensitivity (cf. [5]). Moreover, changing its connectivity and/or coupling strength, a neuronal system can tune itself to signals with different frequencies.

In conclusion, we have shown that, in populations of coupled noise-driven elements, exhibiting in the thermodynamic limit the Ising-type transition, in the ordered phase (i.e., for relatively small noise and large coupling) the response to a periodic force achieves maximum at a certain size of the system. We demonstrated this effect for the Ising model, as well as for lattices and globally coupled ensembles of noisy oscillators. We expect the system size resonance to occur also in purely deterministic systems demonstrating the Ising-type transition, e.g., in the Miller-Huse coupled map lattice [20]. The system size resonance is described theoretically by reducing the dynamics of the mean field to a low-dimensional bistable model with an effective noise that is inverse proportional to the system size. The stochastic resonance in the mean field dynamics then manifests itself as the system size resonance.

We thank N. Brilliantov, A. Neiman, J. Parrondo, F. J. de la Rubia, and R. Toral for useful discussions, and M. Rosenblum for help in analysis of Eq. (6). M. C. thanks the DGESEIC Project No. PB97-0076 and the

[1] L. Gammaitoni, P. Hänggi, P. Jung, and F. Marchesoni, Rev. Mod. Phys. **70**, 223 (1998); P. Jung, Phys. Rep. **234**, 175 (1993).

[2] R. Benzi, A. Sutera, and A. Vulpiani, J. Phys. A **14**, L453 (1981).

[3] A. Longtin, A. Bulsara, and F. Moss, Phys. Rev. Lett. **67**, 656 (1991); A. Simon and A. Libchaber, Phys. Rev. Lett. **68**, 3375 (1992); M. L. Spano, M. Wun-Folge, and W. L. Ditto, Phys. Rev. A **46**, 5253 (1992); S. Barbay, G. Giacomelli, and F. Marin, Phys. Rev. E **61**, 157 (2000).

[4] A. Pikovsky and J. Kurths, Phys. Rev. Lett. **78**, 775 (1997); A. Neiman, P. I. Saparin, and L. Stone, Phys. Rev. E **56**, 270 (1997).

[5] P. Jung, U. Behn, E. Pantazelou, and F. Moss, Phys. Rev. A **46**, R1709 (1992); M. Morillo, J. Gómez-Ordoñez, and J. M. Casado, Phys. Rev. E **52**, 316 (1995); J. M. Casado and M. Morillo, Phys. Rev. E **52**, 2088 (1995); H. Gang, H. Haken, and X. Fagen, Phys. Rev. Lett. **77**, 1925 (1996); P. Jung and G. Mayer-Kress, Phys. Rev. Lett. **74**, 2130 (1995).

[6] J. F. Lindner *et al.,* Phys. Rev. Lett. **75**, 3 (1995); Phys. Rev. E **53**, 2081 (1996).

[7] A. Neiman, L. Schimansky-Geier, and F. Moss, Phys. Rev. E **56**, R9 (1997); B. Hu and C. Zhou, Phys. Rev. E **61**, R1001 (2000).

[8] R. C. Desai and R. Zwanzig, J. Stat. Phys. **19**, 1 (1978).

[9] D. A. Dawson and J. Gärtner, Stochastics **20**, 247 (1987); A. S. Pikovsky and J. Kurths, Physica (Amsterdam) **76D**, 411 (1994); A. Hamm, Physica (Amsterdam) **142D**, 41 (2000).

[10] A. Pikovsky and S. Ruffo, Phys. Rev. E **59**, 1633 (1999).

[11] A. S. Pikovsky, K. Rateitschak, and J. Kurths, Z. Phys. B **95**, 541 (1994).

[12] P. Jung and P. Hänggi, Phys. Rev. A **44**, 8032 (1991).

[13] Z. Néda, Phys. Rev. E **51**, 5315 (1995); J. Javier Brey and A. Prados, Phys. Lett. A **216**, 240 (1996); U. Siewert and L. Schimansky-Geier, Phys. Rev. E **58**, 2843 (1998).

[14] M. E. J. Newmann and G. T. Barkema, *Monte Carlo Methods in Statistical Physics* (Clarendon, Oxford, 1999).

[15] C. V. der Broeck, J. M. R. Parrondo, and R. Toral, Phys. Rev. Lett. **73**, 3395 (1994); C. V. der Broeck *et al.,* Phys. Rev. E **55**, 4084 (1997).

[16] P. Landa, A. Zaikin, and L. Schimansky-Geier, Chaos Solitons Fractals **9**, 1367 (1998).

[17] A. A. Zaikin, J. Kurths, and L. Schimansky-Geier, Phys. Rev. Lett. **85**, 227 (2000); A. A. Zaikin, K. Murali, and J. Kurths, Phys. Rev. E **63**, 020103(R) (2001).

[18] P. A. Tass, *Phase Resetting in Medicine and Biology: Stochastic Modelling and Data Analysis* (Springer-Verlag, Berlin, 1999).

[19] J. K. Douglas, L. Wilkens, E. Pantazelou, and F. Moss, Nature (London) **365**, 337 (1993); D. F. Russell, L. A. Wilkens, and F. Moss, Nature (London) **402**, 291 (1999).

[20] J. Miller and D. A. Huse, Phys. Rev. E **48**, 2528 (1993).

Simple electronic circuit model for doubly stochastic resonance

A. A. Zaikin,[1] K. Murali,[2] and J. Kurths[1]

[1]*Institute of Physics, University of Potsdam, Am Neuen Palais 10, 14469 Potsdam, Germany*
[2]*Department of Physics, Anna University, Chennai 600 025, India*
(Received 17 October 2000; published 22 January 2001)

We have recently reported the phenomenon of doubly stochastic resonance [Phys. Rev. Lett. **85**, 227 (2000)], a synthesis of noise-induced transition and stochastic resonance. The essential feature of this phenomenon is that multiplicative noise induces a bimodality and additive noise causes stochastic resonance behavior in the induced structure. In the present paper we outline possible applications of this effect and design a simple lattice of electronic circuits for the experimental realization of doubly stochastic resonance.

Investigations of phenomena such as noise-induced phase transitions [1–5], stochastic transport in ratchets [6], or noise-induced pattern formation [7] have shown that the energy of noise, which was usually considered as a nuisance in any communication, can be potentially useful to induce order in nonlinear nonequilibrium systems. One of the most important examples is stochastic resonance (SR) [8,9], which has been found in different engineering [10] and natural systems [11]. In the conventional situation this effect consists of the following: additive noise can optimize the signal processing in a bistable system, i.e., it increases the signal-to-noise ratio in the output if a periodic signal acts upon a system. In addition to this conventional situation, SR has been also found in monostable systems [12], systems with excitable dynamics [13], noisy nondynamical systems [14], systems without an external force [15] (note also coherence resonance [16]), systems without any kind of threshold [17], and systems with transient noise-induced structure [18].

However, the energy of noise can be used much more efficiently: The main point is to use noise not only for a synchronization of output hops across a potential barrier with an external signal, but also for the construction of this barrier. This happens in the effect of doubly stochastic resonance (DSR) [19]. In DSR the influence of noise is twofold: additive noise induces resonancelike behavior in the structure, which has been, in turn, induced by multiplicative noise. DSR occurs in a spatially distributed system of coupled overdamped oscillators and can be considered as a synthesis of two basic phenomena: SR and a noise-induced phase transition [20].

An important question is, How can we observe DSR in experimental systems? We have mentioned in Ref. [19] several appropriate real systems: analog circuits [21], liquid crystals [22], photosensitive chemical reactions [23], Rayleigh-Bénard convection [24], or liquid helium [25]. In the present Rapid Communication we design an electronic circuit for the observation of DSR. The most direct way is the realization through analog circuits, but there are complications due to the complex construction of every unit; hence, it is worth looking for a simpler electronic circuit model that exhibits the DSR property. With this aim we consider an electrical circuit which consists of N coupled elements (i,j). A circuit of one element is shown in Fig. 1. Three ingredients in this circuit are important: the input current, a time-varying resistor (TVR), and a nonlinear resistor. Every ele-

ment is coupled with its neighbors by the resistor R_c (i.e., by diffusive coupling). The capacitor is shown by C. The nonlinear resistor R_N can be realized with a set of ordinary diodes [26,27], whose characteristic function is a piecewise-linear function

$$i_N = f_1(V) = \begin{cases} G_b V + (G_a - G_b) B_p & \text{if } V \leq -B_p \\ G_a V & \text{if } |V| < B_p \\ G_b V - (G_a - G_b) B_p & \text{if } V \geq B_p, \end{cases} \quad (1)$$

where i_N is the current through the nonlinear resistor (R_N), V is the voltage across the capacitor (C), and parameters G_a, G_b, and B_p determine the slopes and the breakpoint of the piecewise-linear characteristic curve. Another way to realize the nonlinear resistor is via a third-order polynomial function,

$$i_N = f_2(V) = g_1 V + g_2 V^3.$$

The next important ingredient is a time-varying resistor (TVR) [28,27]. The conductance $G(t)$ of TVRs varies with time. Presently, we consider the case that the function which represents the variation of the TVR is Gaussian δ-correlated in space and time noise, i.e., $G(t) = \xi(t)$, where

$$\langle \xi_i(t) \xi_j(t') \rangle = \sigma_m^2 \delta_{i,j} \delta(t - t').$$

An external action on the circuit is performed by the current input $I(t)$, which is a periodic signal (with amplitude A, frequency ω, and initial phase φ), additively influenced by independent Gaussian noise $\zeta(t)$,
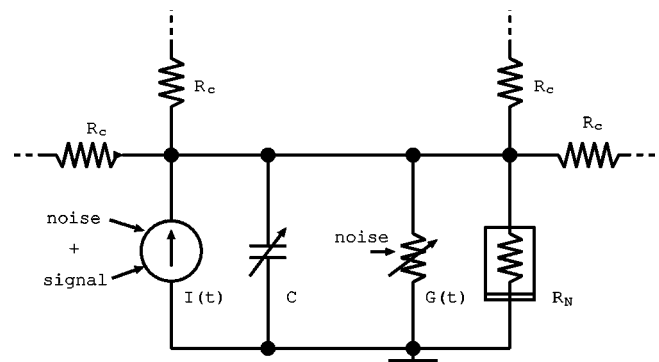

FIG. 1. Electronic circuit of the element (i,j).

$$I(t) = \zeta(t) + A\cos(\omega t + \varphi),$$

where

$$\langle \zeta_i(t)\zeta_j(t')\rangle = \sigma_a^2 \delta_{i,j}\delta(t-t').$$

The electronic circuit with respect to the element (i,j) can be described by a set of Kirchoff's equations,

$$C\frac{dV_{i,j}}{dt} = I(t) - G(t)V_{i,j} - f_{1,2}(V_{i,j})$$

$$+ \frac{1}{R_c}(V_{i+1,j} + V_{i-1,j} + V_{i,j+1} + V_{i,j-1} - 4V_{i,j}). \tag{2}$$

Hence, the following set of Langevin equations describes the considered system,

$$\frac{dV_{i,j}}{dt} = -f_{1,2}(V_{i,j}) + V_{i,j}\xi_{i,j}(t) + \frac{D}{4}(V_{i+1,j} + V_{i-1,j} + V_{i,j+1}$$

$$+ V_{i,j-1} - 4V_{i,j}) + \zeta_{i,j}(t) + A\cos(\omega t + \varphi), \tag{3}$$

where C is set to unity by normalization of time and D denotes a strength of coupling equal to $4/CR_c$. In the case when f_2 represents the TVR, the model is the time-dependent Ginzburg-Landau equation, which is a standard model to describe phase transitions and critical phenomena in both equilibrium and nonequilibrium situations [3]. It is important that we consider only the situation when the potential of one element is monostable ($G_a = 0.5$, $G_b = 10$, and $B_p = 1$ for f_1; $g_1 > 0$ and $g_2 = 1$ for f_2), avoiding the possibility to observe SR without multiplicative noise (The effect of SR in the system, which consists of bistable elements, is well-known and beyond the scope of this paper).

We are interested in the behavior of the mean field $m(t) = (1/N)\Sigma_{i=1}^N\Sigma_{j=1}^N V_{i,j}(t)$ and consider it as an output and the periodic signal as an input of the whole system. SR behavior can be expected if the system is bistable for the chosen set of parameters. Regions of bistability can be determined by means of a standard mean-field theory (MFT) procedure [3]. The mean-field approximation consists of replacing the nearest-neighbor interaction by a global term in the Fokker-Planck equation corresponding to Eq. (3). In this way, we obtain the following steady-state probability distribution w_{st}:

$$w_{st}(x,m) = \frac{C(m)}{\sqrt{\sigma_m^2 g^2(x) + \sigma_a^2}}$$

$$\times \exp\left(2\int_0^x \frac{f_{1,2}(y) - D(y-m)}{\sigma_m^2 g^2(y) + \sigma_a^2}dy\right), \tag{4}$$

where $C(m)$ is a normalization constant and m is a mean field, defined by the equation

$$m = \int_{-\infty}^{\infty} x w_{st}(x,m)dx. \tag{5}$$
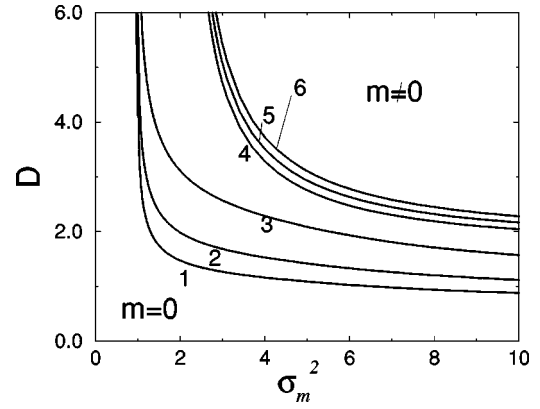
FIG. 2. Transition lines for the equation with function f_1: $\sigma_a^2 = 0.3$ (label 1), 0.5 (label 2), and 1 (label 3). Also the case with f_2 (the potential of every element is monostable: $g_1 > 0, g_2 = 1$); $g_1 = 1, \sigma_a^2 = 0.8$ (label 4), 0.9 (label 5), and 1 (label 6).

A self-consistent solution of Eq. (5) determines the mean field and the transition lines between ordered bistable ($m \neq 0$) and disordered monostable ($m = 0$) phases. Transition boundaries for functions f_1 and f_2 are shown in Fig. 2. Note that bistability is impossible without multiplicative noise and without coupling between elements. Since the SR effect, described below, appears due to the variation of additive noise, it is also important that a change of the additive noise intensity shifts transition boundaries.

Next we estimate the signal-to-ratio (SNR) analytically. Following the short-time evolution approximation, first introduced in [29] and further developed in [30,19], the dynamics of the mean field is governed by an ''effective'' potential $U_{eff}(x)$, which has the form

$$U_{eff}(V) = U_0(V) + U_{noise} = \int f(V)dx - \frac{\sigma_m^2 V^2}{4}, \tag{6}$$

where $U_0(V)$ is a monostable potential and U_{noise} represents the influence of the multiplicative noise. Note that this approach is valid only if a suppression of fluctuations, performed by the coupling, is sufficient. It means that the coupling strength should tend to infinity, or actually be large enough. DSR is expected for the regions where this effective potential has a bistable form. To obtain an analytical estimation of SNR for one element we use a standard linear response theory [9,31], yielding

$$SNR_1 = \frac{4\pi A^2}{\sigma_\zeta^4}r_k, \tag{7}$$

where r_k is the corresponding Kramers rate [32]

$$r_k = \frac{\sqrt{(|U_{eff}''(V)|_{V=V_{min}}|U_{eff}''(V)|_{V=V_{max}})}}{2\pi}\exp\left(-\frac{2\Delta U_{eff}}{\sigma_\zeta^2}\right). \tag{8}$$

Further, we rescale this value by the number N of elements in the circuit [33] and take into account the processing

FIG. 3. (a) Numerical SNR (circles) vs analytical estimation (solid line) for the equation with f_1 and $D=3, \sigma_m^2=3$. Numerical results are shown by closed circles for the mean field and open circles for its two-state approximation. The stochastic resonance 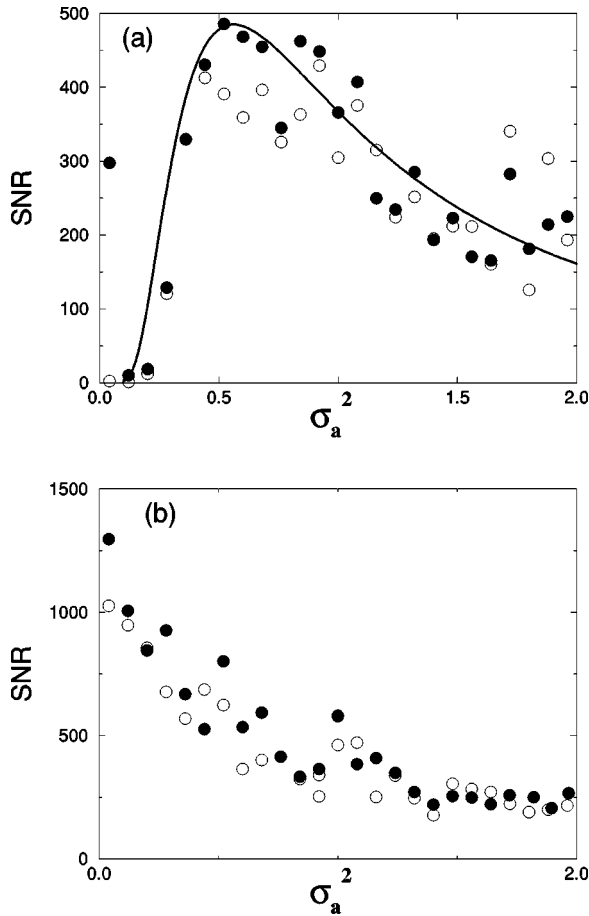effect is supported by noise. If we decrease the intensity of multiplicative noise, we do not observe it; e.g., for (b) $D=3, \sigma_m^2=0.5$.

gain G and the bandwidth Δ in the power spectral density [31]. The SNR_N of the mean field of the whole system of N elements is then

$$SNR_N = SNR_1 \frac{NG}{\Delta} + 1. \qquad (9)$$

For the parameters, used below for numerical simulations ($\sigma_m^2=3$, $A=0.1$, $N=324$, $G=0.7$, and $\Delta=0.012$), we obtain the analytic estimation of the SNR, shown in Fig. 3(a) by the solid line. Except for the application for electronic circuits, this calculation also shows that DSR can be observed not only in the specific model described in Ref. [19].

In order to verify the results obtained by our rough analytical approximation, we have performed simulations of model (3) using numerical methods described in Ref. [34]. We have taken a set of parameters within the region of two coexisting ordered states with nonzero mean field. As a total system, we take a two-dimensional lattice of 18×18 elements, which was simulated numerically with a time step $\Delta t = 2.5 \times 10^{-4}$. The amplitude of the external signal was set to 0.1, i.e., sufficiently small to avoid hops between two states in the absence of additive noise. To describe the SR

effect quantitatively, we have calculated the SNR by extracting the relevant phase-averaged power spectral density $S(\omega)$ and taking the ratio between its signal part with respect to the noise background [9]. The dependence of the SNR on the intensity of the additive noise is shown in Fig. 3(a) for the mean field (closed circles) and the mean field in a two-state approximation (open circles). In this two-state approximation, we have replaced the value of the mean field in time-series by its sign before calculating the power spectral density, using the method of symbolic dynamics [35], standardly used to investigate SR [9]. Both curves demonstrate well-known bell-shaped dependence that is typical for SR. In contrast to two-state approximation, for the mean field, SNR tends to infinity for small values of multiplicative noise intensity (see closed circles for $\sigma_a^2 < 0.1$). It can be explained by intrawell dynamics in the same way as in the conventional SR [9]. Numerical simulations agree very well with our theoretical estimation despite the very rough approximation via "effective" potential (we will study the question, what is the parameters regions of its validity, in a future publication).

Note that this SR effect is created by multiplicative noise, since a bimodality is induced by the combined actions of the multiplicative noise and the coupling. If we decrease only the intensity of multiplicative noise, other parameters fixed, the SR effect is not observed, as is shown in Fig. 3(b). The reason is that in this case our system is not bistable (see Fig. 2). For f_2 the behavior is similar: DSR is observed for $g_1 = 1, g_2 = 1, D = 5$, $\sigma_m^2 = 5$, but not for $\sigma_m^2 = 3, D = 5$. For the experimental setup a minimal number of elements, which is neccessary for DSR observation, can be important. Reduction of the element number in this system leads to the fact that a system can spontaneously (even in the absence of forcing) perform a hop between two states. These jumps hide the DSR effect, since they destroy a coherence between input and output. For the system size 18×18, considered here, such jumps are rather seldom [36] and do not hinder DSR. Our calculations have shown that a size 10×10 is still satisfactory, whereas further decrease of the element number will destroy the effect.

In conclusion, we have proposed a rather simple electronic circuit implementation of the DSR effect in order to encourage observers to perform this or a similar experiment. It is important to add that in spite of the fact that the DSR can be interpreted as some modification of SR, there are several important distinctions between DSR and conventional SR. First, a potential barrier is supported by multiplicative noise; it means that DSR is very efficient from the energetic viewpoint. Another consequence is that this SR effect can be controlled by a variation of multiplicative noise intensity. Second, in contrast to SR, the amplitude of hops is changed if we change the intensity of additive noise (similar to Fig. 3 from [19]). This is explained by the fact that an increase of additive noise influences the transition lines (see Fig. 2) and decreases the mean field, which corresponds to a stable position in the absence of the external force.

[1] W. Horsthemke and R. Lefever, *Noise-Induced Transitions* (Springer, Berlin, 1984).

[2] J. Smythe, F. Moss, and P. McClintock, Phys. Rev. Lett. **51**, 1062 (1983).

[3] J. García-Ojalvo and J. M. Sancho, *Noise in Spatially Extended Systems* (Springer, New York, 1999).

[4] P. Landa, A. Zaikin, V. Ushakov, and J. Kurths, Phys. Rev. E **61**, 4809 (2000).

[5] P. Landa and P. McClintock, Phys. Rep. **323**, 4 (2000).

[6] F. Marchesoni, Phys. Lett. A **237**, 126 (1998).

[7] J.M.R. Parrondo, C. Van den Broeck, J. Buceta, and F.J. de la Rubia, Physica A **224**, 153 (1996).

[8] R. Benzi, A. Sutera, and A. Vulpiani, J. Phys. A **14**, L453 (1981).

[9] L. Gammaitoni, P. Hänggi, P. Jung, and F. Marchesoni, Rev. Mod. Phys. **70**, 223 (1998).

[10] B. McNamara, K. Wiesenfeld, and R. Roy, Phys. Rev. Lett. **60**, 2626 (1988).

[11] J. Douglass, L. Wilkens, and L. Pantazelou, Nature (London) **365**, 337 (1993).

[12] N. Stocks, N. Stei, and P. McClintock, J. Phys. A **26**, 385 (1993).

[13] K. Wiesenfeld *et al.*, Phys. Rev. Lett. **72**, 2125 (1994).

[14] Z. Gingl, L. Kiss, and F. Moss, Europhys. Lett. **29**, 191 (1995).

[15] H. Gang, T. Ditzinger, C. Ning, and H. Haken, Phys. Rev. Lett. **71**, 807 (1993).

[16] A. Pikovksy and J. Kurths, Phys. Rev. Lett. **78**, 775 (1997).

[17] S. Bezrukov and I. Vodyanoy, in *Unsolved Problems of Noise and Fluctuations*, edited by D. Abbott and L. Kiss, AIP Conf. Proc. No. 511 (AIP, New York, 1999).

[18] A. Fuliński, Phys. Rev. E **52**, 4523 (1995).

[19] A. Zaikin, J. Kurths, and L. Schimansky-Geier, Phys. Rev. Lett. **85**, 227 (2000).

[20] C. Van den Broeck, J.M.R. Parrondo, and R. Toral, Phys. Rev. Lett. **73**, 3395 (1994).

[21] F. Moss (private communication).

[22] S. Kai, T. Kai, and M. Takata, J. Phys. Soc. Jpn. **47**, 1379 (1979).

[23] J. Micheau, W. Horsthemke, and R. Lefever, J. Chem. Phys. **81**, 2450 (1984).

[24] C. Meyer, G. Ahlers, and D. Cannell, Phys. Rev. A **44**, 2514 (1991).

[25] D. Griswold and J. Tough, Phys. Rev. A **36**, 1360 (1987).

[26] N. Inaba, T. Saito, and S. Mori, Trans. IEICE **E70-A**, 744 (1987).

[27] L. Chua, C. Desoer, and E. Kuh, *Linear and Nonlinear Circuits* (McGraw-Hill Book Co., New York, 1987).

[28] Y. Nishio and S. Mori, IEICE Trans. Fundam. Electron. Commun. Comput. Sci. **E76-A**, 467 (1993).

[29] C. Van den Broeck, J.M.R. Parrondo, R. Toral, and R. Kawai, Phys. Rev. E **55**, 4084 (1997).

[30] A. Zaikin and L. Schimansky-Geier, Phys. Rev. E **58**, 4355 (1998).

[31] B. McNamara and K. Wiesenfeld, Phys. Rev. A **39**, 4854 (1989).

[32] H. Kramers, Physica (Amsterdam) **7**, 284 (1940).

[33] L. Schimansky-Geier and U. Siewert, in *Stochastic Dynamics*, edited by L. Schimansky-Geier and T. Pöschel (Springer, Heidelberg, 1997), p. 245.

[34] P. Kloeden and E. Platen, *Numerical Solution of Stochastic Differential Equations* (Springer-Verlag, Berlin, 1992).

[35] A. Witt, A. Neiman, and J. Kurths, Phys. Rev. E **55**, 5050 (1997).

[36] R. Müller, K. Lippert, A. Kühnel, and U. Behn, Phys. Rev. E **56**, 2658 (1997).

Doubly Stochastic Resonance

A. A. Zaikin,[1] J. Kurths,[1] and L. Schimansky-Geier[2]

[1]*Institute of Physics, University of Potsdam, Am Neuen Palais 10, 14469 Potsdam, Germany*
[2]*Institute of Physics, Humboldt University at Berlin, Invalidenstraße 110, 10115 Berlin, Germany*
(Received 9 November 1999)

We report the effect of doubly stochastic resonance which appears in nonlinear extended systems if the influence of noise is twofold: A multiplicative noise induces bimodality of the mean field of the coupled network and an independent additive noise governs the dynamic behavior in response to small periodic driving. For optimally selected values of the additive noise intensity stochastic resonance is observed, which is manifested by a maximal coherence between the dynamics of the mean field and the periodic input. Numerical simulations of the signal-to-noise ratio and theoretical results from an effective two state model are in good quantitative agreement.

The subject of this Letter is at the borderline of two basic phenomena nowadays attracting significant interest of a broad readership. Both phenomena are marked out by the surprising ability of noise to create more order in the behavior of nonlinear systems when the intensity of the noise is increased. The first class of phenomena is noise-induced phase transitions, intensively investigated since the 1980s. Within the investigated models the appearance of new maxima in the system probability distribution, which has no counterpart in the deterministic description, has been observed [1]. The excitation of noise-induced oscillations [2,3] and the creation of a mean field in spatially extended systems [4–6] are further examples; various applications are discussed widely and a description of many other noise-induced behaviors, even of inhomogeneous structures, can be found in [1,4,6], and references therein.

The second basic phenomenon is stochastic resonance (SR) [7,8], which has been found in many natural systems [9]. The conventional situation is the Brownian motion in a bistable potential modulated by an external periodic force. For an optimally selected strength of noise, the Brownian particle hops coherently to the periodic input between the two wells. In addition to this situation, SR has been also found and investigated in a large variety of different classes of systems: monostable systems [10], systems with excitable dynamics [11], noisy non-

dynamical systems [12], systems without an external force [13], and systems without any kind of threshold [14].

However, SR has not been considered in systems with a noise-induced structure [15]. Therefore, we present in this Letter a new type of SR in a system with a noise-induced nonequilibrium phase transition resulting in a bistable behavior of the mean field. We call this effect *doubly stochastic resonance* (DSR) to emphasize that additive noise causes a resonancelike behavior in the structure, which in its own turn is induced by multiplicative noise.

This DSR is demonstrated on a nonlinear lattice of coupled overdamped oscillators first introduced in [5] and further studied in [6,16]. The following set of Langevin equations describes the considered system:

$$\dot{x}_i = f(x_i) + g(x_i)\xi_i(t) + \frac{D}{2d}\sum_j (x_j - x_i) + \zeta_i(t) + A\cos(\omega t + \varphi),$$
(1)

where $x_i(t)$ represents the state of the ith oscillator, $i = 1, \ldots, L^d$, in the cubic lattice of the size L in d dimensions and with $N = L^d$ elements. The sum runs over $2d$ nearest neighbors of the ith cell, and the strength of the coupling is measured by D. The noisy terms $\xi_i(t)$ and $\zeta_i(t)$ represent mutually uncorrelated Gaussian noise, with zero mean and uncorrelated both in space and time

$$\langle \xi_i(t)\xi_j(t') \rangle = \sigma_\xi^2 \delta_{i,j} \delta(t - t'), \qquad (2)$$

$$\langle \zeta_i(t)\zeta_j(t') \rangle = \sigma_\zeta^2 \delta_{i,j} \delta(t - t'). \qquad (3)$$

The last item in (1) stands for an external periodic force with amplitude A, frequency ω, and initial phase φ.

For the sake of simplicity, the functions $f(x)$ and $g(x)$ are taken to be of the form [5]:

$$f(x) = -x(1 + x^2)^2, \qquad g(x) = 1 + x^2. \qquad (4)$$

In the absence of external force ($A = 0$) this model can be solved analytically by means of a standard mean-field theory (MFT) procedure [4]. The mean-field approximation consists in replacing the nearest-neighbor interaction by a global term in the Fokker-Planck equation corresponding to (1). In this way, one obtains the following steady-state probability distribution w_{st}:

$$w_{\mathrm{st}}(x, m) = \frac{C(m)}{\sqrt{\sigma_\xi^2 g^2(x) + \sigma_\zeta^2}} \\ \times \exp\left(2 \int_0^x \frac{f(y) - D(y - m)}{\sigma_\xi^2 g^2(y) + \sigma_\zeta^2} \, dy\right), \tag{5}$$

where $C(m)$ is a normalization constant and m is a mean field, defined by the equation

$$m = \int_{-\infty}^{\infty} x w_{\mathrm{st}}(x, m) \, dx. \qquad (6)$$

Solving Eq. (6) self-consistently with respect to the variable m one determines transitions between ordered ($m \neq 0$) and disordered ($m = 0$) phases. Transition boundaries between different phases are shown in Fig. 1 and the corresponding dependence of the order parameter on σ_ξ^2 is presented in Fig. 2. In addition to [5], we show influence of additive noise resulted in the shift of transition lines. For $\sigma_\zeta^2 = 0$ an increase of the multiplicative noise causes a disorder-order phase transition, which is followed by the reentrant transition to disorder [5]. In the ordered phase the system occupies one of two symmetric possible states with the mean fields $m_1 = -m_2 \neq 0$, depending on initial conditions.

Now let us turn to the problem of how system (1) responds to periodic forcing. We have taken a set of parameters $(\sigma_\xi^2; D)$ within the region of two coexisting ordered states with nonzero mean field. In particular, we choose values given by the dot in Fig. 1. As for the network, we take a two-dimensional lattice of $L^2 = 18 \times 18$ oscillators, which is simulated numerically [17] with a time step $\Delta t = 2.5 \times 10^{-4}$ under the action of the harmonic external force. The amplitude of the force A has to be set sufficiently small to avoid hops in the absence of additive noise during the simulation time of a single run which is much larger than the period of the harmonic force [18]. Jumps between $m_1 \leftrightarrow m_2$ occur only if additive noise is additionally switched on. Runs are averaged over different initial phases.

Time series of the mean field and the corresponding periodic input signal are plotted in Fig. 3 for three different values of σ_ζ^2. The current mean field is calculated as $m(t) = \frac{1}{L^2} \sum_{i=1}^{N} x_i(t)$. For a small intensity of the additive noise, hops between the two symmetric states m_1 and m_2 are rather seldom and not synchronized to the external force. If we increase the intensity σ_ζ^2, we achieve a situation when hops occur with the same periodicity as the external force and, hence, the mean field follows with high probability the input force. An increase of additive noise provides an optimization of the output of the system which is stochastic resonance. If σ_ζ^2 is increased further, the order is again destroyed, and hops occur much more frequently than the period of the external force.

Figure 3 illustrates that additive noise is able to optimize the signal processing in the system (1). In order to characterize this SR effect we have calculated signal-to-noise ratio (SNR) by extracting the relevant phase-averaged power spectral density $S(\omega)$ and taking the ratio between its signal part with respect to the noise background [8]. The dependence of SNR on the intensity of the additive noise is shown in the Fig. 4 for the mean field (filled points) and the mean field in a two-state approximation (opaque point). In this two-state approximation we have replaced $m(t)$ by its sign and put approximately $m(t) = +1$ or $m(t) = -1$, respectively. Both curves exhibit the well-known bell shaped dependence on σ_ζ^2 typically for SR. Since the bimodality of the mean field is a noise-induced effect we call that whole effect *doubly stochastic resonance*. For the given parameters and $A = 0.1$, $\omega = 0.1$ the maximum of the SNRs is approximately located near $\sigma_\zeta^2 \sim 1.8$.

Next we intend to give analytic estimates of the SNR. If A, D, and σ_ζ^2 vanish, the time evolution of the first moment of a single element is given simply by the drift part in the corresponding Fokker-Planck equation (Stratonovich case)

$$\langle \dot{x} \rangle = \langle f(x) \rangle + \frac{\sigma_\xi^2}{2} \langle g(x)g'(x) \rangle. \qquad (7)$$

As it was argued in [6], the mechanism of the noise-induced transition in coupled systems can be explained by means of a short time evolution approximation [19]. It means that we start with an initial Dirac δ function, follow it only for a short time, such that fluctuations are small and the probability density is well approximated by a Gaussian. A suppression of fluctuations, performed by coupling, makes this approximation appropriate in our case [20]. The equation for the maximum of the probability, which is also the average value in this approximation $\bar{x} = \langle x \rangle$, takes the following form

$$\dot{\bar{x}} = f(\bar{x}) + \frac{\sigma_\xi^2}{2} g(\bar{x})g'(\bar{x}), \qquad (8)$$

which is valid if $f(\langle x \rangle) \gg \langle \delta x^2 \rangle f''(\langle x \rangle)$. For this dynamics an "effective" potential $U_{\mathrm{eff}}(x)$ can be derived, which has the form

$$U_{\text{eff}}(x) = U_0(x) + U_{\text{noise}} = -\int f(x)\,dx - \frac{\sigma_\xi^2 g^2(x)}{4},$$
$$(9)$$

where $U_0(x)$ is a monostable potential and U_{noise} represents the influence of the multiplicative noise. In the ordered region, inside the transition lines (Fig. 1), the potential $U_{\text{eff}}(x)$ is of the double-well form, e.g., $U(x)_{\text{eff}} = -x^2 - 0.25x^4 + x^6/6$, for given $f(x)$, $g(x)$, and $\sigma_\xi^2 = 3$.

Now we consider a conventional SR problem in this potential with an external periodic force of the amplitude A and the frequency ω. If we neglect intrawell dynamics and follow linear response theory the SNR is well known [8,21]

$$\text{SNR}_1 = \frac{4\pi A^2}{\sigma_\zeta^4} r_k, \qquad (10)$$

where r_k is the corresponding Kramers rate [22]

$$r_k = \frac{\sqrt{(U_{\text{eff}}''(x)|_{x=x_{\min}}|U_{\text{eff}}''(x)|_{x=x_{\max}})}}{2\pi} \exp\left(-\frac{2\Delta U_{\text{eff}}}{\sigma_\zeta^2}\right)$$
$$(11)$$

for surmounting the potential barrier ΔU_{eff}. Using Eqs. (9)–(11), we get an analytical estimate for a single element inside the lattice. Further on, rescaling this value by the number N of oscillators in the lattice [23] and taking into account the processing gain G and the bandwidth Δ in the power spectral density [21], the SNR_N of the mean field of the network of N elements can be obtained

$$\text{SNR}_N = \text{SNR}_1 \frac{NG}{\Delta} + 1. \qquad (12)$$

This dependence is shown in Fig. 4 by the solid line and demonstrates, despite the rough approximation, a good agreement with the results of the numerical simulations. Nearly exact agreement is found in the location of the maximum as well as for the quantitative values of the SNR ("scalloping loss" [21] has been avoided in simulations by setting the frequency ω to be centered on one of the bins in the spectrum). A more satisfying theory of DSR is left as an open question in this Letter.

In conclusion, we have reported the existence of doubly stochastic resonance, which results from the twofold influence of noise on a nonlinear system. DSR is a combined effect which consists of a noise-induced phase transition and conventional SR.

Some remarks should be added. First, we have considered a system which undergoes a *pure* noise-induced transition, in the sense that a transition is impossible in the absence of noise. This is an important distinction of the DSR effect from SR in any variation of the mean-field model [24]. Second, in the considered system the so-called "stochastic" potential [1] for a single oscillator in the lattice [which differs from (9)] always remains monostable. Third, there are clear distinctions between SR and DSR behavior, because, in contrast to SR, in DSR additive noise does not only help an input/output synchronization, but also changes the properties of the system in the absence of the external force (see Figs. 1 and 2). As a consequence, in DSR amplitude of hops is decreased (bistability disappears) for large noise intensities σ_ζ^2 (compare Fig. 3 and Fig. 4 from [8]). Finally, not every system with noise-induced bistability demonstrates DSR, e.g., we did not find DSR in zero-dimensional systems, which are described in [1].

We expect that these theoretical findings will stimulate experimental works to verify DSR in real physical
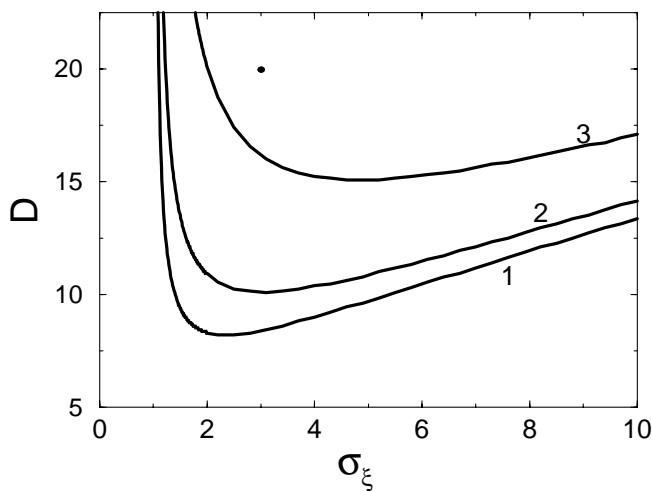

FIG. 1. Transition lines between ordered and disordered phase on the plane $(\sigma_m^2; D)$ for different intensities of the additive noise $\sigma_\zeta^2 = 0$ (1); 1 (2), and 5 (3). The black point corresponds to $D = 20$, $\sigma_\xi^2 = 3$.
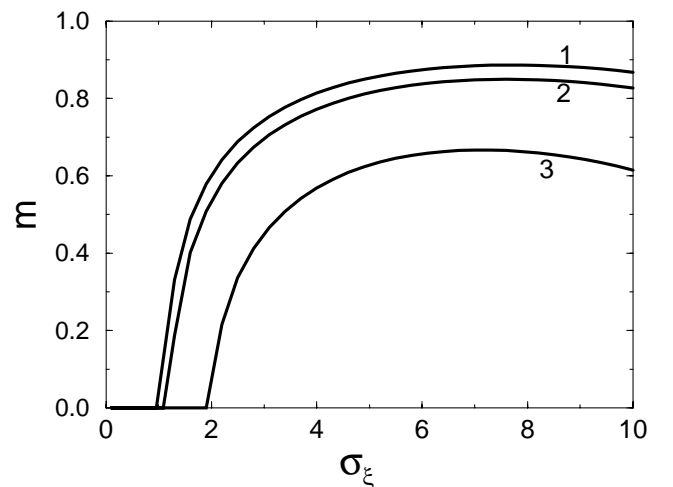

FIG. 2. The order parameter $|m|$ vs the intensity of multiplicative noise for $D = 20$ and $\sigma_\zeta^2 = 0$ (label 1), 1 (label 2), and 5 (label 3).
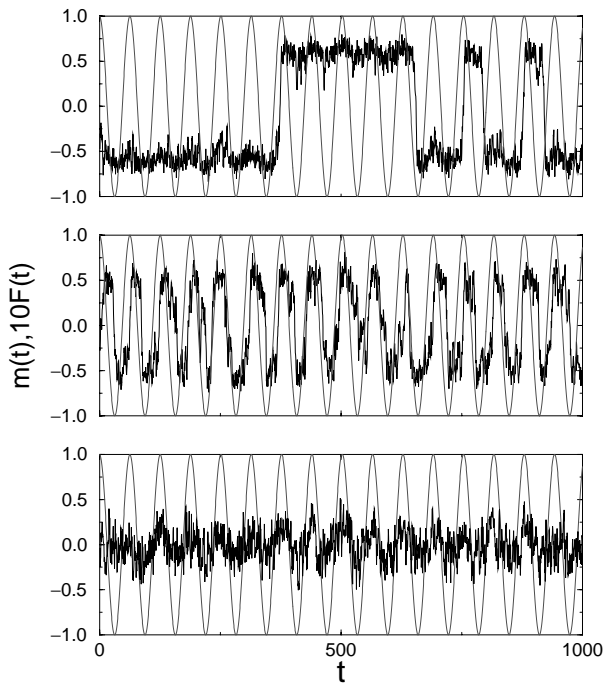
FIG. 3. Example of input/output synchronization. The time evolution of the current mean field (output) and the periodic external force $F(t)$ (input) for different intensities of additive noise (from top to bottom) $\sigma_\zeta^2 = 0.01$, 1.05, and 5.0. If the intensity of the additive noise is close to their optimal value (middle row), hops occur with the period of the external force. The remaining parameters are $A = 0.1$, $\omega = 0.1$, $D = 20$, and $\sigma_\xi^2 = 3$.

systems (for experiments on noise-induced bistability, see [25]). Appropriate situations can be found in electronic circuits [26], as well as in system, which demonstrate a
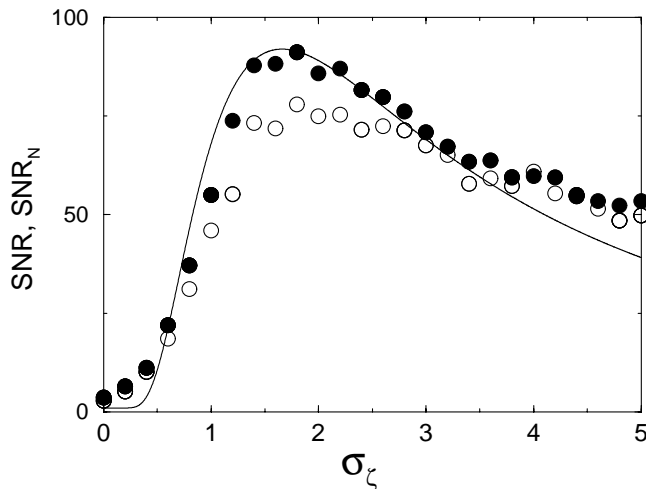

FIG. 4.   The dependence of SNR on the additive noise intensity for the output (filled points) and its two-states approximation (opaque points). The solid line corresponds to the analytical estimation SNR_N (12), performed on the base of derivation of the "effective" potential and linear response theory. The parameters are the same as for Fig. 3 and the processing gain $G = 0.7$.

noise-induced shift of the phase transition, e.g., in liquid crystals [27], photosensitive chemical reactions [28], or Rayleigh-Bénard convection [29]. It can be crucial for such experiments that, in contrast to conventional SR, in DSR the energy of noise is used in a more efficient way: not only for the optimization of the signal processing, but also for the support of the potential barrier to provide this optimization.

[1] W. Horsthemke and R. Lefever, *Noise-Induced Transitions* (Springer, Berlin, 1984).

[2] P. Landa and A. Zaikin, Phys. Rev. E **54**, 3535 (1996).

[3] P. S. Landa, A. A. Zaikin, V. G. Ushakov, and J. Kurths, Phys. Rev. E **61**, 4809 (2000); P. S. Landa and P. V. E. McClintock, Phys. Rep. **323**, 4 (2000).

[4] J. García-Ojalvo and J. M. Sancho, *Noise in Spatially Extended Systems* (Springer, New York, 1999).

[5] C. Van den Broeck, J. M. R. Parrondo, and R. Toral, Phys. Rev. Lett **73**, 3395 (1994).

[6] C. Van den Broeck, J. M. R. Parrondo, R. Toral, and R. Kawai, Phys. Rev. E **55**, 4084 (1997).

[7] R. Benzi, A. Sutera, and A. Vulpiani, J. Phys. A **14**, L453 (1981); M. Dykman and P. McClintock, Nature (London) **391**, 344 (1998); V. S. Anishchenko, A. B. Neiman, F. Moss, and L. Schimansky-Geier, Sov. Phys. Usp. **42**, 7 (1999).

[8] L. Gammaitoni, P. Hänggi, P. Jung, and F. Marchesoni, Rev. Mod. Phys. **70**, 223 (1998).

[9] J. Douglass, L. Wilkens, and L. Pantazelou, Nature (London) **365**, 337 (1993); K. Wiesenfeld and F. Moss, Nature (London) **373**, 33 (1995); S. Bezrukov and I. Vodyanoy, Nature (London) **378**, 362 (1995); J. Collins, T. Imhoff, and P. Grigg, Nature (London) **383**, 770 (1996); P. Cordo *et al.,* Nature (London) **383**, 769 (1996).

[10] N. Stocks, N. Stei, and P. McClintock, J. Phys. A **26**, 385 (1993); J. Vilar and J. Rubí, Phys. Rev. Lett. **77**, 2863 (1996).

[11] K. Wiesenfeld *et al.,* Phys. Rev. Lett. **72**, 2125 (1994).

[12] Z. Gingl, L. Kiss, and F. Moss, Europhys. Lett. **29**, 191 (1995).

[13] H. Gang, T. Ditzinger, C. Ning, and H. Haken, Phys. Rev. Lett. **71**, 807 (1993); Note also A. Pikovsky and J. Kurths, Phys. Rev. Lett. **78**, 775 (1997).

[14] S. Bezrukov and I. Vodyanoy, in *Unsolved Problems of Noise and Fluctuations,* edited by D. Abbott and L. Kiss, AIP Conf. Proc. No. 511 (AIP, New York, 1999), p. 169.

[15] Note that SR in connection with a noise-induced transition has been considered in A. Fuliński, Phys. Rev. E **52**, 4523 (1995), but in a zero-dimensional system with noise-induced transient states.

[16] A. Zaikin and L. Schimansky-Geier, Phys. Rev. E **58**, 4355 (1998); S. Mangioni, R. Deza, H. S. Wio, and R. Toral, Phys. Rev. Lett. **79**, 2389 (1997).

[17] P. Kloeden and E. Platen, *Numerical Solution of Stochastic Differential Equations* (Springer-Verlag, Berlin, 1992).

[18] For small L hops can be observed even without external force [R. Müller, K. Lippert, A. Kühnel, and U. Behn, Phys. Rev. E **56**, 2658 (1997)]. With $L = 18$ such hops are very rare.

[19] Note that the effective potential does not always appropriately explain the transition in this system [A. A. Zaikin, J. García-Ojalvo, and L. Schimansky-Geier, Phys. Rev. E **60**, R6275 (1999)].

[20] C. Van den Broeck, in *Stochastic Dynamics,* edited by L. Schimansky-Geier and T. Pöschel (Springer, Heidelberg, 1997), p. 7.

[21] B. McNamara and K. Wiesenfeld, Phys. Rev. A **39**, 4854 (1989).

[22] H. Kramers, Physica (Amsterdam) **7**, 284 (1940).

[23] L. Schimansky-Geier and U. Siewert, in *Stochastic Dynamics,* edited by L. Schimansky-Geier and T. Pöschel (Springer, Heidelberg, 1997), p. 245.

[24] M. Morillo, J. Gómez-Ordonez, and J. Casado, Phys. Rev. E **52**, 316 (1995).

[25] D. Griswold and J. T. Tough, Phys. Rev. A **36**, 1360 (1987).

[26] F. Moss (private communication).

[27] S. Kai, T. Kai, and M. Takata, J. Phys. Soc. Jpn. **47**, 1379 (1979); M. Wu and C. Andereck, Phys. Rev. Lett. **65**, 591 (1990).

[28] J. Micheau, W. Horsthemke, and R. Lefever, J. Chem. Phys. **81**, 2450 (1984); P. de Kepper and W. Horsthemke, *Synergetics: Far From Equilibrium* (Springer, New York, 1979).

[29] C. Meyer, G. Ahlers, and D. Cannell, Phys. Rev. A **44**, 2514 (1991).

Additive noise in noise-induced nonequilibrium transitions

A. Zaikin and J. Kurths
Institute of Physics, University of Potsdam, Am Neuen Palais 10, 14469 Potsdam, Germany

We study different nonlinear systems which possess noise-induced nonequilibrium transitions and shed light on the role of additive noise in these effects. We find that the influence of additive noise can be very nontrivial: it can induce first- and second-order phase transitions, can change properties of on–off intermittency, or stabilize oscillations. For the Swift–Hohenberg coupling, that is a paradigm in the study of pattern formation, we show that additive noise can cause the formation of ordered spatial patterns in distributed systems. We show also the effect of doubly stochastic resonance, which differs from stochastic resonance, because the influence of noise is twofold: multiplicative noise and coupling induce a bistability of a system, and additive noise changes a response of this noise-induced structure to the periodic driving. Despite the close similarity, we point out several important distinctions between conventional stochastic resonance and doubly stochastic resonance. Finally, we discuss open questions and possible experimental implementations. © *2001 American Institute of Physics.* [DOI: 10.1063/1.1380369]

In the majority of investigations, devoted to the study of noise-induced processes, a supplement of additive noise leads only to smoothing of transition diagrams. Contrary to this situation, in this contribution we show that additive noise can play a much more crucial role. In oscillatory systems, additive noise is able to excite oscillations, to influence on–off intermittency, and to stabilize stochastic oscillations. In spatially extended systems, which consist of coupled overdamped oscillators, additive noise can induce first- and second-order phase transitions, which in particular cases manifest themselves in the appearance of spatially ordered patterns. Another interesting behavior occurs if a system works as a signal processor. Then additive noise is able to optimize the response of a system to an external periodic signal, if this system possesses a property of multiplicative noise induced bistability.

I. INTRODUCTION

Intensive investigations in nonlinear physics in the last two decades have shown that there are many nonequilibrium systems which demonstrate phenomena manifesting noise-induced ordering. Among these phenomena we emphasize several basic ones, such as stochastic resonance (SR)[1,2] (for SR in natural systems see Ref. 3), noise-induced transitions (NIT),[4–6] noise-induced transport in ratchets,[7] or coherence resonance.[8] This classification does not pretend to be complete, because there are various modifications and extensions of these basic phenomena (e.g., resonance activation[9] or noise-induced pattern formation[10]). On the another hand, there are phenomena which possess properties of different groups from this classification. Two interesting examples may illustrate this point: a synthesis of a ratchet mechanism and noise-induced phase transition,[11] and a synthesis of stochastic resonance and noise-induced transition.[12]

In the present review we focus on one of these basic

phenomena, namely noise-induced transitions (NIT). In its turn, NIT can be classified into three main groups: (i) NIT which lead to the appearance of additional maxima in the system's probability distribution,[4] (ii) NIT which lead to the excitation of oscillations,[13,14] and (iii) NIT in extended systems which lead to breaking of symmetry and the creation of a mean field.[5,15–17,19] In the majority of the papers on these topics only multiplicative noise is perceived to be responsible for the transitions. However, it was recently shown,[6,18,20–22] that under certain conditions additive noise can also be very important and nontrivial in NIT. The aim of the present paper is to discuss several aspects and recent results of this investigation and also to point out open questions and unsolved problems connected with the influence of additive noise on transitions in nonlinear systems.

First we analyze *oscillatory* systems under the action of noise. In Sec. II we start by considering a transition induced by multiplicative noise in a pendulum with randomly vibrated suspension axis. We investigate the role of additive noise in this effect and show that additive noise influences a transition as well as on–off intermittency, observed in the excited oscillations. In contrast to this situation in which additive noise only smoothes the transition, in the next investigated oscillatory model, a standard epidemiological model with random excitation, the transition can be induced both by multiplicative and additive noise (Sec. III). Moreover, additive noise is able to stabilize stochastic oscillations, which are unstable if only multiplicative noise is present. Another class of models under consideration are spatially extended systems, which consist of coupled *overdamped* oscillators. We show that in such systems second- and first-order transitions induced by additive noise are possible (Sec. IV). If a nonlinear distributed system is under the action of additional external force, then doubly stochastic resonance (DSR) can be observed (Sec. V). In DSR the influence of noise is twofold: multiplicative noise induces a bistability of a mean field, and additive noise helps the system to respond coher-

ently to an external signal. Finally, we summarize the results and discuss open questions of the problem under consideration in order to show that there are a lot of unsolved problems in this particular field, which is rapidly developing and attracting constantly growing attention in the modern nonlinear physics.

II. TRANSITIONS IN THE PRESENCE OF ADDITIVE NOISE: ON–OFF INTERMITTENCY

A pendulum with randomly vibrated suspension axis is a typical example of oscillatory system, in which parametric action of noise can lead to the excitation of oscillations via a second-order phase transition.[6,13,18] In this case the intensity of multiplicative noise plays the role of temperature and the average amplitude is the order parameter. Here we discuss the question "what happens if additionally additive noise is acting upon the system?" Therefore we consider a pendulum whose suspension axis is vibrating in the direction making the angle γ with respect to the vertical. As shown in Ref. 6, for moderately small vibrations of a suspension axis, the equation of motion can be written as follows:

$$\ddot{\varphi}+2\beta(1+\alpha\dot{\varphi}^2)\dot{\varphi}+\omega_0^2(1+\xi_1(t))\varphi=\omega_0^2\xi_2(t), \qquad (1)$$

where φ is the pendulum angular deviation from the equilibrium position, ω_0^2 is the natural frequency of small free pendulum oscillations, β is a damping factor with the nonlinear coefficient α, $\xi_1(t)=\xi(t)\cos\gamma$ is the multiplicative component of the suspension vibration, and $\xi_2(t)=-\xi(t)\sin\gamma$ is its additive component, $\xi(t)$ is a comparatively wide-band random process (or white noise), responsible for the shift of the suspension axis in the direction of vibration.

In the absence of additive noise ($\xi_2=0$, $\gamma=0$, i.e., a vibration is performed strictly in the vertical direction), the system can be analyzed analytically. Looking for the solution in the form $\varphi(t)=A(t)\cos(\omega_0 t+\phi)$ and using the Krylov–Bogolyubov method for stochastic equations,[23] we obtain the following truncated equations for the amplitude A and the phase ϕ of the pendulum's oscillations:

$$\dot{u}=\frac{1}{8}\omega_0^2\kappa(2\omega_0)-\beta\left(1+\frac{3}{4}\beta\alpha\omega_0^2\exp^{2u}\right)+\frac{\omega_0^2}{2}\zeta_1(t),$$

$$\dot{\phi}=\omega_0\zeta_2(t), \qquad (2)$$

where $u=\ln A$, $\zeta_1(t)$, and $\zeta_2(t)$ are white noise with intensities

$$K_1=\tfrac{1}{2}\kappa(2\omega_0), \quad K_2=\tfrac{1}{4}(\kappa(0)+\tfrac{1}{2}\kappa(2\omega_0)). \qquad (3)$$

Here $\kappa(\omega)=\int_{-\infty}^{\infty}\langle\xi(t)\xi(t+\tau)\rangle\cos(\omega\tau)d\tau$ is the power spectrum density of the process $\xi(t)$ at the frequency ω, and the angular brackets signify averaging over statistical ensemble. It is important that in the equation for the amplitude $u=\ln A$, we have a constant term $\omega_0^2\kappa(2\omega_0)/8$, which appeared due to the parametric action of noise. Namely, this fact is responsible for the excitation of noise-induced oscillations.

Solving the Fokker–Planck equation associated with Eq. (1), a probability density for the amplitude $w(A)$ and amplitude squared $w(A^2)=(1/2A)\,w(A)$ can be found.[13] Using the function $w(A^2)$ we obtain

$$\langle A^2\rangle = \begin{cases} \dfrac{4\eta}{3\alpha\omega_0^2} & \text{for } \eta\geq 0, \\[2mm] 0 & \text{for } \eta\leq 0, \end{cases} \qquad (4)$$

where

$$\eta=\frac{\omega_0^2}{8\beta}\left(\kappa(2\omega_0)-\frac{8\beta}{\omega_0^2}\right)$$

is proportional to the difference between the noise intensity at the frequency $2\omega_0$ and the critical noise intensity.

It is clear from this that for $\eta\geq 0$ the parametric excitation of the pendulum's oscillations occur under the effect of noise via a noise-induced transition. This manifests itself in the fact that the mean value of the amplitude squared becomes different from zero. The corresponding dependence of the order parameter $\langle A^2\rangle$ on the parameter η is plotted in Fig. 1(a). Numerical simulation of the original Eq. (1) shows that if the noise intensity is slightly over a threshold, then on–off intermittency can be observed in the form of oscillations.[24] This means that for the same external action the system is sometimes in the state "on" (the amplitude is large), which is intermittent with the state "off" (the amplitude is rather small).

Now let us discuss which changes happen in the presence of additive noise. The analytical consideration for this case can be found in Ref. 22; here we present the results of numerical simulations. The results are shown in Fig. 1(a). The presence of additive noise leads to the fact that the probability distribution below the threshold is no longer a δ-function, and the transition is now smoothed and not so well-defined, as in the case without additive noise. It is interesting to note that in both cases, with or without additive noise, no additional extrema in the system probability distribution $w(A^2)$ are observed in the course of the transition.

The additive noise also influences the effect of on-off intermittency [see Fig. 1(b)]. For supercritical values of the multiplicative noise intensity on–off intermittency is now hidden and not observable in the form of oscillations, but can be detected for subcritical values, below a threshold. Hence in the presence of additive noise on–off intermittency, a sign of noise-induced transition, can be observed even before this transition occurs with respect to the increase of the control parameter.

It is necessary to note that in the same system chaotic oscillations can be observed, if the external parametric action is periodic. A comparison with this case is discussed in Ref. 13. Chaotic pendulum's oscillations are very similar in its form to noise-induced oscillations. However, a calculation of the probability distribution of the average amplitude squared allows to distinguish between both cases of the external action by means of the Rytov–Dimentberg criterion.[13]
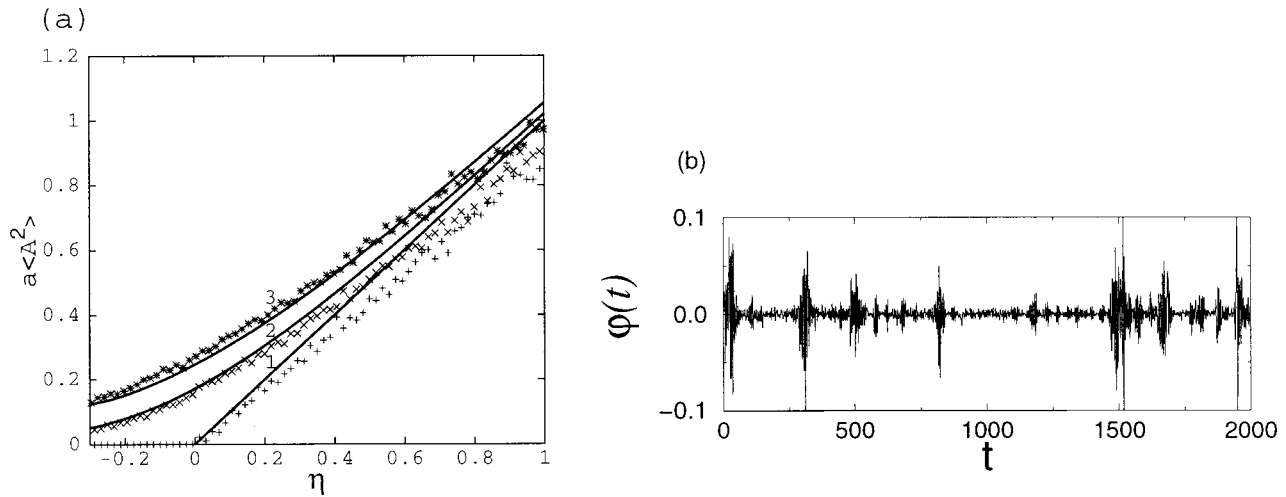
FIG. 1. (a) A noise-induced phase transition in a pendulum with randomly vibrated suspension axis [Eq. (1)]. The dependence of the averaged amplitude squared multiplied by the parameter $a = 3\alpha\omega_0^2/4$ on η, where η is an extent on which multiplicative noise intensity exceeds the threshold value. The curve 1 corresponds to the case without additive noise, curves 2 and 3 to the cases with additive noise intensities $k1$ and $k2$, where $k2 > k1$ (for details and analytical expressions see Ref. 6). Analytical and numerical results are shown by solid and symbol curves, respectively. (b) On–off intermittency for subcritical values of multiplicative noise intensity. In contrast to this situation, if additive noise is absent, on–off intermittency is observed near a threshold but for supercritical values of the multiplicative noise intensity.

As is shown by further examples in this contribution, this effect of transition smoothing and influence on on–off intermittency is not a single effect of additive noise in oscillatory systems.

III. TRANSITIONS INDUCED BOTH BY MULTIPLICATIVE AND ADDITIVE NOISE: STABILIZATION OF NOISE-INDUCED OSCILLATIONS

In this section we study a system under the action of noise, which has both additive and multiplicative components. We show that these both multiplicative and additive components of noise, considered separately, can induce a transition, and, what is especially interesting, the combination of their actions stabilizes noise-induced oscillations. To demonstrate these effects, we use a standard epidemiological model for the dynamics of children diseases.[25] Two variants of excitation are possible, either by periodic force[26,27] or by noise.[14] In both cases this system exhibits chaotic or noise-induced oscillations which closely resemble oscillations observed in experimental data.

We analyze the influence of additive component of noise in the following model system:[14]

$$\dot{S} = e(1-S) - bSI, \quad \dot{E} = bSI - (e+l)E,$$
$$\dot{I} = lE - (e+g)I, \tag{5}$$

where S, E, and I denote the number of susceptible, exposed but not yet infected, and invective children, respectively. The parameters $1/e$, $1/l$, $1/g$ are the average expectancy, latency and infection periods of time. The contact rate b is the parameter of excitation and equal to $b = b_0(1+b_1\xi(t))$ where $\xi(t)$ is a harmonic noise with the peak of spectral density at the circle frequency 2π (seasonal noisy oscillations with a period equal to one year) and the parameter b_1 is the amplitude of noise. The excited oscillations are executed in the vicinity of the stable singular point with the coordinates

(S_0, E_0, I_0). Hence, one can easily rewrite the equations for the new variables $x = S/S_0 - 1$, $y = E/E_0 - 1$, and $z = I/I_0 - 1$ which are deviations from the equilibrium point:

$$\dot{x} + ex = -b_0 I_0 (1+b_1\xi(t))(x+z+xz) - b_0 b_1 I_0 \xi(t),$$

$$\dot{y} + (e+l)y = (e+l)(1+b_1\xi(t))(x+z+xz)$$
$$+ (e+l)b_1\xi(t), \tag{6}$$

$$\dot{z} + (e+g)z = (e+g)y.$$

This form of equations clearly shows that the action of noise is multiplicative as well as additive.

An increase of the noise intensity causes noise-induced oscillations of the variables S, I, E [Fig. 2(a)]. Their oscillatory behavior closely resembles observed epidemiological data [compare Fig. 2(a) with figures in Ref. 28]. These oscillations are excited after a noise-induced transition [see Fig. 2(b)]. There the variance of oscillations together with an approximating straight line is shown. The point where the straight line crosses the abscissa axis can be taken as a critical point of the transition. To prove this, we remove artificially the multiplicative component of noise from Eqs. (6). In this case the variance of oscillations is equal to zero if $b_1 < b_{1cr}$ and goes to infinity shortly after the noise intensity exceeds its critical value. So, additive noise indeed is able to induce a phase transition. The same situation happens if the additive component of noise is absent but the multiplicative one is present.

To conclude, this transition can be induced by noise which contains both multiplicative and additive components. As shown by its separate consideration, both components play an important role in this transition. What is even more interesting, if the additive and multiplicative components of noise act together, as in the model, a stabilization of noise-induced oscillations occurs: in this case the dependence of
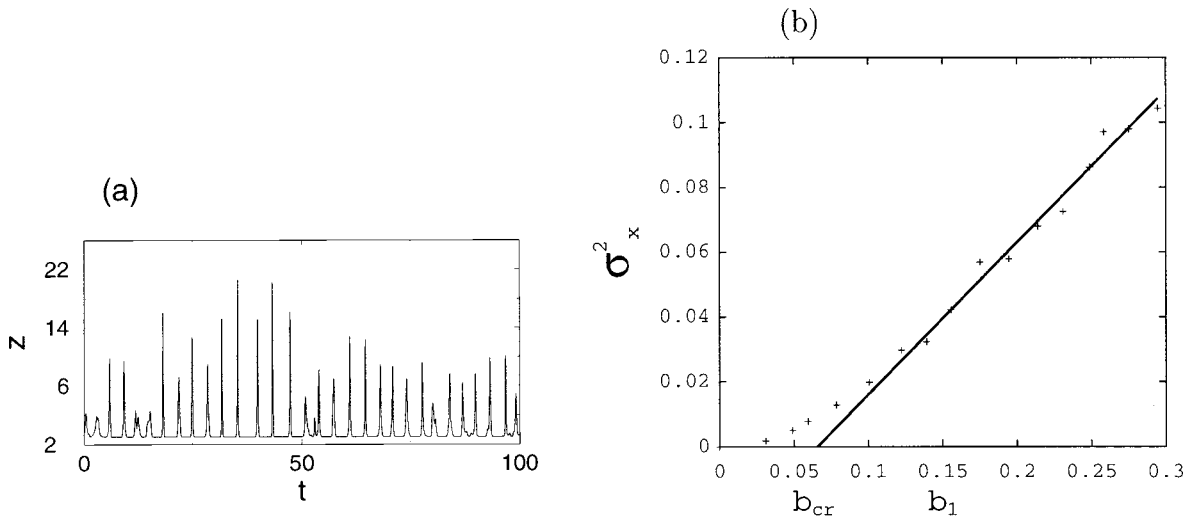
FIG. 2. (a) Noise-induced oscillations (epidemics) in the epidemiological model Eqs. (6). (b) The dependence of oscillation variance for the variable x on the parameter b_1, which is responsible for the noisy variation of a contact rate (see the text).

the variance on the noise intensity does not increase to infinity, that is not a case if multiplicative component of noise acts separately.

IV. TRANSITIONS INDUCED BY ADDITIVE NOISE

Now we extend our study to spatially extended systems and show that additive noise is able to induce second- and first-order phase transitions. Due to a special form of coupling these transition can also lead to the formation of spatially ordered patterns.

A. Second-order phase transitions: Noise-induced pattern formation

We investigate a nonlinear lattice of overdamped coupled stochastic oscillators[10,21] under the action of noise. In this system a transition manifests itself in the formation of spatially ordered patterns, as a consequence of a special form of coupling *a la* Swift–Hohenberg. The system is described by a scalar field $x_{\mathbf{r}}$, defined on a spatial lattice with points $\mathbf{r}$:

$$\dot{x}_{\mathbf{r}} = f(x_{\mathbf{r}}) + g(x_{\mathbf{r}})\xi_{\mathbf{r}} + \mathcal{L}x_{\mathbf{r}} + \zeta_{\mathbf{r}} \qquad (7)$$

with f and g taken in the form (for the discussion, which functions can be chosen to observe a transition see Ref. 29)

$$f(x) = -x(1+x^2)^2, \quad g(x) = a^2 + x^2 \qquad (8)$$

and $\xi_{\mathbf{r}}$, $\zeta_{\mathbf{r}}$ are independent zero-mean-value Gaussian white noises:

$$\langle \xi_{\mathbf{r}}(t)\xi_{\mathbf{r}'}(t')\rangle = \sigma_m^2 \delta_{\mathbf{r},\mathbf{r}'}\delta(t-t'),$$
$$\langle \zeta_{\mathbf{r}}(t)\zeta_{\mathbf{r}'}(t')\rangle = \sigma_a^2 \delta_{\mathbf{r},\mathbf{r}'}\delta(t-t'). \qquad (9)$$

Note that for these functions $f(x)$ and $g(x)$ the transitions described are *pure* noise-induced phase transitions, in the sense that they do not exist in the system without noise. The coupling operator $\mathcal{L}$ is a discretized version of the Swift–Hohenberg coupling term $-D(q_0^2 + \nabla^2)^2$.[21]

To study the influence of the additive noise, we consider two limiting cases of correlation between additive and mul-

tiplicative noise: strong correlation ($\zeta_{\mathbf{r}}=0$ and parameter a is varied), and no correlation ($a=0$ and the intensity of $\zeta_{\mathbf{r}}$ is varied).

Using the generalized Weiss mean field theory (MFT),[5] the conditions of phase transition can be found. Substituting the value of the scalar variable $x_{\mathbf{r}'}$ at the sites coupled to $x_{\mathbf{r}}$ by its special average:

$$\langle x_{\mathbf{r}'}\rangle = \langle x\rangle \cos[\mathbf{k}\cdot(\mathbf{r}-\mathbf{r}')], \qquad (10)$$

we obtain for $x=x_{\mathbf{r}}$

$$\dot{x} = f(x) + g(x)\xi(t) + D\omega(\mathbf{k})x - D_{\text{eff}}(x-\langle x\rangle) + \zeta(t), \qquad (11)$$

where

$$D_{\text{eff}} = \left[\left(\frac{2d}{\Delta^2} - q_0^2\right)^2 + \frac{2d}{\Delta^2} + \omega(\mathbf{k})\right]D \qquad (12)$$

and a dispersion relation $\omega(\mathbf{k})=0$ for the most unstable mode, which is only of interest here.[10]

Now the value $\langle x\rangle$ plays the role of the amplitude of the spatial patterns with an effective diffusion coefficient D_{eff}. The steady state solution of the Fokker–Planck equation corresponding to Eq. (10) is written then as follows:

$$w_{st}(x) = \frac{C(\langle x\rangle)}{\sqrt{\sigma_m^2 g^2(x) + \sigma_a^2}} \exp\left(2\int_0^x \frac{f(y) - D_{\text{eff}}(y-\langle x\rangle)}{\sigma_m^2 g^2(y) + \sigma_a^2}dy\right), \qquad (13)$$

and $C(\langle x\rangle)$ is the normalization constant.

For the mean field value $\langle x\rangle$ we obtain[21]

$$\langle x\rangle = \int x w_{st}(x,\langle x\rangle)dx. \qquad (14)$$

Solving Eq. (14) with parameters D, σ_m^2, and σ_a^2, we obtain a boundary between two phases: a disordered ($|\langle x\rangle|=0$) and an ordered one ($|\langle x\rangle|\neq 0$). The ordered phase corresponds to the appearance of spatially ordered patterns, because its average amplitude becomes nonzero. This happens due to the special form of coupling which includes
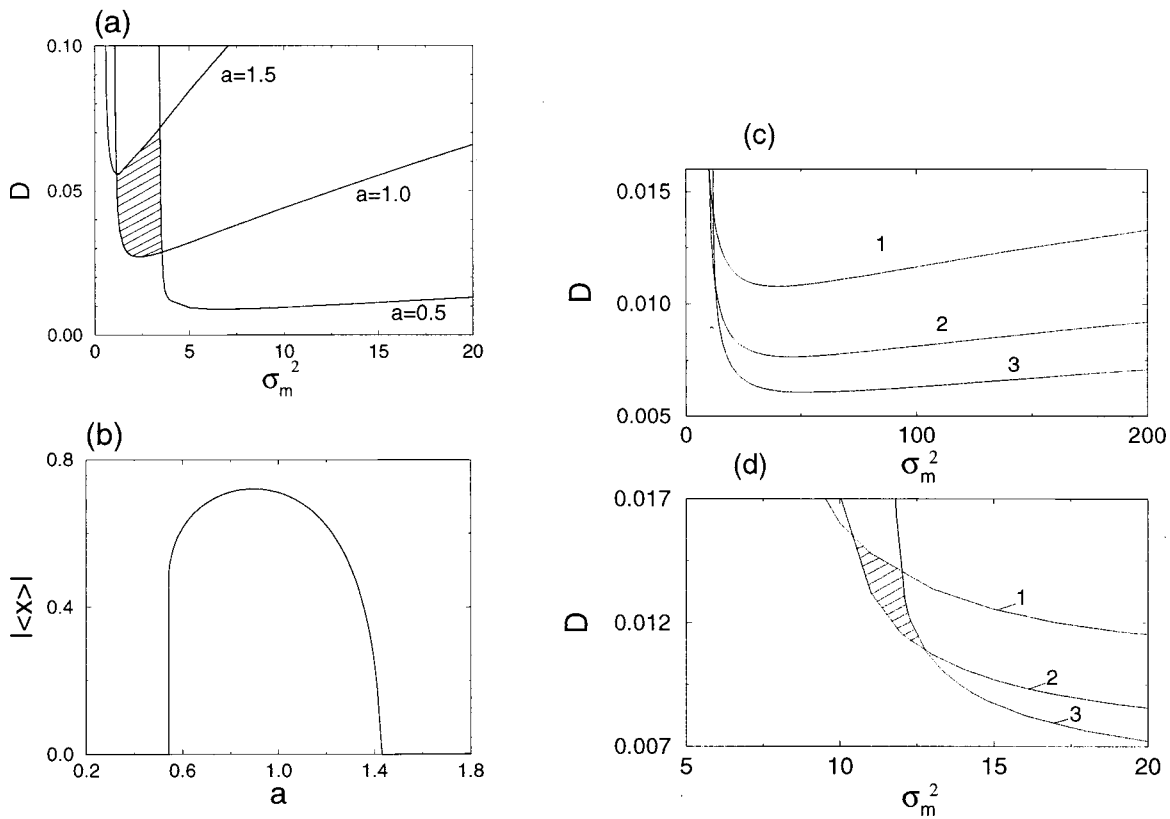
FIG. 3. Additive noise induced phase transition in a nonlinear lattice Eq. (7): predictions of the mean field theory. (a) The boundaries of the transition on the plane (σ_m^2, D) for different values of a Eqs. (8). It is clearly seen that by variation of a a point from the dashed region is a point of the transition induced by additive noise. (b) Dependence of order parameter $|\langle x \rangle|$ if the additive noise intensity is varied. (c) The transition lines for the case when additive and multiplicative noise are independent: $\sigma_a^2 = 1$ (label 1), 0.5 (label 2), and 0.3 (label 3). (d) Large scaled region from the plot in (c).

wave length of these patterns q_0. It is known that in the considered system multiplicative noise induces a phase transition.[10] We focus our attention to the influence of additive noise. The boundary of the phase transition on the plane (σ_m^2, D) is shown in Fig. 3(a), which demonstrates that variation of the intensity of correlated additive noise [the parameter a in Eq. (8)] causes a shift of the transition boundary. The most interesting situation occurs in the dashed region. Here, the increase of the additive noise intensity causes the re-entrant (disorder–order–disorder) phase transition. The corresponding dependence of the order parameter on the parameter a is shown in Fig. 3(b).

For the case of uncorrelated additive noise ($a = 0$), the observed behavior is qualitatively the same [Figs. 3(c) and 3(d)]. Here the transition lines are plotted on the plane (σ_m^2, D) and the intensity σ_a^2 of uncorrelated additive noise

is varied. It is evident that again dashed region corresponds to the phase transition. If we take parameters from this dashed region (in both cases of correlation), and change the intensity of additive noise (varying the parameter a or σ_a^2), we observe a formation of patterns and further their destruction (see results of numerical simulations in Fig. 4).

To understand the mechanism behind this transition, it is necessary to note that there is no bistability either in the "usual" potential or in the so-called "stochastic" potential.[4] Nevertheless, using some approximations it can be shown[17,21] that the short-time evolution of the mean field can be described by the "effective" potential, which becomes bistable after a transition. If D, and σ_a^2 vanish, the time evolution of the first moment of a single element is simply given by the drift part in the corresponding Fokker–Planck equation (Stratonovich case)
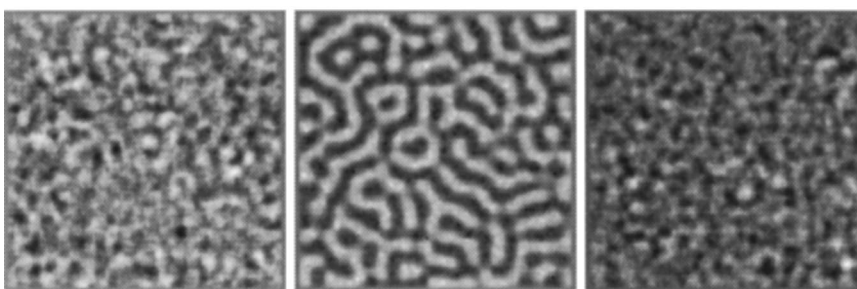

FIG. 4. A formation of spatial patterns induced by additive noise. From left to right the intensity of additive noise is increased ($a = 0$): $\sigma_a^2 = 0.001$, 0.7, and 10 (from left to right). The field in the nonlinear lattice of 128×128 elements is coded from white (minimum) to black (maximum) colors.
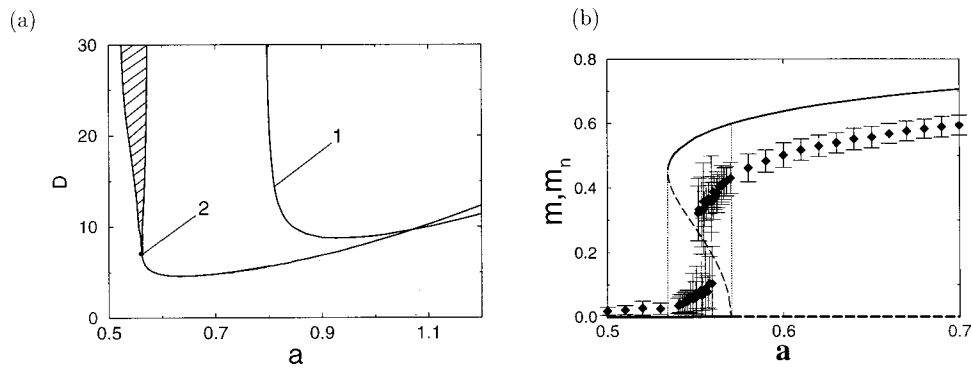
FIG. 5. The nonlinear lattice Eqs. (18): (a) Transition lines on the plane (a,D) for $\sigma_a = 0$ and two different intensities of the multiplicative noise (curve 1: $\sigma_m^2 = 1.6$; curve 2: $\sigma_m^2 = 3.0$). The dashed region (starting with the dot) corresponds to the coexistence of disordered and ordered phase. (b) The corresponding dependence of the order parameters m, m_n on a for $D = 20$, $\sigma_m^2 = 3.0$, and $\sigma_a^2 = 0.0$ are plotted by solid lines (MFT predictions) and by diamonds (numerical simulations). The dotted line delimits the coexistence region exhibited by MFT (a region of the hysteresis effect). The unstable state is plotted by the dashed line.

$$\langle \dot{x} \rangle = \langle f(x) \rangle + \frac{\sigma_m^2}{2} \langle g(x) g'(x) \rangle. \tag{15}$$

As it was argued in Ref. 17, the mechanism of the noise-induced transition in coupled systems can be explained by means of a short-time evolution approximation.[30] It means that we start with an initial Dirac δ function, follow it only for a short time, such that fluctuations are small and the probability density is well approximated by a Gaussian. A suppression of fluctuations, performed by coupling, makes this approximation appropriate in our case.[31] The equation for the maximum of the probability, which is also the average value in this approximation $\bar{x} = \langle x \rangle$, takes the following form:

$$\dot{\bar{x}} = f(\bar{x}) + \frac{\sigma_m^2}{2} g(\bar{x}) g'(\bar{x}), \tag{16}$$

which is valid if $f(\langle x \rangle) \gg \langle \delta x^2 \rangle f''(\langle x \rangle)$. For this dynamic, an "effective" potential $U_{\text{eff}}(x)$ can be derived, which has the form

$$U_{\text{eff}}(x) = U_0(x) + U_{\text{noise}} = -\int f(x)dx - \frac{\sigma_m^2 g^2(x)}{4}, \tag{17}$$

where $U_0(x)$ is a monostable potential and U_{noise} represents the influence of the multiplicative noise. In the ordered region, this "effective" potential has additional $x = 0$ minima that explain the nonzero solutions for the amplitude of spatial patterns.[21]

B. First-order phase transitions

In Ref. 33 a first-order phase transition has been reported, which is induced by multiplicative noise. Now we show that *first-order* nonequilibrium transitions in spatially extended systems can also be induced by additive noise. It is important, that in contrast to second-order transitions, in a first-order transition very tiny fluctuation of the control parameter can lead to a drastic change of the order parameter. The study is performed on a nonlinear lattice of coupled stochastic overdamped oscillators introduced in Ref. 16 and

further studied in Refs. 20, 21, 17, and 32. The time evolution of the system is described by the following set of Langevin equations:

$$\dot{x}_i = f(x_i) + g(x_i)\xi_i(t) + \frac{D}{2d} \sum_j (x_j - x_i) + \zeta_i(t), \tag{18}$$

where $x_i(t)$ represents the state of the ith oscillator, and the sum runs over all nearest neighbors of cell i. The strength of the coupling is measured by D, and d is the dimension of the lattice, which has $N = L^d$ elements. The noise terms $\xi_i(t)$ and $\zeta_i(t)$ are the same as defined in Eqs. (9): mutually uncorrelated, Gaussian distributed, with zero mean and white in both space and time. The functions $f(x)$ and $g(x)$ are defined in Eqs. (8).

We study the behavior of this system by means of a standard MFT procedure. Solving the corresponding Eq. (14) with respect to the variable $m = \langle x \rangle$, and w_{st} defined by Eq. (13) with $D_{\text{eff}} = D$, one can set the transition boundaries. In this way obtained order–disorder transition lines are shown in Fig. 5(a). Here we consider only the case when $\sigma_a^2 = 0$ and the parameter a is varied. Curve 1 separates regions of disorder (below the curve) and order (above the curve) for small multiplicative noise intensity. In this case, the ordered region is characterized by three self-consistent solutions of Eq. (14), one of them unstable ($m = 0$) and the other two stable and symmetrical. These new solutions appear continuously from $m = 0$ in the course of the transition. Hence, if we fix the coupling strength, e.g., $D = 20$, and increase the intensity of additive noise (the parameter a) a *second-order* phase transition from disorder to order occurs, followed by a re-entrant transition back to disorder, also of second order.

The *first-order* transition can be observed when the multiplicative noise intensity increases. In that case [curve 2 in Fig. 5(a)], a region appears where Eq. (14) has five roots, three of which ($m = 0$ and two symmetrical points) are stable. This region is marked dashed in the figure. Thus, for large enough values of D, a region of coexistence appears in the transition between order and disorder. This region is limited by discontinuous transition lines between $m = 0$ and a nonzero, finite value of m. Hence, additive noise is seen to

induce a *first-order* phase transition in this system for large enough values of the coupling strength and multiplicative noise intensity. The re-entrant transition is again of second order. When the first-order phase transition appears, hysteresis can be expected to occur in the coexistence region (if a certain algorithm is applied[34]). The dependence of the order parameter m on the control parameter a as predicted by MFT is shown in Fig. 5(b) with a solid line. The region of possible hysteresis is bounded by dotted lines.

In order to contrast the analytical results, we have performed simulations of the complete model (18) using the numerical methods described in Refs. 5 and 17. The order parameter m_n is computed as

$$m_n = \left\langle \left| \frac{1}{L^2} \sum_{i=1}^{N} x_i \right| \right\rangle,$$

where $\langle \rangle$ denotes time average. Results for a two-dimensional lattice with lateral size $L = 32$ are shown with diamonds in Fig. 5(b). Analyzing this figure one can observe that MFT overestimates the size of the coexistence region. This effect, analogous to what was observed for multiplicative-noise induced transitions,[16] can be explained in terms of an "effective potential" derived for the system at short times (see discussion below). For instance, as a increases the system leaves the disordered phase not when this state becomes unstable but earlier, when the potential minima corresponding to the ordered states become much lower than the minimum corresponding to the state $m = 0$. It should also be mentioned that the numerical simulations did not show hysteresis, because in the coexistence region the system occupied any of the three possible states, independently of the initial conditions. It can be explained by the small size of the simulated system, which permits jumps between steady states when the system is sufficiently perturbed (e.g., by slightly changing the parameter a).

We have thus seen so far that numerical simulations qualitatively confirm the existence of a first-order phase transition induced by additive noise in this system, as predicted by MFT. We note that the transition occurs in the two limiting cases of correlation between multiplicative and additive noise. We also emphasize that variation of both the multiplicative noise intensity and the coupling strength can change the order of this transition.

Let us now discuss a possible mechanism behind this effect. As pointed out above, the collective behavior of this system can be described by the "effective" potential [see Eq. (17)]. We can trace the behavior of this potential in the presence of multiplicative noise, for the case $\sigma_a^2 = 0$ and $a \neq 0$. Its evolution for increasing a is shown in Fig. 6. This approach can be clearly seen to successfully explain the mechanism of the first-order transition: first, only the zero state is stable (curve 1), then there is a region where three stable states coexist (curve 2), and finally, the disordered state becomes unstable (curve 3). This approach also explains why a variation of the multiplicative noise intensity influences the order of the transition: for another (lower) σ_m^2 there is no region where ordered and disordered phases simultaneously exist. We emphasize that the "effective" potential is derived only
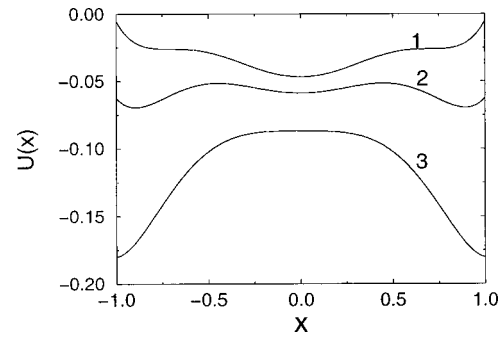

FIG. 6. An "effective" potential for the short-time evolution of m in the lattice Eqs. (18), for $a^2 =: 0.25$ (curve 1), 0.28 (curve 2), and 0.34 (curve 3). Other parameters are $\sigma_m^2 = 3.0$ and $\sigma_a^2 = 0.0$. A coexistence of ordered and disordered phases is observed for the curve 2.

for short-time evolution, and should not be confused with the "stochastic" potential,[4] which for this system remains always monostable. For the other case of correlation between multiplicative and additive noise, in the region of additive noise induced transition, the "effective" potential always has three minima (two symmetric minima are lower than the central one). Sufficiently large (above a threshold of the transition) additive noise causes an escape from zero state and leads to the transition. The value of a critical additive noise intensity for this transition can be estimated by the "effective" potential approach, only by MFT. Here we have considered only a case of strong correlation between multiplicative and additive noise. As described in Ref. 35, if additive noise is independent, it can also induce a first-order phase transition. The level of correlation between additive and multiplicative noise can be considered as an additional parameter in this system, what we leave as an open question here.

In conclusion, we have reported that additive noise can induce a first-order phase transition in a spatially extended system. This transition leads to breaking of symmetry and the creation of a mean field. It should also be mentioned that for another form of coupling, *a la* Swift–Hohenberg as in Sec. IV A, spatial patterns can appear as a result of a first-order phase transition.

V. ADDITIVE NOISE IN DOUBLY STOCHASTIC RESONANCE

Doubly stochastic resonance (DSR)[12] is a synthesis of two basic phenomena: noise-induced phase transition and stochastic resonance (SR).

In the conventional situation SR manifests itself as follows: additive noise optimizes the response of a bistable system to an external periodic force. In addition to this situation, SR has also been found and investigated in a large variety of different class systems: monostable systems,[36] systems with excitable dynamics,[37] noisy non-dynamical systems,[38] systems with sensitive frequency SR dependence,[39] systems without an external force,[8,40] and systems without any explicit threshold.[41] In all these works SR has been observed in the structure, given by the system, and not in the noise-induced structure. In contrast to it, here we address the prob-
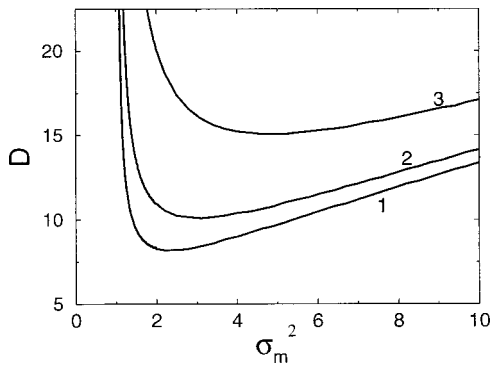
FIG. 7. Transition lines between ordered (inside the curves) and disordered (outside) phase in the lattice Eqs. (19) on the plane $(\sigma_m^2; D)$ for different intensities of the additive noise $\sigma_a^2 = 0$ (1), 1 (2), and 5 (3). The black dot corresponds to $D = 20$, $\sigma_m^2 = 3$.

lem whether SR can be observed in the bistable structure, which in its own turn is induced by multiplicative noise via phase transition.

We study DSR in the nonlinear lattice of coupled over-damped oscillators Eq. (18), but now under the action of an additional periodic force. Hence, the following set of Langevin equations describes the considered system:

$$\dot{x}_i = f(x_i) + g(x_i)\xi_i(t) + \frac{D}{2d}\sum_j (x_j - x_i) + \zeta_i(t)$$
$$+ A\cos(\omega t + \varphi),\qquad(19)$$

where all notations and functions $f(x)$ and $g(x)$ are taken as above. The last term in (19) stands for an external periodic force with amplitude A, frequency ω, and initial phase φ.

Obtained by a standard MFT procedure (see Sec. IV B) transition boundaries between different phases are shown in Fig. 7. In addition to Ref. 16, we show that the influence of additive noise resulted in the shift of transition lines. For $\sigma_a^2 = 0$ an increase of the multiplicative noise causes a disorder–order phase transition, which is followed by the re-entrant transition to disorder.[16] In the ordered phase the system occupies one of two symmetric possible states with the mean fields $m_1 = -m_2 \neq 0$, depending on initial conditions (for a visualization of this transition see Fig. 8).

Now let us consider the problem, how the system (19) responds to periodic forcing. We have taken a set of parameters $(\sigma_m^2; D)$ within the region of two coexisting ordered states with a nonzero mean field. In particular, we choose values given by the dot in Fig. 7. For numerical simulations we take a two-dimensional lattice of $L^2 = 18 \times 18$ oscillators, which is simulated numerically[42] with a time step $\Delta t = 2.5 \times 10^{-4}$ under the action of the harmonic external force. The amplitude of the force A has to be set sufficiently small to avoid hops in the absence of additive noise during the simulation time of a single run which is much larger than the period of the harmonic force.[43] Jumps between $m_1 \leftrightarrow m_2$ occur only if additive noise is additionally switched on. Runs are averaged over different initial phases.

Time series of the mean field along the corresponding periodic input signal are plotted in Fig. 9 for three different values of σ_a^2. The current mean field is calculated as $m(t) = (1/L^2)\Sigma_{i=1}^{N} x_i(t)$. For a small intensity of the additive noise, hops between the two symmetric states m_1 and m_2 are rather seldom and not synchronized to the external force. If we increase the intensity σ_a^2, we achieve a situation when hops occur with the same periodicity as the external force

increase
of
noise
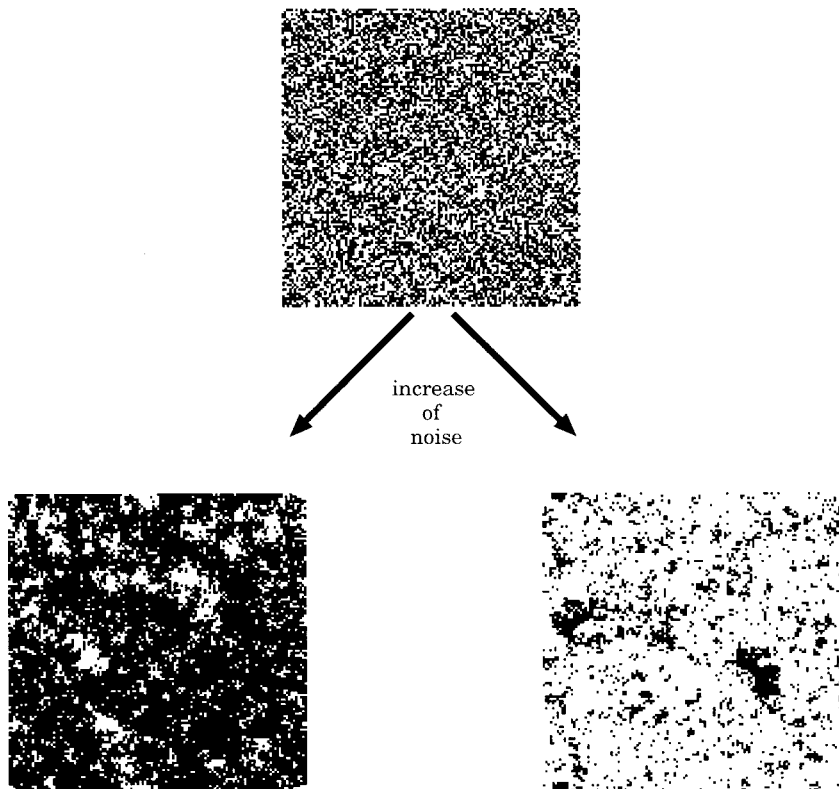
FIG. 8. A symbolic visualization of a phase transition in the model Eqs. (19), which leads to the formation of a mean field. In the disordered phase the mean field is zero due to the random deviation of different elements around zero (up). In the ordered phase, induced by noise, the symmetry is broken and the mean field is either positive (right) or negative (left). The elements in the lattice 128×128 are coded in accordance to its sign: if positive or zero, white; if negative, black.
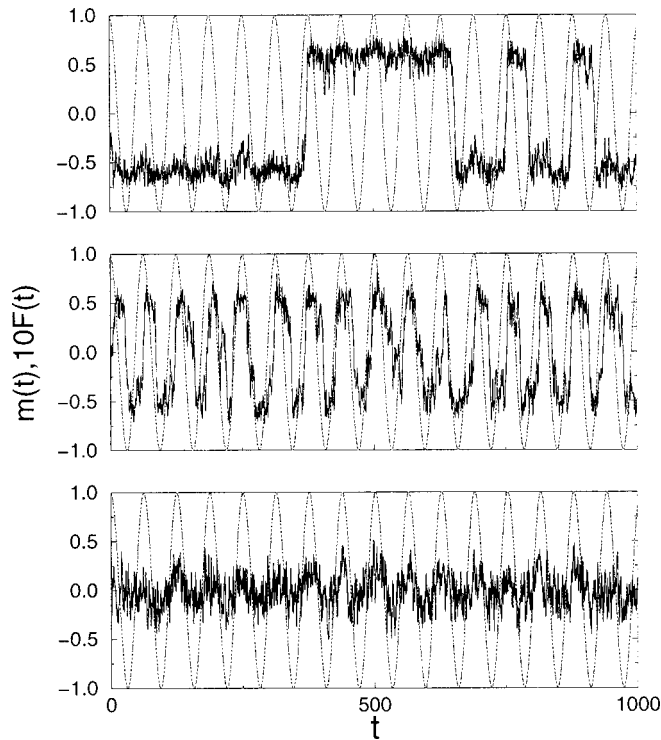
FIG. 9. Doubly stochastic resonance in the lattice (19): a coherent response to periodic driving induced by additive noise. The time evolution of the current mean field (output) and the periodic external force $F(t)$ (input) for different intensities of additive noise (from top to bottom) $\sigma_a^2 = 0.01$, 1.05, and 5.0. For the optimal value of the additive noise intensity (middle row), hops occur mostly with the period of the external force. The remaining parameters are $A = 0.1$, $\omega = 0.1$, $D = 20$, and $\sigma_m^2 = 3$.

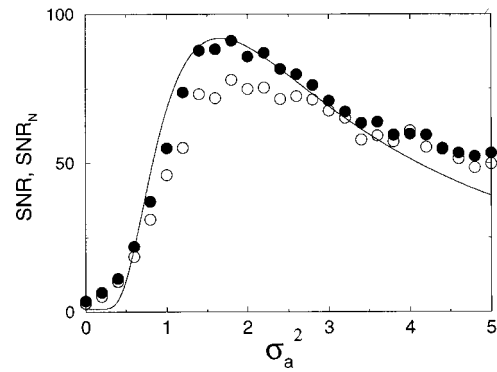FIG. 10. The dependence of SNR vs the additive noise intensity in the lattice (19). The full output and its two-states approximation are plotted by filled and opaque points, respectively. The solid line shows the analytical estimation SNR_N (22), performed on the base of derivation of the "effective" potential and linear response theory. The parameters are the same as for Fig. 9 and the processing gain $G = 0.7$.

and, hence, the mean field follows with high probability the periodic input force. An increase of additive noise provides an optimization of the output of the system which is stochastic resonance. If σ_a^2 is increased further, the order is again destroyed, and hops occur much more frequently than the period of the external force. Note also that for large σ_a^2 the value of the mean field which corresponds to the stable state is becoming smaller. It is caused by the fact that additive noise also influences transition lines.[20] An increase of σ_a^2 results in the reduction of the ordered region (Fig. 7, curves 2 and 3) and decreasing the value $m_1 = -m_2$.

Figure 9 illustrates that additive noise is able to optimize the signal processing in the system (19). In order to characterize this SR effect quantitatively, we have calculated signal-to-noise ratio (SNR) by extracting the relevant phase-averaged power spectral density $S(\omega)$ and taking the ratio between its signal part with respect to the noise background.[2] The dependence of SNR on the intensity of the additive noise is shown in the Fig. 10 for the mean field (filled points) and the mean field in a two-state approximation (opaque point). In this two-states approximation we have replaced $m(t)$ by its sign and put approximately $m(t) = +1$ or $m(t) = -1$, respectively. Both curves exhibit the well known bell shaped dependence on σ_a^2 typically for SR.

Next we estimate the SNR analytically, in order to compare it with numerical simulations. If A, D, and σ_a^2 are equal to zero, the dynamics of the system is described by the "effective" potential $U_{eff}(x)$ [see Eq. (17)]. In the ordered re-

gion, inside the transition lines (Fig. 1), the potential $U_{eff}(x)$ is of the double-well form, e.g., $U(x)_{eff} = -x^2 - 0.25x^4 + x^6/6$, for given $f(x)$, $g(x)$, and $\sigma_m^2 = 3$.

From the analytical form of the system's bistable potential, we can solve a conventional SR problem in this potential with an external periodic force of the amplitude A and the frequency ω. Using the well-known approach of a linear response theory,[2,44] we get the following expression for SNR:

$$SNR_1 = \frac{4\pi A^2}{\sigma_a^4} r_k, \qquad (20)$$

where r_k is the corresponding Kramers rate[45]

$$r_k = \frac{\sqrt{|U''_{eff}(x)|_{x=x_{min}} |U''_{eff}(x)|_{x=x_{max}}}}{2\pi} \exp\left(-\frac{2\Delta U_{eff}}{\sigma_a^2}\right) \qquad (21)$$

for surmounting the potential barrier ΔU_{eff}. Using Eqs. (17), (20), and (21) we get analytical estimates for a single element inside the lattice. Further on, rescaling this value by the number N of oscillators in the lattice[46] and taking into account the processing gain G and the bandwidth Δ in the power spectral density,[44] the SNR_N of the mean field of the network of N elements can be obtained

$$SNR_N = SNR_1 \frac{NG}{\Delta} + 1. \qquad (22)$$

This dependence is shown in Fig. 10 by the solid line and demonstrates despite the rough approximation a good agreement with the results of the numerical simulations. Nearly exact agreement is found in the location of the maximum as well as for the quantitative values of the SNR ("scalloping loss"[44] has been avoided in simulations by setting the frequency ω to be centered on one of the bins in the spectrum).

In conclusion, we have reported the existence of doubly stochastic resonance, which is resulted from the twofold influence of noise on a nonlinear system. DSR is a combined effect which consists of a noise-induced phase transition and conventional SR. It is important to add, that there are clear

distinctions between SR and DSR behavior, because, in contrast to SR, in DSR additive noise does not only help an input/output synchronization, but also changes the properties of the system in the absence of the external force (see Fig. 7). As a consequence, in DSR amplitude of hops is decreased (bistability disappears) for large noise intensities σ_a^2, that is not the case for standard SR (compare Fig. 9 and Fig. 4 from Ref. 2). It means also that a decrease of SNR with the increase of the additive noise intensity can be explained not only by disordered hops induced by large additive noise, but also by the fact that the system loses its bistability. Another distinction is that DSR can be controlled by multiplicative noise, and this control is not possible in a conventional SR. It happens because change of multiplicative noise results in the change of the ''effective'' potential [Eq. (17)], which governs the behavior of the system.

VI. SUMMARY AND OPEN QUESTIONS

We have reported here recent results concerning the influence of additive noise on noise-induced nonequilibrium phase transitions. We have shown that the role of additive noise can be crucial in various aspects: (i) In oscillatory systems, represented by a single oscillator, additive noise is able to induce such NIT, it strongly influences this transition and stabilizes oscillations occurred as a result of this transition. (ii) In spatially extended systems, which are lattices of coupled overdamped oscillators, additive noise can induce first- as well as second-order phase transitions, cause the formation of spatial patterns, and optimize the response of such a system to periodic driving. In the latter case, it is important that the bistability of the collective behavior is supported by multiplicative noise.

Despite these findings there are several open questions and promising directions of future research. Note that the topic of nonequilibrium phase transitions induced by additive noise is rather new. We see three main directions in the study of these transitions.

(1) Theory of noise-induced phase transitions. The phenomena described here are demonstrated by a large variety of models, and the question naturally arises whether these transitions belong to any of the existing universality classes. A discussion about it can be found in Ref. 17 for the transitions which leads to the breaking of symmetry and creation of the mean field. In general, however, this is still an open question as well as a question whether dependencies in the presented models are universal for other models demonstrating these transitions. Another interesting problem is a search of combined effects, as, e.g., a synthesis of white noise driven ratchets and noise-induced nonequilibrium phase transitions,[11] globally synchronized oscillations in subexcitable media[47] or DSR. One should investigate the translation of the transitions discussed into other phenomena, probably systems of coupled excitable elements. It is interesting also to find hidden transitions induced by additive noise in oscillatory systems in the absence of multiplicative noise.[48] Another group of open questions is connected to DSR. We expect that DSR or its modifications can be found not only in the system, described here, but probably in oscillatory systems (see also a case considered in Ref. 19), or systems with a bistable ''stochastic'' potential.[49]

(2) Experimental confirmation of noise-induced transitions predicted by theoretical studies. For the pendulum, modelling a real mechanical object (Sec. II), and the epidemiological model, describing a real experimental data (Sec. III), the connection to the experiment is clear. Concerning spatially extended systems with noise, described in Secs. IV and V, we suggest the following potential experimental implementations. As proposed in Ref. 17, it is worth to re-evaluate experiments in physical systems for which noise-induced shifts[15,16] or purely noise-induced transitions may be relevant. Some examples of noise-induced shifts can be mentioned here, such as processes in photosensitive chemical reactions under the influence of fluctuating light intensity,[50,51] in liquid crystals,[52–55] or in the Rayleigh–Bénard instability with a fluctuating temperature at the plates.[56]

We expect also that our theoretical findings will stimulate experimental works to verify DSR in real physical systems (for the first experimental observation of noise-induced bistability see Ref. 57). Appropriate situations can be found in analog[58] or electronic circuits,[59] as well as in systems, which demonstrate noise-induced shifts of the phase transition (see the discussion above). It can be crucial for such experiments, that, in contrast to conventional SR, in DSR the energy of noise is used in a more efficient way: not only for the optimization of the signal processing, but also for the support of the potential barrier to provide this optimization. This can be of a large importance in the communication.

(3) Modelling transitions and irregular oscillations observed in experimental data by stochastic models. As shown in Ref. 14, already known phenomena which have been explained in the frames of a deterministic theory, could also be successfully described by stochastic models. Note that deterministic and noise-induced processes are very difficult to be distinguished in many situations. Moreover, sometimes a noisy excitation looks more justified. It is worth to mention a recently outlined hypothesis that turbulence in nonclosed flows is a result of noise-induced phase transition (Ref. 60 and the experiment in Ref. 61). Also we expect that noise-induced processes may be very important for understanding of complex natural systems studied in neuroscience (e.g., Ref. 62) or such as microseismic oscillations,[63] or phase transitions observed in physiological systems, especially in bimanual movements.[64,65] Despite the fact that up to now these tempo-induced transitions in the production of polyrhythm are explained by deterministic mechanisms in the presence of noise, we expect that models with noise-induced oscillations will also be relevant in this case.

Another open question, closely associated with modelling is the identification of the excitation mechanism by the analysis of irregular time series. This problem is of high importance, because to model a system one should know the physical mechanism of an excitation. At the same time, time series are often the single source of the information about a nonlinear system: ''black box.'' At this point, it is essential to note that classical methods of analysis, such as a spectral analysis or a calculation of a correlation dimension are some-

times unable to distinguish between noise-induced irregular oscillations and chaotic oscillations of the deterministic nature.[13]

ACKNOWLEDGMENTS

[1] R. Benzi, A. Sutera, and A. Vulpiani, J. Phys. A **14**, L453 (1981); M. Dykman and P. McClintock, Nature (London) **391**, 344 (1998); V. S. Anishchenko, A. B. Neiman, F. Moss, and L. Schimansky-Geier, Sov. Phys. Usp. **42**, 7 (1999).

[2] L. Gammaitoni, P. Hänggi, P. Jung, and F. Marchesoni, Rev. Mod. Phys. **70**, 223 (1998).

[3] J. Douglass, L. Wilkens, and L. Pantazelou, Nature (London) **365**, 337 (1993); K. Wiesenfeld and F. Moss, ibid. **373**, 33 (1995); S. Bezrukov and I. Vodyanoy, ibid. **378**, 362 (1995); J. Collins, T. Imhoff, and P. Grigg, ibid. **383**, 770 (1996); P. Cordo et al., ibid. **383**, 769 (1996).

[4] W. Horsthemke and R. Lefever, Noise-Induced Transitions (Springer, Berlin, 1984).

[5] J. García-Ojalvo and J. M. Sancho, Noise in Spatially Extended Systems (Springer, New York, 1999).

[6] P. Landa, A. Zaikin, V. Ushakov, and J. Kurths, Phys. Rev. E **61**, 4809 (2000).

[7] F. Marchesoni, Phys. Lett. A **237**, 126 (1998).

[8] A. Pikovksy and J. Kurths, Phys. Rev. Lett. **78**, 775 (1997).

[9] C. Doering and J. Gadoua, Phys. Rev. Lett. **69**, 2318 (1992).

[10] J. M. R. Parrondo, C. Van den Broeck, J. Buceta, and F. J. de la Rubia, Physica A **224**, 153 (1996).

[11] P. Reimann, R. Kawai, C. Van den Broeck, and P. Hänggi, Europhys. Lett. **45**, 545 (1999).

[12] A. Zaikin, J. Kurths, and L. Schimansky-Geier, Phys. Rev. Lett. **85**, 227 (2000).

[13] P. Landa and A. Zaikin, Phys. Rev. E **54**, 3535 (1996).

[14] P. Landa and A. Zaikin, in Applied Nonlinear Dynamics and Stochastic Systems Near the Millenium, edited by J. Kadtke and A. Bulsara (AIP Conference Proceedings, Woodbury, NY, 1997), Vol. 411, pp. 321–329.

[15] J. García-Ojalvo, A. Hernández-Machado, and J. Sancho, Phys. Rev. Lett. **71**, 1542 (1993).

[16] C. Van den Broeck, J. M. R. Parrondo, and R. Toral, Phys. Rev. Lett. **73**, 3395 (1994).

[17] C. Van den Broeck, J. M. R. Parrondo, R. Toral, and R. Kawai, Phys. Rev. E **55**, 4084 (1997).

[18] P. Landa and A. Zaikin, in Computing Anticipatory Systems, edited by D. Dubois (AIP Conference Proceedings, Woodbury, NY, 1998), Vol. 465, pp. 419–434.

[19] P. Reimann, C. Van den Broeck, and R. Kawai, Phys. Rev. E **60**, 6402 (1999).

[20] P. Landa, A. Zaikin, and L. Schimansky-Geier, Chaos, Solitons Fractals **9**, 1367 (1998).

[21] A. Zaikin and L. Schimansky-Geier, Phys. Rev. E **58**, 4355 (1998).

[22] P. Landa and A. Rabinovitch, Phys. Rev. E **61**, 1829 (2000).

[23] R. Stratonovich, Topics in the Theory of Random Noise (Gordon and Breach, New York, 1963), Vol. 1.

[24] P. Landa, A. Zaikin, M. Rosenblum, and J. Kurths, Chaos, Solitons Fractals **9**, 1367 (1997).

[25] K. Dietz, Lect. Notes Biomath. **11**, 1 (1976).

[26] L. Olsen and W. Schaffer, Science **249**, 499 (1990).

[27] R. Engbert and F. Drepper, Chaos, Solitons Fractals **4**, 1147 (1994).

[28] R. Pool, Science **243**, 25 (1989).

[29] J. Sancho and J. García-Ojalvo, in Stochastic Processes in Physics, Chemistry, and Biology, edited by J. Freund and T. Pöschel (Springer, New York, 2000), pp. 235–246.

[30] Note that not always the effective potential description appropriately explains the phase transition in this system (Ref. 33).

[31] C. Van den Broeck, in Stochastic Dynamics, edited by L. Schimansky-Geier and T. Pöschel (Springer, Heidelberg, 1997), p. 7.

[32] S. Mangioni, R. Deza, H. S. Wio, and R. Toral, Phys. Rev. Lett. **79**, 2389 (1997).

[33] R. Müller, K. Lippert, A. Kühnel, and U. Behn, Phys. Rev. E **56**, 2658 (1997).

[34] The hysteresis may appear if we slowly change c^* during integration, i.e., the solution x_i for the previous value $c^* = c - \Delta c$ is the initial condition for the next point $c^* = c$ by a monotonical variation of c^*, where c^* is a control parameter (a or σ_a^2) and varied upwards and downwards.

[35] A. Zaikin, J. García-Ojalvo, and L. Schimansky-Geier, Phys. Rev. E **60**, R6275 (1999).

[36] N. Stocks, N. Stei, and P. McClintock, J. Phys. A **26**, 385 (1993).

[37] K. Wiesenfeld et al., Phys. Rev. Lett. **72**, 2125 (1994).

[38] Z. Gingl, L. Kiss, and F. Moss, Europhys. Lett. **29**, 191 (1995).

[39] H. Gang, H. Haken, and X. Fagen, Phys. Rev. Lett. **77**, 1925 (1996).

[40] H. Gang, T. Ditzinger, C. Ning, and H. Haken, Phys. Rev. Lett. **71**, 807 (1993).

[41] S. Bezrukov and I. Vodyanoy, in Unsolved Problems of Noise and Fluctuations, edited by D. Abbott and L. Kiss (AIP Conference Proceedings, NY, in press).

[42] P. Kloeden and E. Platen, Numerical Solution of Stochastic Differential Equations (Springer-Verlag, Berlin, 1992).

[43] For small L hops can be observed even without external force (Ref. 33). With $L = 18$ such hops are very rare.

[44] B. McNamara and K. Wiesenfeld, Phys. Rev. A **39**, 4854 (1989).

[45] H. Kramers, Physica **7**, 284 (1940); P. Hänggi, P. Talkner, and M. Borkovec, Rev. Mod. Phys. **62**, 251 (1990).

[46] L. Schimansky-Geier and U. Siewert, in Stochastic Dynamics, edited by L. Schimansky-Geier and T. Pöschel (Springer, Heidelberg, 1997), p. 245.

[47] H. Hempel, L. Schimansky-Geier, and J. García-Ojalvo, Phys. Rev. Lett. **82**, 3713 (1999).

[48] P. Landa and P. McClintock, Phys. Rep. **323**, 4 (2000).

[49] A. Fuliński, Phys. Rev. E **52**, 4523 (1995).

[50] J. Micheau, W. Horsthemke, and R. Lefever, J. Chem. Phys. **81**, 2450 (1984).

[51] P. de Kepper and W. Horsthemke, Synergetics: Far From Equilibrium (Springer, New York, 1979).

[52] S. Kai, T. Kai, and M. Takata, J. Phys. Soc. Jpn. **47**, 1379 (1979).

[53] M. Wu and C. Andereck, Phys. Rev. Lett. **65**, 591 (1990).

[54] S. Kai, H. Fukunaga, and H. Brand, J. Phys. Soc. Jpn. **56**, 3759 (1987).

[55] S. Kai, H. Fukunaga, and H. Brand, J. Stat. Phys. **54**, 1133 (1989).

[56] C. Meyer, G. Ahlers, and D. Cannell, Phys. Rev. A **44**, 2514 (1991).

[57] D. Grisowld and J. Tough, Phys. Rev. A **36**, 1360 (1987).

[58] F. Moss (private communication).

[59] A. Zaikin, K. Murali, and J. Kurths, Phys. Rev. E **63**, 020103(R) (2001).

[60] P. Landa, Europhys. Lett. **36**, 401 (1996).

[61] P. Landa, A. Zaikin, A. Ginevsky, and Y. V. Vlasov, Int. J. Bifurcation Chaos Appl. Sci. Eng. **9**, 397 (1999).

[62] M. Usher and M. Feingold, Biol. Cybern. **83**, L11 (2000).

[63] A. Correig, M. Urquizu, V. Ryabov, and A. Zaikin (unpublished).

[64] C. Scheffczyk et al., Int. J. Bifurcation Chaos Appl. Sci. Eng. **7**, 1441 (1997).

[65] R. Engbert et al., Phys. Rev. E **56**, 5823 (1997).

Influence of additive noise on transitions in nonlinear systems

P. S. Landa,[1] A. A. Zaikin,[2] V. G. Ushakov,[1] and J. Kurths[2]

[1]*Lomonosov Moscow State University, 119899 Moscow, Russia*
[2]*Institute of Physics, University of Potsdam, Am Neuen Palais 10, 14469 Potsdam, Germany*

The effect of additive noise on transitions in nonlinear systems far from equilibrium is studied. It is shown that additive noise in itself can induce a hidden phase transition, which is similar to the transition induced by multiplicative noise in a nonlinear oscillator [P. Landa and A. Zaikin, Phys. Rev. E **54**, 3535 (1996)]. Investigation of different nonlinear models that demonstrate phase transitions induced by multiplicative noise shows that the influence of additive noise upon such phase transitions can be crucial: additive noise can either blur such a transition or stabilize noise-induced oscillations.

PACS number(s): 05.40.−a, 05.70.Fh

I. INTRODUCTION

Noise-induced transitions occupy an important place among phenomena that demonstrate a strong influence of weak noise on the behavior of a system [2]; e.g., *stochastic resonance* [3–5], *noise-induced transport* [6], *coherence resonance* [7] or *noise-induced pattern formation* [8]. Intensive investigations of recent years have shown that noise-induced phase transitions can manifest themselves in the appearance of new extrema in the system probability distribution [9,10], in the creation of a mean field [11–13], and in the excitation of oscillations [1,14,15]. The last two types of transitions [16] have been termed nonequilibrium noise-induced phase transitions [17,1].

In these and other works multiplicative noise is perceived to be responsible for the transitions. However, as has been recently shown in [18–20], additive noise plays a crucial role in these transitions. Hence, studying the influence of additive noise is of great importance. In this paper we study several major aspects of the influence of additive noise by consideration of typical models in which a transition leads to noise-induced oscillations.

First, we study a transition induced by multiplicative noise in the presence of additive noise. We investigate such a transition theoretically and numerically in a pendulum with randomly vibrating suspension axis. In this model the additive noise blurs the transition induced by multiplicative noise. The pendulum is a key model for understanding another effect: a hidden phase transition induced purely by additive noise. We demonstrate it for an oscillator with quadratic nonlinearity and random force by showing that autoparametrical excitation occurs due to the additive noise and quadratic nonlinearity. At the same time the presence of additive noise makes this transition hidden. The mechanism of this transition is similar to subharmonic resonance [14]. Another mechanism, combination resonance, can also be associated with a phase transition induced by additive noise. This mechanism is illustrated by an electromechanical vibrator energized from a source of sufficiently high-frequency random current in place of a periodic source [21,14]. The combination resonance is caused by nonlinear interaction of random oscillations of the source current and the oscillations

induced in the high-frequency subsystem. Then we consider a standard epidemiological model [22–24] with a random action and show that this action can be split into additive and multiplicative parts. In contrast to the pendulum, here the transition can be induced by both additive and multiplicative noise. The mechanisms are likely to be the same as in the oscillator with quadratic nonlinearity and in the pendulum, respectively. The combined action of additive and multiplicative noise in this system extends the range of the parameters where noise-induced oscillations are stable, so we interpret this phenomenon as stabilization of noise-induced oscillations by additive noise.

The organization of the paper is as follows. In Sec. II we consider a pendulum with multiplicative and additive noise, which demonstrates a phase transition induced by multiplicative and influenced by additive noise. In Sec. III systems with additive noise alone are considered: an oscillator with quadratic nonlinearity and an electromechanical vibrator. Section IV is devoted to the study of transitions induced by both additive and multiplicative noise and of the stabilizing influence of additive noise in an epidemiological model. In Sec. V we summarize the results obtained.

II. NOISE-INDUCED PHASE TRANSITIONS IN THE PRESENCE OF ADDITIVE NOISE

First, we study the problem of excitation of a nonlinear oscillator under parametric and forcing random actions. We give an approximate analytical solution of this problem to reveal the influence of additive noise on a phase transition induced by multiplicative noise in a pendulum with a randomly vibrated suspension axis. In the absence of additive noise such a transition has been considered in [1,25]. It should be noted that the additive constituent of noise appears by itself if the vibration of the pendulum's suspension axis occurs in a certain direction making a nonzero angle with the vertical [18].

In the presence of additive noise the equation of motion for this system can be written as

$$\ddot{\varphi} + 2\beta(1 + \alpha\dot{\varphi}^2)\dot{\varphi} + \omega_0^2[1 + \xi_1(t)]\sin\varphi = \omega_0^2\xi_2(t), \quad (1)$$

where φ is the pendulum's angular deviation from the equilibrium position, ω_0 is the natural frequency of a small free pendulum's oscillations, β is the damping factor, α is the coefficient of nonlinear friction, and $\xi_1(t)$ and $\xi_2(t)$ are comparatively broadband random processes with zero mean values. We assume that the suspension axis vibration is moderately small in amplitude, i.e., the pendulum oscillations can be considered small enough for φ to be substituted in place of $\sin \varphi$ in Eq. (1).

An approximate analytical solution of this problem can be obtained from the assumptions that $\beta/\omega_0 \sim \epsilon$, $\xi_1(t) \sim \sqrt{\epsilon}$, and $\xi_2(t) \sim \sqrt{\epsilon}$, where ϵ is a certain small parameter which should be put equal to unity in the final results. Equation (1) can then be solved by the Krylov-Bogolyubov method; to do this we set $\varphi = A(t)\cos \psi(t) + \epsilon u_1 + \cdots$, where $\psi(t) = \omega_0 t + \phi(t)$,

$$\dot{A} = \epsilon f_1 + \cdots, \quad \dot{\phi} = \epsilon F_1 + \cdots, \tag{2}$$

and $u_1, \ldots, f_1, \ldots, F_1, \ldots$ are unknown functions. By using the Krylov-Bogolyuov technique for stochastic equations (see [26]), we find expressions for the unknown functions f_1 and F_1. Substituting these expressions into Eqs. (2) we obtain

$$\dot{A} = -\beta(1 + \tfrac{3}{4}\alpha\omega_0^2 A^2)A + \omega_0 \overline{g_1(A, \omega(t), \xi_1(t), \xi_2(t))}, \tag{3}$$

$$\dot{\phi} = \omega_0 \overline{g_2(A, \psi(t), \xi_1(t), \xi_2(t))}, \tag{4}$$

where

$$g_1(A, \phi, t) = \frac{A}{2}\xi_1(t)\sin 2\psi(t) - \xi_2(t)\sin \psi(t),$$

$$g_2(A, \phi, t) = \xi_1(t)\cos^2 \psi(t) - \frac{1}{A}\xi_2(t)\cos \psi(t).$$

The bar over an expression denotes averaging over time.

As follows from [26], the Fokker-Planck equation associated with Eqs. (3) and (4) is

$$\frac{\partial w(A, \phi, t)}{\partial t} = -\frac{\partial}{\partial A}\{[-\beta(1 + \tfrac{3}{4}\alpha\omega_0^2 A^2)A + \omega_0^2 R_1]$$

$$\times w(A, \phi, t)\} - \omega_0^2 R_2 \frac{\partial w(A, \phi, t)}{\partial \phi} + \frac{\omega_0^2}{2}$$

$$\times \left\{ \frac{\partial^2}{\partial A^2}\left[\left(\frac{K_{11}}{4}A^2 + K_{12}\right)w(A, \phi, t)\right] \right.$$

$$\left. + \left(K_{21} + \frac{K_{22}}{A^2}\right)\frac{\partial^2 w(A, \phi, t)}{\partial \phi^2} \right\}, \tag{5}$$
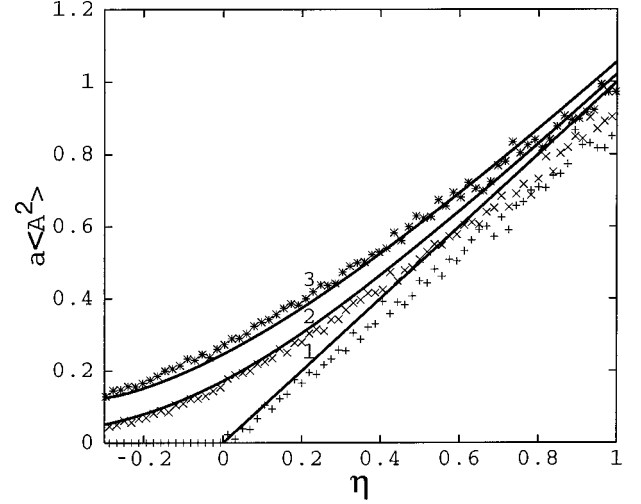
where

FIG. 1. The influence of additive noise on a noise-induced phase transition in a pendulum with randomly vibrated suspension axis. The dependence of the value $a\langle A^2\rangle$, which is proportional to the mean amplitude squared, on η without additive noise $q_0 = 0$ and with additive noise $q_0 = 0.005$ and 0.02 for curves 1–3 respectively. Theoretical (solid lines) and numerical results (symbols). In the presence of additive noise the dependence is smooth. The remaining parameters are $\beta = 0.1$, $\alpha = 100$, and $\omega_0 = 1$.

$$R_1 = \int_{-\infty}^0 \left(\left\langle \overline{\frac{\partial g_1(A, \phi, t)}{\partial A}g_1(A, \phi, t + \tau)} \right\rangle \right.$$

$$\left. + \left\langle \overline{\frac{\partial g_1(A, \phi, t)}{\partial \phi}g_2(A, \phi, t + \tau)} \right\rangle \right) d\tau, \tag{6}$$

$$R_2 = \int_{-\infty}^0 \left(\left\langle \overline{\frac{\partial g_2(A, \phi, t)}{\partial A}g_1(A, \phi, t + \tau)} \right\rangle \right.$$

$$\left. + \left\langle \overline{\frac{\partial g_2(A, \phi, t)}{\partial \phi}g_2(A, \phi, t + \tau)} \right\rangle \right) d\tau, \tag{7}$$

(the angular brackets denoting averaging over the statistical ensemble),

$$K_{11} = \tfrac{1}{2}\kappa_{\xi_1}(2\omega_0), \quad K_{12} = \tfrac{1}{2}\kappa_{\xi_2}(\omega_0), \tag{8}$$

$$K_{21} = \tfrac{1}{4}[\kappa_{\xi_1}(0) + \tfrac{1}{2}\kappa_{\xi_1}(2\omega_0)],$$

$$K_{22} = \tfrac{1}{4}[\kappa_{\xi_2}(0) + \tfrac{1}{2}\kappa_{\xi_2}(\omega_0)], \tag{9}$$

and

$$\kappa_\xi(\omega) = \int_{-\infty}^\infty \langle \xi(t)\xi(t + \tau)\rangle \cos \omega\tau \, d\tau$$

is the power spectrum density of the process $\xi(t)$ at the frequency ω.

Let us now calculate the integrals (6) and (7), taking into account the expressions for g_1 and g_2. As a result, we obtain

$$R_1 = \frac{3A}{8} \int_{-\infty}^{0} \langle \xi_1(t)\xi_1(t+\tau) \rangle \cos 2\omega_0\tau d\tau$$

$$+ \frac{1}{2A} \int_{-\infty}^{0} \langle \xi_2(t)\xi_2(t+\tau) \rangle \cos \omega_0\tau d\tau$$

$$= \frac{3K_{11}}{8}A + \frac{K_{12}}{2A}, \qquad (10)$$

$$R_2 = \frac{1}{4} \int_{-\infty}^{0} \langle \xi_1(t)\xi_1(t+\tau) \rangle \sin 2\omega_0\tau d\tau$$

$$- \frac{1}{A^2} \int_{-\infty}^{0} \langle \xi_2(t)\xi_2(t+\tau) \rangle \sin \omega_0\tau d\tau. \qquad (11)$$

The value of R_2 depends on the characteristics of the random processes $\xi_1(t)$ and $\xi_2(t)$: if they are white noises then $R_2 = 0$; but if, for example, $\xi_2(t)$ is white noise and $\xi_1(t)$ has a finite correlation time and its power spectrum density is

$$\kappa_{\xi_1}(\omega) = \frac{a_1^2 \kappa_{\xi_1}(2\omega_0)}{(\omega - 2\omega_0)^2 + a_1^2},$$

then

$$R_2 = -\frac{a_1\omega_0\kappa_{\xi_1}(2\omega_0)}{4(16\omega_0^2 + a_1^2)}.$$

It should be noted that in this case R_2 is negative, which results in a decrease of the mean oscillation frequency with increasing noise intensity. The Langevin equations which can be related to the Fokker-Planck equation (5) in view of Eqs. (10) and (11) are presented in Appendix A.

First we consider *the case when additive noise is absent*, i.e., $\kappa_{\xi_2} \equiv 0$. In this case the steady-state solution of Eq. (5), satisfying the condition of zero probability flux, is

$$w(A,\phi) = \frac{C}{2\pi A^2} \exp\left[\frac{3}{1+\eta}\left(\eta \ln A - \frac{aA^2}{2}\right)\right], \qquad (12)$$

where $a = 3\alpha\omega_0^2/4$ is the nonlinear parameter and $\eta = 3\omega_0^2 K_{11}/8\beta - 1$. The constant C is determined from the normalization condition

$$\int_0^{2\pi}\int_0^{\infty} w(A,\phi)A\,dA\,d\phi = 1.$$

Upon integrating Eq. (12) over ϕ, we find the expression for the probability density w of the oscillation amplitude:

$$w(A) = CA^{(2\eta-1)/(1+\eta)}\exp\left(-\frac{3aA^2}{2(1+\eta)}\right). \qquad (13)$$

From the normalization condition we get

$$C = 2 \times \begin{cases} \left(\frac{3a}{2(1+\eta)}\right)^{3\eta/2(1+\eta)} \dfrac{1}{\Gamma(3\eta/2(1+\eta))} & \text{for } \eta \geq 0 \\ 0 & \text{for } \eta \leq 0. \end{cases} \qquad (14)$$

Hence,

$$w(A) = 2 \times \begin{cases} \left(\dfrac{3a}{2(1+\eta)}\right)^{3\eta/2(1+\eta)} \dfrac{A^{(2\eta-1)/(1+\eta)}}{\Gamma(3\eta/2(1+\eta))}\exp\left(-\dfrac{3aA^2}{2(1+\eta)}\right) & \text{for } \eta \geq 0 \\ \delta(A) & \text{for } \eta \leq 0. \end{cases} \qquad (15)$$

The fact that for $\eta \leq 0$ the probability density of the amplitude turns out to be a δ function is associated with the absence of additive noise (see below).

Using Eq. (15), we can determine $\langle A \rangle$ and $\langle A^2 \rangle$:

$$\langle A \rangle = \begin{cases} \sqrt{\dfrac{3}{2a(1+\eta)}}\dfrac{\Gamma((4\eta+1)/2(1+\eta))}{\Gamma(3\eta/2(1+\eta)+1)}\eta & \text{for } \eta \geq 0 \\ 0 & \text{for } \eta \leq 0, \end{cases} \qquad (16)$$

$$\langle A^2 \rangle = \begin{cases} \dfrac{\eta}{a} & \text{for } \eta \geq 0 \\ 0 & \text{for } \eta \leq 0. \end{cases} \qquad (17)$$

Therefore, it is evident that for $\eta > 0$ the parametric excitation of pendulum oscillations occurs under the influence of multiplicative noise. This manifests itself in the fact that the mean values of the amplitude and of the amplitude squared become nonzero (Fig. 1, curve 1). This parametric excitation implies a transition of the system to a new state, which can be treated as a phase transition. The condition $\eta = 0$ is the threshold for the onset of this phase transition. It follows that, in the absence of additive noise, the critical value of the multiplicative noise intensity is

$$\kappa_\xi^{cr}(2\omega_0) \equiv \kappa_{cr} = \frac{16\beta}{3\omega_0^2}. \qquad (18)$$

Hence, the parameter η characterizes the extent to which the intensity of the multiplicative noise component exceeds its critical value.

It should be noted that, for $\eta > 0$, the steady state $A = 0$ loses its stability and the state $A \neq 0$ becomes stable. At the

same time, Eq. (15) implies that the probability density of A^2 is monotonically decreasing with increasing A^2 for any value of $\eta > 0$. Hence, in contrast to the transitions considered in [9], the appearance of a new stable state need not be accompanied by the appearance of a new maximum in the system probability distribution [see Fig. 2(a)].

Now let us consider *the case when the intensity of additive noise is not equal to zero*. The steady-state solution of Eq. (5), satisfying the condition of zero probability flux, is conveniently written as

$$w(A,\phi) = \frac{Ca}{2\pi(aA^2+q)} \exp\left[\int \frac{3(\eta - aA^2)aA^2 + q}{(1+\eta)(aA^2+q)A} dA \right],$$
(19)

where $q = 4aK_{12}/K_{11}$ characterizes the ratio between the intensities of additive and multiplicative noise.

Following the calculations presented in Appendix B, we get an expression for

$$a\langle A^2\rangle \approx (1+\eta)\left\{ \frac{4\mu}{3}\Gamma(2\mu)\Gamma(\tfrac{3}{2}-2\mu)(1+2\mu)\left(2(1-2\mu)+(5-4\mu)\frac{3q}{2(1+\eta)} \right) - \frac{3q}{2(1+\eta)} \right.$$
$$\times\left[\sqrt{\pi}\Gamma(-2\mu)(1-2\mu)\left(\frac{3q}{2(1+\eta)} \right)^{2\mu} + 2\Gamma(2\mu)\Gamma(\tfrac{3}{2}-2\mu)(1+2\mu) \right]\right\}\left[\frac{\sqrt{\pi}}{2}\Gamma(-2\mu)(1-2\mu)\left(\frac{3q}{2(1+\eta)} \right)^{2\mu} \right.$$
$$\left.\times\left(2(1+2\mu)+\frac{9q}{2(1+\eta)} \right) + \Gamma(2\mu)\Gamma(\tfrac{3}{2}-2\mu)(1+2\mu)\left(2(1-2\mu)+\frac{3(3-4\mu)q}{2(1+\eta)} \right) \right]^{-1},$$
(20)

where $\mu = 3(\eta + q)/4(1+\eta)$. Note that, similarly to the case without additive noise, after a transition no additional maxima appear in the system probability distribution and the shape of this distribution is not qualitatively changed [Fig. 2(b)].

Next we compare these analytical results with numerical simulations. The corresponding dependence of $a\langle A^2\rangle$ on η for different values of the parameter q_0 is illustrated in Fig. 1. We see that additive noise of small intensity results in a smoothing of the dependence of the mean oscillation amplitude squared on the multiplicative noise intensity: it becomes without the break inherent in a phase transition induced by only multiplicative noise. If we increase the additive noise intensity, the transition becomes less detectable (Fig. 1, curve 3).

In a numerical experiment it is more convenient to calculate the variance of the corresponding variable instead of the mean amplitude squared. It is evident that the dependencies of these values on the noise intensity should be similar. Indeed, in the case when the amplitude A is a slowly changing function, the variance is equal to $\langle A^2\rangle/2$. The dependencies of $a\langle A^2\rangle$ on η found by numerical simulation of Eq. (1) for both the presence of additive noise and its absence are shown also in Fig. 1. We find that near the threshold the simulations match the analytical results very well and that the dependencies for $q=0$ can be approximated by a straight line intersecting the abscissa at $\eta=0$. With an increase of η, the growth rate of the variance in numerical simulations is smaller than in the analytical results. This can be explained by the fact that the Krylov-Bogolyubov method is valid only near a threshold.

III. PHASE TRANSITIONS INDUCED BY ADDITIVE NOISE

A. Oscillator with quadratic nonlinearity

In this section we show that the mechanism of the noise-induced phase transition may exist also in an oscillatory system with additive noise only. For this we consider an oscillator with a quadratic nonlinearity and additive random force.

The oscillator under consideration can be described by

$$\ddot{x} + 2\beta\dot{x} + \omega_0^2(1+x+\gamma x^2)x = \omega_0^2 b\xi(t),$$
(21)

where the friction factor β is assumed to be sufficiently small in comparison with the natural frequency ω_0, $\xi(t)$ is an external force, which is a sufficiently broadband random process with zero mean value, the parameter b is responsible for the noise intensity, and the term γx^3 is introduced to avoid the solution going to infinity [caused by the presence of an unstable singular point of Eq. (21) for $\gamma < 0.25$].

At this point it is necessary to note that direct use of the Fokker-Planck equation [26] and its stationary solution does not show that the system probability distribution for variables $(x,\dot{x})$ is qualitatively changed with increase of the noise intensity. However, as we learned from the example in the previous section, the transition can take place despite the facts that there is no noise-induced maximum in the system probability distribution (see Fig. 2) and that the transition is not observable in the dependence of variance on noise intensity (see Fig. 1, curve 3). Obviously, the presence of moderately strong additive noise makes every transition hidden and undetectable. Nevertheless, the mechanism of the noise-induced transition is present in the model and, therefore, we call this phenomenon a *hidden phase transition induced by additive noise*.

To demonstrate the physical mechanism that is responsible for the hidden noise-induced phase transition, we will use the same procedure as for the calculation of subharmonic resonances [14]. First, we decompose x into

$$x(t) = y(t) + \chi(t),$$
(22)

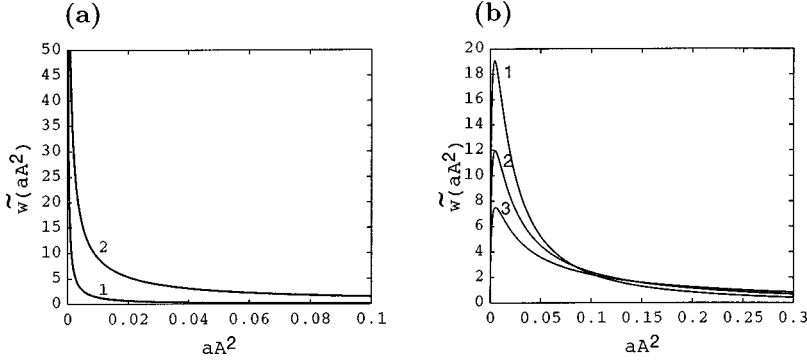where $\chi(t)$ is a random process satisfying the equation

(a)

(b)

FIG. 2. The system probability distribution for a pendulum. (a) The case without additive noise. The probability distribution $\tilde{w}(aA^2) = w(A)/2aA$ for $\eta = 0.01$ (curve 1) and $\eta = 0.2$ (curve 2). (b) The case with additive noise. The dependence of $\tilde{w}(aA^2) = w(A)/2aA$ for $q = 0.01/(1+\eta)$ and $\eta = -0.2$, 0, and 0.2 for curves 1–3, respectively.

$$\ddot{\chi} + 2\beta\dot{\chi} + \omega_0^2\chi = \omega_0^2 b\xi(t). \tag{23}$$

Now we will show that the system described by the variable y undergoes a noise-induced transition. Substituting Eq. (22) into Eq. (21) and taking into account Eq. (23), we get the equation for the variable y,

$$\ddot{y} + 2\beta\dot{y} + \omega_0^2\{1 + y + \xi_2(t) + \gamma y[y + 3\chi(t)]\}y = \omega_0^2\xi_1(t), \tag{24}$$

where $\xi_1(t) = -\chi^2(t)[1 + \gamma\chi(t)]$ is additive noise and $\xi_2(t) = \chi(t)[2 + 3\gamma\chi(t)]$ is multiplicative noise. Comparing Eq. (24) with Eq. (1), we find that these equations are similar. In the absence of additive noise $\xi_1(t)$, Eq. (24) is similar also to Eq. (1) in [1], except that the role of the random process $\xi(t)$ is played by the noise $\xi_2(t)$. In the previous section we have shown analytically and numerically that in the oscillator described by such an equation multiplicative noise causes a phase transition. Hence, the noise $\xi_2(t)$ is responsible for the phase transition, whereas, as will be seen from subsequent results, the additive noise makes the transition hidden.

An approximate analytical analysis of Eq. (24), in view of Eq. (23), is possible in the specific case when the random force in Eq. (23) is nonresonant. Owing to this, $\chi(t)$ is sufficiently small, and we can ignore in Eq. (24) both $\xi_1(t)$ and $3\gamma\chi^2 y$. As a result we obtain the following approximate equation for y:

$$\ddot{y} + 2\beta\dot{y} + \omega_0^2[1 + y + 2\chi + \gamma y(y + 3\chi)]y = 0. \tag{25}$$

Putting $y = A(t)\cos\psi(t) + \cdots$, where $\psi(t) = \omega_0 t + \phi(t)$, and using now the Krylov-Bogolyubov method for stochastic equations, we obtain the following truncated equations for $A(t)$ and $\phi(t)$:

$$\dot{A} = (\eta - aA^2)A + \omega_0\zeta_1(t), \quad \dot{\phi} = M_1 + \omega_0\zeta_2(t), \tag{26}$$

where

$$\eta = \frac{3\omega_0^2 K_1}{2\beta} - 1, \quad a = \frac{3\gamma}{4}\left(1 - \frac{15\gamma\omega_0^2}{8\beta}\right)(K_2 + K_3),$$

$$M_1 = \int_{-\infty}^0 \langle\chi(t)\chi(t+\tau)\rangle\left(\sin 2\omega_0\tau + \frac{9\gamma^2 A^3}{4}\right.$$

$$\left. \times (3\sin\omega_0\tau + \sin 3\omega_0\tau)\right)d\tau,$$

$\zeta_1(t)$ and $\zeta_2(t)$ are white noises with intensities

$$N_1 = \left(K_1 + \frac{9\gamma^2 A^2}{16}(K_2 + K_3)\right)A^2$$

and

$$N_2 = 2K_0 + K_1 + \frac{9\gamma^2 A^2}{16}(K_2 + K_3),$$

respectively, $K_1 = \kappa_\chi(2\omega_0)/2$, $K_2 = \kappa_\chi(\omega_0)/2$, $K_3 = \kappa_\chi(3\omega_0)/2$, $K_0 = \kappa_\chi(0)/2$, and $\kappa_\chi(\omega)$ is the spectral density of the random process $\chi(t)$ at the frequency ω.

Solving the Fokker-Planck equation associated with Eqs. (26), we get the probability density $w(A)$:

$$w(A) = CA^{(2\eta-1)/(1+\eta)}(1 + rA^2)^{-[(2+5\eta)r + 3a]/2r(1+\eta)}, \tag{27}$$

where

$$r = \frac{9\gamma^2}{16}\frac{K_2 + K_3}{K_1}.$$

From the normalization condition we find

$$C = 2 \times \begin{cases} \dfrac{a + r\eta}{a} r^{3\eta/2(1+\eta)}\dfrac{\Gamma(3(a+r\eta)/2r(1+\eta))}{\Gamma(3\eta/2(1+\eta))\Gamma(3a/2r(1+\eta))} & \text{for } \eta \geq 0 \\ 0 & \text{for } \eta \leq 0. \end{cases} \tag{28}$$
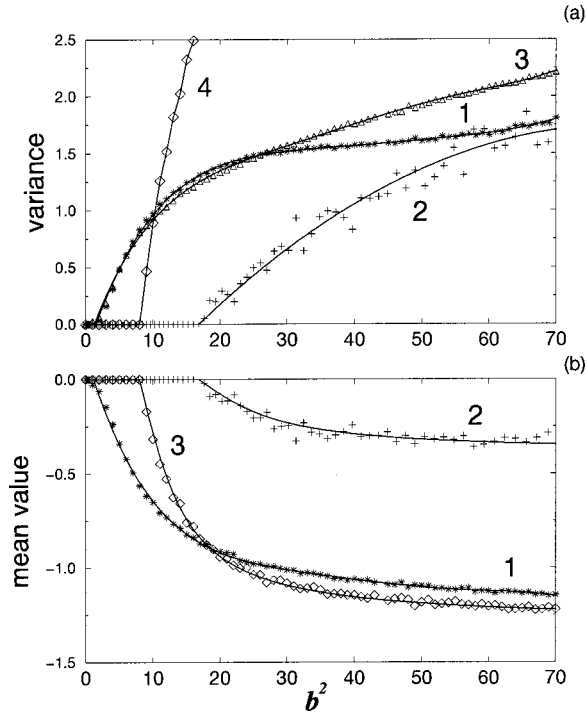
FIG. 3. Dependencies of the first moments of the simulated solutions on b^2 for $\gamma=0.251$, $\omega_0=1$, $\beta=0.1$. (a) variances σ_y^2 (curve 1), $\sigma_{y_r}^2$ (curve 2), σ_x^2 (curve 3), and $\sigma_{y_{rr}}^2$ (curve 4); (b) mean value $\langle y \rangle$ (curve 1), $\langle y_r \rangle$ (curve 2), and $\langle y_{rr} \rangle$ (curve 3) for the same value of γ.

It follows from here that the probability density of the amplitude turns out to be a δ function for $\eta \le 0$, as for the pendulum considered in [1].

Using Eqs. (27) and (28) we calculate $\langle A^2 \rangle$ ($\langle \cdot \rangle$ denotes the statistical average):

$$\langle A^2 \rangle = \begin{cases} \dfrac{3\eta}{3a+r(2+5\eta)} = \dfrac{4\eta}{3\gamma-4r} & \text{for } \eta \ge 0 \\ 0 & \text{for } \eta \le 0. \end{cases} \quad (29)$$

Note that the solution found is valid only for $3\gamma(K_2+K_3) < 4K_1$.

Thus, we have shown analytically that in the absence of the additive noise ξ_1 and the term $3\gamma\chi^2 y$, in a system described by Eq. (24), a noise-induced phase transition indeed occurs. As shown below, numerical simulations demonstrate that this transition remains well defined if the term $3\gamma\chi^2 y$ is included; though the additive noise ξ_1 makes it hidden. The main results of our numerical simulations are as follows.

(1) The results of numerical simulation of the complete equations (23) and (24) in the case of sufficiently broadband noise, which can be considered as white noise, are shown in Fig. 3. For comparison, the results of numerical simulation of Eq. (24) after dropping only the additive noise $\xi_1(t)$ are also given there. We call Eq. (24) with $\xi_1(t) \equiv 0$ the ''reduced equation'' and denote its solution by y_r. The solution of Eq. (25) is denoted by y_{rr}. We see that for the complete equations, which are equivalent to the initial equation, the phase transition is practically undetectable and very noisy (curve 1). For the reduced equation, the phase transition is clearly defined (curve 2). Close to the critical point the de-
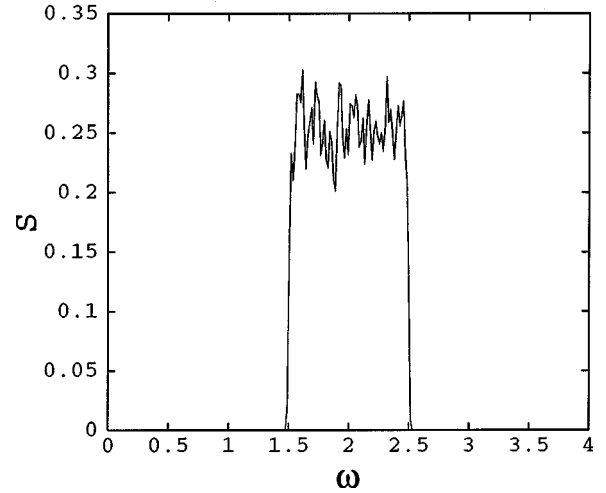

FIG. 4. The spectral density of the noise used in numerical simulations for the oscillator with quadratic nonlinearity to exclude the resonant frequency. The noise is passed through a bandpass filter.

pendence of $\sigma_{y_r}^2$, which can be treated as an order parameter, on the parameter b^2, which can be regarded as temperature, is well approximated by the straight line described by the equation $\sigma_{y_r}^2 = 0.056(b^2 - b_{cr}^2)$, where $b_{cr} \approx 4.1$. This means that the critical index is equal to 1 [see Fig. 3(a)].

(2) Figure 3(b) demonstrates that we can use as an order parameter not only the variance, but the mean value as well. Close to the critical point the dependence of $\langle y_r \rangle$ on b^2 can be approximated by the straight line $\langle y_r \rangle = -0.025(b^2 - b_{cr}^2)$.

(3) To reveal the influence of the term $3\gamma\chi^2 y$ that was dropped in the analytical consideration, we also numerically simulated Eq. (25). The results are given in Fig. 3(a) (curve 4) and Fig. 3(b) (curve 3). We see that the phase transition occurs for a smaller value of b^2 if in the reduced equation the term $3\gamma\chi^2 y$ is ignored, i.e., this term suppresses the phase transition [compare curves 2 and 4 in Fig. 3(a)]. This is also attested by the fact that the slopes of the dependencies of σ_r^2 and σ_{rr}^2 on b^2 are essentially different. Thus, the numerical simulations have shown that in the absence of additive noise ξ_1 only, we obtain a clearly defined phase transition. As mentioned above, the additive noise ξ_1 makes the transition hidden (see the dependence for σ_y^2). It is interesting that the dependence for σ_x^2 is close to that for σ_y^2; the difference appears only for large values of the parameter b. This means that close to the critical point the influence of the noise $\chi(t)$ is negligibly small.

(4) To reduce the noise spectral density at the frequency ω_0, we have passed the noise $\xi(t)$ through a bandpass filter with central frequency $2\omega_0$ and bandwidth ω_0. The spectral density of this noise is shown in Fig. 4. We see that it is indeed very narrowband in the vicinity of ω_0. Next, we simulate Eqs. (23) and (24) using this filtered noise as $\xi(t)$. For comparison we simultaneously simulate the reduced equation (24). Figure 5 illustrates that, even though the spectral density of the filtered noise $\xi(t)$ at ω_0 is very small, the influence of the noise $\xi_1(t)$ and of the term $3\gamma\chi^2 y$ is essential. The reason is that the component of the noise $\chi(t)$ at ω_0 is not small because it is resonant. The smooth increase of
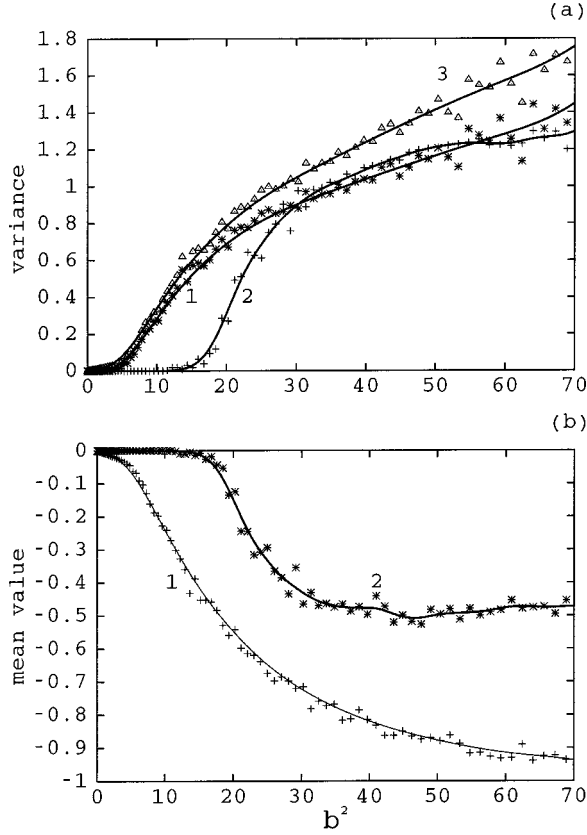
FIG. 5. Dependencies of the first moments of the simulated solutions on b^2 obtained using bandpass filtered noise. (a) Variances σ_y^2 (curve 1), $\sigma_{y_r}^2$ (curve 2), and σ_x^2 (curve 3); (b) mean values $\langle y \rangle$ (curve 1) and $\langle y_r \rangle$ (curve 2).

$\sigma_{y_r}^2$ with increasing b^2 from b_{cr}^2 onward is explained by the fact that the influence of the term $3\gamma\chi^2 y$ is less than for broadband noise.

Coming back to the initial equation (22), we decomposed the initial variable x into the sum of variables y and noise χ, which has practically no influence, since the dependencies for x and y are very similar (Figs. 3 and 5). Dropping the additive constituent of the noise from the equation for y, we get a clearly defined transition with an increase of noise intensity. From this we conclude that the initial equation describes a system in which a hidden nonequilibrium phase transition is induced by additive noise.

The transition under consideration is similar to the transition studied in the previous section, not only in the physical mechanism (autoparametrical and parametrical excitation, respectively), but also in the sense that both these transitions occur via on-off intermittency [27,28]. This is clearly visible from the shape of $y_r(t)$ [Fig. 6(b)]. Because of additive noise the intermittency for $x(t)$ is hidden [Fig. 6(a)]. As for a pendulum with randomly vibrated suspension axis and additive noise [28], the intermittency is defined more clearly for $b < b_{cr}$ [Fig. 6(a)].

At the current stage of investigation we have shown that an oscillator with quadratic nonlinearity may contain a mechanism for a phase transition induced only by additive noise. The strong influence of additive noise makes this transition undetectable in the initial equation, but we guess that it is possible to find a situation when the transition becomes
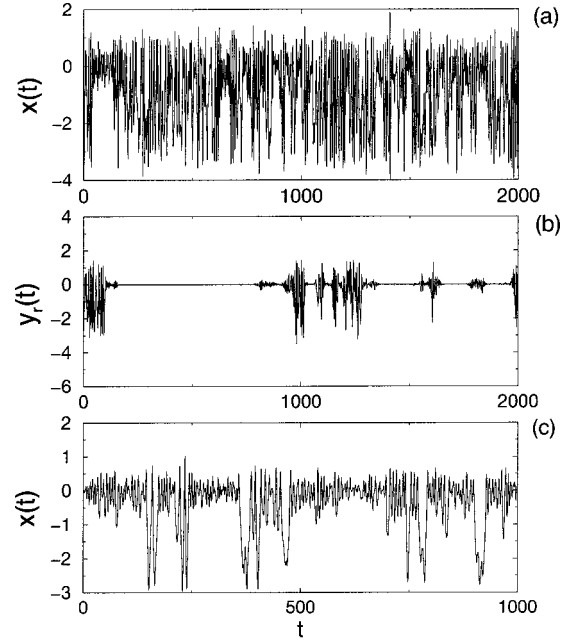

FIG. 6. A phase transition via on-off intermittency. The time series of $x(t)$ (a) and (c), and $y_r(t)$ (b) for $b^2 = 20$ (a) and (b) and $b^2 = 4$ (c). The remaining parameters are the same as in Fig. 4.

well defined just by dropping some terms from the initial system equation. We leave this as an open question in the present paper.

B. Electromechanical vibrator

An electromechanical vibrator energized from a source of periodic alternating current has been considered in [21,14]. It consists of a sprung plate attracted to an electromagnet with a power supply circuit forming an oscillatory circuit. We demonstrated that under certain conditions powerful low-frequency oscillations of the plate can be excited [21,14]. Below we show that similar oscillations can also be excited in the case when the power source is random. The scheme of the vibrator with a random power source is presented in Fig. 7.

The equations of this vibrator can be written as

$$\frac{d^2}{dt^2}\left(\frac{L(x)I}{L_0}\right) + 2\delta_1\frac{dI}{dt} + \Omega_0^2 I = \xi(t),$$

$$\frac{d^2x}{dt^2} + 2\delta_2\frac{dx}{dt} + \nu_0^2 x = F(x,I), \qquad (30)$$

where x is the plate displacement, I is the current in the oscillatory circuit, $L(x) = L_0(1 + a_1 x + a_2 x^2 + a_3 x^3 + \cdots)$ is the inductance of the coil with a core depending on the size of the clearance between the plate and the core, $\delta_1 = R/2L_0$ and $\delta_2 = \alpha/2m$ are the damping factors for the oscillatory circuit and the plate, respectively, $\Omega_0 = 1/\sqrt{L_0 C_0}$ and $\nu_0 = \sqrt{k/m}$ are the corresponding natural frequencies, $F(x,I) = (I^2/2)(dL/dx)$ is the pondermotive force acting on the plate, and $\xi(t)$ is a random process that is proportional the electromotive force of the power source. We set $\xi(t)$ to be described by the following equation:
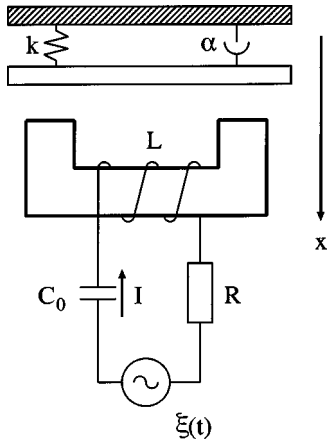
FIG. 7. A schematic image of an electromechanical vibrator with random power source. x is the plate displacement, α the friction, L the inductance, I the current, R the resistance, $\xi(t)$ the random process responsible for the electromotive force of the power source, and k the rigidity of the springs.

$$\ddot{\xi} + 0.5\omega\dot{\xi} + 1.125\omega^2\xi = k\chi(t), \qquad (31)$$

where $\chi(t)$ is white noise. It follows from Eq. (31), that the spectral density of $\xi(t)$ peaks at the frequency ω.

Numerical simulation of Eqs. (30) shows that from a certain value of the power source intensity, low-frequency oscillations of the plate appear. The dependence of the variance of these oscillations (σ_x^2) on k^2, which is proportional to the noise intensity, is illustrated in Fig. 8(a). The form of this dependence closely resembles the corresponding dependence for a pendulum with a randomly vibrated suspension axis and additive noise (see Fig. 1). We find from this plot that, for sufficiently large values of k^2, the dependence can be approximated by a straight line described by the equation $\sigma_x^2 = 0.3(k^2 - 0.025)$. Taking into account the similarity with the dependencies for noise-induced transitions in a pendulum, we can take the point where this straight line crosses the abscissa as the threshold of a noise-induced transition. Hence, the critical value of k is equal to 0.158. Unlike the variance σ_x^2, the variance of the current fluctuations ($\sigma_I^2 = \overline{I^2}$) increases with an approximately constant rate as k^2 increases. The corresponding dependence is presented in Fig. 8(b) (curve 1). It can be approximated by the straight line $\sigma_I^2 = 0.075k^2$. Owing to the presence of a quadratic nonlinearity, the mean value of the plate displacement is nonzero. The dependence of $\bar{x}$ on k^2 is also shown in Fig. 8(b) (curve 2).

Typically for noise-induced transitions that lead to the excitation of oscillations [28], for $k < k_{cr}$ one can detect on-off intermittencylike behavior in oscillations of the variable x [see, for example, Fig. 9(a)]. With increase of k this effect disappears. An example of the oscillations of x, I, and ξ for $k > k_{cr}$ is given in Fig. 9(b).

Power spectra of the random source and excited oscillations are shown in Fig. 10. It is clearly seen that we deal with high-frequency excitation. The mechanism responsible for the excitation seems to be similar to combination resonance.

As in the case of a pendulum with slight additive noise, noise-induced oscillations of the vibrator under consideration
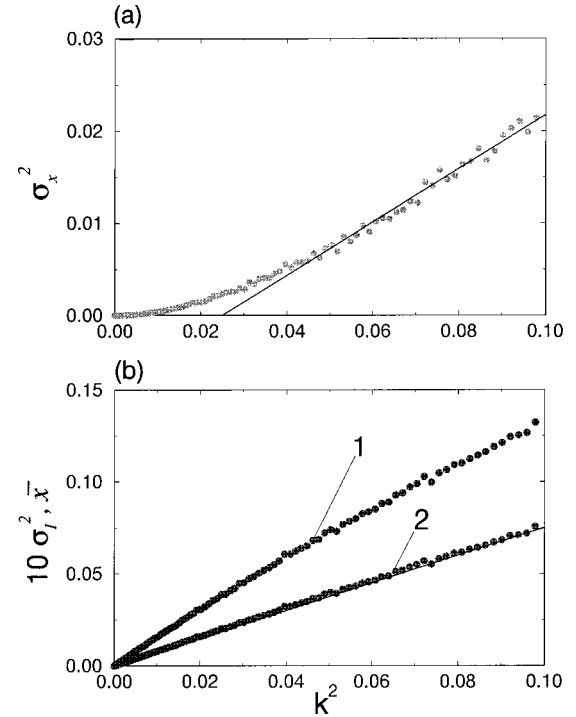

FIG. 8. The noise-induced transition in the electromechanical vibrator caused by a mechanism similar to combination resonance. The dependencies of σ_x^2 (a) and $10\sigma_I^2$ and $\bar{x}$ (b) on k^2 for $\omega = 1$, $\Omega_0 = 0.9$, $\nu_0 = 0.05$, $\delta_1 = 0.1$, $\delta_2 = 0.005$, $L_0/m = 0.1$, $a_1 = 1$, $a_2 = -0.5$, and $a_3 = 0.1$.

can be partially suppressed by additional harmonic action [27]. But, in contrast to the pendulum, the suppression occurs at low-frequency action rather than at high frequency. If the action frequency is high, the action has little or no effect on the variance of the plate oscillations. To describe the additional action, we add the term $a\cos\omega t$ to $\xi(t)$ on the right of the first equation of Eq. (30). Under low-frequency action a considerable constant displacement of the plate appears. Therefore, the study of the suppression is conveniently performed using the variance of the plate velocity instead of the plate displacement. The dependencies of this variance (σ_y^2) on the action amplitude a for a fixed value of the action frequency ω and on ω for a fixed value of a are shown in Fig. 11. We see that for a fixed value of the frequency ($\omega = 0.2$) the variance σ_y^2 initially decreases as the action amplitude increases, and then abruptly increases owing to excitation of oscillations at the frequency ω. For a fixed value of the action amplitude, the dependence of σ_y^2 on ω has a minimum whose location depends on the amplitude a [Fig. 11(b)].

IV. TRANSITIONS INDUCED BY BOTH MULTIPLICATIVE AND ADDITIVE NOISE: STABILIZATION OF NOISE-INDUCED OSCILLATIONS BY ADDITIVE NOISE

In this section we consider an example of a system under the combined action of additive and multiplicative noise. Both multiplicative and additive noise can induce a transition, and, what is especially interesting, a combination of their actions stabilizes noise-induced oscillations. To demon-
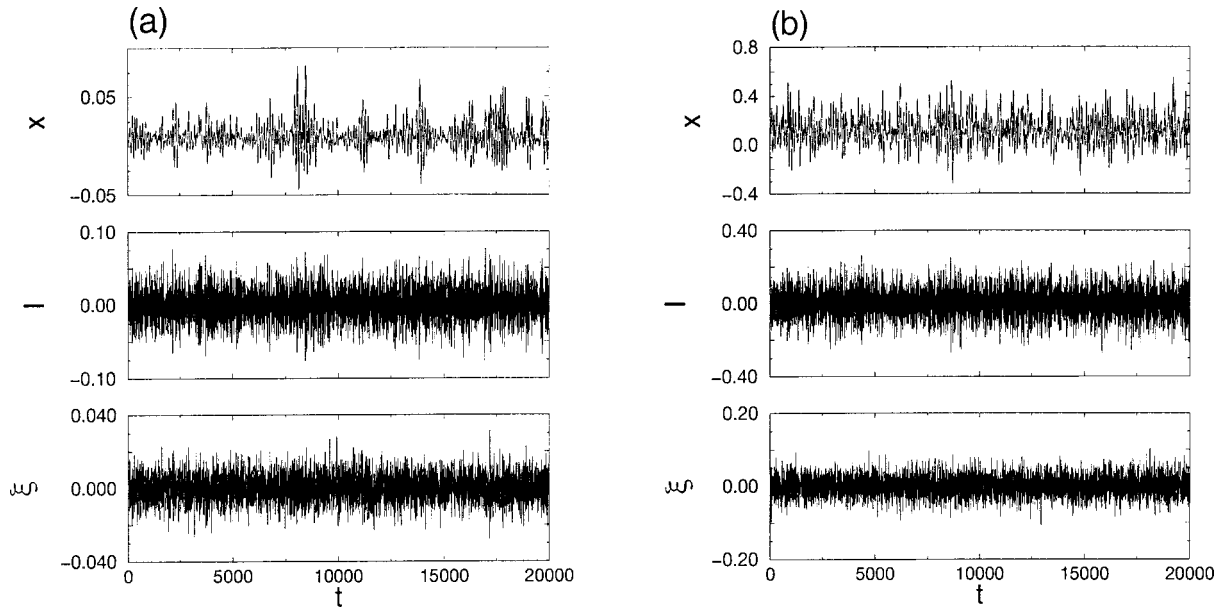
FIG. 9. On-off intermittency in the vibrator. Examples of oscillations of the plate (x), of the current in the oscillatory circuit (I), and of the power source (ξ) for $k=0.08$ (a) and $k=0.3$ (b).

strate these effects, we use a standard epidemiological model for the description of seasonal oscillations of childhood infections, such as chickenpox, measles, mumps, and rubella, under the influence of variations of the contact rate of children susceptible to infection with infective children. This model has been studied in detail both in the case of periodic variation of the contact rate [22–24,29] and in the case of random variation of the contact rate [15,29]. Here we dwell only on one important aspect of this problem, namely, on the stabilizing influence of a combination of additive and multiplicative noise on the excitation of induced oscillations.

The model equations are

$$\dot{S}=m(1-S)-bSI, \quad \dot{E}=bSI-(m+a)E,$$

$$\dot{I}=aE-(m+g)I, \tag{32}$$

$$\dot{R}=gI-mR, \tag{33}$$

where S is the relative number of children susceptible to infection, E is the relative number of children exposed but not yet infective, I is the number of infective children, R is the number of children recovered and immune, $1/m$ is the average expectancy time, $1/a$ is the average latency period, $1/g$ is the average infection period, and b is the contact rate (the average number of susceptibles in contact yearly with

infectives). Let us note that Eqs. (32) do not contain the variable R; hence these equations can be considered independently of Eq. (33).

It is easy to show that Eqs. (32) for $b=b_0=$const, and for any values of the remaining parameters, have one aperiodically unstable singular point with coordinates $S=1, E=I=0$, and one stable singular point with coordinates

$$S_0=\frac{(m+a)(m+g)}{ab_0}, \quad E_0=\frac{m}{m+a}-\frac{m(m+g)}{ab_0},$$

$$I_0=\frac{am}{(m+a)(m+g)}-\frac{m}{b_0}. \tag{34}$$

If the parameter b varies with time then the variables S, E, and I will oscillate, and these oscillations will be executed around the stable singular point with coordinates (34). Therefore, it is convenient to substitute into Eqs. (32) the new variables $x=S/S_0-1$, $y=E/E_0-1$, and $z=I/I_0-1$. Putting $b=b_0[1+b_1f(t)]$, where $f(t)$ is a function describing the shape of the contact rate variation, we rewrite Eqs. (32) in the variables x, y, z:
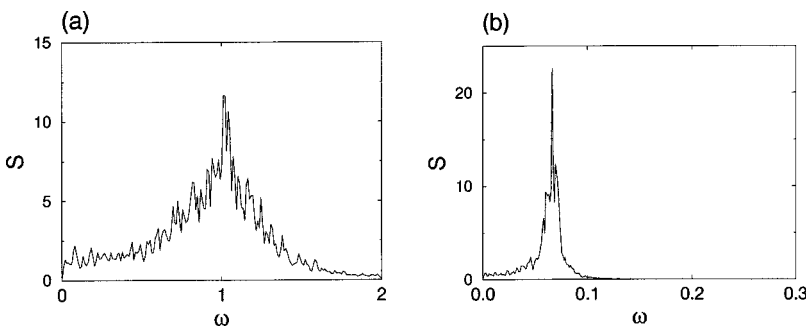
$$\dot{x}+mx=-b_0I_0[1+b_1f(t)](x+z+xz)-b_0b_1I_0f(t),$$

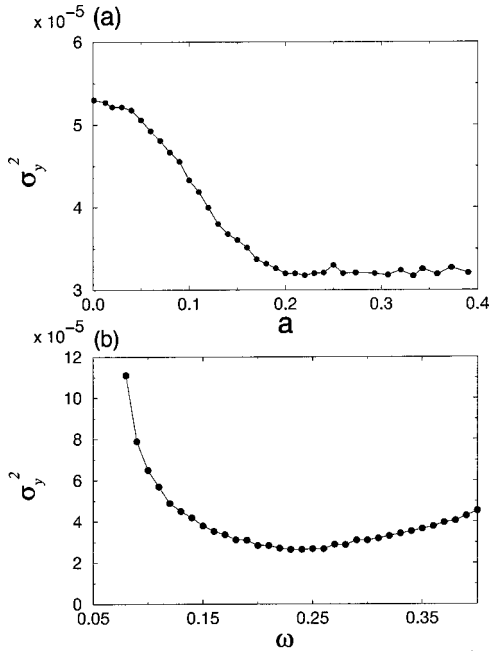FIG. 10. The power spectra of the random power source (a) and of the solution x (b).

FIG. 11. The dependencies of the variance σ_y^2 on the action amplitude a for $\omega = 0.2$ (a) and on the action frequency ω for $a = 0.3$ (b). For $\omega = 0.2$, $a > 0.4$, the variance abruptly increases owing to excitation of oscillations at the frequency ω and goes, in fact, to infinity.

$$\dot{y} + (m+a)y = (m+a)[1 + b_1 f(t)](x+z+xz)$$
$$+ (m+a)b_1 f(t), \qquad (35)$$

$$\dot{z} + (m+g)z = (m+g)y.$$

In Eqs. (35) the term $b_1 f(t)$ can be considered as an external action upon the system. This form of the equations clearly shows that this action is not only multiplicative, i.e., parametric, but additive as well.

Olsen and Schaffer [23] set the following values of the parameters: $m = 0.02$ year^{-1}, $a = 35.84$ year^{-1}, $g = 100$ year^{-1}, $b_0 = 1800$ year^{-1}, and $b_1 = 0.28$. These parameters correspond to estimates made for childhood diseases in first world countries. We follow them.

In [15] we supposed that the contact rate b varies randomly with the main period equal to one year, i.e., $f(t) = \chi(t)$, where $\chi(t)$ is a random process that is a solution of the equation

$$\ddot{\chi} + 2\pi\dot{\chi} + 6\pi^2\chi = k\xi(t), \qquad (36)$$

$\xi(t)$ is white noise, and k is a factor that we choose so that the variance of $\chi(t)$ is equal to 1/2. It is easily seen that the spectral density of $\chi(t)$ peaks at the frequency $\omega = 2\pi$.

Noise-induced oscillations appear as a result of a noise-induced phase transition. To show this let us consider Fig. 12, where the dependence of σ_x^2 on b_1 is presented. With an increase of noise intensity, the intensity of noise-induced oscillations is increased too. For rather large $b_1 > b_{cr}$ this dependence can be approximated by a straight line. The intersection point of this line and the abscissa can be taken as a point of a transition—a threshold value b_{cr}. To prove it let us drop the artificially multiplicative noise from Eqs. (35). In
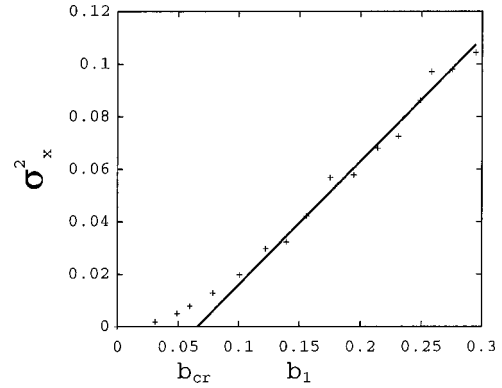

FIG. 12. A noise-induced phase transition in the SEIR model. The dependence of σ^2 on the parameter b_1 in the case of a random variation of the contact rate. The solid line represents $\sigma^2 = 0.47(b_1 - 0.066)$.

this case the variance of oscillations is equal to zero for $b_1 < b_{cr}$ and goes to infinity shortly after the noise intensity represented by the parameter b_1 exceeds its critical value. The same situation is observed if additive noise is absent but multiplicative noise is present. Now it is clear that the point $b_1 = b_{cr}$ is a point of noise-induced phase transition, which can be induced by both multiplicative and additive noise. The physical mechanisms responsible for this effect are likely to be the same as for the pendulum (Sec. II) and the nonlinear oscillator (Sec. III A), respectively.

It is even more interesting that the combined action of additive and multiplicative noise performs a stabilization of noise-induced oscillations: in this case the dependence of variance on noise intensity does not go to infinity. Again, as for previously considered models [28], the transition can be accompanied by the effect of on-off intermittency. In the absence of additive noise one can observe on-off intermittency near the threshold (Fig. 13).

V. CONCLUSIONS

We have studied in this paper the role of additive noise in noise-induced phase transitions and have shown that it can be nontrivial. We have found several phenomena by consideration of different typical models; each of them has demonstrated a certain aspect of the problem. Consideration of a pendulum under the action of multiplicative and additive noise has shown that, if a noise-induced transition occurs in
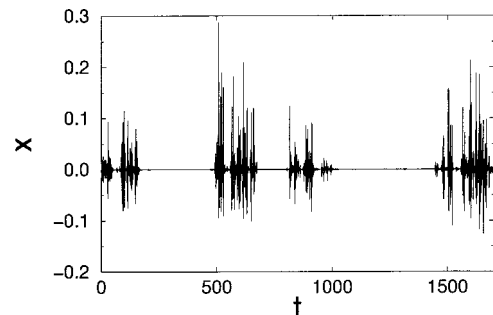

FIG. 13. On-off intermittency in the SEIR model. An example of oscillations of the variables x and y for $b_1 = 0.099$ for the case of multiplicative random action alone.

the presence of additive noise, it is blurred by this noise and becomes hidden. We have presented results of an analytical study confirmed by numerical simulations. By the examples of Sec. III we have demonstrated that there are mechanisms which allow additive noise alone to induce a hidden transition. Consideration of an epidemiological model has shown that, moreover, there exist nonlinear systems in which only the combined action of multiplicative and additive noise causes stable noise-induced oscillations. In such systems the joint influence of additive and multiplicative noise can be interpreted as the stabilization of noise-induced oscillations. In the present study we have considered only transitions that lead to the excitation of oscillations (e.g., in contrast to [20,30,31]). It should be mentioned also that we have recently shown in [19,20] that the role of additive noise may also be crucial in noise-induced transitions that lead to the creation of a mean field in a spatially extended system.

APPENDIX A: LANGEVIN EQUATIONS

The following Langevin equations can be related to the Fokker-Planck equation (5) in view of Eqs. (10) and (11):

$$\dot{A} = \beta \left(\eta - \frac{3\omega_0^2}{4} \alpha A^2 \right) A + \frac{\omega_0^2}{2A} K_{12} + \frac{\omega_0}{2} A \zeta_{11}(t) + \omega_0 \zeta_{12}(t),$$

$$\dot{\phi} = \omega_0^2 M + \omega_0 \left(\zeta_{21}(t) + \frac{\zeta_{22}(t)}{A} \right), \tag{A1}$$

where $\zeta_{11}(t)$, $\zeta_{12}(t)$, $\zeta_{21}(t)$, and $\zeta_{22}(t)$ are white noises with zero mean value and uncorrelated with A. The intensities of these noises are K_{11}, K_{12}, K_{21}, and K_{22}, respectively. We note that even in the case with $\kappa_{\xi_2} = 0$ Eqs. (37) differ from that derived in [26]. The reason is that there the variable $u = \ln A$ in place of A was used, i.e., the correlation between the noise $\xi(t)$ and the amplitude A was implicitly ignored [14,1,25].

APPENDIX B: CALCULATIONS IN THE CASE WITH ADDITIVE NOISE

The dependence of the mean amplitude squared on the multiplicative noise intensity in the case where additive noise also acts on the pendulum can be calculated as follows. Upon integrating Eq. (19) over ϕ and calculating the integral within the exponential, we obtain

$$w(A) = 2\pi A w(A, \phi) = CA^2 (A^2 + q/a)^{3(q-1)/2(1+\eta)}$$

$$\times \exp\left(-\frac{3aA^2}{2(1+\eta)} \right). \tag{B1}$$

It follows from the normalization condition that

$$C^{-1} = \int_0^\infty A^2 (A^2 + q/a)^{3(q-1)/2(1+\eta)} \exp\left(-\frac{3aA^2}{2(1+\eta)} \right) dA. \tag{B2}$$

The integral on the right-hand side of Eq. (B2) can be expressed in terms of a Whittaker function [32]. As a result we find

$$C^{-1} = \frac{\sqrt{\pi}}{4a^{2\mu} q^{1/2-\mu}} \left(\frac{3}{2(1+\eta)} \right)^{-\mu-1/2} \exp\left(\frac{3q}{4(1+\eta)} \right)$$

$$\times W_{\mu-1,\mu}\left(\frac{3q}{2(1+\eta)} \right), \tag{B3}$$

where $\mu = 3(\eta + q)/4(1+\eta)$.

We obtain the expression for C in explicit form in the limiting case when the additive noise intensity is small compared to that of the multiplicative noise, so that

$$q \ll 1. \tag{B4}$$

In this case we can use a representation of the Whittaker function $W_{\lambda,\mu}(z)$ in terms of two other Whittaker functions $M_{\lambda,\mu}(z)$ and $M_{\lambda,-\mu}(z)$ [32]:

$$W_{\lambda,\mu}(z) = \frac{\Gamma(-2\mu)}{\Gamma(1/2-\mu-\lambda)} M_{\lambda,\mu}(z)$$

$$+ \frac{\Gamma(2\mu)}{\Gamma(1/2+\mu-\lambda)} M_{\lambda,-\mu}(z). \tag{B5}$$

We then expand each of the functions $M_{\lambda,\mu}(z)$ and $M_{\lambda,-\mu}(z)$ in powers of z [32]:

$$W_{\lambda,\mu}(z) = \sqrt{z} \exp\left(-\frac{z}{2} \right) \left[\frac{\Gamma(-2\mu)}{\Gamma(1/2-\mu-\lambda)} z^{\mu} \right.$$

$$\times \left(1 + \frac{1-2(\lambda-\mu)}{2(1+2\mu)} z + \cdots \right)$$

$$+ \frac{\Gamma(2\mu)}{\Gamma(1/2+\mu-\lambda)} z^{-\mu} \left(1 + \frac{1-2(\lambda+\mu)}{2(1-2\mu)} z + \cdots \right) \right]. \tag{B6}$$

Substituting Eq. (B6) into Eq. (B3) we get

$$C^{-1} = \frac{\sqrt{\pi}}{4a^{2\mu}} \left[\frac{\Gamma(-2\mu)}{\Gamma(3/2-2\mu)} q^{2\mu} \left(1 + \frac{9q}{4(1+2\mu)(1+\eta)} + \cdots \right) \right.$$

$$+ \frac{\Gamma(2\mu)}{\Gamma(3/2)} \left(\frac{2(1+\eta)}{3} \right)^{2\mu}$$

$$\times \left. \left(1 + \frac{3(3-4\mu)q}{4(1-2\mu)(1+\eta)} + \cdots \right) \right]. \tag{B7}$$

The expression (14), obtained in the absence of additive noise, follows at once from Eq. (B7) for $q \to 0$.

The probability distribution (B1) for $q \neq 0$ differs essentially from Eq. (15): first, it is not a δ function for $\eta < 0$ and, secondly, $w(A) = 0$ for $A = 0$.

Using Eqs. (B1) and (B3) we can calculate $\langle A \rangle$ and $\langle A^2 \rangle$. For example, for $\langle A^2 \rangle$ we obtain

$$a\langle A^2 \rangle = \sqrt{\frac{3q(1+\eta)}{2}} \frac{W_{\mu-3/2,\mu+1/2}[3q/2(1+\eta)]}{W_{\mu-1,\mu}[3q/2(1+\eta)]}. \tag{B8}$$

Taking into account the recursion relation [32]

$$W_{\lambda,\mu}(z) = \sqrt{z}\,W_{\lambda-1/2,\mu+1/2}(z) + (\tfrac{1}{2}-\lambda-\mu)W_{\lambda-1,\mu}(z),$$

the expression (B8) can be rewritten as

$$a\langle A^2\rangle = (1+\eta)\left(1 - (\tfrac{3}{2}-2\mu)\frac{W_{\mu-2,\mu}[3q/2(1+\eta)]}{W_{\mu-1,\mu}[3q/2(1+\eta)]}\right).$$
(B9)

The expression for $\langle A^2\rangle$ can be obtained in explicit form only with the constraint (B4). Using Eq. (B6) we find for $W_{\mu-2,\mu}(z)/W_{\mu-1,\mu}(z)$ the following approximate expression:

$$\frac{W_{\mu-2,\mu}(z)}{W_{\mu-1,\mu}(z)} \approx \frac{2}{(3-4\mu)}\left[\frac{\sqrt{\pi}}{2}\Gamma(-2\mu)z^\mu(1-2\mu)\right.$$

$$\times[2(1+2\mu)+5z]+\Gamma(2\mu)\Gamma(\tfrac{3}{2}-2\mu)$$

$$\times\left(1-\frac{4\mu}{3}\right)z^{-\mu}(1+2\mu)[2(1-2\mu)$$

$$\left.+(5-4\mu)z]\right]\left(\frac{\sqrt{\pi}}{2}\Gamma(-2\mu)z^\mu(1-2\mu)[2(1\right.$$

$$+2\mu)+3z]+\Gamma(2\mu)\Gamma(\tfrac{3}{2}-2\mu)z^{-\mu}$$

$$\left.\times(1+2\mu)[2(1-2\mu)+(3-4\mu)z]\right)^{-1}.$$
(B10)

Substituting Eq. (B10) in Eq. (B9) we get the required Eq. (20).

---

[1] P. Landa and A. Zaikin, Phys. Rev. E **54**, 3535 (1996).

[2] P. Landa and P. McClintock, Phys. Rep. (to be published).

[3] L. Gammaitoni, P. Hänggi, P. Jung, and F. Marchesoni, Rev. Mod. Phys. **70**, 223 (1998).

[4] M. Dykman and P. McClintock, Nature (London) **391**, 344 (1998).

[5] P. Hänggi, P. Talkner, and M. Borkovec, Rev. Mod. Phys. **62**, 251 (1990).

[6] F. Marchesoni, Phys. Lett. A **237**, 126 (1998).

[7] A. Pikovksy and J. Kurths, Phys. Rev. Lett. **78**, 775 (1997).

[8] J. M. R. Parrondo, C. Van den Broeck, J. Buceta, and F. J. de la Rubia, Physica A **224**, 153 (1996).

[9] W. Horsthemke and R. Lefever, *Noise-Induced Transitions* (Springer, Berlin, 1984).

[10] J. Smythe, F. Moss, and P. McClintock, Phys. Rev. Lett. **51**, 1062 (1983).

[11] J. García-Ojalvo, A. Hernández-Machado, and J. Sancho, Phys. Rev. Lett. **71**, 1542 (1993).

[12] C. Van den Broeck, J. M. R. Parrondo, and R. Toral, Phys. Rev. Lett. **73**, 3395 (1994).

[13] J. García-Ojalvo and J. M. Sancho, *Noise in Spatially Extended Systems* (Springer, New York, 1999).

[14] P. Landa, *Nonlinear Oscillations and Waves in Dynamical Systems* (Kluwer Academic Publ., Dordrecht, 1996).

[15] P. Landa and A. Zaikin, in *Applied Nonlinear Dynamics and Stochastic Systems Near the Millenium*, edited by J. Kadtke and A. Bulsara, AIP Conf. Proc. No. 411 (AIP, New York, 1997), pp. 321–329.

[16] We call the transitions considered in this paper noise-induced *phase* transitions. In our terminology we follow the concept suggested by Haken in [33], where he shows that the name *phase transitions* can be used for the transitions considered by us on the basis of analogy with phase transitions in equilibrium systems. Such a name expresses that these new transitions are closely akin to the classical equilibrium phase transitions and to a more recent class of nonequilibrium phase transitions (see also the Introduction in [9]). However, there is also another point of view [13,12], arguing that the name noise-induced *phase* transitions can be used only for transitions in spatially extended systems.

[17] C. Van den Broeck, J. M. R. Parrondo, R. Toral, and R. Kawai, Phys. Rev. E **55**, 4084 (1997).

[18] P. Landa and A. Zaikin, in *Computing Anticipatory Systems*, edited by D. Dubois, AIP Conf. Proc. No. 465 (AIP, New York, 1998), pp. 419–434.

[19] P. Landa, A. Zaikin, and L. Schimansky-Geier, Chaos Solitons and Fractals **9**, 1367 (1998).

[20] A. Zaikin and L. Schimansky-Geier, Phys. Rev. E **58**, 4355 (1998).

[21] P. Landa and Y. Duboshinsky, Usp. Fiz. Nauk. **158**, 729 (1989) [Sov. Phys. Usp. **32**, 723 (1989)].

[22] K. Dietz, Lect. Notes Biomath. **11**, 1 (1976).

[23] L. Olsen and W. Schaffer, Science **249**, 499 (1990).

[24] R. Engbert and F. Drepper, Chaos Solitons and Fractals **4**, 1147 (1994).

[25] P. Landa and A. Zaikin, Zh. Eksp. Teor. Fiz. **84**, 358 (1997) [JETP **84**, 197 (1997)].

[26] R. Stratonovich, *Topics in the Theory of Random Noise* (Gordon and Breach, New York, 1963), Vol. 1.

[27] P. Landa, A. Zaikin, M. Rosenblum, and J. Kurths, Phys. Rev. E **56**, 1465 (1997).

[28] P. Landa, A. Zaikin, M. Rosenblum, and J. Kurths, Chaos, Solitons and Fractals **9**, 1367 (1997).

[29] P. Landa and A. Rabinovitch, Phys. Rev. E. **61**, 1829 (2000).

[30] H. Fujisaka and S. Grossman, Z. Phys. B: Condens. Matter **43**, 69 (1981).

[31] L. Brenig and N. Banai, Physica D **5**, 208 (1982).

[32] E. Whittaker and G. Watson, *A Course of Modern Analysis* (Cambridge Univ. Press, Cambridge, 1927).

[33] H. Haken, *Synergetics* (Springer-Verlag, Berlin, 1978).

Nonequilibrium first-order phase transition induced by additive noise

A. A. Zaikin,[1] J. García-Ojalvo,[2] and L. Schimansky-Geier[3]

[1]*Institute of Physics, University of Potsdam, Am Neuen Palais 10, 14469 Potsdam, Germany*
[2]*Departament de Física i Enginyeria Nuclear, Universitat Politècnica de Catalunya, Colom 11, E-08222 Terrassa, Spain*
[3]*Humboldt Universität zu Berlin, Invalidenstraße 110, 10115 Berlin, Germany*
(Received 9 September 1999)

We show that a nonequilibrium first-order phase transition can be induced by additive noise. As a model system to study this phenomenon, we consider a nonlinear lattice of overdamped oscillators with both additive and multiplicative noise terms. Predictions from mean field theory are successfully confirmed by numerical simulations. A physical explanation for the mechanism of the transition is given. [S1063-651X(99)51912-0]

Among all the counterintuitive phenomena observed in nonlinear systems with noise (such as stochastic resonance [1], noise-induced transport [2], coherence resonance [3], resonant activation [4], etc.) an important place is occupied by noise-induced transitions. Discovered in the 1980s [5] and confirmed by numerous experiments (see, for example, [6]), noise-induced transitions have attracted intensive attention due to the surprising ability of noise to produce order in the system. These transitions can be characterized by a qualitative change in the probability distribution of the system (e.g., by a change in the number of maxima). In the 1990s other kinds of transitions were found, such as those giving rise to noise-induced oscillations in single nonlinear oscillators [7,8]. On the other hand, systems of spatially coupled overdamped oscillators have been recently shown to display noise-induced *phase* transitions. In this case, contrary to the previous phenomena, the system exhibits ergodicity breaking and the transition can be characterized by standard tools in equilibrium statistical mechanics [9]. Several models have exhibited so far the existence of noise-induced second-order (continuous) phase transitions leading to the creation of a nonzero mean field [9–12]. In [13] it was shown that noise-induced phase transitions can also be of first order (discontinuous).

In the majority of the above-mentioned studies, phase transitions are induced by multiplicative noise. However, recent results [14–16] have shown that additive noise can play a crucial role in this phenomenon, and even induce a transition by itself. Such an influence has been observed both in oscillatory [14] and in nonoscillatory (overdamped) systems [15,16]. The present Rapid Communication shows that additive noise can also induce *first-order* nonequilibrium transitions in spatially extended systems. These are *pure* noise-induced phase transitions, in the sense that they do not exist in the system in the absence of noise. The study is performed on a nonlinear lattice of coupled stochastic overdamped oscillators introduced in [11] and further studied in [15,16,18,19]. It is described by the following set of Langevin equations:

$$\dot{x}_i = f(x_i) + g(x_i)\xi_i(t) + \frac{D}{2d}\sum_j (x_j - x_i) + \zeta_i(t), \quad (1)$$

where $x_i(t)$ represents the state of the ith oscillator, and the sum runs over all nearest neighbors of cell i. The strength of

the coupling is measured by D, and d is the dimension of the lattice, which has $N = L^d$ elements. The noise terms $\xi_i(t)$ and $\zeta_i(t)$ are mutually uncorrelated, Gaussian distributed, with zero mean and white in both space and time,

$$\langle \xi_i(t)\xi_j(t') \rangle = \sigma_\xi^2 \delta_{i,j}\delta(t-t'), \quad (2)$$

$$\langle \zeta_i(t)\zeta_j(t') \rangle = \sigma_\zeta^2 \delta_{i,j}\delta(t-t'). \quad (3)$$

For the sake of simplicity, the functions $f(x)$ and $g(x)$ are taken to be of the form [11]

$$f(x) = -x(1+x^2)^2, \quad g(x) = a^2 + x^2, \quad (4)$$

so that two different sources of additive noise can be considered to exist in this system: the first one, controlled by σ_ζ, is completely uncorrelated with the multiplicative noise; the second one, controlled by a, is strongly correlated with it.

The behavior of this system can be analytically studied by means of a standard mean-field theory (MFT) procedure [9]. The mean-field approximation consists of replacing the nearest-neighbor interaction by a global term in the Fokker-Planck equation corresponding to Eq. (1). In this way, one obtains the following steady-state probability distribution w_{st}:

$$w_{st}(x,m) = \frac{C(m)}{\sqrt{\sigma_\xi^2 g^2(x) + \sigma_\zeta^2}}\exp\left(2\int_0^x \frac{f(y)-D(y-m)}{\sigma_\xi^2 g^2(y) + \sigma_\zeta^2}dy\right), \quad (5)$$

where $C(m)$ is a normalization constant and m is a mean field, defined by the equation

$$m = \int_{-\infty}^{\infty} x w_{st}(x,m)dx. \quad (6)$$

By solving Eq. (6) self-consistently with respect to the variable m, one can find transitions between ordered ($m \neq 0$) and disordered ($m=0$) phases. As shown in [11], for $a=1$ and $\sigma_\zeta=0$ the system exhibits a disorder-order phase transition, followed by a reentrant transition back to disorder, both induced by multiplicative noise. When a or σ_ζ are used to control the system, additive noise is seen to lead to similar transitions [15,16]. In all cases, the transition (which exists only in the presence of noise) is of second order. But when the complete system is analyzed more carefully, new aspects
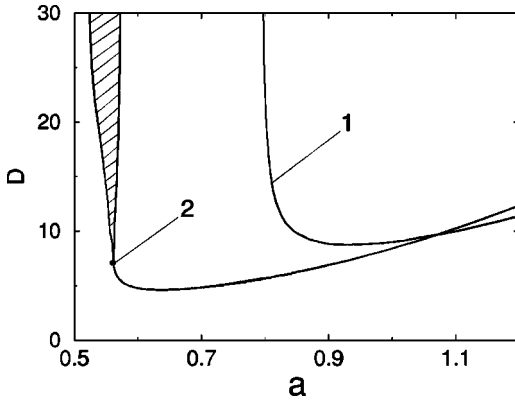
FIG. 1. Phase transition boundaries on the plane (a,D) for $\sigma_\zeta = 0$ and two different intensities of the multiplicative noise (curve 1, $\sigma_\xi^2 = 1.6$; curve 2, $\sigma_\xi^2 = 3.0$). The dashed region (starting with the dot) corresponds to the coexistence of the disordered and ordered phases.

FIG. 2. First-order phase transition induced by additive noise. Order parameters m, m_n vs a for $D=20$, $\sigma_\xi^2 = 3.0$ and $\sigma_\zeta^2 = 0.0$. MFT predictions (solid line) and numerical simulations (diamonds) are presented. The dotted line delimits the coexistence region exhibited by MFT. The unstable state is plotted by the dashed line.

arise. Figure 1 shows order-disorder transition lines in the plane (a,D), for $\sigma_\zeta = 0$ and two different values of the multiplicative noise intensity σ_ξ^2. Curve 1 separates regions of disorder (below the curve) and order (above the curve) for small multiplicative noise intensity. In this case, the ordered region is characterized by three self-consistent solutions of Eq. (6), one of them unstable ($m=0$) and the other two stable and symmetrical. These new solutions appear continuously from $m=0$ in the course of the transition. Hence, curve 1 corresponds to a *second-order* phase transition from disorder to order as a increases, followed by a reentrant transition back to disorder (also of second order).

The situation changes noticeably when the multiplicative noise intensity increases. In that case (curve 2 in Fig. 1), a region appears where Eq. (6) has five roots, three of which ($m=0$ and two symmetrical points) are stable. This region is shown as dashed in the figure. Thus, for large enough values of D, a region of coexistence appears in the transition between order and disorder. This region is limited by discontinuous transition lines between $m=0$ and a nonzero, finite value of m. Hence, additive noise is seen to induce a *first-order* phase transition in this system for large enough values of the coupling strength and multiplicative noise intensity. The reentrant transition is again of second order.

When the first-order phase transition appears, hysteresis can be expected to occur in the coexistence region (if a certain algorithm is applied [17]). The dependence of the order parameter m on the control parameter a as predicted by MFT is shown in Fig. 2 by a solid line. The region of possible hysteresis is bounded by dotted lines.

In order to contrast the previous MFT results, we have performed simulations of the complete model (1)–(4) using the numerical methods described in [9,18]. The order parameter m_n is computed as

$$m_n = \left\langle \left| \frac{1}{L^2} \sum_{i=1}^{N} x_i \right| \right\rangle,$$

where $\langle \rangle$ denotes time average. Results for a two-dimensional lattice with lateral size $L=32$ are shown with diamonds in Fig. 2. Analyzing this figure one can observe
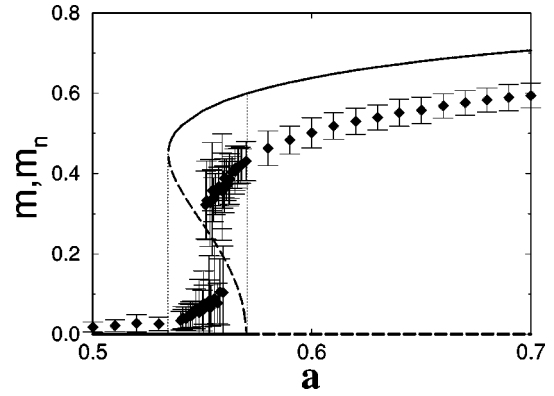
that MFT overestimates the size of the coexistence region. This effect, analogous to what was observed for multiplicative-noise-induced transitions [11], can be explained in terms of an ''effective potential'' derived for the system at short times (see the discussion below). For instance, as a increases the system leaves the disordered phase not when this state becomes unstable but earlier, when the potential minima corresponding to the ordered states become much lower than the minimum corresponding to the state $m=0$. It should also be mentioned that the numerical simulations did not show hysteresis, because in the coexistence region the system occupied any of the three possible states, independently of the initial conditions. This fact can be explained by the small size of the simulated system, which permits jumps between steady states when the system is sufficiently perturbed (e.g., by slightly changing the parameter a).

Now we consider the second kind of additive noise present in the system, namely, the one uncorrelated with the multiplicative noise ($a=0$ and $\sigma_\zeta^2 \neq 0$). MFT results are presented in the phase diagram of Fig. 3, which shows transitions lines in the plane (σ_ξ^2, D) for three different values of the additive noise intensity σ_ζ^2. A coexistence region is again found in the disorder-order transition (left) branch for all three values of σ_ζ^2. For points in the dashed region (inset plot in Fig. 3), the system is in a disordered phase for small and large values of σ_ζ^2, and in an ordered phase for intermediate values of this parameter. Hence, in that region additive noise is able to induce two consecutive phase transitions from disorder to order and back to disorder. The character of the first transition is very sensitive to the parameter values: as can be clearly seen in Fig. 4 (curves 1 and 2), for very close values of D and σ_ξ^2, additive noise can induce either a second- or a first-order phase transition. Note also that, if we consider the multiplicative noise intensity as a control parameter, the width of the coexistence region as predicted by MFT decreases with an increase of the additive noise intensity.

Numerical simulations for this kind of additive noise are shown as diamonds in Fig. 4, again for a two-dimensional lattice with $L=32$. MFT overestimates once more the loca-
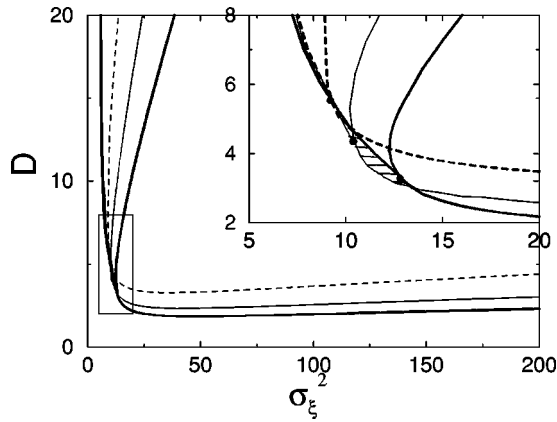
FIG. 3. Phase diagram in the plane (σ_ξ^2, D) for $a = 0$ and three different values of the additive noise intensity: $\sigma_\zeta^2 = 0.3$ (thick solid line), 0.5 (thin solid line), and 1.0 (dashed line). For large coupling D additive noise shrinks the region of coexisting solutions, whereas its left boundary coincides for different σ_ζ^2 and remains unaffected. The inset plot shows peculiarities of the transition lines in the small box. Inside the dashed region an increase of additive noise induces disorder-order and the reentrant transition (see the text and Fig. 4).

tion of the transition, hence if, according to MFT, a transition is observed for $D = 4.15$, in numerical simulations it occurs for $D = 6.5$. The region of possible hysteresis for this set of parameters is too thin to be shown in Fig. 4; this fact is also confirmed by numerical simulations. But if we slightly increase D, hysteresis appears [17]. For example, for $D = 7.0$ the hysteresis region spans even from $\sigma_\xi^2 = 0.0$ to 0.2.

We have thus seen so far that numerical simulations qualitatively confirm the existence of a first-order phase transition induced by additive noise in this system, as predicted by MFT. We note that in the two limiting cases of correlation between multiplicative and additive noise, the transition occurs. We also note that variation of both the multiplicative noise intensity and the coupling strength can change the order of this transition.

Let us now present a possible physical mechanism behind this effect. In [16,18] it was argued that the short-time evolution of the average value of the local field can be described by the equation
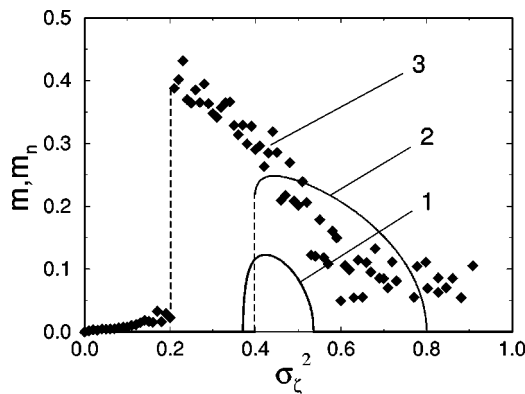

FIG. 4. First- and second-order phase transitions induced by uncorrelated additive noise. Curves 1 ($D = 3.5$, $\sigma_\xi^2 = 12.0$) and 2 ($D = 4.15$, $\sigma_\xi^2 = 11.0$) correspond to MFT results, diamonds to numerical simulations ($D = 6.5$, $\sigma_\xi^2 = 11$).
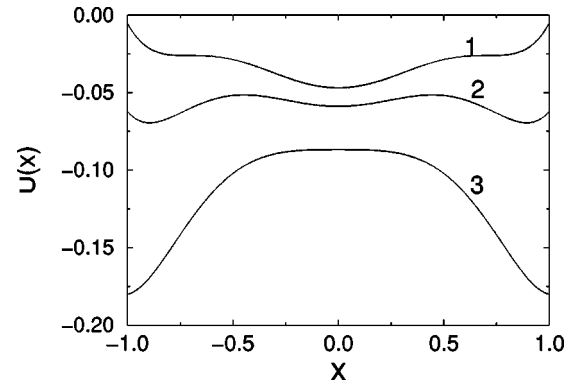

FIG. 5. ''Effective'' potential for the short-time evolution of m for $a^2 = 0.25$ (curve 1), 0.28 (curve 2), and 0.34 (curve 3). Other parameters are $\sigma_\xi^2 = 3.0$ and $\sigma_\zeta^2 = 0.0$.

$$\dot{\bar{x}} = f(\bar{x}) + \frac{\sigma_\xi^2}{2} g(\bar{x}) g'(\bar{x}), \tag{7}$$

for which an ''effective'' potential can be derived. It is described by $U(x) = U_0(x) + U_{\text{noise}} = -\int f(x) dx - \sigma_\xi^2 g^2(x)/4$, where U_{noise} represents the influence of the multiplicative noise. We can trace the behavior of this potential in the presence of multiplicative noise, for the case $\sigma_\zeta^2 = 0$ and nonzero a. Its evolution for increasing a is shown in Fig. 5. This approach can be clearly seen to successfully explain the mechanism of the first-order transition: first, only the zero state is stable (curve 1), then there is a region where three stable states coexist (curve 2), and finally, the disordered state becomes unstable (curve 3). This approach also explains why a variation of the multiplicative noise intensity influences the order of the transition: for another (lower) σ_ξ^2 there is no region where ordered and disordered phases simultaneously exist. We emphasize that the ''effective'' potential is derived only for short-time evolution, and should not be confused with the ''stochastic'' potential [5], which for this system remains always monostable. For the other case of correlation between multiplicative and additive noise, in the region of additive noise induced transition, the ''effective'' potential always has three minima (two symmetric minima are lower than the central one). Overcritical additive noise causes an escape from zero state and leads to the transition. Hence, the ''effective'' potential approximation does not explain all results of MFT: it explains well the transition but not an existence of threshold in the additive noise intensity. It is important to add that the transition under consideration has much in common with the phenomenon of stochastic resonance: in both cases there is a multistability, and there exists an optimal value of the additive noise intensity for which the ordering is the most effective one. This similarity is limited by the fact that here the multistability is induced only in short-time terms, and there is no external signal to be synchronized with (see also [16]).

In conclusion, we have reported the existence of nonequilibrium first-order phase transitions induced by additive noise. Such a phenomenon can be expected to be experimentally observed [18] in systems exhibiting shifts in a transition induced by multiplicative noise. Possible candidates could be photosensitive chemical reactions [20,21], liquid crystals

[22,23], and Rayleigh-Bénard convection under a fluctuating temperature gradient [24]. It should also be mentioned that another form of coupling, Swift-Hohenberg, is possible in the presented model. In that case, one can observe ordered spatial patterns appearing as a result of a first-order phase transition induced by additive noise.

The results presented here open up several questions. First, it should be determined whether the behaviors reported are universal. Second, one should investigate the translation of these effects into other phenomena, such as globally synchronized oscillations in subexcitable media [25], transport properties in coupled ratchets [26], and relation between noise-induced transitions and stochastic resonance in systems with external forcing. Finally, these results could be of relevance for the stochastic modeling of transitions and irregular oscillations that have been explained in the frames of deterministic theory [8,14,27].

[1] L. Gammaitoni, P. Hänggi, P. Jung, and F. Marchesoni, Rev. Mod. Phys. **70**, 223 (1998).

[2] P. Hänggi and R. Bartussek, in *Nonlinear Physics of Complex Systems*, edited by J. Parisi, S. Müller, and W. Zimmermann (Springer, Berlin, 1996).

[3] A. Pikovksy and J. Kurths, Phys. Rev. Lett. **78**, 775 (1997).

[4] C. Doering and J. Gadoua, Phys. Rev. Lett. **69**, 2318 (1992).

[5] W. Horsthemke and R. Lefever, *Noise-Induced Transitions* (Springer, Berlin, 1984).

[6] J. Smythe, F. Moss, and P.V.E. McClintock, Phys. Rev. Lett. **51**, 1062 (1983).

[7] P. Landa and A. Zaikin, Phys. Rev. E **54**, 3535 (1996).

[8] P. Landa and A. Zaikin, in *Applied Nonlinear Dynamics and Stochastic Systems Near the Millenium* (AIP 411, San Diego, CA, 1997), pp. 321–329.

[9] J. García-Ojalvo and J. M. Sancho, *Noise in Spatially Extended Systems* (Springer, New York, 1999).

[10] J. García-Ojalvo, A. Hernández-Machado, and J. Sancho, Phys. Rev. Lett. **71**, 1542 (1993).

[11] C. Van den Broeck, J.M.R. Parrondo, and R. Toral, Phys. Rev. Lett. **73**, 3395 (1994).

[12] J. García-Ojalvo, J.M.R. Parrondo, J.M. Sancho, and C. Van den Broeck, Phys. Rev. E **54**, 6918 (1996).

[13] R. Müller, K. Lippert, A. Kühnel, and U. Behn, Phys. Rev. E **56**, 2658 (1997).

[14] P. Landa, A. Zaikin, V. Ushakov, and J. Kurths (unpublished).

[15] P. Landa, A. Zaikin, and L. Schimansky-Geier, Chaos Solitons Fractals **9**, 1367 (1998).

[16] A. Zaikin and L. Schimansky-Geier, Phys. Rev. E **58**, 4355 (1998).

[17] The hysteresis may appear if we slowly change c^* during integration, i.e., the solution x_i for the previous value $c^* = c - \Delta c$ is the initial condition for the next point $c^* = c$ by a monotonical variation of c^*, where c^* is a control parameter (a or σ_ζ^2) and variated upwards and downwards.

[18] C. Van den Broeck, J.M.R. Parrondo, R. Toral, and R. Kawai, Phys. Rev. E **55**, 4084 (1997).

[19] S. Mangioni, R. Deza, H.S. Wio, and R. Toral, Phys. Rev. Lett. **79**, 2389 (1997).

[20] J. Micheau, W. Horsthemke, and R. Lefever, J. Chem. Phys. **81**, 2450 (1984).

[21] P. de Kepper and W. Horsthemke, *Synergetics: Far From Equilibrium* (Springer, New York, 1979).

[22] S. Kai, T. Kai, and M. Takata, J. Phys. Soc. Jpn. **47**, 1379 (1979).

[23] M. Wu and C. Andereck, Phys. Rev. Lett. **65**, 591 (1990).

[24] C. Meyer, G. Ahlers, and D. Cannell, Phys. Rev. A **44**, 2514 (1991).

[25] H. Hempel, L. Schimansky-Geier, and J. García-Ojalvo, Phys. Rev. Lett. **82**, 3713 (1999).

[26] P. Reimann, R. Kawai, C. Van den Broeck, and P. Hänggi, Europhys. Lett. **45**, 545 (1999).

[27] P. Landa, Europhys. Lett. **36**, 401 (1996).

Spatial patterns induced by additive noise

A. A. Zaikin and L. Schimansky-Geier

Humboldt-Universität zu Berlin, Invalidenstraße 110, 10115 Berlin, Germany

(Received 18 May 1998)

We consider a nonlinear lattice with spatial coupling under the influence of multiplicative and additive noise. In contrast to other studies, we pay attention mainly to the role of the additive noise and show that additive noise, much like multiplicative noise, is able to induce spatial patterns. The reason is that the increase of additive noise causes a nonequilibrium phase transition that manifests itself in the formation of ordered spatial patterns. The presence of the additive noise correlated or uncorrelated with the multiplicative noise is a necessary condition of the phase transition. We review the mean field theory for this model and show that this theory predicts a reentrant phase transition caused by additive noise. Theoretical predictions are confirmed by numerical simulations. [S1063-651X(98)12510-2]

PACS number(s): 05.40.+j, 47.54.+r, 05.70.Fh

I. INTRODUCTION

Over the past two decades nonlinear systems with noise have been continuously attracting attention. The reason is the ordering role of noise in such phenomena as stochastic resonance [1], noise-induced transport [2], or noise-induced transitions [3]. A large variety of models [4–12] appear to demonstrate nonequilibrium noise-induced phase transition. In these studies only multiplicative noise is shown to be the reason for the transition and much less attention has been paid to the role of additive noise. Recently, we started to study the influence of an additive noise on noise-induced transitions. It was shown that this influence can be crucial because the additive noise may shift the boundaries of the noise-induced phase transition [13] or even cause these transitions [13,14].

In the present paper we continue to study the influence of additive noise on noise-induced phase transitions. We consider the role of the additive noise in the formation of the ordered spatially inhomogeneous patterns. For this we investigate a paradigmatic model introduced in [7] (for the history of the subject see also [15–18]). As noted in [19], investigation of this model is helpful for the understanding of results of experiments on electrohydrodynamic convection in nematic liquid crystals with thermal fluctuations (additive noise) and an external stochastic voltage (multiplicative noise). We show that this model displays noise-induced spatial patterns with an increase of additive noise. After exceeding an optimal level of the additive noise a further increase destroys the structures again.

First we review mean field theory for this model [7]. The theory predicts the existence of the reentrant phase transition by increasing the additive noise for two limiting cases of correlation between both additive and multiplicative noises. The transition manifests itself in breaking the symmetry and appearing ordered spatial structures. Next we perform numerical calculations and confirm some results of the theoretical considerations. After a discussion about understanding of the phenomena observed we summarize results obtained.

II. MODEL AND MEAN FIELD THEORY

We consider a scalar field $x_{\mathbf{r}}$ defined on a spatial lattice with points $\mathbf{r}$. The time evolution of the field is described by a set of Langevin equations [7]

$$\dot{x}_{\mathbf{r}} = f(x_{\mathbf{r}}) + g(x_{\mathbf{r}})\xi_{\mathbf{r}} + \mathcal{L}x_{\mathbf{r}} + \zeta_{\mathbf{r}}, \tag{1}$$

with f and g defined as

$$f(x) = -x(1+x^2)^2, \quad g(x) = a^2 + x^2 \tag{2}$$

and $\xi_{\mathbf{r}}, \zeta_{\mathbf{r}}$ independent zero-mean-value Gaussian white noise sources

$$\langle \xi_{\mathbf{r}}(t)\xi_{\mathbf{r}'}(t')\rangle = \sigma_\xi^2 \delta_{\mathbf{r},\mathbf{r}'}\delta(t-t'), \tag{3}$$

$$\langle \zeta_{\mathbf{r}}(t)\zeta_{\mathbf{r}'}(t')\rangle = \sigma_\zeta^2 \delta_{\mathbf{r},\mathbf{r}'}\delta(t-t'). \tag{4}$$

We note that such a form of the function $g(x)$ implies that the parameter a is responsible for an additive noise strongly correlated with the multiplicative one. To gain knowledge about the influence of additive noise on the noise-induced phase transition we study two different problems. First the constant contribution a^2 of the multiplicative noise $\xi_{\mathbf{r}}$ is changed, setting $\sigma_\zeta^2 = 0$. The origin one could see, for instance, in a decomposition of the multiplicative noise into two parts $g(x)\xi_{\mathbf{r}} = a^2\xi_{\mathbf{r}}^1 + x^2\xi_{\mathbf{r}}^2$. Changing the parameter a would imply an increase or a decrease of additive noise $a^2\xi_{\mathbf{r}}^1$ strongly correlated with the multiplicative one. We prove that the constant contribution of that noise is essential for the nonequilibrium phase transition. Only in the presence of the additive component with an optimally selected value does the system exhibit spatially disordered states.

A different situation is the variation of the noise intensity σ_ζ^2. It models additive noise independently of the multiplicative one. In that case we set $a=0$. Again we will find a strong influence of the additive noise ζ.

The spatial coupling in the model is described by the coupling operator $\mathcal{L}$ [see Eq. (1)], which is a discretized version of the Swift-Hohenberg coupling term $-D(q_0^2+\nabla^2)^2$:

$$\mathcal{L}x_{\mathbf{r}} = -D\left\{ q_0^2 - \frac{1}{\Delta^2}\sum_{i=1}^{2d}\left[1 - \exp\left(\Delta\mathbf{e}_i \cdot \frac{\partial}{\partial\mathbf{r}}\right)\right]\right\}^2 x_{\mathbf{r}}. \tag{5}$$
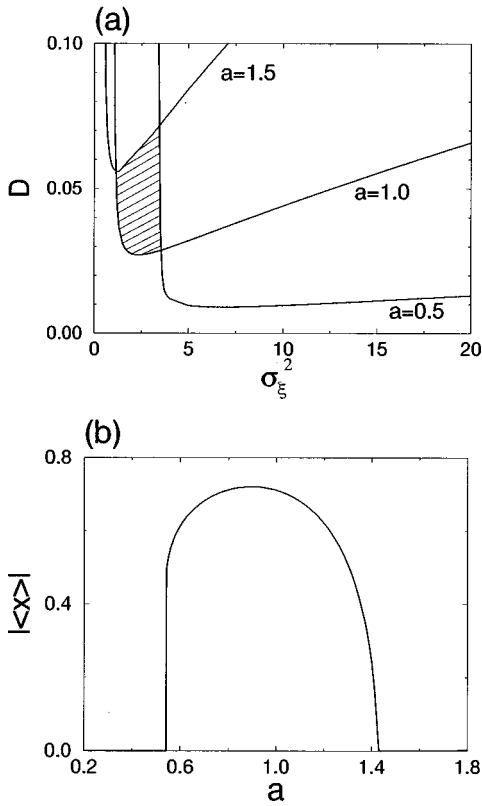
FIG. 1. (a) Boundaries of the phase transition on the plane (σ_ξ^2, D) in the case of correlated additive noise. The values of parameter a are shown in the picture. (b) Dependence of the order parameter $|\langle x \rangle|$ on the control parameter a for $D = 0.06$ and $\sigma_\xi^2 = 3.0$.

Here $\mathbf{e}_i$ are the unit vectors associated with the cubic lattice of the dimension d, and Δ is the lattice space.

The conditions of phase transition can be found using generalized Weiss mean field theory [7]. According to this theory, we replace the value of the scalar variable $x_{\mathbf{r}'}$ at the sites coupled to $x_{\mathbf{r}}$ by its averaged value, assuming the specific nonuniform average field

$$\langle x_{\mathbf{r}'} \rangle = \langle x \rangle \cos[\mathbf{k} \cdot (\mathbf{r} - \mathbf{r}')]. \qquad (6)$$

Substituting Eq. (6) into Eq. (5) we get for $x_{\mathbf{r}}$

$$\dot{x} = f(x) + g(x)\xi + D\omega(\mathbf{k})x - D_{\text{eff}}(x - \langle x \rangle) + \zeta, \qquad (7)$$

where

$$D_{\text{eff}} = \left[\left(\frac{2d}{\Delta^2} - q_0^2 \right)^2 + \frac{2d}{\Delta^2} + \omega(\mathbf{k}) \right] D \qquad (8)$$

and

$$\omega(\mathbf{k}) = -D \left[q_0^2 - \frac{2}{\Delta^2} (2 - \cos k_x \Delta - \cos k_y \Delta) \right]^2. \qquad (9)$$

The expression for $\omega(\mathbf{k})$ can be obtained if one considers how $\mathcal{L}$ acts on a plane wave $e^{i\mathbf{k} \cdot \mathbf{r}}$ for the case of a two-dimensional lattice:

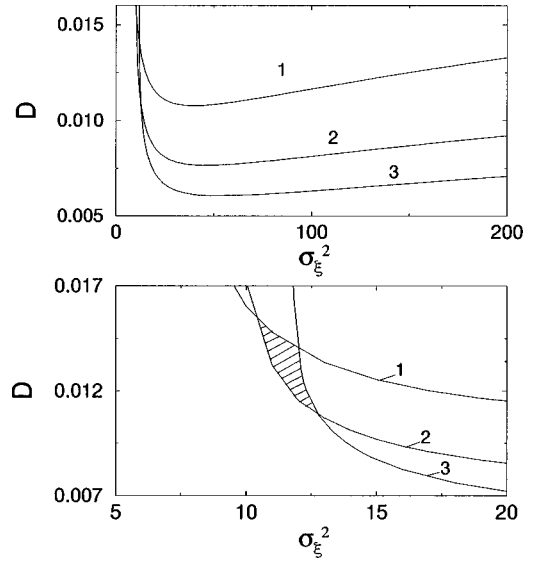$$\mathcal{L} e^{i\mathbf{k} \cdot \mathbf{r}} = \omega(\mathbf{k}) e^{i\mathbf{k} \cdot \mathbf{r}}. \qquad (10)$$

FIG. 2. Boundaries of the phase transition on the plane (σ_ξ^2, D) in the case of uncorrelated additive noise. The parameter σ_ζ^2 is equal to 1.0 (label 1), 0.5 (label 2), and 0.3 (label 3).

Note that for $|\mathbf{k}| \ll 2\pi/\Delta$ the dispersion relation $\omega(\mathbf{k})$ reduces to the relation for the continuous Swift-Hohenberg model: $-D(q_0^2 - |\mathbf{k}|^2)^2$. For the most unstable mode in the discrete case $\omega(\mathbf{k}) = 0$ (see [7]).

Now the value $\langle x \rangle$ plays the role of the amplitude of the spatial patterns with an effective diffusion coefficient D_{eff}. The Fokker-Planck equation corresponding to Eq. (7) in the case $\omega(\mathbf{k}) = 0$ is

$$\frac{\partial w}{\partial t} = -\frac{\partial}{\partial x} \left[[f(x) - D_{\text{eff}}(x - \langle x \rangle)]w - \frac{\sigma_\xi^2}{2} \left(g(x) \frac{\partial}{\partial x}[g(x)w] \right) \right.$$
$$\left. - \frac{\sigma_\zeta^2}{2} \frac{\partial w}{\partial x} \right].$$

For this equation it is possible to find the exact steady state probability, parametrically dependent on $\langle x \rangle$:

$$w_{\text{st}}(x) = \frac{C(\langle x \rangle)}{\sqrt{\sigma_\xi^2 g^2(x) + \sigma_\zeta^2}} \exp\left(2 \int_0^x \frac{f(y) - D_{\text{eff}}(y - \langle x \rangle)}{\sigma_\xi^2 g^2(y) + \sigma_\zeta^2} dy \right), \qquad (11)$$

where $C(\langle x \rangle)$ is the normalization constant determined by

$$C^{-1}(\langle x \rangle) = \int_{-\infty}^{\infty} \frac{1}{\sqrt{\sigma_\xi^2 g^2(x) + \sigma_\zeta^2}}$$
$$\times \exp\left(2 \int_0^x \frac{f(y) - D_{\text{eff}}(y - \langle x \rangle)}{\sigma_\xi^2 g^2(y) + \sigma_\zeta^2} dy \right) dx. \qquad (12)$$

For the value $\langle x \rangle$ we obtain

$$\langle x \rangle = \int x w_{\text{st}}(x, \langle x \rangle) dx, \qquad (13)$$
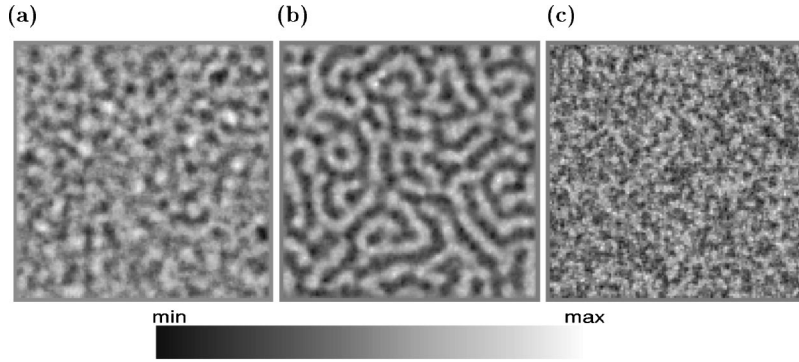
FIG. 3. Snapshots of the field for $D=1.0$, $\sigma_\xi^2=1.8$, and $\sigma_\zeta^2=0$. The parameter a is equal to (a) 0.1, (b) 1.0, and (c) 10.0. The increase of the additive noise induces spatial patterns. The scalar field from minimum to maximum value is coded in accordance with the color scale shown in the same figure.

which is nonlinear equation for the unknown value $\langle x \rangle$ and closes the system of equations.

Solving Eq. (13), we can calculate boundaries of phases with $\langle x \rangle \neq 0$ (order) and $\langle x \rangle = 0$ (disorder) for specific $\mathbf{k}$ whose modes are excited first. Nonzero solution of Eq. (13) means excitation of the corresponding mode and hence existence of the phase transition. Due to the special form of the spatial coupling, the transition manifests itself in a formation of ordered spatial patterns with the wave number defined by the parameter q_0.

The computation of Eq. (13) shows that the condition for the existence of nonzero solutions is

$$\left| \frac{dF}{dm} \right|_{m=0} \geqslant 1. \tag{14}$$

We note that for rather large D four nonzero roots (two stable and two unstable) of Eq. (13) may be observed. It is an open question whether this indicates that additionally also noise-induced first-order phase transition may be found in this model (to this point see also [19,20]).

III. ADDITIVE NOISE AND NOISE-INDUCED TRANSITION

First we study the case if an additive noise is strongly correlated with multiplicative noise (in this case $\sigma_\zeta^2=0$). For different values of a the boundary of the phase transition on the plane (σ_ξ^2, D) is shown in Fig. 1. As it is seen from this plot, the reentrant phase transition occurs for the specific value of a with the increase of σ_ξ^2 [7]. Solving Eq. (13) for other values of a, we find that as a decreases the boundary of the phase transition significantly drops and is right shifted (see Fig. 1). Hence there is a set of parameters (σ_ξ^2, D) for which the reentrant phase transition occurs with the increase of a (dashed region in Fig. 1). This means that for fixed values of σ_ξ^2 and D an increase of additive noise intensity will first induce the spatial patterns and then destroy them. We note that this phase transition is possible only in the presence of multiplicative noise. The corresponding dependence of the order parameter $|\langle x \rangle|$ on the control parameter a is shown in Fig. 1(b).

Now we study the case where the additive noise is uncorrelated (independent) from the multiplicative noise ($a=0$, $\sigma_\zeta^2 \neq 0$). As Fig. 2 shows in this case the behavior of the system is qualitatively the same: For fixed parameters (D, σ_ζ^2) an increase of the multiplicative noise intensity σ_ξ^2 causes the noise-induced phase transition. Hence for large enough coupling D one expects the formation of the spatially ordered patterns if σ_ξ^2 exceeds it critical value. As concerns the influence of the additive noise on the transition, an amplification of the additive noise intensity shifts the transition boundaries and therefore causes the reentrant disorder-order-disorder nonequilibrium phase transition. It can be clearly seen if one take a point with fixed parameters (D, σ_ξ^2) from the dashed region in the Fig. 2: With an increase of σ_ζ^2 this point first belongs to the disordered phase, then to the ordered one, and then again to the disordered phase.

IV. NUMERICAL SIMULATIONS

We check the relevance of the theory presented above by numerical simulations of the initial equations (1). We use an Euler scheme for stochastic differential equations interpreted in the Stratonovich sense [21,22]. The time step has been set $\Delta t = 5 \times 10^{-4}$. For simulations we integrate the scalar field $x_{\mathbf{r}}(t)$ on a two-dimensional square lattice 128×128 with conditions $x_{\mathbf{r}}=0$ and $\mathbf{n} \cdot \nabla x_{\mathbf{r}}=0$ at the boundaries. Here $\mathbf{n}$ is the vector normal to the boundary.

First we set $\sigma_\zeta^2=0$ and $a \neq 0$. The remaining parameters are $D=1$, $q_0=0.7$, $\Delta=0.5$, and $\sigma_\xi^2=1.8$. For these values the mean field theory predicts the existence of spatial patterns of the most unstable mode $|k|=1.0478$ for $a=1$. For additive noise intensities significantly larger than this value, for example, $a=10.0$, or significantly smaller, $a=0.1$, according to the mean field theory no spatial patterns will be exhibited.

In Fig. 3 the picture of the field after 100 time units has been plotted for three different noise intensities. Clearly one can see the appearance of the spatial patterns with the increase of the additive noise and its further destruction. These calculations confirm the predictions of the mean field theory for the case of correlated additive noise.

The ordered patterns in Fig. 3(b) have rotational symmetry, which can be clearly observed in the two-dimensional

(a)
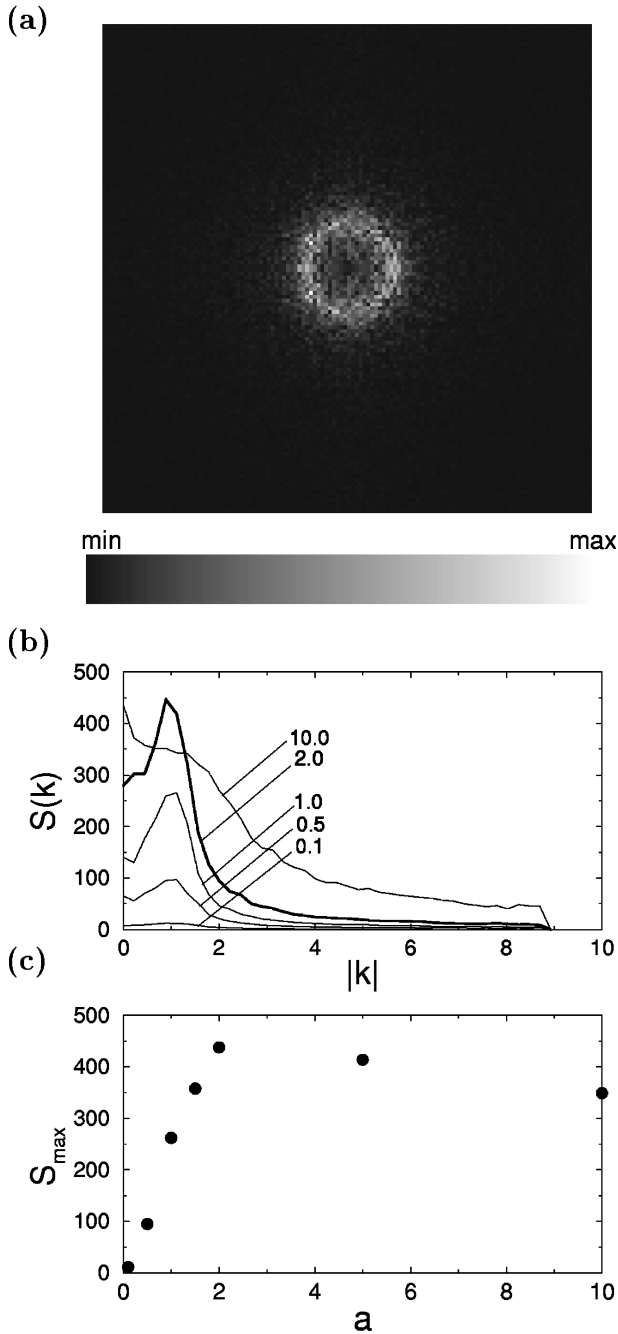

min max

(b)

(c)

FIG. 4. (a) 2D Fourier transform of the pattern shown in Fig. 3(b). Rotational symmetry is observed. (max,min) values are (1337,0.1). (b) Fourier transform averaged over angles for $D=1.0$ and $\sigma_\xi^2=1.8$. Values of parameter a are shown in the figure. (c) Dependence of S_{max} on a.

Fourier transform of the field represented in Fig. 4. To make the transition more evident we have plotted the Fourier transform of the field averaged over the angles of the wave vector. It is shown in Fig. 4 for different values of a. With an increase of a a maximum in this structure function is found. It corresponds to the dominating value $|k|_{max}$, indicating the appearance of a spatial pattern with a wavelength $2\pi/|k|_{max}$. After an optimal value of a the maximum of the structure function disappears, again signaling the destruction of the order.

Next we consider the case of uncorrelated additive noise, in which $a=0$ and $\sigma_\zeta^2\neq0$. Numerical simulations show that the behavior of the model is quite similar to the case of the correlated additive noise. An increase of the additive noise causes the formation of the rotationally symmetric spatial patterns. A further increase of the additive noise destroys this pattern (see Fig. 5). These results are also in good agreement with the predictions of mean field theory.

V. DISCUSSION

Now we discuss the mechanism providing the appearance of the ordered spatially patterns with the increase of the additive noise and its further destruction. The appearance of the ordered state is a manifestation of the phase transition, so one should understand which factors lead to this transition. To do this, let us follow the argumentation suggested in [6] to give an explanation of the phase transition induced by the multiplicative noise but now influenced by the additive noise.

For a single element of the lattice the time evolution of the first moment is given simply by the drift part in the Fokker-Planck operator, which reads (Stratonovich case)

$$\langle\dot{x}\rangle=\langle f(x)\rangle+\frac{\sigma_\xi^2}{2}\langle g(x)g'(x)\rangle. \qquad (15)$$

As it was argued in [6], the evolution over short times of an initial δ function is well approximated by a Gaussian whose extremum obeys

$$\dot{\bar{x}}=f(\bar{x})+\frac{\sigma_\xi^2}{2}g(\bar{x})g'(\bar{x}). \qquad (16)$$

Here $\bar{x}=\langle x\rangle$ is the maximum of the probability, which is the average value in this approximation. For this dynamics one is able to introduce a potential $U(x)=U_0(x)+U_{noise}=-\int f(x)dx-\sigma_\xi^2 g^2(x)/4$, where $U_0(x)$ is the unperturbed potential and $U_{noise}<0$ describes the action of the noise. In the case under consideration $U_0(x)=x^2(1+x^2+x^4/3)/2$, which is monostable with a minimum at $x_0=0$.

Let us consider how additive noise modifies the potential $U(x)$. We start with the case of $\sigma_\zeta^2=0$ and additive noise is included in the equations through $g(x)=a^2+x^2$ by the constant a. For small a the potential $U(x)$ remains monostable and there is no possibility of a phase transition in the system. If we increase a, i.e., the intensity of the correlated additive noise, the potential $U(x)$ becomes bistable if $a>a_{crit}=1/\sqrt{\sigma_\xi^2}$ [see Fig. 6(a)]. For sufficiently strong coupling this bistability will be the reason for the local ordered regions at short time scales, which coarsen and grow with time. Hence the additive part of the noise in the function g is essential for the occurrence of the nonequilibrium phase transition.

The situation with uncorrelated additive noise ($a=0$ and $\sigma_\zeta^2\neq0$) is more complicated. In this case the state $x=0$ always remains stable since the noisy part $U_{noise}(x)\propto x^4$ [see Fig. 6(b)]. Nevertheless, as it is seen from this figure, for
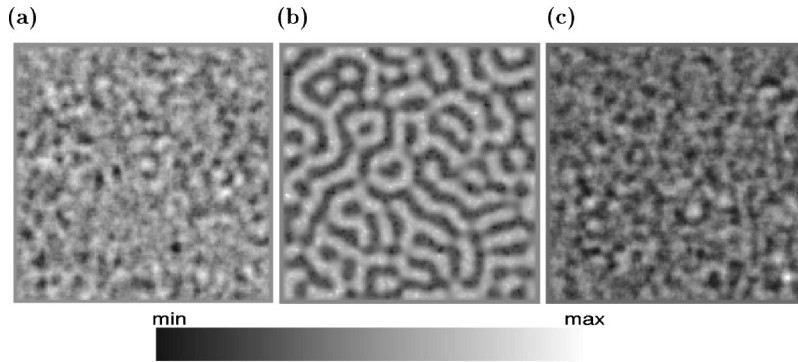
FIG. 5. Snapshots of the field for in the case of the uncorrelated additive noise. The parameter σ_ζ^2 is equal to (1) 0.001, (b) 0.7, and (c) 10.0. The remaining parameters are $D=3.5$, $\sigma_\xi^2=13$, $a=0$, and $\Delta t=10^{-7}$. (max,min) values are $(0.0072,-0.0075)$, $(7.14,-6.33)$, and $(1.07,-0.61)$.

large enough intensity σ_ξ^2, in addition to the stable state $x=0$, the potential $U(x)$ has two minima more, precisely if $\sigma_\xi^2>4$. Therefore, in this case the phase transition is a result of hard excitation and requires independent additive noise. Sufficiently large additive noise causes escapes from the central minimum and the system does not return if the new minimal states are lower than the central one. This argumentation can be considered as an intuitive explanation of the observed noise-induced phase transition by uncorrelated additive noise.

Another interesting finding to be mentioned is the relation between phenomena discussed and the well-known problem of stochastic resonance (SR). Namely, we trace the parallels between the nonmonotonic behavior of the signal to noise ratio (SNR) in SR phenomena and the reentrant phase transitions dependent on the additive noise.

Let us consider possible reasons for this similarity. For that purpose we reformulate the process of ordering in the bistable potential $U(x)$ as a situation typically occurring in SR. The influence of the neighbors supplied by the coupling serves as a driving force for the single system in the lattice with a bistable potential. Under this influence every single system is trying to obey the rules of the whole system, for example, to choose the proper minimum of a potential. Accordance with stochastic resonance becomes evident since this information is best transmitted to the single system if the

intensity of an additive noise is optimally selected. For smaller and larger values of noise intensity the ordering process is not effective as in stochastic resonance. As a result and quite analogously to the shape of the SNR, the maximum of the structure function behaves nonmonotonically dependently on the parameter a. The similarities are obviously bounded since in SR the input is independent from the reaction of the system. In our case it differs due to the mutual interaction between the elements of the lattice. It determines the structure of the output, which plays the role of the input for another element.

VI. CONCLUSION

In conclusion, we have shown by the example of the nonlinear model with coupling term similar to that of *Swift and Hohenberg* that an increase of the additive noise may surprisingly induce ordered spatial patterns. The reason is the reentrant phase transition caused by the additive noise. The further increase of the additive noise destroys these structures. In both limiting cases of the correlation between additive and multiplicative noise the pictures are similar but the origins differ. We stress that this phase transition is possible only in the presence of multiplicative noise. As we have discussed, we interpret the phenomenon observed as a coop-
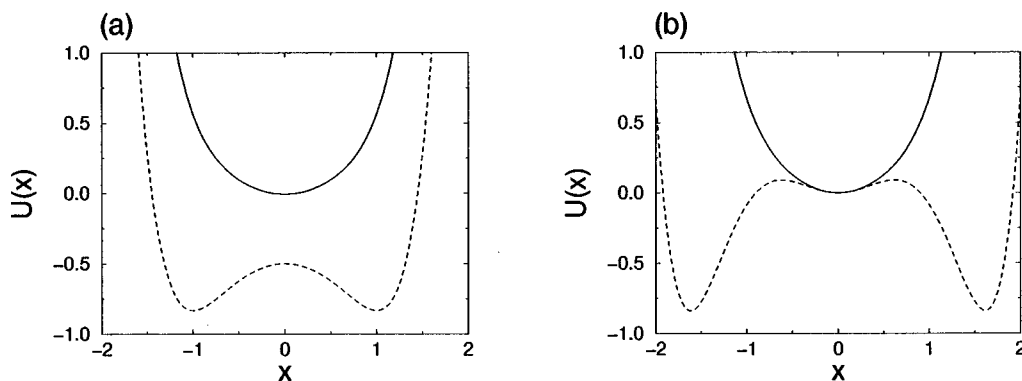

FIG. 6. Potential for the short time evolution of the average value $\langle x(t)\rangle$. (a) $\sigma_\xi^2=2$: solid line, $a^2=0.1$; dashed line, $a^2=1.0$. (b) $a=0$: solid line, $\sigma_\xi^2=2$; dashed line, $\sigma_\xi^2=5$. In case (a) the short time behavior can be described by the bistable potential if the constant a is sufficiently large. In case (b) the situation is more complicated: the state x_0 remains stable, but large enough additive noise can force a system to leave the zero state and form a mean field.

erative work of a noise-induced phase transition and ordering process with an optimal value of the additive noise. From this point of view the phenomena observed can be understood as a mixture of the phase transition induced by the multiplicative noise and processes that have similarities to features of stochastic resonance.

[1] L. Gammaitoni, P. Hänggi, P. Jung, and F. Marchesoni, Rev. Mod. Phys. **70**, 223 (1998).

[2] P. Hänggi and R. Bartussek, in *Nonlinear Physics and Complex Systems—Current Status and Future Trends*, edited by J. Parisi, S.C. Müller, and W. Zimmerman, Lecture Notes in Physics Vol. 476 (Springer, Berlin, 1996), p. 294.

[3] W. Horsthemke and R. Lefever, *Noise-Induced Transitions* (Springer-Verlag, Berlin, 1984).

[4] C. Van den Broeck, J.M.R. Parrondo, and R. Toral, Phys. Rev. Lett. **73**, 3395 (1994).

[5] C. Van den Broeck, J.M.R. Parrondo, J. Armero, and A. Hernández-Machado, Phys. Rev. E **49**, 2639 (1994).

[6] C. Van den Broeck, J.M.R. Parrondo, R. Toral, and R. Kawai, Phys. Rev. E **55**, 4084 (1997).

[7] J.M.R. Parrondo, C. Van den Broeck, J. Buceta, and F.J. de la Rubia, Physica A **224**, 153 (1996).

[8] J. García-Ojalvo, J.M.R. Parrondo, J.M. Sancho, and C. Van den Broeck, Phys. Rev. E **54**, 6918 (1996).

[9] P.S. Landa and A.A. Zaikin, Phys. Rev. E **54**, 3535 (1996).

[10] P.S. Landa and A.A. Zaikin, JETP **84**, 197 (1997).

[11] P.S. Landa, *Nonlinear Oscillations and Waves in Dynamical Systems* (Kluwer Academic, Dordrecht, 1996).

[12] P.S. Landa and A.A. Zaikin, in *Applied Nonlinear Dynamics and Stochastic Systems Near The Millenium*, edited by James B. Kadtke, AIP Conf. Proc. No. 411 (AIP, Woodbury, NY, 1997).

[13] P.S. Landa, A.A. Zaikin, and L. Schimansky-Geier, Chaos Solitons Fractals (to be published).

[14] P.S. Landa, A.A. Zaikin, V.G. Ushakov, and J. Kurths (unpublished).

[15] J. García-Ojalvo, A. Hernández-Machado, and J.M. Sancho, Phys. Rev. Lett. **71**, 1542 (1993).

[16] A. Becker and L. Kramer, Phys. Rev. Lett. **73**, 995 (1994).

[17] J. García-Ojalvo and J.M. Sancho, Int. J. Bifurcation Chaos **4**, 1337 (1994).

[18] J. García-Ojalvo and J.M. Sancho, Phys. Rev. E **53**, 5680 (1996).

[19] R. Müller, K. Lippert, A. Kühnel, and U. Behn, Phys. Rev. E **56**, 2658 (1997).

[20] S. Kim, S.H. Park, and C.S. Ryn, Phys. Rev. Lett. **78**, 1616 (1997).

[21] L. Ramirez-Piscina, J.M. Sancho, and A. Hernández-Machado, Phys. Rev. B **48**, 125 (1993).

[22] J.M. Sancho, M. San Miguel, S.L. Katz, and J.D. Gunton, Phys. Rev. A **26**, 1589 (1982).